END-TO-END FLOOD RISK ASSESSMENT: A COUPLED MODEL CASCADE WITH UNCERTAINTY ESTIMATION

Hilary Katherine McMillan

This dissertation is submitted

for the degree of Doctor of Philosophy

University of Cambridge, UK

Selwyn College

2006

DECLARATION

This thesis is submitted for the degree of Doctor of Philosophy at the University of Cambridge. It is the result of my own work and includes nothing which is the outcome of work done in collaboration except where specifically indicated in the text. It is within the prescribed word limit (80,000 words) of the Degree Committee for Earth Sciences and Geography.

Hilary McMillan

ACKNOWLEDGEMENTS

It is a pleasure to thank those people who helped me to complete this thesis.

Firstly, I am very grateful to my supervisor, Dr. James Brasington, for his guidance in direction and technique throughout my PhD. Particular thanks are due for his valuable comments on the first draft of the dissertation.

Thank you to my colleagues in the hydrology group, with whom I was able to discuss and share ideas. I am also indebted to many others in the Geography Department, particularly to Adrian Hayes, John Clarke and Mark Theobald for their support in building and installation of field equipment.

This project was funded by a NERC studentship, in association with my CASE partner, Hannah Reed Associates. Grants from the British Geomorphological Research Group, British Hydrological Society and Philip Lake II Fund enabled attendance at international conferences. Linton Parish Council provided funding for field equipment and I am grateful to their chairman, Val Urwin, for her essential work in collection of survey data.

Finally, I would like to thank Tom, for his love and support, and for proofreading the final manuscript.

Abstract

This thesis aims to establish a contemporary framework for flood risk assessment, using a cascade of coupled models which incorporate the best new hydrological data and modelling techniques, within a structure which allows uncertainty estimation to be integrated into the analysis. The method is tested and validated through an application to the Linton catchment of the River Granta in Cambridgeshire, allowing an assessment of its suitability for use in a typical small, lowland catchment.

Several factors provide the motivation to improve on conventional methods of flood risk assessment. Recent evidence of non-stationarity in the flood generation process suggests that a process-based model of catchment behaviour is required to replace the traditional ‘curve-fitting’ approach to flood frequency analysis. Further, it is no longer sufficient to limit the procedure to prediction of discharge; a distributed model of floodplain inundation based on sound hydraulic principles must be integrated into the analysis in order to support today’s ‘soft engineering’ solutions to flood risk. Finally, a rigorous uncertainty estimation procedure must replace outdated deterministic forecast techniques.

In order to achieve these aims, three component models were developed: a stochastic rainfall model, a rainfall-runoff model and a floodplain inundation model. The process-based technique of continuous simulation is employed to allow direct analysis of flow characteristics, using simulated rainfall series produced by the first model to drive the rainfall-runoff model and thereby produce continuous discharge simulation. Direct analysis of flow regime is then possible, which in turn provides the boundary conditions for the inundation model. This takes the form of a 2d raster storage cell model which benefits from airborne laser altimetry (LIDAR) mapping of floodplain topography to allow high resolution simulation of floodplain inundation. Improvements in efficiency through the use of sub-grid scale information are explored.

The results of the case study demonstrate that the coupling of the three models to form an ‘End-to-End’ flood risk assessment structure provides a practical and rigorous flood risk assessment tool. A comparison of results with a study using conventional techniques suggests that the new method achieves a valuable improvement.

Contents

Chapter 1

INTRODUCTION

Abstract

This chapter introduces the thesis by setting the research question in terms of its wider context. The thesis is concerned with the design of a process-based, integrated, spatially distributed, flood risk assessment structure: this chapter considers the situation which has led to deficiencies in current methods and the need for such a framework to be established.

Firstly the nature of flooding itself must be examined. Scientific, political and public opinion is agreed that we live in a period of accelerated flood risk; the forcing factors which underlie this trend are set out in Section 1.3. This leads on to a consideration of societal response to flooding: the perception of an increased threat has led to a period of intense research into flood defence and mitigation strategies. Increased understanding of the limited ability of structural flood defence measures to protect inappropriately sited development, and the possible damage caused by removing the natural role of the floodplain, has encouraged catchment-wide flood management strategies which emphasise planning controls and floodplain restoration.

The step change in response to flood risk has not however been reflected in methods of flood risk assessment. The standard methods in use today (Section 1.3.3) were designed to facilitate 'hard' engineering works which aimed to increase channel conveyance capacity. Their unsuitability for use in a society concerned with non-stationarity in flood frequency and the need for flexible and environmentally sound 'soft' engineering solutions is documented in Section 1.4.1. These findings provide the stimulus for the design of a new flood risk assessment framework (Section 1.4.3).

1.1 Introduction

In recent years, Britain has experienced several major and widespread flood events, notably those of Easter 1998 and Autumns 2000 and 2001. In addition to these, more recent flood events have had a smaller spatial extent but similarly damaging consequences. For example, in January 2005, floods in Carlisle inundated 2000 properties and caused 2 fatalities. Flash floods also have the capacity to cause devastation, such as those in North Yorkshire in June 2005 which washed away roads and bridges and caused £5 million damage, and the destructive flooding of Boscastle in August 2004 by what was described as a 3 m 'wall of water'. Floods in the UK have been mirrored by widely reported floods in mainland Europe, such as those of Germany, the Czech Republic, Austria, Russia, Romania, Italy and Switzerland in 2002 (79 fatalities), Romania, Germany, Switzerland, Bulgaria and Austria in 2005 (42 fatalities), and Hungary, the Czech Republic, Serbia, Romania and Bulgaria in 2006. Further afield, the July 2005 flooding of Mumbai resulted in 1000 deaths, and in August 2005 Hurricane Katrina hit New Orleans causing widespread devastation from flooding and over 1200 confirmed deaths.

The causes of these flood events are diverse: from the exotic of monsoon and hurricane, to the more mundane of snowmelt, thunderstorm and prolonged rainfall. Those causes relating to the UK are discussed in Section 1.2. However, despite their disparate causes, all the events resulted in huge economic, social and environmental cost, and in many cases prolonged displacement of residents. In response to these events, bolstered by speculation in the press as to the possible future impacts of climate change on precipitation and flood regime, a high level of public and political awareness of flood hazard has been achieved. Authorities have thus been pressurised into being seen to take action to prevent repetition of flooding in affected areas, leading to a high demand for accurate flood frequency estimates and risk mapping. In some cases, the resulting action has taken the form of extensive and expensive engineering work such as the building of the Jubilee River to protect areas of Maidenhead and Windsor; in others focus has shifted to the restoration of the natural flood attenuation function of the floodplain. In some, the difficult process has begun of explaining to residents that a cost-benefit analysis has not justified any further intervention; an outcome only ameliorated in some instances by provision of an improved flood warning system. These different responses and the philosophies underlying them are discussed in Section 1.3.2.

In the UK, the extent of public concern, the high numbers of people affected by flooding and the large sums of money spent on flood protection measures have served to drive scientific research into methods of flood risk assessment and inundation modelling. To a certain extent, however, there remains a mismatch between those techniques being developed in the research arena, and those being applied in standard flood risk assessment applications. By examining the conventional methods being applied in the UK (Section 1.3.3) and their limitations in providing a response which enables modern solutions to today's flood risk conditions (Section 1.4), the conception of a contemporary flood risk assessment framework, which takes advantage of advances in data collection and modelling techniques, is a logical outcome of this chapter.

1.2 Research Context: Background to Flood Forecasting in UK

1.2.1 A Brief History of UK Flooding

Recent reports and media stories often seem to suggest that flooding in Britain is a 21st century phenomenon, never experienced before the effects of climate change began to be felt. However a study of the literature soon reveals that flooding has been an integral part of our history, documented since records began. An archive of textual information on British hydrological events before 1935 is being created by the British Hydrological Society (Black and Law, 2004). Some of the earliest floods recorded there are Thames floods in AD 9 and AD 48, and a flood in Cheshire in AD 353 in which "5000 persons and an innumerable quantity of cattle perished"; however it seems certain that there were many floods before these. This section takes a short overview of such historical flood events in the context of some of their forcing factors.

All inland floods originate in meteorological conditions, despite the many other causative factors which may exacerbate their effects. They may be broadly classified into Summer and Winter storms, of which the former have traditionally been more often recorded; however, this may be due to their suddenness and novelty value (Newson, 1975). Summer rainstorms may be due to weather fronts becoming stationary over a vulnerable area; these conditions have caused several notable floods in Eastern Scotland. Alternatively, simple 'cloudbursts' giving rainfall totals of up to 150 mm cause localised floods. In comparison, winter floods are generally caused by prolonged wet weather bringing saturation conditions which curtail the ability of the catchment to attenuate the flood peak. These conditions generally give rise to more widespread flood events, often affecting the major lowland rivers. The great floods of 1894 on the Thames, Wye, Severn and Bristol Avon are one example. A further cause of floods less commonly seen in recent years is snowmelt. This was the case in the infamous floods of 1947, which have commonly been used to set a benchmark protection level for flood defence works (Newson, 1975). A thaw of snow accumulated over 2 months was accompanied by 25 mm of rainfall to cause major floods on the Lea, Great Ouse, Trent and Medway.

Topography is another essential control on flood magnitude. Historically, areas suffering particularly severe floods have been the West Country and North-East Scotland, and this has been attributed to their typically small, steep catchments (Newson, 1975). The similarity of the floods of August 1829 and August 1956 in Moray - those of 1829 recorded by a plaque marking the 15 m rise of the River Findhorn - has been attributed to the control that the area's topography exerts on the flood regime. One of the floods with the most prominent position in the public consciousness, that of Lynmouth in 1952, had its dominant cause in the relative position of the rainfall over the topography. The storm was centred on several merging streams at the headwaters of the Lyn, around 9 inches of rain falling in 24 hours onto saturated ground. This water then flowed down the narrow and deeply incised valleys, showing the unusual occurrence of significant overland flow (Huxtable, 2005). A very similar mechanism caused the devastating flooding of Boscastle in 2004.

Although the topography of an area is largely beyond the control of its inhabitants, human influence is apparent in another major factor in flood development: land-use and structures within the catchment. The bare earth left by agricultural activities has been stripped of the natural interception qualities of vegetation cover, and heavy rain can cause gullying of the soil which greatly reduces the lag time between precipitation and channel peak. This was demonstrated in Louth, Lincolnshire in 1920 where such action caused the River Ludd to rise 5 m in 15 minutes. Flooding which causes rivers to form in otherwise dry valleys may often meet obstacles such as stone walls. In Somerset and the Mendips in 1968 such blockages caused damaging flood surges. More recent studies into the effects of land use change are described in Section 1.2.2.2.

1.2.2 Accelerated Flood Risk and its Causes

The previous section considered some of the postulated causes for historical flood events. Today we are in a period of what is widely considered to be 'accelerated' flood risk caused by human factors. Public and political perception of this process has been influenced by floods at home and abroad (Section 1.1); however these opinions have been backed up scientific studies which both look for non-stationarity exhibited in the recent precipitation and flood record, and aim to predict the occurrence of such behaviour in the future. The causative factors may be broadly divided into those relating to climate change and those relating to land-use change. Wheater (2006) presents a useful summary of the possible reasons for increased flood hazard in the UK, comparing these two causes.

Studies which demonstrate existing trends include that of Osborn and Hulme (2002) who modelled daily precipitation amounts in the UK between 1961 and 2000 using a gamma distribution, and found that winter rainfall had on average become more intense over the period. Increasing trends in precipitation volume and intensity have also been found in other studies of mid-latitude areas of the Northern Hemisphere, suggesting an intensification of the hydrological cycle (Dai *et al*., 1997; Easterling *et al*., 2000; Groisman *et al*., 2004; Huntington, 2006). Staeger *et al*. (2003) extended their analysis to test for anthropogenic forcing in precipitation fields and conclude that in some regions of Europe, human behaviour has already caused significant changes to the climate. However, evidence for trends in rainfall is stronger than that for flood frequency or magnitude, and studies choosing to examine trends in UK flood regime have found no significant changes (Robson, 2002; Robson *et al*., 1998). This may in part be due to lack of long-term data series and limitation of many recordings to flood peak magnitude rather than the full flood hydrograph.

1.2.2.1 Causes Relating to Climate Change

Supporting evidence for precipitation increases comes from observations of global warming in the recent past, with average global temperature increase since 1900 estimated to be in the range 0.4 – 0.6 ºC (Folland *et al*., 2001). By using this change to alter the parameters of a numerical climate model, the likely effect of this temperature rise in terms of precipitation regime may be examined. The results of such studies in general concur with the observed changes in rainfall patterns, suggesting increased frequency of heavy precipitation in winter (Hulme and Osborn, 1998).

As well as predicting past and current consequences of global warming, numerical Global Climate Models (GCMs) are also widely used to estimate the possible future effects and magnitudes of climate change. A widely-used model is the UK Hadley centre 11-layer GCM which gives standardised fields of temperature and rainfall indices on monthly basis. The forecast available from this model for 2050 is commonly used as a basis for

UK applications. It predicts changes of temperature up to 3.6 ºC in South-East England, and rainfall increases from 10% in South-East England to 20% in North-West England (Sefton and Boorman, 1997). This forecast is used as a basis for guidance given by the government (MAFF, 2001; ODPM, 2004) that an allowance for 20% increase in peak river flow due to climate change should be made in any new flood risk applications. The estimates of precipitation increase can only be used as a 'best guess'; there are numerous sources of uncertainty in the calculations. For example, the model relies on an emissions forecast from IPCC predictions which is an estimate based on possible world development scenarios and governmental success in reducing emissions. The model itself may also be run using different structures and parameterisations: models using equilibrium versus transient scenarios have found annual runoff to increase or decrease respectively (Holt and Jones, 1996; Pilling and Jones, 1999).

The uncertainty of climate change effect on river flows makes it difficult to design flood defence strategies to cope with such changes. There are many different ways in which climate change may effect catchment behaviour, such as changes in rainfall totals, locations, seasonality, and intensity, effects on temperatures and evaporation (Roberts, 1998), effects on channel morphology and sediment transport (Rumsby and Macklin, 1994), and effects on drainage density (Moglen *et al*., 1998). There are indications that the frequency of heavy rainfall events is likely to increase (Arnell *et al*., 2001), and studies have shown that variability is expected to increase with changes in monthly totals greater than annual change (Arnell and Reynard, 1996). Attempts have been made to model this type of response, for example by assuming that all extra rainfall predicted occurs as heavy rainfall (Reynard *et al*., 1998). However in general it is difficult to quantify these effects as they occur at higher resolutions in space and time than can be predicted by a GCM (Arnell and Reynard, 1996; Sefton and Boorman, 1997).

1.2.2.2 Causes Relating to Land-Use Change

Section 1.2.1 highlighted briefly ways in which land-use change was observed to affect flow regimes as early as 1920. In more recent years, urban development and intensive cultivation of the land have led to widespread consequences in terms of infiltration rates, soil structure and drainage patterns, and therefore in the ability of catchments to store flood water and to attenuate flood peaks. The causes of catchment response change may be subdivided in various ways: Wheater (2006) draws a distinction between those relating to urban development, and those relating to rural land-use changes, providing a comprehensive review of reasons behind recent increases in flood hazard. Alternatively, a useful distinction might be drawn between those causes which affect the rainfall-runoff response of the catchment, and those which relate to the functionality of the floodplain.

Those causes associated with urbanisation of areas of a catchment, whether affecting source or floodplain areas, are relatively well studied and well understood. This is due both to the limited scale of such developments, and to the short timescales over which they typically occur, leading often to dramatic changes in hydrological regime and easily monitored results. Planning regulations also tend to focus on such urban developments. Causes in source areas include reduced infiltration rates, reduced evapotranspiration rates due to vegetation loss and reduced soil storage capacity. Urbanisation may have particularly severe effects on small head-water catchments, where a high percentage of the catchment area may undergoes a change in land-use within a short time period. In a larger catchment, the effects of land-use change would to a greater extent be damped by the remainder of the catchment area (Orr and Carling, 2006; Rosso and Rulli, 2002; Tollan, 2002). Measured effects are also more pronounced at smaller flood magnitudes and during dry seasons, where previously the catchment had a capacity to attenuate the flood peak; during higher return period and winter floods saturation of the soil and resulting overland flow gives a natural response closer to that of an urbanised catchment and therefore the effects are reduced (Camorani *et al.*, 2005; Liu *et al.*, 2004). Where urbanisation occurs on the floodplain itself, the ability of the floodplain to attenuate a flood peak by promoting storage, infiltration and alternative flow pathways is reduced. This effect is greatly enhanced where flood defences are erected; such structural measures may also cause residents to lose their sense of natural river dynamics and reduce the perceived risk for further development (van Stokkom *et al.*, 2005).

The Linton catchment is largely rural, and those land-use factors relating specifically to the Granta catchment are discussed in Section 3.2.3. Here, rural areas in general are considered, where the effects of land-use change are often less dramatic and more difficult to quantify than for urban sites. Where rural areas of the floodplain are used for valuable arable crops and hence protected by flood defences, the effects may be similar to that of urbanisation; an understanding of the associated increase in flood peak heights was demonstrated by the decision in Romania in April 2006 to deliberately breach defences and flood farmland in order to protect towns. Other changes relating to vegetation cover, infiltration rates, soil structure and artificial drainage usually take place more gradually, meaning that cause-effect relationships are more difficult to establish. Sullivan *et al*. (2004) studied a basin in Cornwall which had seen a significant increase in magnitude and frequency of flood flows, but only a weak rising trend in rainfall. Although it was suggested that the increased flood risk could be attributed to land-use change, it was not found possible to distinguish the effects of climate change, increased agricultural activity and urban expansion. Other authors have suggested that this interaction of different forcing factors could be exploited, for example by offsetting urbanisation with forestation, or climate change by land-use change (De Roo *et al*., 2003; Naef *et al*., 2002; Reynard *et al*., 2001). Crooks and Davies (2001) studied the causes and effects of land-use change by identification of those periods of UK history producing the most dramatic changes in land-use in the Thames catchment. They highlighted significant urban expansion during the inter-war years, and rapid rural land-use changes during the Second World War as large areas of grasslands were converted to arable land in order to increase crop production. In comparison, the years since 1960 had seen only gradual land-use change which had a very small effect on flood frequency compared with observed changes in precipitation regime.

1.3 Flood Forecasting and Assessment of Flood Risk: Standard Methods

1.3.1 Flood Gauging and Reconstruction

Essential to both our understanding of causes and impacts of floods, and to our ability to plan for future ones, is the capacity to reconstruct past events. Data retrieved from previous floods ranges from time series of flow for modern gauges, to estimated maximum levels or discharges for earlier events. The standard methods for use of such data in the context of flood management are considered further in Section 1.3.3.

The UK currently has a relatively dense network of river flow gauges, created through a programme of instrumentation that was largely initiated by the Water Resources Act of 1963, and encouraged through incentives provided as part of the United Nations Educational, Scientific and Cultural Organization's (UNESCO) International Hydrological Decade 1965-1974. These gauges are currently maintained by the Environment Agency (EA) in England and Wales, and the Scottish Environmental Protection Agency (SEPA) in Scotland. The records are held in the National River Flow Archive, managed by the Centre for Ecology and Hydrology (CEH) at Wallingford. Over 1300 gauging stations provide daily or better flow data which can be used to reconstruct flood hydrographs. Although data form the underpinning of most flood management applications, the average length of gauged record in the UK is relatively short. The average length of the 'Annual Maximum Discharge' series found to be available in the Flood Estimation Handbook was 23.4 years (Bayliss, 1999), which without extrapolation is often insufficient to predict the levels of protection required by flood defence works.

Alongside the gauging network, there are numerous alternative sources of data on flood events. These may be used either for the reconstruction of historical floods before the gauging network was widespread, or as supplementary data when rainfall and flow gauges malfunction. They can also serve to refine magnitude-frequency relations to reduce the influence of recent outliers (Kidson and Richards, 2005; Kidson *et al*., 2005; Salas *et al*., 1992). There are many accounts in the literature of the failure of gauges in extreme conditions: rain gauges are flooded or buried in landslides, flow gauges are unsuitable for accurate monitoring of high flows or simply washed away. Even when gauged data is presented as a complete and accurate record, it must be borne in mind that the gauging process includes many possible sources of error, most notably through uncertainty in the stage-discharge relationship (especially for extreme flows). The most obvious benefits of including alternative data sources is the extension of the flood record, however it may also bring greater understanding of flood production mechanisms, information on land-use change and flood seasonality, and improved confidence in flood frequency estimation results (Archer, 1991; Bayliss and Reed, 2001). The types of supplementary data available are many and varied. The gauging authorities themselves may hold historical data previous to formal records. Peak levels are some of the most widely available data, in the form of flood stones or other marks. Levels may also be remarked upon in journals or newspapers from the time of the flood. These sources may also give clues that are less easy to interpret into hard figures, such as the description of the River Findhorn during the 1829 floods "passing with the velocity of a swift horse" (Newson, 1975).

The field of paleohydrology provides methods suitable for estimating or creating a lower bound for the stage, discharge or velocity of the very largest of floods, even if these have occurred many thousands of years ago. Perhaps the most common source of river level information is from slack water deposits: depositions of suspended clay, silt or sand from stagnated water behind constrictions or in low-velocity eddies present during high flood stages, whose age may be determined by carbon-dating methods. Other stage indicators may include the study of fluvial landforms or vegetation types (Salas *et al*., 1992), or vegetation debris ('trashpoint') evidence (Kidson *et al*., 2006). Bounds on floodwater velocity may be possible to define in some cases by studying the sizes of boulders moved by the flood (Huxtable, 2005). While sedimentary and other evidence provides valuable information on river stage, transforming this into an estimate for discharge in order to create or extend a magnitude – return period relationship for the catchment can be extremely challenging. Typically a 1D model such as HEC-RAS is used to generate the discharge estimates (Sheffer *et al*., 2003; Thorndycraft *et al*., 2005), however the results are dependant on the unknown value of the friction coefficient Manning's n. Uncertainty in this parameter, due to a common lack of high-magnitude floods with known discharge for calibration, may lead to high uncertainties in the discharge value (Kidson *et al*., 2006;

Wohl, 1998). It is therefore important that such reconstruction evidence should only be used with appropriate consideration of its inherent uncertainties (Archer, 1991; Fanok and Wohl, 1997).

1.3.2 Philosophies of Flood Prevention and Mitigation

In order to put into context the current standard methods of flood forecasting and risk assessment, this section considers the type of flood prevention and mitigation measures in use today. An understanding of these measures explains the aims behind current risk assessment techniques and the information which they are required to provide. Considering changing responses to flood risk also highlights the shortfalls of such techniques and the areas where they are less able to provide the data required for modern flood management strategies.

1.3.2.1 Historical Perspective on Flood Prevention Measures

Humans have long attempted to control the effects of flood and tide on their settlements. Some of the earliest defences on record in the UK are defence banks built into the Wash in Roman times. In more recent history, the Thames Barrier was built at a cost of £535m in response to the flood of 1953 which claimed 307 lives (Hart and Hart, 2005). This structure typifies the ‘positive’ approach to flood management, which holds that the objectives should be to allow exploitation and the use of the natural resources of the floodplain wherever possible (Penning-Rowsell and Parker, 1973); the expectation being that this will be made possible by expenditure on flood protection works. A similar philosophy was in evidence in 1964-1973 when flood protection measures were put in place on the Bristol Avon (Newson, 1975). Costing £2m, the works included creation of new river walls, installation of new sluices and bridges, the grading of the river bed and removal of bends, and channel dredging. This demonstrates the removal of the traditional role of the floodplain as a facility for storage and conveyance of flood flows, and instead an expectation that the channel conveyance should be expanded such that it is capable of accommodating the event water. In the case of the Avon, the channel conveyance was increased from 170 cumecs to 340 cumecs.

To a large extent, the reliance on structural flood defences was still in evidence when MAFF published its flood strategy in 1993, quoting its aim as “To reduce risks to people and the developed and natural environment from flooding … by encouraging the provision of … defence measures” (MAFF & the Welsh Office, 1993). The document specified that the priorities for funding were urban areas where risk to life was greatest; the emphasis was on coping with the effects of flooding rather than studying its causes. This was reinforced by the lack of central provision or guidance: flood control measures were left to local River Authorities to implement, reducing the capacity for a holistic view of basin management as these authorities had no legal say in floodplain development planning (Davies, 1992). This reflected previous feelings that watershed management awaited a ‘coming-of-age’ of scientific hydrology before becoming widespread (Newson, 1975). Although the era of structural flood defence solutions is now coming to an end, for reasons given in the following two sections, there are still instances where such measures continue to be used. Notably the ‘Jubilee River’, an 11.6 km long diversion channel built to alleviate floods in Maidenhead and Windsor, was opened in 2003 at a cost of £100 million.

1.3.2.2 Drivers for Change

In recent years, significant changes in scientific, public and government opinion have brought about a reappraisal of flood management policy in Britain. Above all, there has been an acceptance that nature cannot always be tamed by science, that engineering works cannot be used to solve all flooding problems. Indeed public perception now commonly holds that science and modernisation are at the root of many of the risks we face (Beck, 1992; Giddens, 1998). This is demonstrated in the growing public view that the perceived increased flooding in areas of the UK may be caused by both international human actions such as global warming, and local ones such as floodplain development. In turn, this understanding has led to a decreased trust in authority, and at the same time an increased willingness to understand the scientific process behind policy decisions and to take a greater part in these processes (Jamieson, 1990; Saraiva *et al.*, 1992; Watts, 1996).

The shift in public view has increasingly been recognised and accepted by policy makers. The importance of public opinion on flood defence provision has been highlighted by studies showing large increases in public approval of flood strategy where communication has been made a priority (Parker and Handmer, 1998). This change in attitude has had several major impacts on flood planning, notably that the concept of risk assessment has been extended from purely economic considerations to cover wider social and environmental values. This is demonstrated by the Department of the Environment, Food and Rural Affairs (DEFRA) scoring system which is used to decide grant allocations for flood and coastal defence capital works, in which a base score is modified to account for the vulnerability of the area's residents and also the impact on valuable habitat affected by the proposed scheme (DEFRA, 2002). The idea of vulnerability of a population has become an important one, and has been quantified in terms of social and economic variables, property and infrastructure variables, flood characteristics, flood warning provision variables and official responses variables (Green *et al*., 1994; Reitano, 1992). Continuity across communities is another recent concern, to ensure that residents living in lower-cost housing do not lose out in traditional benefit-cost analyses (Environment Agency, 2001).

1.3.2.3 Current Government standpoint

In response to the drivers identified above, the current governmental policies on flood prevention and mitigation measures increasingly favour 'soft' solutions over 'hard' engineering solutions. Latest government guidance states that "Continued construction of hard-engineered flood defences to protect development in areas exposed to frequent or extensive flooding may not be sustainable in the long term" (ODPM, 2004). The fact that flood defences cannot reasonably be built to protect against the most extreme floods has become apparent through several recent costly failures. For example, the Easter 1998 floods caused 5 deaths and £440m damage; in Autumn 2000 although flood defences protected 280,000 homes, 10,000 homes were still flooded and £1bn damage was caused. In 26% of cases this was due to overtopping of defences, in 14% of cases defences were outflanked (Environment Agency, 2001). The changing nature of river flow characteristics due to climate change, urbanisation and land-use change on floodplains has brought about increasing flood peak magnitudes which were not planned for when existing flood defences were designed. Some modern structural schemes have responded to similar problems using adaptable flood defences measures, which may be upgraded to maintain the required level of protection at reduced additional expenditure. There is also government recognition of the problem of existing flood defences encouraging further development of protected land, and hence rising costs when such defences are breached.

Environmental considerations are becoming increasingly integrated into flood management policy, as the habitat, amenity and cultural values of floodplains are recognised. Studies have shown that some communities would prefer to live with some level of flood risk than be subjected to intrusive flood defence works, especially where the flood risk is not well understood (Correia *et al*., 1994; Saraiva *et al*., 1992), and assessment of recreational, environmental and social impacts is therefore becoming an important contributing factor in flood management policy decisions (Brouwer and van Ek, 2004; Rasid and Haider, 2002). Floodplains form an important habitat, and flood management plans must balance the need for flood cycles which sustain biodiversity, with protection against extreme events, possibly caused in part by human impacts, which damage habitats and soils (Richards *et al*., 2002). Measures such as biodiversity action plans, statutory conservation sites, and environmental impact assessments for flood relief works have all contributed to the heightened role of environmental considerations.

All these considerations have led authorities to seek a ‘step change’ in the role of the land-use planning system in the control of flood risks, as demonstrated by the guidance put forward in the document PPG25 (ODPM, 2004) and its successor PPS25 (ODPM, 2005). In efforts to reduce unnecessary expenditure on structural flood defences, increasingly strict guidance on planning has been given. Developers are now responsible for carrying out Flood Risk Assessments in the planning stage of new developments, and for managing and funding any flood management measures necessary as a result of construction. This is particularly pertinent as pressure on housing provision forces consideration of development on land at risk from flood events, including initiatives such as the use of brownfield sites (ODPM, 2000) which are often situated close to waterways. Such new planning regulations demonstrate determination to provide centralised guidance and policy, and are backed up by an increased emphasis on the Environment

Agency as the leading supervisory and regulatory body for all matters relating to flood defence. This allows flood management to be considered at a regional scale, with planning policies that cross administrative boundaries.

Basin-wide planning is central to many of the new ‘soft-engineering’ flood defence options suggested for consideration. These centre on the restoration, enhancement or creation of the natural functions of the floodplain, recognising that the floodplain is a “transitional environment between terrestrial and fully aquatic systems” (Brookes *et al*., 1996). By reintroduction of natural defences such as flood meadows, wetlands, washlands, salt marshes or mud flats, the importance of a ‘functional floodplain’ is recognised and flood events can be greatly attenuated. This type of management is used to good effect in the Ouse Washes which provide a wide, shallow river in times of flood (Pask, 1992). The Environmental Stewardship Scheme offers an option to pay land owners to set land aside as ‘inundation grassland’ or to create wet grassland, reed bed or swamp habitats, recognising the financial value of dedicated river corridors. It is estimated that up to 0.5 million hectares of agricultural land lies behind non-viable flood defences and could be returned to its natural state as part of the floodplain. Other measures to be considered which require greater intervention include the setting back or removal of flood banks, reintroduction of river meanders and restoration of variable bed morphology (DEFRA, 2003)

Complementing strategic regional planning, there is an increased emphasis on individual responsibility. There is no statutory duty for the government to provide flood defences; the owner is ultimately response for safeguarding property against flooding. Studies have shown that in the past, structural flood defences have led to a false feeling of security amongst property owners, discouraging flood proofing and emergency preparedness, and weakening community resolve to implement land-use regulations (Ericksen, 1986; Handmer, 1990). This has then led to unnecessary disruption when defences have been overtopped, which could have been prevented by houseowner preparedness. To address this issue, there has been a concerted effort by the Environment Agency to raise public awareness of flood risk (Environment Agency, 2001). Central to the campaign has been the introduction of the new codes ‘Flood Watch’, ‘Flood Warning’, ‘Severe Flood Warning’ and ‘All Clear’ which are represented by graphics and have been introduced in collaboration with national television and radio networks. These have been accompanied by the telephone advisory service ‘Floodline’, which provides a central point of information for concerned members of the public. In order to target flood information correctly, a national database of at-risk properties has also been compiled using indicative floodplain maps produced by the Environment Agency. These flood risk maps are also available online for consultation by the public, to improve awareness of high risk areas. In the future this information will have to be included in the Sellers Pack for property sales. Improved public awareness has been shown to encourage public feelings of efficacy in flood management and an improved uptake of flood prevention measures (Waterstone, 1977). Measures promoted to the public include installing removable flood-proof screens and air-brick covers, stockpiling of sandbags and preparation of an emergency plan. In the case of property refurbishment more invasive measures can be considered such as raising of floor levels and electrical circuits.

1.3.3 Standard Methods in Flood Forecasting

In order to meet the aims of the previous section in the provision of catchment and basin-wide management strategies, planning of structural and non-structural flood defence works, and provision of information to emergency planners and the public, a range of flood risk assessment results are required. In order to harmonize these results across regional boundaries, standard methods are employed in several different aspects of the process. These include methods for the estimation of flood peaks, flood hydrographs, and inundated areas. All these variables are typically required in terms of the ‘T-year flood’, although other standards that are used include the maximum recorded flood, probable maximum flood (if such a thing is deemed to exist) or reconstruction of a particular known event such as the 1947 floods. The estimation of peak discharge is perhaps the most common; it is used to determine the height and location of flood defences required for a certain standard of protection. In some cases however an estimate of the whole flood hydrograph is required; this would be the case if the likely flood volume was needed for the design of storage reservoir solutions. Finally, flood risk mapping is increasingly in demand from insurers, planners and flood warning agencies, both to specify the current levels of risk and to allow feasibility assessments of non-structural flood defence measures. These maps may show different variables apart from simply flood frequency (Marco, 1992).

Standardised methods are important in the creation and implementation of national ‘Standards of Service’ which can be used to compare flood defence provision across the country (Birks *et al*., 1992). The concept of these guidelines dates from 1984 when a MAFF working party was set up. This was then followed by a pilot study by the Thames Water Authority in 1986 to set up a ‘Levels of Service’ database. Today the standards are monitored by DEFRA, which uses them in relation to cost:benefit analyses in order to rule on proposed flood defence expenditure. Birks *et al*. (1992) quote the then current target for flood defence provision as being such that 0.5 – 1 houses per km per year (or the equivalent value of other assets) may be damaged by flooding, corresponding to approximately a 50-100 year return period for flooding in residential areas. Today, guidance from DEFRA stresses the more flexible approach taken to flood defence standards, while giving indicative standards of protection as a 50-200 year return period for flooding in residential areas, 5-50 years for high-grade agricultural land (DEFRA, 2000).

1.3.3.1 Estimation of peak discharges using Statistical Methods

When gauged records of flow are available in a catchment, a statistical analysis of peak flows provides a well-established and widely-researched method of estimating frequency characteristics of flood discharge. In the UK, this method is widely used in engineering applications, and guidance is provided by the Flood Estimation Handbook (Robson and Reed, 1999). The method is particularly well-suited to large catchments (> 1000km^2) which are likely to experience significant differences in precipitation across the catchment during a single storm, making the use of flow records more appropriate than rainfall records.

The data required for the statistical analysis is either an annual maximum record (AM) or partial duration series (PDS), the latter being more suitable for record lengths less than 13 years (Reed, 1999). Data series covering the UK are provided by the Institute of Hydrology in both forms (Bayliss and Jones, 1992; Robson and Reed, 1999; Spencer, 2005). In order to interpolate or extrapolate from the recorded data to make an estimate of flood discharge for a particular return period, an extreme value distribution is fitted to the data series (Naden, 1992). Distributions used include those of the Log Normal, Gumbel, Pearson, Generalised Pareto and Generalised Logistic distributions; a summary is given by Kidson (2004). The distribution is fitted using a parameter estimation procedure such as the Method of Moments, the L-Moment Method (Hosking, 1990), or Maximum Likelihood Estimation. There is, however, often no process-based strategy for choice of distribution, leading to different models being officially mandated in different countries, often judged purely on goodness-of-fit (Kidson, 2004; Vogel *et al*., 1993). This may lead to varying estimates of extreme flood magnitudes, none of which include a sound hydrological justification for the extrapolation procedure chosen.

In addition to the empirical nature of the extrapolation procedure, the method has disadvantages in terms of the length of gauged flow series required for accurate estimation of discharges. The Flood Estimation Handbook recommends that a record twice the length of the modelled return period should be used, this would usually be achieved by flood regionalisation: using data from 'donor catchments' close to the site of interest, or hydrologically similar 'analogue catchments'. Although standardised methods for choosing these catchments are provided, there is still a lack of consensus as to the optimal method (Acreman and Sinclair, 1986; Wiltshire and Beran, 1986). It is especially difficult to group ungauged catchments where extreme value behaviour cannot be used as a similarity measure (Reed, 1992). There are also particular difficulties in using a Peaks-Over-Threshold analysis in conjunction with regionalisation methodology (Birikundaugi and Rouselle, 1992).

In order to mitigate some of these problems, historical or paleoflood data may be used in addition to the gauged record (see Section 1.3.1). This data has the potential to substantially extend the record of extreme floods in the catchment, and is therefore of great benefit when estimates of low-frequency events are required, having been shown to reduce both uncertainty and bias in the results of a flood risk assessment (O'Connell *et al*., 2002). Paleoflood evidence may be used to improve the parameter estimates for standard extreme value distribution models, often using the technique of Maximum Likelihood Estimation based on the combined record (Guo and Cunnane, 1991; Martins and Stedinger, 2001; Pilon and Adamowski, 1993; Stedinger and Cohn, 1986). More recently, ideas borrowed from multi-parameter validation strategies have popularised the use of Bayesian methods to incorporate gauged, historical and paleoflood data (O'Connell, 2005; O'Connell *et al.*, 2002; Reis and Stedinger, 2005). Paleoflood data analysis has also provided the stimulus for a critique of traditional flood risk assessment, as a result of often substantial modifications to flood frequency estimates where paleoflood data has been available. In particular, a longer record may identify non-stationarity in the flood-generating mechanism that was not apparent in a shorter gauged record, a finding that would violate the assumptions of the standard statistical analysis (Kidson and Richards, 2005; Thorndycraft *et al.*, 2005). This issue is explored in more detail in Section 1.4.1.1.

1.3.3.2 Estimation of flood hydrographs using Rainfall-Runoff Methods

Using rainfall-runoff methods for the estimation of a design flood discharge or hydrograph provides a preferable alternative to statistical methods when the required return period is greater than 200 years. Often it is possible and desirable to combine the two approaches to achieve an improved estimate. The methodology dates back to work by Eagleson (1972) who recognised the importance of, and provided a technique for using climatic and catchment data to predict streamflow characteristics when flow records were not available. In Britain this is a very useful technique since rainfall records are available for more sites and generally for much longer periods than flow data. Since its conception, the method has been widely used in flood frequency estimation: a summary is provided by Beven (2001b).

Dependant on the data available and the return period of the estimate required, the rainfall-runoff model may be used in different ways. Where the observed rainfall record is long, transformation via the model into flow records allows direct estimation of flow magnitudes. Eagleson’s initial proposal was that the rainfall record could be characterised by probability distributions of storm characteristics, which could then be transformed into distributions of flow magnitudes. This technique allows for extrapolation beyond observed rainfall extremes. In recent years the increasing computing power available has allowed more complex representations of rainfall characteristics and runoff-producing mechanisms, as numerical rather than analytical methods can be used to produce the corresponding flow distributions. The rainfall distributions can be used stochastically to generate thousands of years of simulated rainfall series, which then drive the rainfall-runoff model to produce the corresponding flow series in the same way as observed rainfall series.

There are various reasons for uncertainty in results produced by this method. The results of any application depend on the rainfall-runoff method used. Hydrologists have experimented with a range of different models, from physically-based and distributed models e.g. IHDM (Calver, 1993), to hybrid models such as TOPMODEL (Troch *et al*., 1994), to lumped models such as IHACRES (Steel *et al*., 1999). The Flood Estimation Handbook suggests a simple estimation of the unit hydrograph from existing rainfall-runoff records if available, or from physical catchment characteristics as a last resort in an ungauged catchment (Houghton-Carr, 1999). As well as uncertainty in model type, parameter estimation introduces further challenges as the model is usually calibrated from a selected period of observed data, but is required to make predictions of the catchment behaviour in more extreme climatic states. Finally, as with statistical methods for discharge estimation, when catchment variables such as storm characteristics are fitted with frequency distributions there is uncertainty in distribution choice and fitting method. Despite these problems, rainfall-runoff modelling is the method of choice for many applications involving rare events and may be used for estimates with return periods of up to 5000 years (Reed, 1999).

1.3.3.3 Flood Risk Mapping

Mapping of expected water levels during a flood is often required in addition to discharge predictions. National standards are particularly important when such maps are used for purposes such as insurance calculations, when some properties may even be marked out as uninsurable. An indicative map of flood risk in the UK was drawn up by Morris and Flavin (1996) using a simple hydrological model. This map was used together with further modelling and historical records to produce the Environment Agency’s Indicative Floodplain Extent map of 1999. This is currently being updated to show two area bands: those areas estimated to be flooded in the 1 in 100 year flood, and those at risk in the more extreme 1 in 1000 year flood. It will also show the influences of strategic defences.

In order to create depth mapping, assumptions must be made as to the nature of flows on the floodplain. Usually a rainfall-runoff method such as those outlined in Section 1.3.3.2 is used, together with a hydraulic model. Typically the model is a one-dimensional hydraulic approximation applied to the channel only, such as with the popular computer model HEC-RAS (US Army Corps of Engineers, 2005). The model results can then be used to map water elevations onto a digital elevation model of the catchment. This requires the assumption that the water forms a horizontal surface perpendicular to flow direction; however this may not be the case in short duration events, for high velocity flows with strong dynamic effects, or for shallow braided flows. These types of effects cannot be accounted for without hydraulic modelling of the whole floodplain rather than purely the channel. This type of modelling can be computationally expensive but provides a more accurate simulation of the conditions found in extreme flood events; it also allows the effects of flood defence works to be more easily incorporated.

By extending modelling of flood extent to other variables, many advantages may be gained. Predicted damage from flooding to a particular property can only be rudimentarily estimated from a map of flood extent; flood depth is a more important control that may usually be easily estimated using the same modelling techniques. Depth is typically related to damage by a nonlinear relationship recognising both the relatively minor effects of very shallow floods, and the decreased rate of further damage at very high levels. Where it is possible to use hydraulic modelling of the floodplain, Marco (1992) points to many of the additional benefits to be gained. For example, by mapping flow velocity, danger to life during flood evacuation may be estimated. A map of flood duration may show accumulative damage, for example over agricultural land where crops may be resistant to a short period of inundation, but damaged during a longer flood.

1.4 Updating the Approach to Flood Risk Assessment

Section 1.3 has attempted to summarise the philosophy and aims of flood management strategy in the UK, and the methods of flood risk analysis currently used to provide the data to meet those aims. However, closer inspection shows several areas in which such conventional methods make unwarranted assumptions with regard to catchment behaviour, or fail to provide the flexibility or scope required for modern 'soft' engineering applications. This section presents further detail on some of those shortcomings, and makes the case for a new, process-based modelling strategy. This strategy would use the established principles of continuous simulation as the basis for a coupled model cascade, providing 'End-to-End' modelling of the complete flood generation process.

1.4.1 Non-Stationarity of the Flood Generation Process

1.4.1.1 Changes in Flood Frequency

Section 1.2.2 identified a variety of causes behind the modern experience of accelerated flood risk, grouped into those that reflected climate change (i.e. change in precipitation regime) and those that reflected land-use change (i.e. change in catchment response to precipitation). However, if non-stationarity exists in the flood generation process, this violates a critical assumption of conventional, statistical flood risk assessment; namely that floods occur as independent, identically distributed, random events from a single, stationary distribution. The empirical nature of the distribution fitting procedure, as described in Section 1.3.3.1, does not allow any adjustment based on understanding of trend or quasi-oscillatory behaviour in the climate record.

One consequence of this problem is the lack of a sound methodology by which to allow for the effects of future climate change: non-stationarity of precipitation characteristics threatens the relevance of historical gauged flow and flood records. Despite this, the continuing evidence for climate change as monitored by the Intergovernmental Panel on Climate Change (Arnell *et al*., 2001) suggests that a failure to plan for increases in flood risk could jeopardise the country's ability to cope with future events. As such, a similarly empirical principle, that of allowing for a 20% increase in peak flow in any new flood risk applications (Section 1.2.2.1), has been adopted in order to act on the current government advice to adopt the precautionary principle with respect to flood hazard: ‘Where there are threats of serious or irreversible damage, lack of full scientific certainty shall not be used as a reason for postponing cost-effective measures to prevent environmental degradation’ (ODPM, 2004). The figure of 20% was arrived at after a preliminary modelling study in the Thames and Severn catchments (ODPM, 2004), however in applying this factor arbitrarily throughout the UK without regard to catchment-specific response, any justification for its use based on process understanding is lost. Similar limitations on the ability of the method to account for land-use change are also apparent. Even where future trends in land-use patterns in a catchment may be estimated, the curve-fitting exercise of the flood frequency assessment does not readily allow the inclusion of such knowledge.

1.4.1.2 Flood Risk in New Locations

In addition to changing flood frequency characteristics at sites known to be prone to flooding, climate change (and to a lesser extent land-use change) may cause flood events in locations not previously considered to be at risk. As high intensity storm events increase, the IPCC concludes that small headwater streams especially may demonstrate increased flood activity. This is a particular problem in Britain as there is central control of flood protection and channel maintenance only for sections of channel designated as ‘main river’; headwater streams will generally fall outside of this bracket. Smaller rivers are also less likely to be gauged, and their large numbers make a complete gauging programme infeasible. Therefore flood risk assessments may increasingly need to be made without the traditional advantage of discharge records, forcing the adoption of alternative methods such as flood risk estimates based on precipitation data (Section 1.3.3.2).

Lack of gauged data is also a problem in urban areas which are more likely to be affected by intra-urban flooding in a flashier precipitation regime. The Foresight ‘Future Flooding’ report (Office of Science and Technology, 2004), which aims to inform long-term policy on flood defence, identifies this as a major challenge to future strategy with a possible 80,000 individuals at risk. Damages through intra-urban flooding may be low until the current excess capacity is exceeded, after which damages will rapidly increase. This must be anticipated many years in advance due to the long lead-in time required for major engineering works; for example, replacement of Victorian sewers is estimated to need 10-15 years notice. New strategies will be needed for assessment of risk from urban flooding in order to commission such works in time.

1.4.2 Connectivity of Channel and Floodplain

Despite the benefits described in Section 1.3.3.3 of presenting flood frequency data in terms of flood risk mapping rather than river levels, such a transformation has conventionally been regarded as disconnected from the main task of flood risk assessment. The chief focus of a study has previously been seen as the derivation of discharge or level magnitude for a given set of return periods, with spatial mapping an optional extra. This attitude reflected a reliance on structural flood defence works whose aim was to contain flood flows within the designated channel. As shifts in attitude towards a preference for 'soft' engineering solutions and floodplain restoration have increased requirements for spatially distributed flood risk information, the 1D hydraulic models typically used to study levels within the channel have been extended to provide water elevation mapping over the floodplain. A widely-used example of this is the 'GEO-RAS' add-on to the channel model 'HEC-RAS' (US Army Corps of Engineers, 2005) which enables water level output from the channel model to be draped over a terrain model of the surrounding area. This typifies the simplistic view of the role of the floodplain implicit in such a modelling strategy: the floodplain is seen purely as a storage reservoir and water movement over the floodplain as the river reaches bank-full and out-of-bank stages is not seen as an integral part of the floodwater transport mechanism. The view mimics the disconnection of channel and floodplain which has occurred where structural flood defence measures have been employed.

Contrary to the assumptions behind the view of a floodplain disconnected from the river channel, flood defence circumvention or failure during extreme events has demonstrated that these two areas function together as a coupled system during times of flood. Water is routed downstream as the floodplain assumes a transport as well as storage capacity.

Where paleochannels exist these often become active; in other cases where natural routes have been blocked by urban development then strong flows may occur even through built-up areas. It is here that deficiencies in the hydraulic approximations made by a 1D model become apparent. Firstly the model is unable to properly represent the lateral flows between the river and the floodplain. Being extremely dependent on the cross-section survey locations used to create the channel structure, the true shape, width variations and sinuosity of the channel is unlikely to be fully captured. Further to this, the 1D format cannot account for the pressure gradients which force water flows at highly variable rates between the two areas. Secondly, once water has reached the floodplain, the model cannot properly route flows through complex terrain. An urban environment presents a multitude of obstacles to flood water which cause a complicated response differing greatly from a 'basin-fill' scenario. Barriers and constrictions cause the creation of preferential pathways for water transport, while other areas are protected from the greatest water depths. The increased expectation of flood flows through urban areas, due to changes in flood defence strategy, leads to a requirement for flood risk mapping based on 2D models which couple channel and floodplain flows and provide a dynamic representation of water transport on the floodplain in order to overcome these difficulties.

1.4.3 End-to-End Modelling: A Process-Based Continuous Simulation Methodology

In order to address some of the deficiencies in standard flood risk assessment (FRA) techniques which have been outlined in the previous section, this thesis proposes a preliminary structure for a modern FRA methodology which seeks to include the benefits of the latest modelling techniques. These may previously have been used in research exercises but before now have rarely been seen as appropriate for wide scale application. The requirement to combine such techniques in an efficient and practical way is an important theme of the study.

A critical criterion for the structure is that it should embody a process-based approach to FRA. This greatly increases the predictive power of the system: it is only with a correct representation of dominant process that the model may be expected to react correctly to novel input and boundary conditions, a point emphasised by Oreskes and Belitz (2001). The use of a process-based approach also allows the structure and parameters of the system to be modified to reflect knowledge of changing conditions of climate and land-use, a vital attribute for a modern FRA technique which will be used in a period of changing climate regime and catchment response. In order to achieve this, the FRA structure is underpinned by the technique of continuous simulation. This was introduced in Section 1.3.3.2 as part of the discussion on the use of rainfall-runoff models as a replacement for statistical flood frequency analysis.

Continuous simulation uses the available precipitation record for the catchment as a basis for creation of long synthetic rainfall series typical of those experienced by the catchment. These series are used as input to a rainfall-runoff model to produce the corresponding discharge series, from which extreme event frequencies may be calculated explicitly. An important advantage of the method is that it provides continuous soil moisture accounting which gives implicit consideration of antecedent wetness conditions in the catchment. The stochastic generation of the rainfall series is achieved by creating frequency distributions for a variety of rainstorm characteristics such as duration, mean intensity and time between storms. Where the historical record is not felt to fully capture the possible range of catchment behaviour, the empirical distributions may be fitted using a standard distribution or be modified by the addition of an upper tail. The rainfall series is then created by sampling randomly from the distributions. Many variations on the method exist; these are explored more fully in Chapter 4. Using this flexible method, climate change might be represented via a modification of the rainfall frequency distributions, land-use change by a modification of the rainfall-runoff model structure or parameters, such as an increase in runoff coefficient. Although the method of continuous simulation is not new, and it has previously been used to forecast the discharge magnitude of extreme floods (Cameron *et al*., 1999), it has not been considered suitable for integration into the standard FRA framework due to the computational overhead required. However, by using a relatively simple rainfall-runoff model, it proves to be a practical and valuable tool.

The new structure is also defined by its integrated, ‘End-to-End’ approach to FRA. As management plans become catchment- or basin-wide in their scope, so too should FRA methods be spatially and temporally ambitious. It is clear to the observer that no part of the catchment acts in isolation, and the process-based approach attempts to replicate this connected system through a cascade of coupled models representing precipitation regime, rainfall-runoff characteristics and floodplain inundation behaviour. As such, discharge estimates from the continuous simulation of runoff are used to drive a 2D model of floodplain hydraulics which aims to simulate the dominant behaviour of the floodplain as a dynamic system with a key role in the control of flood behaviour. By using a 2D model which couples channel and floodplain behaviour, many of the limitations outlined in Section 1.4.2 are overcome. The advantages of the particular choice of inundation model are explained more fully in Chapter 5, however amongst them is the opportunity to benefit from new, high-resolution elevation data which provides an explicit topographical boundary condition for the model. By enabling 2D urban flood modelling with extremely low grid sizes, the accuracy required to properly capture flow dynamics within the built environment may be achieved. A spatially distributed flood forecast available at high resolution also paves the way for additional modules for vulnerability and damage assessment, calculating social and economic impacts of floods, for example using information on building use or value (Apel *et al*., 2004; Merz *et al*., 2004). In the UK a simple way to access such information might be through ties to a postcode database.

Finally, the aspiration to produce an ‘End-to-End’ modelling structure is also important in order to include uncertainty estimation as an integral part of the FRA procedure. Uncertainty cascades through any FRA system as outputs from one component go on to become the input or boundary conditions for the next. By treating the procedure as a coupled system, it may be run within a proven uncertainty estimation framework (further details are given in Chapters 4 and 7).

1.5 Conclusion

This introductory chapter has sought to set flood risk assessment in both its historical and contemporary context. Firstly, the underlying phenomenon, flooding itself, was examined. The causes which provide the forcing factors behind flood risk were set out, with examples of recorded flood events resulting from each. This provided the background for a discussion of flood risk today, which is widely perceived as an increasing threat. Possible reasons for such a rising trend were considered, broadly categorised into those relating to climate change and those relating to land-use change.

In a society increasingly concerned by the threat of flood inundation, flood risk assessment is an essential tool to enable emergency and strategic planning. Section 1.3 examined the conventional methods used to carry out such an assessment. These methods were found to be strongly influenced by the use to which the results of any estimate of flood frequency would be put. An important part of this section was therefore a look at the type of flood prevention and mitigation measures typically used in the UK. In recent years, understanding of the need to manage flood risk at a catchment or basin scale, integrating economic, social and environmental concerns, has led to a step-change in flood defence strategies from structural to non-structural solutions. This has in many cases left behind the standard methods of flood risk assessment, which are no longer able to provide the information needed to plan and implement such solutions.

Section 1.4 examined in more detail some of the reasons behind the inability of standard flood risk assessment methods to adapt to today’s demands. In particular, the lack of a process-based approach was identified as a major limitation which left the system unable to respond to non-stationarity in the flood generation process. In addition, the disconnection of channel and floodplain in the modelling process was particularly damaging to the system’s usefulness in assessment of spatially dispersed flood mitigation measures. These problems led to the identification of a need for a contemporary, flexible, flood risk assessment structure, able to take advantage of recent improvements in data availability and modelling techniques to meet the diverse demands of a modern catchment management plan.

1.6 Structure of the thesis

The preceding discussion of conventional methods of flood frequency analysis, together with a critical analysis of their ability to deliver the data required for contemporary catchment and flood management plans, led to the conception of a modern structure for flood risk assessment. This thesis aims to establish such a system, using a case study catchment to test and demonstrate its ability to perform under the typical conditions of a lowland UK catchment. The thesis falls naturally into three parts:

Part I: Hydrological Setting for the Study

Part II: Component Model Development

Part III: ‘End-to-End’ Flood Risk Assessment with Uncertainty

The objective of **Part I** is to set the study in context. **Chapter 2** does this from a methodological perspective, examining the current and evolving themes in hydrological research which have provided the stimulus for a modernisation of the flood risk assessment procedure. These include the effects that increased data availability has had on hydrological modelling, the emergence of process-based modelling, an acceptance of uncertainty leading to the rejection of deterministic forecasts, and the increased emphasis placed on providing hydrological forecasts in an accessible format.

Chapter 3 provides the context for the thesis in terms of the study catchment. The essential part that field data sets play in hydrological modelling is highlighted in Chapter 2, and this chapter provides details of data availability in the catchment and additional information collected through fieldwork. This includes both flow gauging and the collection of point inundation data through a survey of residents. It also provides a physiographical, climatological and hydrological review of the catchment. Finally, the methods and outcome of previous modelling of the catchment is examined.

Part II details the development of the three component models which go on to make up the coupled flood risk assessment system. The first of these is the stochastic rainfall series generator described in **Chapter 4**. Different methodologies for rainfall simulation are reviewed, and a profile-based method is chosen. The gauged rainfall series from the catchment is then processed and used to create simulated series using two variants of the method. These are evaluated in their ability to reproduce statistics of the catchment rainfall regime.

The continuous simulation methodology requires that the simulated rainfall series should form the input to a rainfall-runoff model which predicts the associated river discharge. **Chapter 5** describes the choice of rainfall-runoff model, together with detail of model structure identification and parameterisation, using both Environment Agency gauged data and that collected during fieldwork. It also introduces the Generalised Likelihood Uncertainty Estimation (GLUE) philosophy, used to support a set theoretic approach to model structure and parameter choice, and to estimate uncertainty in model output. The results of the rainfall-runoff modelling exercise are produced in terms of this probabilistic approach.

As the final part of the chain of coupled models, **Chapter 6** describes the floodplain inundation model. The benefits of using reduced-complexity techniques for high resolution floodplain modelling are discussed, and the model structure is described in detail. Developments to the model to ensure numerical stability and correct model functionality at small scales are described. A method to enable the incorporation of sub-grid scale information, one of the themes discussed in Chapter 2, is established. The chapter then describes the model application to the study catchment, including calibration and multi-criteria validation of the model. Model performance is compared across scales and the value of sub-grid scale information is assessed.

Part III synthesises the results of the three chapters of Part II to create, apply and assess the ‘End-to-End’ modelling framework for flood risk assessment. **Chapter 7** first gives a detailed explanation of the framework, discussing issues of efficiency and data preparation. The framework is then applied to produce a flood magnitude and inundation frequency analysis for the study catchment, with integral estimation of the predictive uncertainty in the results. The role of uncertainty estimation in the risk assessment is then considered further with an attempt to quantify the relative magnitude of uncertainty originating from different aspects of the system, and therefore the opportunities to constrain such uncertainty.

Finally, **Chapter 8** concludes the thesis by assessing the success of the study in establishing a modern, rigorous and efficient framework for flood risk assessment, together with a summary of achievements in terms of methodological improvements.

Part I

HYDROLOGICAL SETTING FOR THE STUDY

Chapter 2

NEW DIRECTIONS IN FLOOD FORECASTING

Abstract

This chapter aims to summarise the current and evolving themes in hydrological research which have provided the stimulus and direction for this thesis. First, the characterisation of recent years as a new 'data-rich' age of hydrology is discussed, including the relationship between data availability, hydrological understanding and refinements in model process representation. It is the availability of high-resolution remotely-sensed topographical data sets which has enabled development of floodplain inundation models capable of simulating flow through complex urban environments. Consideration is given to conflicts which can occur between spatial data availability for different hydrological variables, leading to possible bias in process representation or calibration strategy.

High resolution spatial data sets encourage the use of distributed, process-based models; however these models are often highly scale-dependent. Section 2.2.2 examines the difficulties associated with the use of 'effective' parameter values where it is not possible to measure quantities at the model grid scale. Another important theme is that of reconciling the availability of extremely high resolution data with the scales required to retain efficient model performance; this leads to consideration of sub-grid variability.

The difficulties of deterministic specification of model structure and parameterisation, in the face of limited data for calibration or validation, are discussed in Section 2.3. Increasing acceptance of the necessity of probabilistic forecasts has resulted in methodological frameworks which accept uncertainty in all aspects of model deployment, such as the GLUE method which is outlined here and later used in Chapters 5 and 7. Finally, the challenges of communicating the strengths and weaknesses of current modelling and uncertainty mitigation strategies, both within the hydrological community, and to a wider audience, are considered in Section 2.4.

2.1 A Resource-Rich Age?

2.1.1 A Spatial Revolution

The advent of remote sensing has brought about a spatial revolution in hydrological data and has precipitated a change in focus in catchment modelling. Historically, data collection methods tended to bias records towards at-a-point temporal patterns. These records naturally lent themselves to models lumped at the catchment scale, and provided only limited support for distributed hydrological modelling. In order to use point input measurements such as gauged rainfall depth, interpolation or extrapolation was required. Similarly, point validation data typically only measures bulk catchment response such as river discharge and cannot be used to distinguish correct spatially-distributed process representation. Today, however, Bates (2004) suggests that availability of remotely-sensed data has ushered hydrology into a new ‘data-rich’ age where distributed data highlights the importance of spatial variability and models are redesigned to take full advantage of the data influx. Grayson and Bloschl (2000c) explore many of the same themes and discuss their consequences for model structural design. They demonstrate the consequences of assumptions of spatial uniformity by comparing the runoff simulations in two implementations of the THALES model, one assuming a random soil moisture deficit field, the other organised by wetness index. Very different responses to rainfall inputs were observed in the two cases (Figure 2.1).

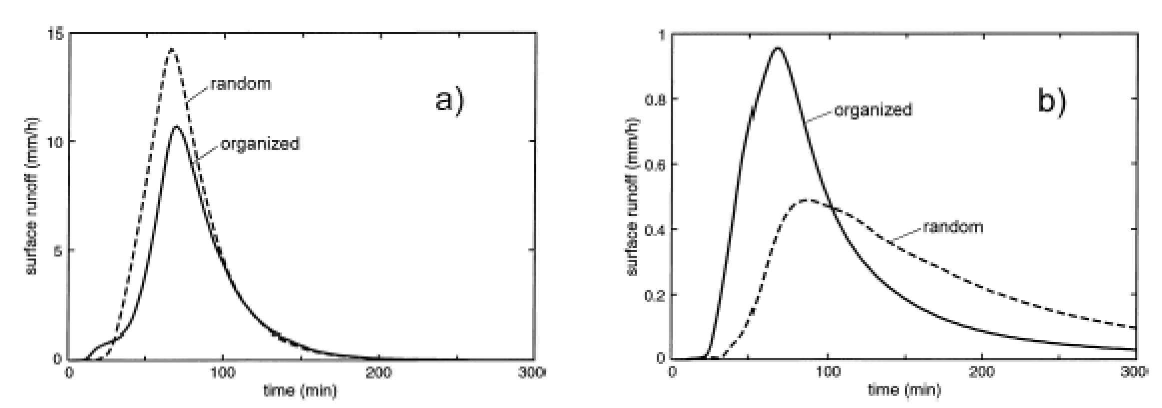

Figure 2.1: Runoff simulations using the Thales model with both random and organised saturation deficit scenarios, for a rainfall event of (a) 30 mm and (b) 5 mm over 1 hour. From Grayson and Bloschl (2000c).

One of the most common forms of data made available by new remote sensing techniques are digital elevation models (DEMs) of the land surface. Previous such datasets were coarsely obtained by interpolation from digitised contours or aerial photogrammetry. These techniques have been replaced by collection via airborne laser altimetry (LIDAR) or interferometric synthetic aperture radar (INSAR), either airborne or from satellite. These new methods allow large scale collection of data at very high horizontal spatial resolutions (0.5 – 2 m) and high vertical precisions of the order of 10^{-1} m. Amongst other applications, DEMs may be used explicitly within a hydrological model as a topographic boundary condition, or to derive other variables such as slope, aspect or wetness index. These now ubiquitous DEMs have been seen as a major catalyst in the increasing awareness of the importance of spatially-distributed data (Dietrich and Montgomery, 1998; Grayson and Bloschl, 2000c).

Remote sensing does not only provide elevation mapping; it has provided important techniques for collection of many other variables (Schmugge *et al*., 2002). The LIDAR and SAR measurements may, in addition to collection of elevation data, be used to determine vegetation types and land cover (e.g. Kasischke *et al*., 1997; Moffiet *et al*., 2005), soil moisture (Pauwels *et al*., 2001), snow cover (Andreadis and Lettenmaier, In Press) or flood extent (Bates and De Roo, 2000; Frappart *et al*., In Press). The collection of precipitation information, vital for rainfall-runoff modelling, has been transformed by the emergence of ground-based weather radar. Data from these instruments allows distributed rainfall mapping with resolutions of 2 – 4 km, relaxing the traditional dependency on discrete rain-gauge sources and offering the prospect of real-time distributed measurements over large catchments (Collier, 1999; Schultz, 1988).

Despite the profound effect that remote sensing has had on hydrology, it might be argued that this has been only a ‘partial’ data revolution, due to conflicts between the extent to which spatial data is available for different hydrological variables. While the impact has been strongest on systems dominated by surficial processes (e.g. hydraulic systems, runoff production systems in steep catchments), remotely sensed data has proved less valuable for subsurface model development where characteristics are not measurable from the air. The inaccessibility of key data required to establish process descriptions, parameterise and validate such models is highlighted by Anderson *et al*. (1996) in their review of data capture issues. Subsurface water storage and water flows are an essential part of a full description of catchment behaviour, yet these are conditioned on soil structures and bedrock topography that is not readily apparent from the surface (Freer *et al*., 2002). Although techniques for subsurface remote-sensing are being developed, such as ground-penetrating radar (Knight, 2001), they currently lack the essential capability to capture small-scale heterogeneity and structural features. For example, it is not yet possible to map macropore distribution within soil layers, and yet these provide preferential flow pathways which are a significant contributor to storm flow (Flury *et al*., 1994; Freer *et al*., 2002; Shakya and Chander, 1998).

As well as underground structures, there are also surface features which are difficult to quantify remotely. For example, channel morphology is not usually well represented in DEMs, which may lack definition of fluvial features e.g. bars and banks, and of the channel/floodplain boundary (Dietrich and Montgomery, 1998). Difficulties are also compounded where valley slopes are shallow and therefore drainage directions may not be portrayed accurately, or may lie below the resolving power of the data acquisition method. It may be tempting to ignore the loss of these features and treat the DEM as a complete representation of the landscape, however they can provide important controls on floodplain flows.

In some cases, an inaccessible variable required for understanding of process may be estimated using a surrogate variable which it is easier to measure using remote sensing; Grayson and Bloschl (2000b) provide a brief review. Again the ease of collection of DEMs means that they are a popular source of information, and there are many examples of the use of surrogate terrain indices such as calculation of contributing areas to enable channel definition (Rinaldo and Rodriguez-Iturbe, 1998) or use of topographic soil indices to infer the spatial pattern of water table depth (Famiglietti and Wood, 1994b). Indices not based on terrain include pedotransfer functions which are commonly used in soil science, to translate more easily obtainable measurements such as soil type and texture into hydraulically useful properties such as saturated hydraulic conductivity (Islam *et al*., In Press). Other examples include the use of vegetation types from LANDSAT Thematic mapper data to estimate evapotranspiration rates (Chen *et al*., 2005), and water quality measurements using water reflectance properties to estimate suspended sediment and other pollutants (Schmugge *et al*., 2002).

2.1.2 An Empirical Science

New remotely sensed data streams have reshaped hydrologists' understanding of spatial variability in surficial catchment processes and hence their representation via hydrological models. Subsurface understanding has been correspondingly slower to develop due to reduced availability of high resolution spatial data. This understanding, vital to the development of hydrological theory, is what is referred to by Beven (2001b) as a 'perceptual model' of the catchment. Without the constraints of mathematical formulation, and guided by each individual's study, data analysis and field experience, the model encompasses knowledge of the different hydrological processes at work, their relative importance and interactions. The development of the perceptual model has been recognised as an important first step preceding further hydrological work, and has been the subject of detailed local investigations in study catchments (e.g. McGlynn *et al*., 2002; Ocampo *et al*., In Press). Differences in the perceptual model will lead to different strategies for modelling the catchment, as demonstrated by Botterweg (1995) who compared differences of calibration of a hydrological model by two independent users given the same input data, due to their different understandings of the system.

The completeness of the hydrologist's perceptual model is, however, generally limited by the availability of good field data sets. Despite recent advances, it is often impractical or impossible to collect comprehensive data on hydrological variables at time-scales appropriate to catchment-scale processes. Yet in spite of these difficulties, such information is vital in order to shape understanding of catchment behaviour and response to hydrological events. Silberstein (In Press) questions whether data collection is still necessary in an age where computer models of catchments are becoming increasingly complex, but concludes that without underlying data these models are little more than 'computer games'. Dunne (1982) and Klemes (1986) have called for modellers to work more closely with field hydrologists to ensure model results are backed up by sound data to avoid giving the appearance of hydrological knowledge where it is not justified. Hornberger and Boyer (1995) also conclude that despite advances in modelling, future progress will be reliant on new data and new experimental work. The same sentiment has been echoed by many others (Anderson *et al*., 1996; Bencala *et al*., 1993; Beven, 2001b; PUB Science Steering Group, 2003).

The search for a better understanding of a particular catchment process is therefore often a force for the collection of further data. Developments in theoretical models have guided the investigation of catchment response and generated new areas of ‘data capture’ in their exceptional demand for data for floodplain development and process operation understanding (Anderson *et al*., 1996). In some cases the data demand is too high for collection across the whole catchment, and instead the conceptual model may be built from localised investigation of processes in a subcatchment (Bormann *et al*., 2005). This is particularly the case at small scales where the heterogeneity of the catchment makes complete knowledge of catchment properties impossible. Hydrological advances continue to be reliant on such techniques for improving methods of data collection, information extraction and subsequent model conditioning, and hence hydrology remains very much an empirical science.

2.2 Emergence of Process-Based Modelling

2.2.1 Using catchment understanding to inform model structure

The improving availability and coverage of spatial data has both driven and been driven by developments in distributed, process-based modelling. Historical time series data of integrated variables measured at a point were most easily incorporated into models which were lumped at the catchment or basin scale. Now, where spatially-distributed measurements of catchment form and process are available, these encourage the incorporation of process understanding in model structures. This may range from a relatively simple decomposition of the catchment into hillslope and channel elements, to an attempt to produce a fully distributed model incorporating all the known surface and subsurface processes in the catchment. This latter aim was first described by Freeze and Harlan (1969) in their *'Blueprint for a physically-based digitally simulated hydrological response model'*.

A more recent popular alternative to such spatially explicit methods is distribution function modelling. Here a hydrological similarity index is used to group dispersed locations by hydrological behaviour, assigning each landscape parcel to a conceptual 'Hydrological Response Unit' (HRU). The advent of geographical information systems (GIS) has allowed easy identification of such HRUs based on maps of soil type, vegetation classification, geology, etc. Popular examples of distribution function models include the Probability Distributed Moisture Model (PDM), which extends the concept of lumped storage rainfall-runoff models to allow a probability distribution of different storage capacities throughout a catchment (Moore and Clarke, 1981), and TOPMODEL (Beven and Kirkby, 1979) which uses a topographic index to generate a probability distribution function of soil moisture deficit and hence to determine variable contributing areas within a catchment.

The relationship between catchment understanding and model structure is a two-way process. Patterns in the landscape and process identification through field experiment will guide the choice of processes to be included or excluded from a model structure, or the level of detail at which they are modelled. In turn, sensitivities shown by the model towards structural choices and parameter values will add to process knowledge (Grayson and Bloschl, 2000a). Also included in this cycle is the collection and processing of data; for example data interpolation methods may be guided by the identification of a spatial organisation in the underlying controlling process. Grayson and Western (1998) consider the benefits of using modelling results to refine sampling strategies by investigating the existence of parts of the landscape which consistently exhibit 'mean' behaviour in terms of soil moisture status. These sites may then be used to reduce sampling commitment in the future by allowing an accurate estimate of catchment mean soil moisture from a small number of locations (Figure 2.2)

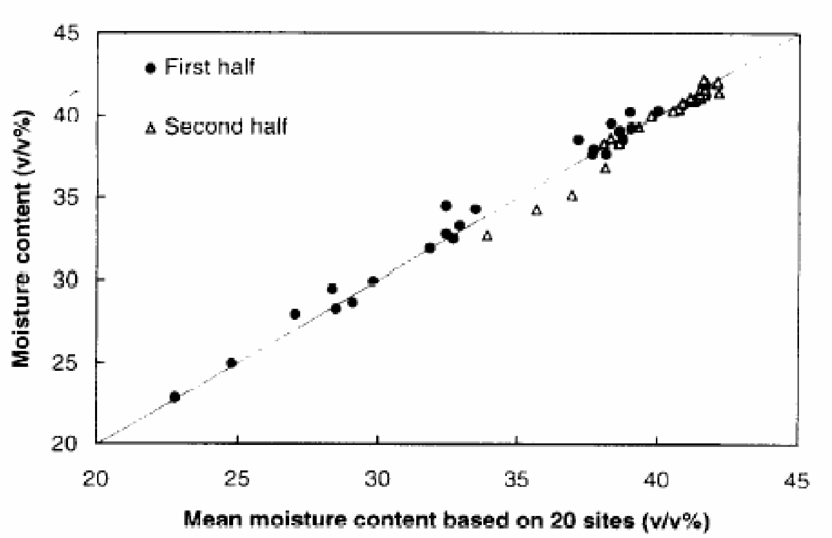

Figure 2.2: Catchment average moisture content for Tarrawarra versus values estimated from 20 sites identified as exhibiting 'mean' behaviour. From Grayson and Western (1998).

2.2.2 Model Scales

2.2.2.1 Process and Parameter Scale Dependency

One important aspect of perceptual models is that they are usually scale dependant. The dominant processes identified in the catchment will change according to the scale of the system considered. The choice of scale acts as a filter on our view of the catchment (Woods, 2005). This is often referred to as the *'scaling problem'* in hydrology: what is the relationship between spatial variability, scale and the governing description of hydrological processes? A change in prevalent process may occur within the same underlying mechanism, for example Lane *et al*. (1997) discuss the different processes controlling sediment yield at various scales, from overland flow processes at the plot and hillslope scale, through gully erosion and channel processes at the sub-watershed scale, to rainfall coverage and transmission losses at the watershed scale. Similarly, Hopmans and Shoups (2005) consider the dynamics of soil water flow; they identify three characteristic scales at which different processes dominate: microscopic pore scale, local scale and regional scale. Woods (2005) gives a summary of the nested characteristic patterns in variables including climate, soils, geology, vegetation and topography, and identifies interactions between time and space scales.

Hydrological models are typically developed for a particular spatial and temporal scale, to facilitate the choice of process representation. Once these choices have been made, the model may be unsuitable for rescaling. For example, if subsurface flow has been represented as soil matrix flow using Darcy's equation for small spatial scales, the model would not be appropriate at the catchment scale where macropore flow dominates. It would therefore need to be reformulated rather than simply scaled up. For a larger scale model there may need to be a change of parameters, state variables and even fundamental equations. An example of the first is given by Yu and Lane (2006a) who examine the effects of mesh resolution on the performance of a two-dimensional diffusion wave model of flood inundation. They find that model response in terms of inundation extent and timing displays strong sensitivity to mesh resolution, and demonstrate the need for recalibration of the effective roughness parameter 'Manning's n' in order to retain simulation accuracy when validating against observed data (Figure 2.3).

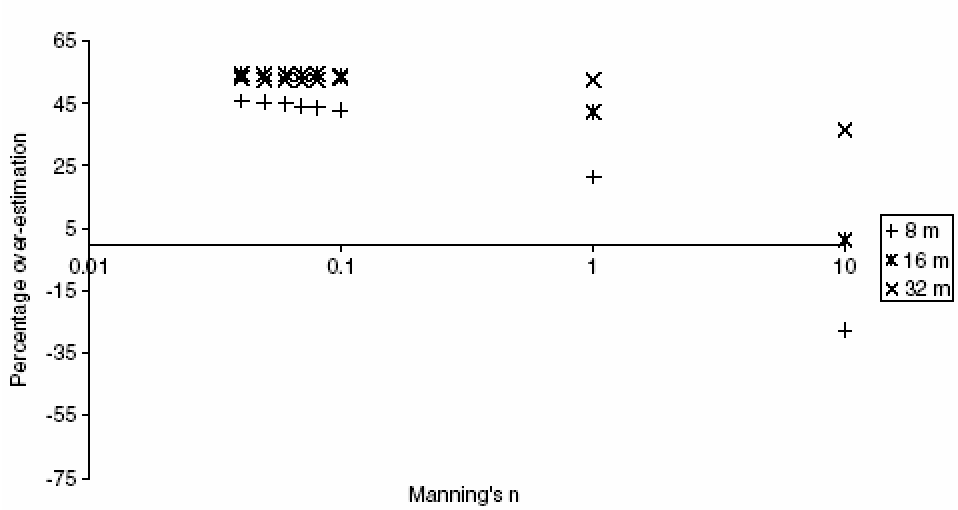

Figure 2.3: Relationship between Model Grid Scale and Value of Calibration Parameter Manning's n in terms of Percentage Over-Estimation of Inundated Extent. From Yu and Lane (2006a).

Questions remain as to the appropriate methods of integrating and representing effects from different spatial and temporal scales in catchment scale or macroscale models. One approach that is often used involves the use of a nested structure of models with appropriate aggregation/disaggregation transfer functions linking these (Famiglietti and Wood, 1994a; Famiglietti and Wood, 1994b; Sivapalan and Wood, 1987). In response to these uncertainties, Sivapalan (2005) calls for development of a unifying theory of hydrology at the catchment scale. This theory would aim to recognise that macroscale response is a function of currently poorly-understood interactions and feedbacks between small-scale processes; that apparently simple measured responses may result from the combination of multiscale heterogeneities.

In some cases it is necessary to use model parameters that have been measured or calibrated at a different scale. This might occur when outputs from models at different scales need to be combined (Bloschl, 2005), or when responses from catchments at different scales are used together in the context of hydrologic regionalisation (Gupta and Waymire, 1998). Alternatively the problem may arise where laboratory or field measurements of parameters have been made at the point scale, but a model requires a parameterisation at a grid-cell or catchment scale. In this case the parameters required by the model are euphemistically termed 'effective parameters'. If the small-scale variation of the process is known completely then it may be possible to calculate the scaling relationship giving rise to the effective parameters deterministically; however typically an approximating function is used. The complexity of this function would depend on the nonlinearity of model process equations relative to the input fields, the spatial autocorrelation and scaling properties of the fields, and the extent of model spatial interaction (Wigmosta and Prasad, 2005; Wood, 1998). Alternatively the parameter values may be determined empirically, using flux matching methodology (Raupach and Finnigan, 1995).

2.2.2.2 Sub-grid variability

The choice of a model scale often brings with it the question of representation of sub-grid variability. In some cases the scale will have been chosen to incorporate the finest measured heterogeneity; however more often the choice of scale will reflect limitations in data-handling capabilities, especially when applying models over large areas. In the latter case there will be catchment information available that would not be captured by using a mean or effective parameter value for each model cell.

Various approaches to sub-grid variability have been suggested. Wood *et al*. (1988) outlined the concept of a representative elementary area (REA); a scale beyond which continuum assumptions could be used without explicit knowledge of the true patterns of variables such as topographic, soil, vegetation or rainfall fields. Therefore by running a model at a scale larger than the REA, typically quoted as around 1 km^2, the patterns of sub-grid variability would not need to be explicitly accounted for. Their experimentation was in runoff production; it has also been repeated for runoff ratio (Wood, 1995) and evaporation (Famiglietti and Wood, 1995). However as Beven (1995) noted, although the trials demonstrated the insensitivity of the model to sub-grid pattern, the macroscale parameters may still need to be adjusted to take account of the distribution of characteristics at the sub-grid scale. A similar attempt to identify a critical scale has been made in geomorphology with the concept of the ‘fundamental hillslope’ (Dietrich and Montgomery, 1998; Montgomery and Dietrich, 1992) which is defined as having no organised persistent convergent areas within it. It is the scale where smaller areas could not generate sufficient overland flow to initiate surface erosion (Horton, 1945).

Where the qualities of the model render sub-grid variability important, it is sometimes possible to adapt the model or model parameters to use some of the information content carried in the variability, without the full cost of using a higher resolution model application. This technique aims to improve on the more usual assumption of uniformity of parameters below grid size. Often it is done using a distribution function method, using the assumption that spatially distributed description of subgridscale variability can be replaced by simpler statistical representation (Famiglietti and Wood, 1994b; Grayson and Bloschl, 2000c; Liang *et al*., 1994). An alternative method is to use the complete spatial pattern but under simplified process assumptions. For example, Koster and Suarez (1992) model the land surface boundary within one cell of a General Circulation Model (GCM) by using a tiling of smaller gridsquares of different vegetation types, each using a simplified form of the energy balance equation. In some model structures such as TOPMODEL, which use similarity theory, questions still remain as to the best way to incorporate sub-grid variability. When using a distribution function, a decision must be made as to the likely nature of the variability and hence the most appropriate representation. In the simplest cases it can be treated as a random variable characterised by its covariance. However, it is important to draw a distinction between 'organised' and 'disorganised' variabilities; an organised variability being one that shows identifiable patterns, demonstrating feedback with other hydrological variables. Kirkby (2005) gives the example of organisation in sediment and solute processes which, through changes in landscape form, shape the hydrological response of the catchment to precipitation, but are themselves strongly affected by the form of flood hydrographs. In cases where organisation of variabilities is shown to exist, a more complex representation of sub-grid variability may be appropriate, together with a larger-scale REA (Bloschl, 2005; Shuttleworth, 1988).

A number of studies have examined the effects of including information on sub-grid variability on modelling results, concluding that inclusion often results in significant changes in predictions. Freeze (1980) compared a stochastic model of rainfall applied to heterogeneous and homogeneous representations of a hillslope. He found significant differences in the runoff predicted by the two representations and stated that distributions of hydraulic conductivities should be included in the model. Wood (1997) examined the effects of using simplified lumped or distribution (statistical) models versus a fully distributed model on the estimated value of the average evaporative fraction parameter. He found that the information included in the statistical model was sufficient to provide a good match to the fully distributed model, however the lumped model produced poor results, tending to overestimate evaporation in low atmospheric demand conditions while underestimating it in high demand situations (Figure 2.4).

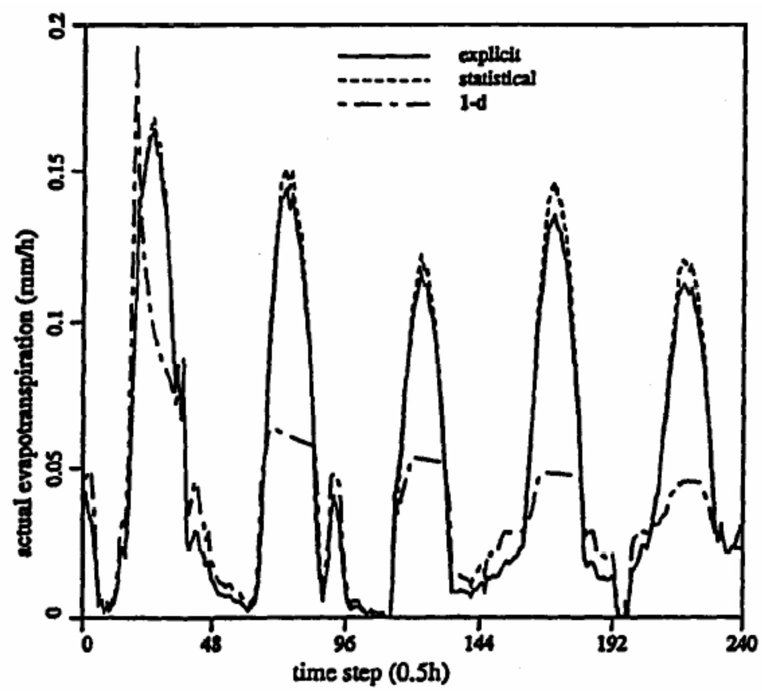

Figure 2.4: A comparison of three models for predicting actual evapotranspiration. (1: explicit) A fully distributed model in which the spatial patterns of the soil-topographic parameters and rainfall are preserved; (2: statistical) A macroscale, distributed model in which the spatial variability in the soil-topographic parameters is accounted for statistically; (3: 1-D) An aggregated, one-dimensional model in which parameters and inputs are spatially constant at their average values.

The advantages of including sub-grid scale topographic information within a 2-D raster floodplain inundation model are explored in detail in Chapter 6. Traditionally, hydraulic models have used a 'roughness' parameter, Manning's n, which subsumes the combined effects of topographical blockage and turbulence production, and hence must be considered as an effective parameter which cannot be calculated directly from the physical properties of the land parcel. Instead, the use of sub-grid scale information provides an opportunity to represent explicitly the effects of complex topography on flow pathways without the penalty in terms of computer time and data storage which would be incurred by running the full model at the higher resolution.

2.2.3 Balancing Data Capabilities and Requirements

The process-based models that have emerged through the partnership of improved hydrological data sets and improved catchment understanding are hungry for distributed data for both calibration and validation. A typical situation arises when a distributed model has been created through availability of a particular high-resolution data set such as a DEM. The model then requires distributed information on other processes, which may not be available. For example, Famiglietti and Wood (1994b) commented on this problem when using a distributed soil-vegetation-atmosphere transfer (SVAT) model which then required distributed water table depths. Grayson and Bloschl (2000a) describe the importance of considering interactions between processes when choosing the conceptual model, as the hydrologist cannot model a detailed process which depends on an unmodelled one. Where such a lack of data occurs, a common response is to impose spatial uniformity of parameters or processes. However this may bias process control to the datasets which do exist (Grayson and Bloschl, 2000c), and typically results in poor performance at internal data sites not used in calibration (Refsgaard, 1997).

When a model has been calibrated, further data is needed for verification or validation. Some dispute the concept of model validation, seeing models as embodiments of hypotheses which cannot be proven or validated, only tested or invalidated through comparison with measured catchment responses (Konikow and Bredehoeft, 1992; Silberstein, In Press). Beven (1993) describes this process as model conditioning rather than validation. Whatever philosophical view is taken towards this process, there remains a requirement for additional field data in order to carry it out. The problems of collecting validation data at proper time-space scales mimic those encountered during the collection of calibration data. Further problems may occur if, for example, extrapolation across scales has been carried out in parts of the modelling process, leaving validation data at a different scale to that at which the model is operating (Wigmosta and Prasad, 2005).

Consideration must also be given to the computational effort that may be required when complex, process-based models are run at high resolutions. Dietrich and Montgomery

(1998) highlight the mismatch that can occur between availability of input data and the resources available to process it within current modelling frameworks. In some cases solutions to this type of problem may be found in the use of sub-grid variability (Section 2.2.2.2); this will be explored further in Chapter 6.

2.3 An Acceptance of Uncertainty

2.3.1 Realisation of Uncertainty

The preceding discussion has outlined the increasing use of process-based models as distributed hydrological data sets have become more widely available. It has also emphasised the many choices that exist as to which processes occur in the catchment, which should be included or emphasised within the model structure, and at which scale the model should be run. As different hydrologists come up with their own answers to these questions, hundreds or even thousands of different hydrological models are created, calibrated, and used in theoretical or practical applications. Just a few of the most popular are summarised by Singh (1995).

Although many of these models have been optimised for use in a particular situation, it is undoubtedly true that in most applications, there are a variety of different models that could be used to provide adequate answers. Often, it would be hard or impossible to identify an 'optimal' model to be used, and yet each model may provide a different interpretation of catchment processes, and so differing predictions in future hydrological scenarios. This question itself hides the dual choices of model structure and parameterisation, which may each independently change the model representation of the catchment at different levels in the hierarchy of decisions required to fully specify model function. This type of situation has increasingly led hydrologists to question the acceptability of making deterministic predictions where no indication of uncertainty in the outcome is given. An engineering application where model choice or parameterisation makes little difference to predicted outcome may deserve a very different treatment to one in which the outcome is highly uncertain, even if both have the same 'best estimate' values.

The realisation that deterministic predictions may not always tell the 'whole story' leads to questions on the role of uncertainty in the modelling process. Here we use 'uncertainty' as a specialist term, in contrast to the colloquial understanding, meaning the absence or lack of information on prior probabilities and the likelihood of particular outcomes (Kundzewicz, 1995). What are the sources of uncertainty, how can these be measured and if possible constrained? These questions are considered in some detail in the following sections.

There is a fundamental difference of opinion on the nature of uncertainty in hydrology. Kundzewicz (1995) poses the question as ‘Is the world deterministic?’ - could uncertainty eventually be removed through improvements in the monitoring and measuring program or is a representation of nature necessarily uncertain? The former standpoint is taken by Beck (1987) and is described as the non-identifiability of the system with respect to some true description. The latter view is taken by Klemes (1996) who attempts to convey the extreme difficulty of quantifying the system at its fundamental level by describing uncertainty as ‘irreducible’. In response to a similar philosophical viewpoint, Beven (1993) introduces the concept of equifinality, which is defined as the situation where points from dispersed areas of the model structure and parameter space give equally good fits to available data for the catchment. Gupta *et al*. (2005) describe different responses to equifinality: it might be seen as an indication that the model structure is too complex for the available data and should be simplified. Alternatively it may be due to a failure to properly specify the calibration problem to exploit the data available. Finally, and following Beven’s (1993) philosophy, it may support the need for a set theoretic approach to model choice where different models are accepted as equally valid.

2.3.2 Overwhelming Uncertainty?

Many authors attempt to classify the different causes or types of uncertainty in a hydrological system. Typically these would include uncertainty in process descriptions, inexact knowledge of parameter values (particularly in the case of effective parameters) and uncertainty in calibration and validation measures (Bardossy, 2005; Beck, 1987; Gupta *et al*., 2005; Melching, 1995). Melching (1995) and Kundzewicz (1995) both highlight the apparent lack of structure in some hydrological processes, referring to this as ‘natural randomness’ and ‘chaotic behaviour’ respectively. Uncertainty may also be caused by non-stationarity in hydrological processes, including trends, periodicities and correlations between variables. This may include trends produced by climate change or land use change (Kundzewicz, 1995; Strupczewski and Mitosek, 1995). Bogardi and Kundzewicz (1996) describe the importance of the pre-hydrological (e.g. meteorology) and post-hydrological (e.g. social, psychological and institutional) sources of uncertainty. Klemes (1996) considers the social and political factors which may govern which sources of uncertainty are considered. Finally there are the sources of uncertainty which are unidentified until a hydrological event or disaster brings them to our attention: these are the ‘unknown unknowns’ (Klemes, 1996).

It seems that the closer one examines a hydrological system, the more sources of uncertainty can be identified. For example, Melching (1995) studies the use of point rainfall measurements to estimate the catchment rainfall input and describes eight different sources of uncertainty (Table 2.1).

1. Depth Measurement error in gauge due to equipment malfunction
2. Representiveness of ground-level precipitation at gauging point
3. Gauge location, e.g. gauges may be in positions that constantly result in high or low readings relative to rainfall.
4. Gauge network areal-mean rainfall versus true areal-mean
5. Rainfall spatial variability.
6. Rainfall temporal variability
7. Lack of synchronisation between time clocks for rain and stream gauges.
8. Lack of synchronisation between time clocks for the various rain gauges in the watershed.

Table 2.1: Eight sources of uncertainty in estimation of rainfall input. From Melching (1995).

Catchments may be particularly susceptible to large uncertainties where there is a lack of data; Kotwicki and Kundzewicz (1995) give the example of an arid catchment which rarely exhibits flow conditions. In this type of system there may be insufficient information to ‘close’ the catchment, leading to large uncertainties in even the most fundamental analysis of mass or energy continuity. Catchments which have multiple controlling mechanisms or mechanisms which switch between states are also prone to high uncertainties, e.g. Romanowicz *et al*. (1995) study the uncertainties in a model of evaporation which has two distinct process states depending on a threshold value of soil moisture in the surface layer. The problems are often exacerbated because uncertainties are at their greatest during extreme events such as flood peaks when accuracy may be at its most critical. Gupta *et al*. (2005) cite the problems of streamflow gauges which suffer from rating curve inaccuracies and bypassing of gauging structures at high flows. Beven (2001a) questions whether, given so many possible faults in any model, a scientist searching for a truthful representation of reality might feel that he should reject all models. This might seem to be the most rigorous response, and might indeed lead to advances in process understanding and refinements in modelling technique as we search for an acceptable model. However, referring back to the theory of equifinality and irreducible uncertainty, it may be necessary to accept and accommodate uncertainty. Given that model predictions are required for many applications, we must instead look for a way to simplify the layers of uncertainty and identify those that are the most important (Beven, 2001a).

Kundzewicz (1995) outlines some of the practical ways that hydrologists and engineers have dealt with uncertainty in the past. The technique of Laplacian Postulates, otherwise known as the principle of insufficient reason, suggests that when probabilities of alternative outcomes are not known, they should be assumed equal. This is the basis the uniform *a priori* distribution commonly used in Monte Carlo sampling applications. Another popular method is simply to use the worst case scenario, or to introduce an arbitrary 'safety factor' (Plate, 1996; Yen, 1996), or to use a measure of central tendency. A slightly more advanced analysis might consider an interval or range of possible outcomes. In some cases it may be justified to ignore uncertainty altogether: Moore (1996) suggests that deterministic forecasts are often sufficient, and that it is only in marginal cases where there is a high probability of false positives or negatives where a probabilistic forecast would be required. Melching (1995) and Troutman (1983) give the example of model errors consisting of systematic bias, which in some cases may be ignored altogether as it would be corrected automatically during calibration of parameter values, or in other cases may be included explicitly as an additional parameter such as a rainfall input scaling factor (Gupta *et al*., 2005).

Recently, hydrologists have tried to take a more thoughtful approach to dealing with uncertainty, using the information that is available about the magnitude of uncertainty, its variability over space and time, and the role that it plays in the modelled system. For example, it may be possible to consider uncertainty in some variables only; Romanowicz *et al*. (1995) modelled dynamic unsaturated flow in spatially variable soils by assuming that soil properties were uniform with depth. This is based on a similar principle to the shallow water approximation to the Navier-Stokes equations; although not uniform, pressure may be expected to behave hydrostatically and hence velocity may be replaced by its mean over depth. We should, however, take care not to fall into the trap of modelling only those uncertainties we know how to analyse (Singh, 1995). In order to make this type of judgement, rigorous methods of uncertainty estimation are required.

2.3.3 Approaches to Uncertainty and Uncertainty Estimation

In order to ensure that model predictions are both reliable and precise, or to assess their progress towards achieving this aim, methods are needed to estimate and report uncertainty. The new generation of physically-based, process-orientated hydrological models require methodological frameworks which are able to accommodate the multiple sources of uncertainty encountered as we try to simulate the hydrological behaviour of a catchment. In particular, models are increasingly being created which simulate linked hydrological systems, and methods must be found to combine the component uncertainties associated with these. Process-orientated models may also be required to incorporate qualitative expert knowledge of a system, an example of 'soft data', and techniques for dealing with the uncertainties of such judgements must be included.

When dealing with such complex systems, an important constraint on the completeness of an uncertainty estimation technique is the way in which uncertainties in input parameters are described. Yen (1996) gives various methods for specifying the uncertainty, from the complete probability density function (pdf) of the parameter, through simpler descriptions such as its statistical moments or as a confidence interval. However, as he points out, only the full pdf will allow a (numeric or analytical) calculation of how two or more uncertainty sources combine. It is important to note that in coupled systems, one model's output uncertainty will be the next model's input uncertainty and so in order to evaluate the combined uncertainty of the system, the uncertainties have to be expressed as complete pdfs. Plate (1995) gives an example of tracking uncertainty through a coupled system; in this case a pollutant transport model describing first pollutant runoff into a river, then transport along the river reach. The complete distributions of the input parameters were not determined, and therefore a distribution function type was imposed, in this case requiring each parameter to conform to a normal distribution. This assumption allowed analytical calculations of combined uncertainty probabilities to be made, using known characteristics of the normal distribution. The technique of imposing analytical distributions is popular for the ease with which such analyses can be made (e.g. Karbowski, 1995; Kozlowski and Lodzinski, 1995).

In many applications, it is possible to capture a complete empirical pdf of input parameters. This is preferable to an assumed statistical distribution function, however it precludes the use of analytical methods for combining uncertainties. In such situations discrete numerical methods such as Monte Carlo analysis must be applied. This involves random sampling from input distributions, which can be of any form, to build up a distribution of associated outputs. Uncertainties from many sources can be accommodated by sampling independently from each distribution for each model run. For example, Fahmy *et al*. (1996) used the technique to include uncertainties in the model, parameters and input samples in an ecological risk model. Melching (1995) describes the Monte Carlo sampling technique as an ‘extremely robust and flexible method’ which is often the only option when the system is highly nonlinear. The method was extended by Beven and Binley (1992) to form the Generalised Likelihood Uncertainty Estimation (GLUE) technique by associating a ‘degree of belief’ with each output sample. Again this measure of belief is extremely flexible and could include fuzzy measures to incorporate soft data (Bender, 1996; Kindler and Tyszewski, 1995). Using the measure allows the output samples to be weighted according to the likelihood that the model used to produce them was a good representation of the catchment. Melching (1995) however sees the need to reject some models as ‘non-behavioural’, i.e. not adequately simulating catchment behaviour, as a shortcoming of the methodology due to the arbitrary choice of threshold value. The GLUE methodology is described more fully in Chapter 5.

A disadvantage of Monte Carlo sampling is the high cost in terms of computational resources when even a moderate number of different parameters are considered uncertain and need to be explored. This has spawned various methods to approximate the response surface to save computer time. Both Melching (1995) and Yen (1996) give reviews of several of these, including Latin hypercube sampling, integral transformation techniques and point estimation methods such as those of Rosenblueth and Harr which assume local linearity of response. Given certain conditions these are found to compare well to full Monte Carlo sampling (Melching, 1995).

2.3.4 Mitigating Uncertainty

The uncertainty estimation methods described in the previous section are undertaken in the hope that knowledge of uncertainty can aid in its mitigation. Our perception of the approach used in mitigation has its roots in the answer to the fundamental question posed in Section 2.3.1 – is the uncertainty inherent in the system? If the answer is yes, the process will be seen as progressive and iterative as we aim to reduce uncertainties in knowledge of structure and parameterisation, rejecting non-behavioural models while retaining a set of behavioural ones. If contrastingly there is a belief that all uncertainty is avoidable, the process will be seen as a pathway to acquiring the knowledge required to remove uncertainty. Typical of this process would be the description by Melching (1995) of the reduction of uncertainty associated with data-handling, timing and reading errors that has been achieved by using telemetry rather than manual reading of raingauges. Despite these conflicting paradigms, the methodology may in fact be very similar. Given the constraint of finite resources for data collection and processing, how may we best reduce uncertainty in model outcome?

One of the crucial roles of uncertainty estimation is to allow the total uncertainty to be disaggregated into its source components. This is not an easy task and sometimes assumptions or simplifications must be made, for example to assume that model structure is correct and focus on uncertainty due to inexact parameter knowledge only. Another possible simplification is to look at uncertainty in classes of variables rather than each individual variable, e.g. Plate (1995) looked at uncertainty in the levels of classes of pollutants which could be separated by behavioural differences. Various methods may be used for disaggregation, depending on the uncertainty estimation technique. Melching (1995) describes the use of reliability analysis, including both sensitivity analysis and estimation of magnitude of parameter error. This technique relies on the assumption that the response surface is locally multivariate normal around the optimum predicted parameter set. When GLUE is used, Monte Carlo simulations can provide a correlation coefficient between the parameter value and output values.

The knowledge of individual uncertainties can be used to identify problem areas in the model, enabling resources to be used in the most efficient way. For example, where the variance of the pdf of a model parameter is small compared to that of the model input samples, it may not be worthwhile to attempt further data collection to improve knowledge of that parameter (Plate, 1995). Instead an attempt may be made to reduce input uncertainty. Many authors have highlighted input uncertainty as a major factor in rainfall runoff models, and have been able to quantify the effects of reducing it by comparing an uncertain estimate of rainfall fields from a gauging network with the ‘true’ field measured by radar, (e.g. Melching, 1995; Moore, 1996) and a summary of other work by Gupta *et al*. (2005). Care must however be taken that in aiming to reduce uncertainty in one part of the system, bias is not created in the balance of process descriptions leading to increased uncertainty in other areas (Gupta *et al*., 2005).

2.4 Use and Communication of New Techniques

2.4.1 Challenges in Communication

The preceding discussion has emphasised the high current level of awareness of uncertainty in the hydrological community, and the understanding of the importance of its role during the interpretation of model predictions. Various authors comment on its centrality to water resource management decisions (Kindler and Tyszewski, 1995; Yen, 1996). Why then is the consideration of uncertainty almost non-existent in commercial application of hydrological models? There are counter-examples to this observation, e.g. Krzysztofowicz (1996) cites the development of a probabilistic hydrometeorological forecasting system for the United States National Weather Service which aims to quantify uncertainty in precipitation quantity and river flow (USNWS, 2006). The system is described as increasing the economic benefit of forecasts, and being at least as reliable as deterministic forecasts, yet it is an example that has been seldom copied elsewhere.

The reality is that many organisations have entrenched modelling frameworks which would require an extreme stimulus to overturn. This prevents both unjustifiably deterministic models and under-performing models being replaced. Oreskes and Belitz (2001) attribute the continuing use of established models and techniques, in the face of poor results, to an effort to avoid legal liability by being seen to follow standard techniques. Anderson and Bates (2001) reiterate this, by considering the government agency endorsement of some models and giving the example of the United States Environmental Protection Agency mandating the use of certain models in environmental risk assessments. Similarly in the United Kingdom, the Environment Agency indicative floodplain map, originally produced using a simple three-parameter model, has been enshrined in statutory governmental guidance (Reed, 2002). However, these types of considerations cannot be the only reason why people continue to use bad models, as hydrologists without these pressures also fall into the same trap on occasion. Oreskes and Belitz (2001) suggest that past failures of the model are either forgotten, or never established due to a lack of comprehensive monitoring. Perhaps particularly true for experienced hydrologists is in fact an *expectation* that models will produce poor results.

With a heightened awareness that models are at best a crude representation of reality, with little or no place for their validation or verification (Konikow and Bredehoeft, 1992), perhaps it is no surprise to produce poor results at times.

With this in mind, one of the most difficult challenges in the drive for recognition of uncertainty is to bring uncertainty estimation into widespread use as a way of increasing the information available from a model, rather than as an excuse for ignoring bad model performance. Anderson and Bates (2001) highlight the importance of differentiating between models which correctly identify the driving processes of the catchment, albeit with uncertain parameters, and those for which parameterisation has allowed a bad representation to produce reasonable results. An instance of the latter is given by Oreskes and Belitz (2001) in the form of a beach erosion model which could reproduce current observations, but incorrectly represented the erosion as a steady process whereas it actually occurred only during rare storms. This is a further example of calibration bias allowing the accommodation of an unreasonable model structure (Section 2.2.3). In order to make the differentiation, methods for visualising uncertainty and the information that this gives us about the model must be developed. This will make uncertainty estimation relevant and useful to researchers, commercial modellers and the wider public.

2.4.2 Using and Visualising Uncertainty

2.4.2.1 Methods in the context of Research

While uncertainty estimation is well established in the field of hydrology in general, Lane and Bates (2000) emphasise its infrequent use in floodplain inundation studies. They suggest that this may be due to a combination of the computational effort needed, and a lack of process knowledge which would be required to specify uncertainties. Perhaps another contributing factor is a greater confidence in the completeness of such physical hydraulic models, which require far fewer parameters than, for example, rainfall-runoff models. The dominant uncertainties in hydraulic models may instead stem from initial and boundary conditions, and model structure (including treatment of numerical instability; see Section 6.3.1.3). Now that models using high-resolution floodplain data, run on high-powered computers, are increasingly able to support detailed process representations, the barriers to inclusion of uncertainty estimation are beginning to be removed. In turn the ability and necessity of including uncertainty in flood inundation predictions is becoming apparent; Wheater (2002) concludes that increased understanding of uncertainty will in particular emphasise the current limits and deterministic nature of floodplain inundation mapping.

Methods must therefore be established to visualise and use uncertainty information in floodplain inundation prediction and mapping. These methods must be suitable for their intended use; Reed (2002) draws the distinction between simple and complex representations of uncertainty depending on specific needs. An example of the former would be a 'statement of ignorance'; that uncertainty is known to exist with a certain magnitude, but nothing further is known. This may be sufficient for applications such as planning decisions. The latter would include more information such as variances or spatial distribution of uncertainty; an example is given of an application to Kriging variance mapping to highlight weak spots in a gauging network where new investment in equipment would reduce uncertainty most effectively.

There are two main cases where there is a need to visualise uncertainty. Firstly the uncertainty in the model input: knowledge of uncertainty in any estimated or calibrated parameters may allow identification of gaps in catchment process understanding or data collection. Secondly the uncertainty in the model output: knowledge of uncertainty in the prediction allows better informed decisions to be made. In the first case, where an uncertainty estimation technique such as GLUE is being used (Section 2.3.3), 'dotty plots' enable a visualisation of the uncertainty in each parameter. These plots show the parameter value against the performance measure, one dot for each model realisation. In effect they are a one dimensional representation of the response space, and show the sensitivity of the model to changes in that parameter (Figure 2.5). The data behind the plots may also be used to create histograms showing the marginal posterior likelihood weighted distributions of individual parameters. Multiple dotty plots may also be made with different performance measures which highlight particular aspects of model behaviour. For example Freer *et al*. (2004) give dotty plots based on performance in predicting near-stream water table levels, hillslope water table levels, discharge and combinations of these to show the control of different parameters on different aspects of model output (Figure 2.5).

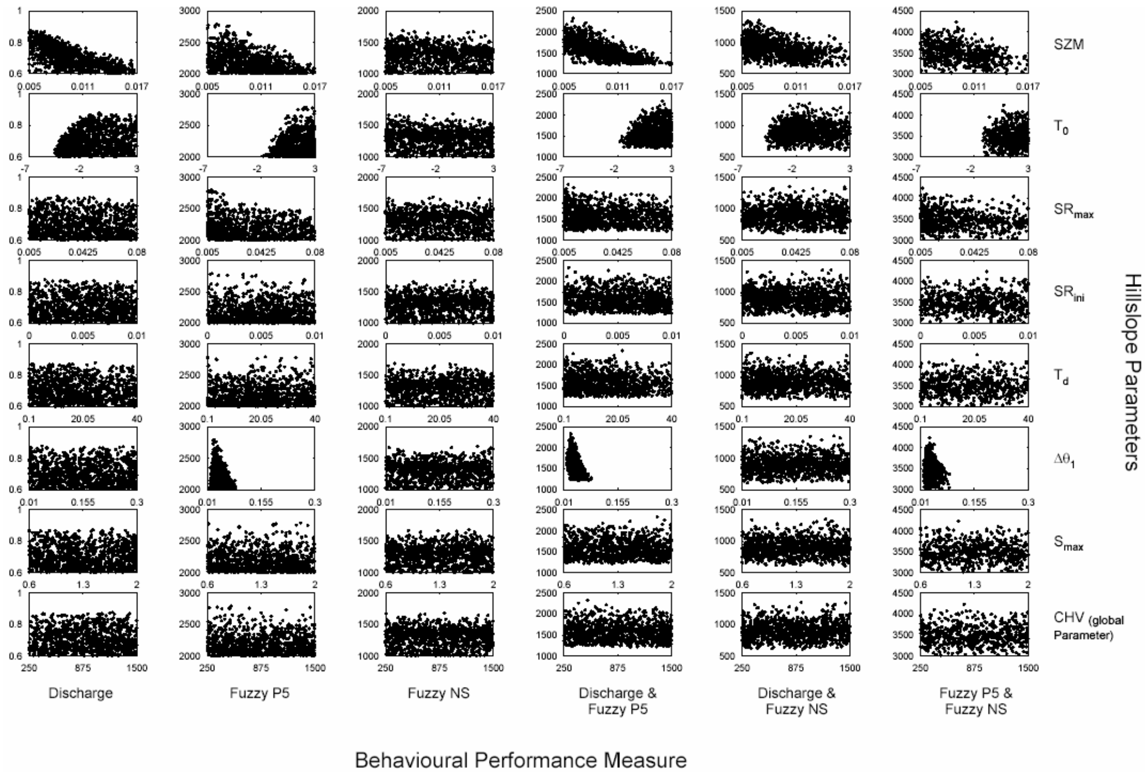

Figure 2.5: Dotty Plots used to visualise uncertainty in 8 parameters of a TOPMODEL application to the MaiMai M8 catchment in New Zealand, in response to 6 different performance measures (validating against discharge, near stream/hillslope water table depth and combinations). Each plot shows performance score against parameter value; each dot represents one behavioural simulation. From Freer et al. (2004).

To extend the concept to interactions between parameters, plots may be made which show one parameter on each axis, with each dot representing the existence of a behavioural model realisation with that combination of parameters. These plots will give visualisations of correlations between parameters which may indicate model process interactions.

In the second case, uncertainty visualisation is needed to demonstrate possible errors in model prediction. From a researcher's point of view, this may often be most usefully expressed in terms of a cumulative probability distribution of each output variable such as discharge at a given time step. This distribution may be created using a combination of predictions from behavioural models weighted by performance measure. The distributions may then be used to create confidence limits for each point of the time-series (Figure 2.6).

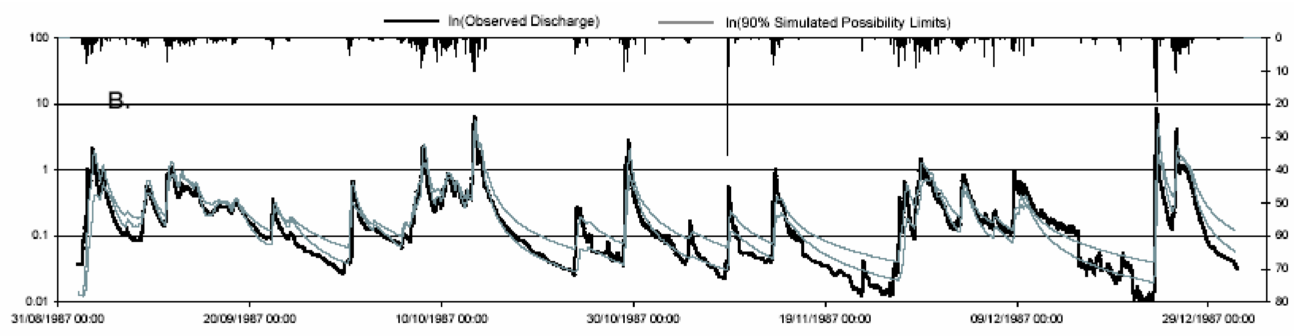

Figure 2.6: 90% Confidence bounds for catchment discharge compared with observed discharge, from an application of dynamic TOPMODEL within a GLUE framework (displayed on a log scale for clarity). From Freer et al. (2004).

Such a type of representation may not be the most easily understood by the public: this issue will be discussed in the following section. It is important to be able to visualise output uncertainty in order to understand how further data collection might serve to reduce it. For example, by plotting prediction bounds of an output variable as additional sets of temporal and spatial data are included in the model conditioning procedure, the value of the data may be demonstrated in terms of a narrowing of these bounds (Freer *et al*., 1996; Lamb *et al*., 1998). This effect is shown in Figure 2.7.

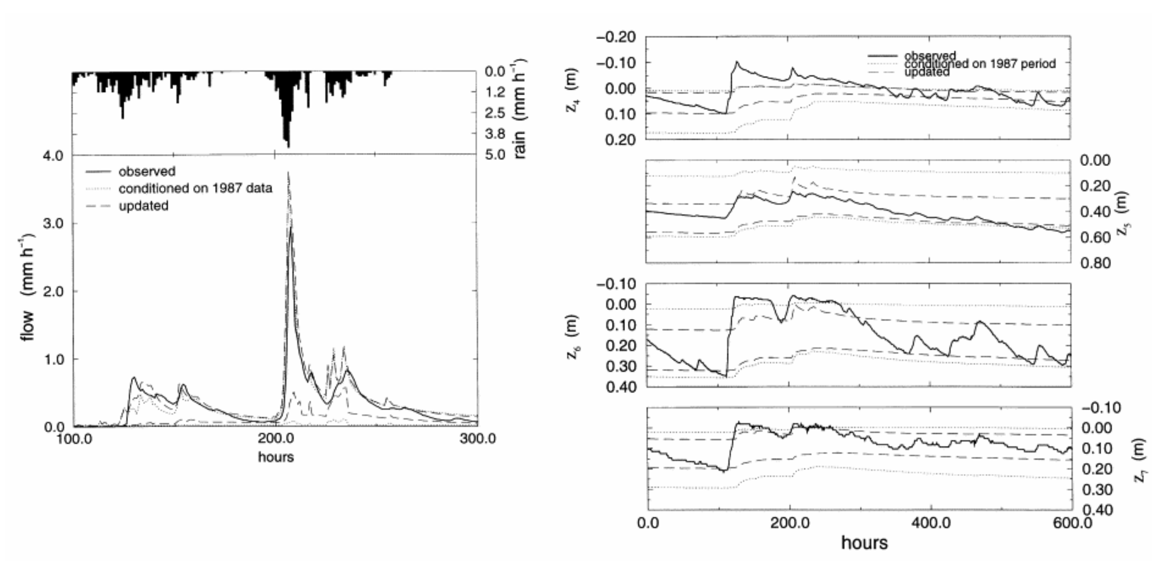

Figure 2.7: Uncertainty bounds for (a) discharge and (b) borehole water levels using a single period of data and updated using a second period. From Lamb et al. (1998).

2.4.2.2 *Methods for Public Understanding*

The techniques used to explain and represent uncertainty in hydrological predictions intended for use by the general public may be quite different to those used by hydrological researchers. The techniques will also differ according to their intended audience: a group of concerned homeowners affected by recent flooding may be more receptive to detailed technical data than populations not previously flooded.

It is important that information is presented in a way that will be accessible to the user community (Wheater, 2002). This may involve the use of different variables to those used in the uncertainty analysis. Keys (1997) uses the example of gauged discharge levels, which are meaningless to the community, being translated into information on the horizontal spread of water on the ground, hence implying the necessity of coupled rainfall-runoff and hydraulic modelling. Alternatively, it may be couched in terms of simple instructions such as avoiding certain roads. The uncertainty within this data must similarly be expressed in an accessible way. Instead of frequency distributions of variables, simplified representations such as an upper and lower bound, best and worst case scenarios, or the percentage chance of a particular area being flooded may be most appropriate.

As well as information provision, uncertainty estimation is also used in public policy for making benefit-cost decisions; this will increasingly be the case as the Water Framework Directive comes into force (Newson and Chalk, 2005). In this case, it is the combination of uncertainty and the possible consequences of that uncertainty that are important: this is referred to as the risk (Kundzewicz, 1995) or vulnerability (Gilard, 1996) associated with the uncertainty (the concept of vulnerability was examined in more detail in Section 1.3.2.2). Public participation and opinion can be seen as the bridge between predictive uncertainty and risk (or the perception of risk) (Newson and Chalk, 2005); hence public understanding of uncertainty is vital. It is not only important in providing informative warning messages, but also in improving public comprehension of hydrological complexity. This will help to prevent the dominance of oversimplified ‘narratives’ of catchment processes (Forsyth, 2005) and allow more complete and reasoned responses to hydrological uncertainty.

2.5 Conclusion

This chapter has discussed a range of the current opportunities and challenges in hydrological science. These have, in the main, been related to the availability of new data sources, emphasising once again the continued status of hydrology as an empirical science. Increasingly powerful computing facilities, while easing problems of data manipulation capability, and allowing more complex, process-based model structures, have not removed the need for improved provision of reliable and wide ranging data sets.

The revolution in data availability has been examined, from the historical prevalence of temporal sources, to new spatially-distributed data sets made available through developments in remote-sensing technology. This expansion has highlighted the interdependence between data collection, hydrological understanding and model design; new information on spatial variation in catchment processes has forced hydrologists to re-examine their own perceptions of catchment behaviour and hence appropriate model structures for simulation.

Some of the problems associated with the sudden deluge of spatial data sets have also been studied. In some cases, the almost unprecedented situation now exists where data availability outstrips computational processing power, leading to exciting new research opportunities into techniques for utilising this data in an efficient way. One method for its inclusion as subgridscale information will be pursued in Chapter 6. It was also argued that this has been only a 'partial' data revolution, with detailed monitoring of surficial processes far exceeding that possible for subsurface structures and behaviour. This may lead to a danger of unwarranted assumptions of uniformity in unmodelled processes and calibration bias towards particular aspects of model behaviour. It has therefore become more important than ever to consider the unavoidable uncertainty present in choice of model structure and parameterisation.

A review of the current approaches to uncertainty estimation was undertaken, particularly with regards to calculation of uncertainties deriving from combinations of sources and within systems of coupled models such as the linked rainfall, rainfall-runoff and hydraulic models that are the subject of this thesis. This emphasised the importance of capturing complete empirical pdfs of parameters or variables, and hence the necessity of numerical methods such as Monte Carlo sampling in order to combine uncertainties.

Improvements in computer resources have increasingly made it possible to integrate such data intensive techniques into standardised hydrological assessment methods for use in commercial and public policy applications. However, to achieve acceptance in such arenas, clear visualisation techniques are required in order to demonstrate the effects of uncertainty on model predictions and make the concepts accessible to a wider audience. This in turn will reinforce the benefits of uncertainty mitigation through additional collection of validation data in terms of improved prediction accuracy. However, to succeed in this aim, uncertainty must be expressed in terms meaningful to the user. Chapter 7 demonstrates how this might be achieved through the use of coupled rainfall-runoff and hydraulic models to translate uncertainty in terms of discharge magnitude into information on inundation extent, the latter being accessible to the general public and more specifically to homeowners on the floodplain.

Chapter 3

STUDY CATCHMENT: THE RIVER GRANTA

Abstract

This Chapter introduces the study catchment which is used throughout the thesis to provide practical application and testing of the ‘End-to-End’ flood risk assessment framework. The catchment chosen is that of the Granta above Linton in Cambridgeshire, UK. The reasons for the choice of site are presented, together with a review of the history of flooding in the catchment. The physical characteristics of the catchment, and the part that these play in controlling the flow regime, are examined in some detail. Information on geology, soils, land-use, climate, water use and river management is presented.

The chapter also describes the data collected in order to structure, calibrate and evaluate the model components developed in the thesis. Rainfall and gauged flow data were provided by the Environment Agency. To further inform the structure of the rainfall-runoff model, flow gauges were installed in the two main tributaries of the Granta above Linton, to provide information on relative subcatchment contributions to total discharge. Data on flood extent and depth was required for the floodplain inundation model; this was collected through a survey of floodplain residents.

The data collected is used to undertake a hydrological review of the catchment. This includes analysis of rainfall and flow characteristics, and presentation of tributary flow gauging results for individual hydrographs. The catchment behaviour is linked to the geological and climatic controls. In addition, the meteorological conditions leading to the floods of October 2001 are examined. Finally, a review is made of the previous flood risk modelling carried out in the catchment. In 2004, the Environment Agency commissioned a report on the standards of flood protection provided in the catchment, to include modelling of channel flows and inundation associated with the 100-year flood. A summary of the methods and results of the study is presented.

3.1 Introduction

3.1.1 Catchment Choice

It is important that this thesis should be not only a theoretical exercise in model design, implementation and coupling, but also be grounded in a practical application, testing techniques in a study catchment. The essential part that field data sets play in hydrological modelling was emphasised in Section 2.1, concluding that model results are rarely justified unless they are backed up by sound data.

The study is based on the River Granta in Cambridgeshire, UK. This site has a recent history of flooding, the effects of which have been exacerbated by the lack of a reliable warning system. This is partly due to the fact that the Granta to Linton falls into a problematic class of catchments, where the speed of response hinders the use of traditional upstream monitoring to aid real-time forecasting and warning systems. Despite these constraints, a combination of climate and land-use change has increasingly put this type of lowland headwater catchment at risk from flooding (Section 1.3.2), and therefore solutions must be found in order to improve flood warning capacity. A strong candidate for such provision is in the use of operational forecasting systems based on forcing precipitation forecasts, i.e. the operational equivalent of the strategic 'end-to-end' flood risk assessment system proposed here. The Granta to Linton therefore provides an ideal opportunity to develop and test the 'end-to-end' framework, and also benefits from a strong data content including rainfall records, hydrometric data and topographic mapping, ease of access and local support for the project.

A map of the surrounding area is shown in Figure 3.1. The map shows the location of the River Granta, which flows in a North-Westerly direction from its headwaters in the South Cambridgeshire chalk uplands to its confluence with the River Cam near Stapleford. A more detailed topographic map of catchment of the Granta to Babraham is shown in Figure 3.2, and more details on the catchment physiography are given in Section 3.2. Figure 3.1 marks the three Environment Agency gauging stations at Linton, Babraham and Stapleford; the data available for the study from these gauges is examined in Section 3.3. Velocity and stage measurements were also made on the two main tributaries

(Camps Tributary and Bourn Tributary), marked upstream of Linton, over a three-year period; the results are presented in Section 3.4.

The study of flood risk is based around the town of Linton. The most recent severe flooding in Linton took place in October 2001, after 70.2 mm of rain fell in 17 hours on top of already saturated ground. River flow is estimated to have exceeded 20 m^3s^{-1}, compared to a typical base flow of 0.2 – 0.4 m^3s^{-1}. The meteorological conditions leading to this flood are examined in Section 3.4.4. Data on the associated floodplain inundation were collected through a survey of floodplain residents and are given in Section 3.3.

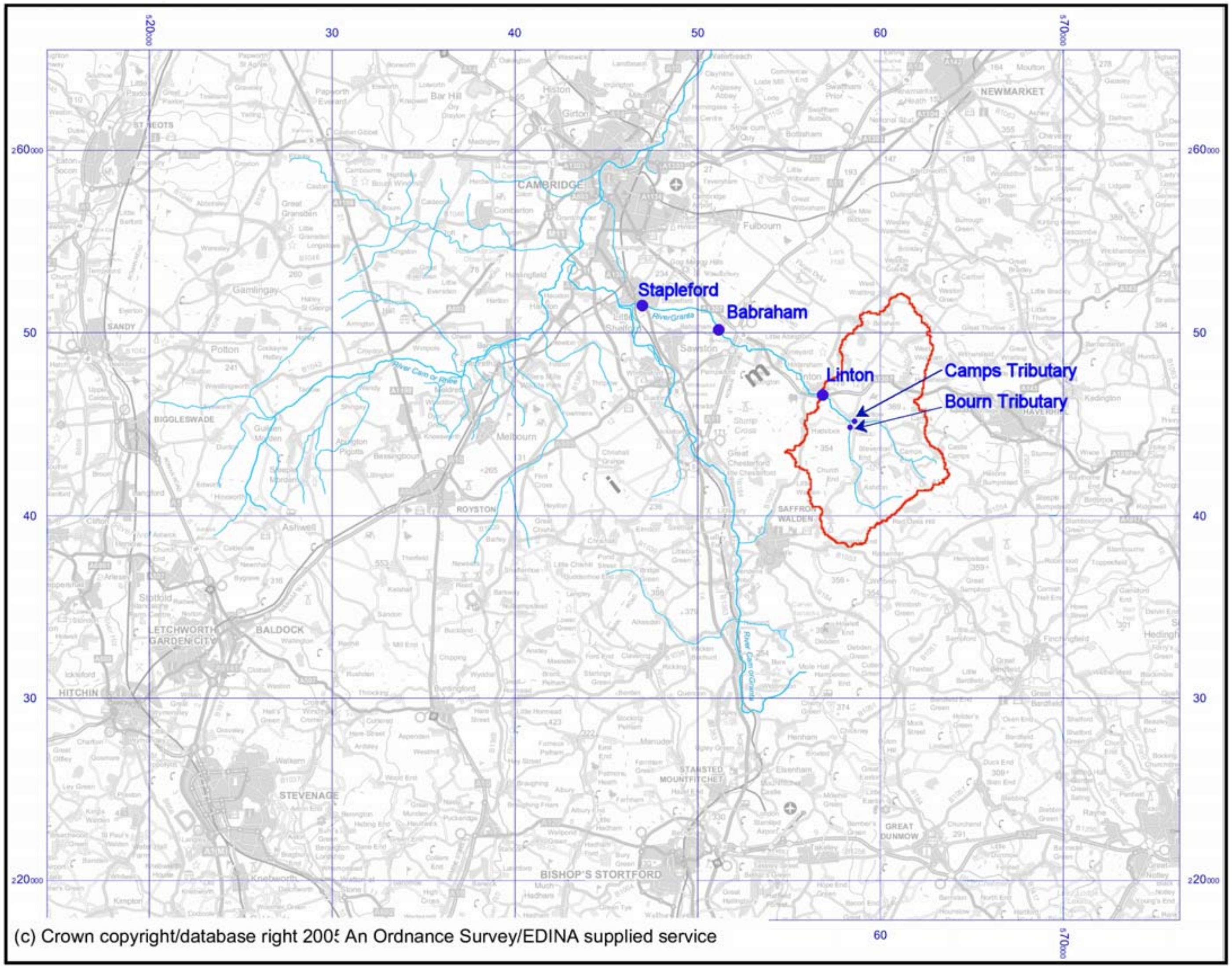

Figure 3.1: Granta to Linton Catchment Location Map. Flow gauges on the River Granta are marked.

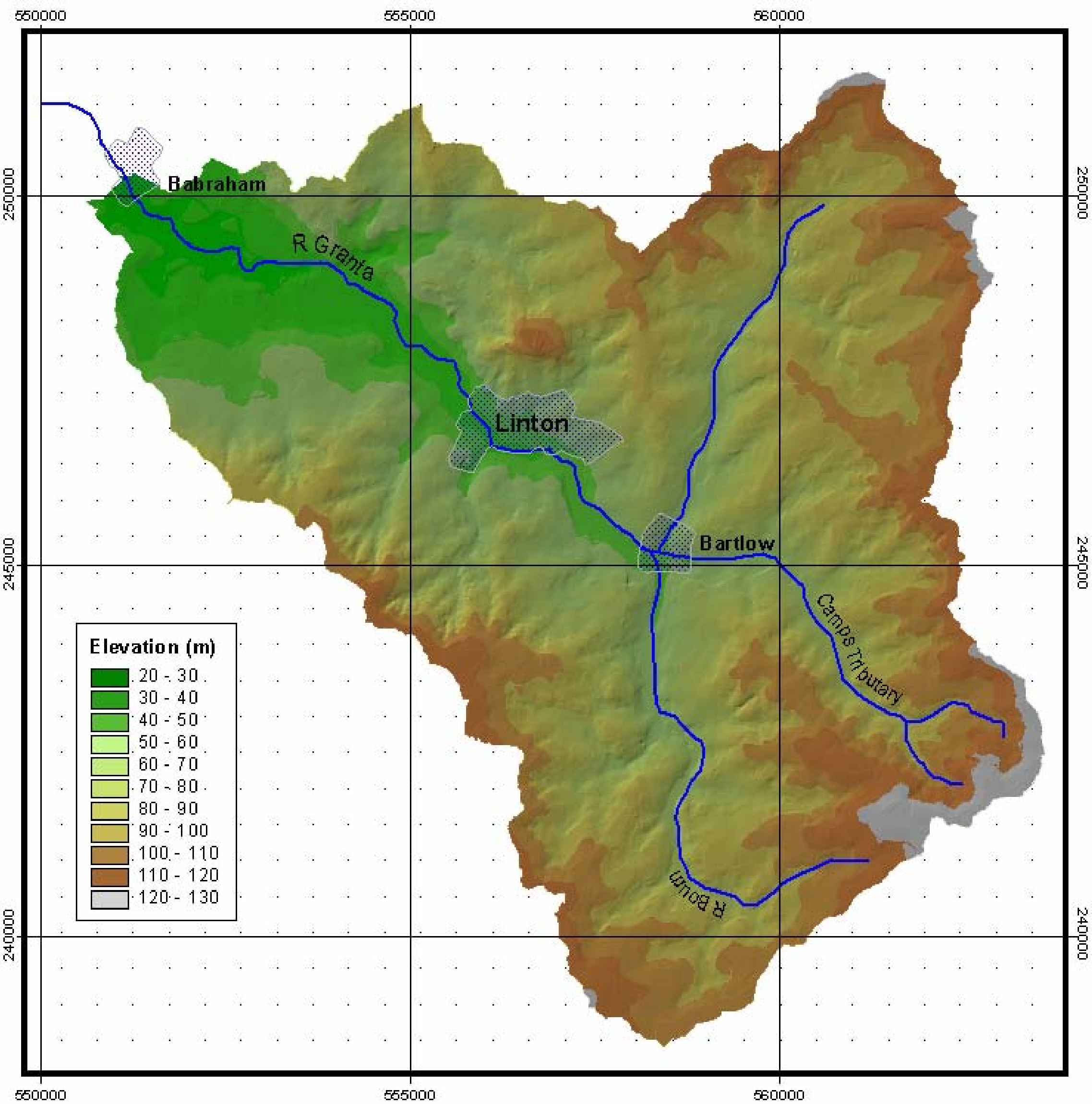

Figure 3.2: Topographic map of the Catchment of the Granta to Babraham

3.1.2 Hydrological History of Linton

Linton has a long history both of habitation and of flooding. Early remains found in the village include a Roman villa on the banks of the river towards Hadstock, further Roman remains on the site of the current secondary school, and Saxon burial mounds on Linton heath (Seaman-Turner, 1987). These finds date the settlement to pre-700 AD. The location of Linton stems from its importance as a crossing-place of the River Granta; the roads and tracks of the town radiate out from what is now the main bridge and was originally a ford ('Chilford'). There were also two main tracks parallel to the river, one on each bank. It is likely that these tracks marked the boundaries of the normal floodplain; they have subsequently become Bartlow Road and Back Road on the North side, Long Lane and Cambridge Road on the South (Linton Parish Council, 1982). Linton High Street joins the Northern track to the old ford at a diagonal; on the South side the connecting track is perpendicular to the river, suggestive of wetter ground on this bank. Figure 3.3 illustrates these roads on a historical map of Linton.

The river has always had an influence on land-use in the town. The relatively steep banks seen today suggest that the Granta was deeper and faster flowing in the past, and the river has been used for boating and bathing within living memory although flows are seldom sufficient to warrant such activities today (Linton Parish Council, 1982). Land close to the river is commonly still waterlogged in winter, suggesting that in the past it would often have been underwater. Further evidence for this lies in the designation of both the floodplain land upstream of Linton and the cricket meadow downstream as 'common land' of low value. It is possible however that such water meadows were encouraged in some places as an early form of irrigation to provide winter and spring feed for sheep. In Cambridgeshire evidence for this is seen in leats or channels along valley sides which then overflow through fields back to the main stream, and this type of system is known to have been introduced by the owner of Babraham manor (Taylor, 1973).

Floods have been a persistent feature of the Granta and have constrained both building and land cultivation. Failure of harvest caused by flooding has been put forward as an explanation for the abandonment of former arable land and decline of population in Linton in the 1300s (Taylor, 1973). Maps of the town commissioned by the Paris and Millicent families of the Linton manors in 1600 show that the lower part of the High

Street was not occupied save for an inn at the bridge, probably due to frequent flooding (Linton Parish Council, 1982). The same map shows dwellings on both sides of '*The Grip*' – a tributary joining the main channel just upstream of the ford; however a series of drainage ditches were used to make this land habitable in times of spate. Population growth, together with improved river management, has however pushed housing towards the river in more recent times. The population grew from 600 in 1600 AD, to 976 in 1731 AD, to 2061 in 1851 AD, and stood at 4412 in the 2001 census. Records referring to the main bridge in Linton also demonstrate a history of flooding. Frequent references to repair of the original wooden foot bridge after storms or floods occurs in the Constable's accounts and money was specifically allocated for this from the Guildhall income from 1564 (Linton Parish Council, 1982). In 1867 the wooden bridge was replaced by a sturdier iron road bridge, which was in turn destroyed by severe flooding in September 1968. To replace it, the current concrete bridge was erected, having greater width and clearance in anticipation of further floods.

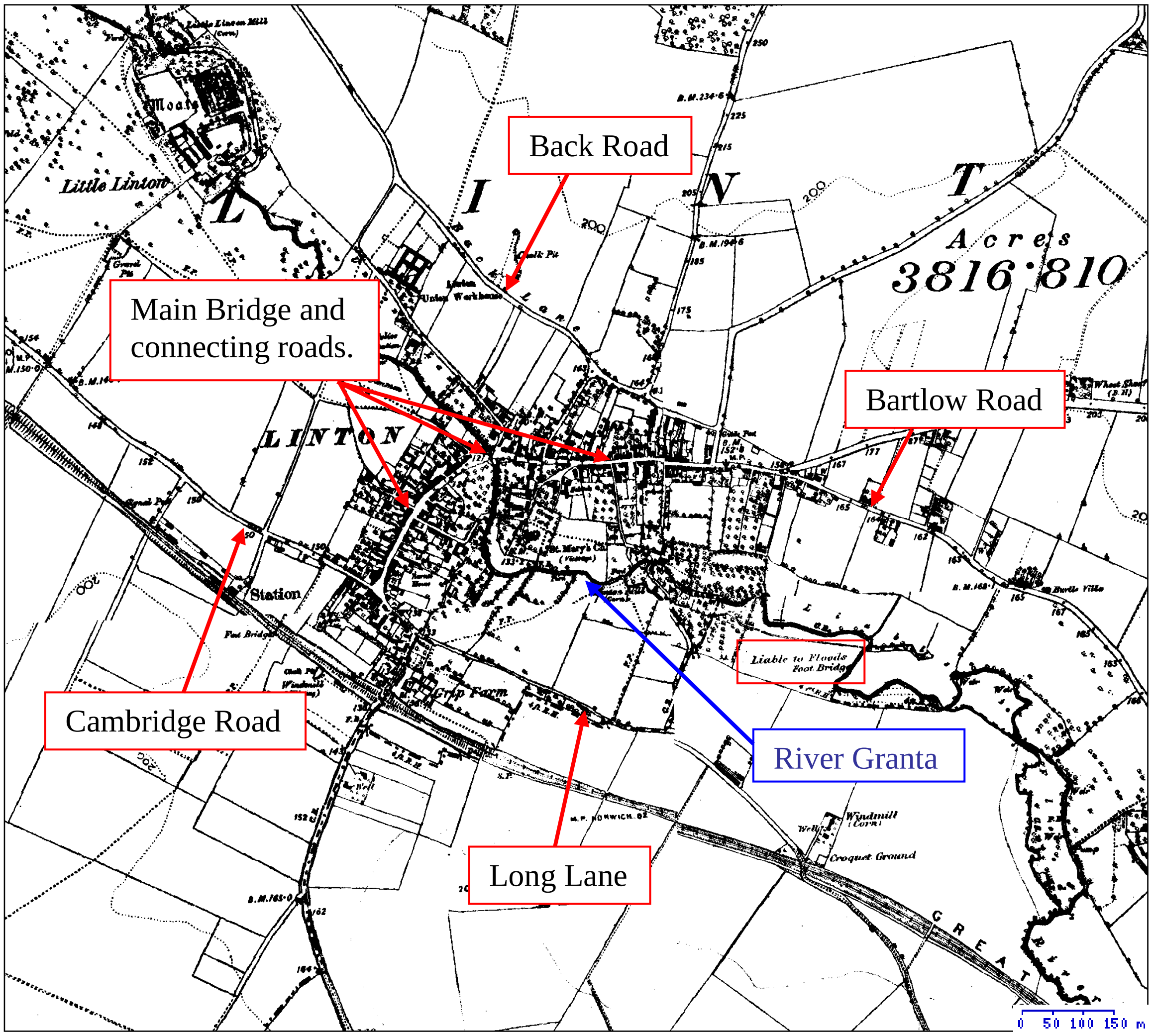

Figure 3.3: Historic Map of Linton, taken from the 1:10560 County Series. Sheet: Cambridgeshire and the Isle of Ely. Published 1891.
Map illustrates major routes parallel to River Granta on North and South sides, marking the boundaries of the historical floodplain. The connecting roads to the main town bridge are also shown. Note the land close to the river marked 'Liable to Floods'.

3.2 The Granta Catchment: Physiography and Climatology

3.2.1 Hydrogeology and Soils

The geology of the Linton catchment is illustrated in Figure 3.4. Linton lies on the edge of the chalk uplands which rise in the South East of the Cambridge Region and are a direct continuation of the Chilterns (Hey and Perrin, 1980). At Stapleford, the impermeable and easily eroded Chalk Marl of the lower Cam valley gives way to a zone of Upper Cretaceous Chalk lying above Totternhoe Stone, forming higher terraces. The Chalk is more permeable and more erosion resistant than the Chalk Marl, and forms scarp slopes in North and West directions, dip slopes of an angle of 1º to the South and East. The mature escarpments now take the form of rounded ridges. The Cam and Granta, in draining the Chalk Uplands, are obsequent streams flowing in the opposite direction to the Strata (Marr and Shipley, 1904; Staff, 1946), and the Granta at Bartlow is thought to have captured a stream which previously flowed South (Staff, 1946). Groundwater flow in the region is in a north-westerly direction, mirroring the surface drainage (Muhlherr and Hiscock, 1997).

Several divisions occur within the Chalk, often classified as Lower, Middle and Upper Chalk. The Lower Chalk (Cenomanian stage) is well and regularly jointed, and largely determines the line of springs following the base of the chalk escarpment, including one at Baslow and one on Rivey Hill above Linton. The Middle Chalk layer (Turonian stage) has a depth of around 60 m, and includes a lower layer of hard Melbourn Rock, overlain with well stratified White Chalk. This is then topped with the Upper Chalk which includes bands of semi-crystalline and rubbly chalk known as ‘Chalk Rock’. Above the Chalk Rock, the layers are much more soft and earthy and include tabular flints between layers.

Above the chalk there are accumulations of late glacial Boulder Clay, a mixture of coarse and fine material containing pebbles and boulders, with the exact constitution determined by the rock floor north of the location in question. Flint and chalk fragments are common, also occurring are other rock types foreign to the region. The Boulder Clay does not occur on steep slopes: accumulations are thickest in valley bottoms and on the flatter upland areas. In some places such as Barrington Hill near Linton, Plateau Gravel overlies the Boulder Clay; these gravels consist of the less soluble residue of the Boulder Clay, with a much smaller proportion of chalky material. On the valley floors, Boulder Clay is overlain by outwash materials of gravels and sands. This occurs at both Bartlow and Linton (Seaman-Turner, 1984).

The soils of the Linton catchment are illustrated in Figure 3.5. The soils of the Granta valley consist of Brown Earths and Brown Calcareous Soils along the valley beds, giving way to Rendzinas (originating from thin Chalky Drift) on the higher slopes and Surface-Water Gleys (originating from Chalky Boulder Clay) on the Chalk Uplands (Steers, 1965). The Surface-Water Gleys have been cracked by wetting and drying cycles, producing a blocky structure at the surface, a prismatic structure lower down. In winter, swelling of the soil causes partial closure of these cracks and percolation of water is slow. Almost all these soils have, however, been heavily modified by the long agricultural history of the region, with the valley soils forming Calcareous Loams and the upland Gleys kept reasonably well aerated by artificial drainage.

The soil and geological features of the region produce a characteristic response to rainfall patterns through the year; three dominant mechanisms which route rainfall into the river channels may be identified. Where rainfall intensity exceeds infiltration capacity, overland flow will result. This may be due to soil saturation, or impermeable surfaces for example in urban areas. Where infiltration does occur, soil throughflow provides a second important transport route. This is particularly likely to occur where soil lies over relatively impermeable bedrock such as the Boulder Clay of the Linton catchment. Thirdly, groundwater movement through the bedrock contributes to river flow either by discharge directly into the channel, or through re-emergence as springs supplied by a rising water table. This mechanism plays a major role in the Linton catchment due to the permeable and fractured nature of the underlying chalk, with between one third and one half of discharge volume thought to result from it (Barrington Local History and Conservation Society, 1979). In particular, this behaviour is caused by the constraint of groundwater circulation by hard bands such as the Totternhoe Stone and Melbourne Rock, while outcrops of fractured Lower Chalk deposits allow the water to return to the surface through springs and groundwater seepage zones. Typically, through the contribution of groundwater to channel slowflow, spring-fed regimes are expected to produce stable hydrological regimes with a narrow range of discharge (Sear *et al*., 1999;

Whiting and Stamm, 1995). However, studies have also shown that the contribution of groundwater to the quickflow storm hydrograph may also be high, due to processes such as pipeflow in connected fracture systems (Sklash and Farvolden, 1979). In Linton therefore, a strong baseflow signal would be expected from the groundwater contribution, overlain by flood peaks resulting from a combination of the three processes identified above. This response may be seen in the flow series illustrated in Section 3.4.2.

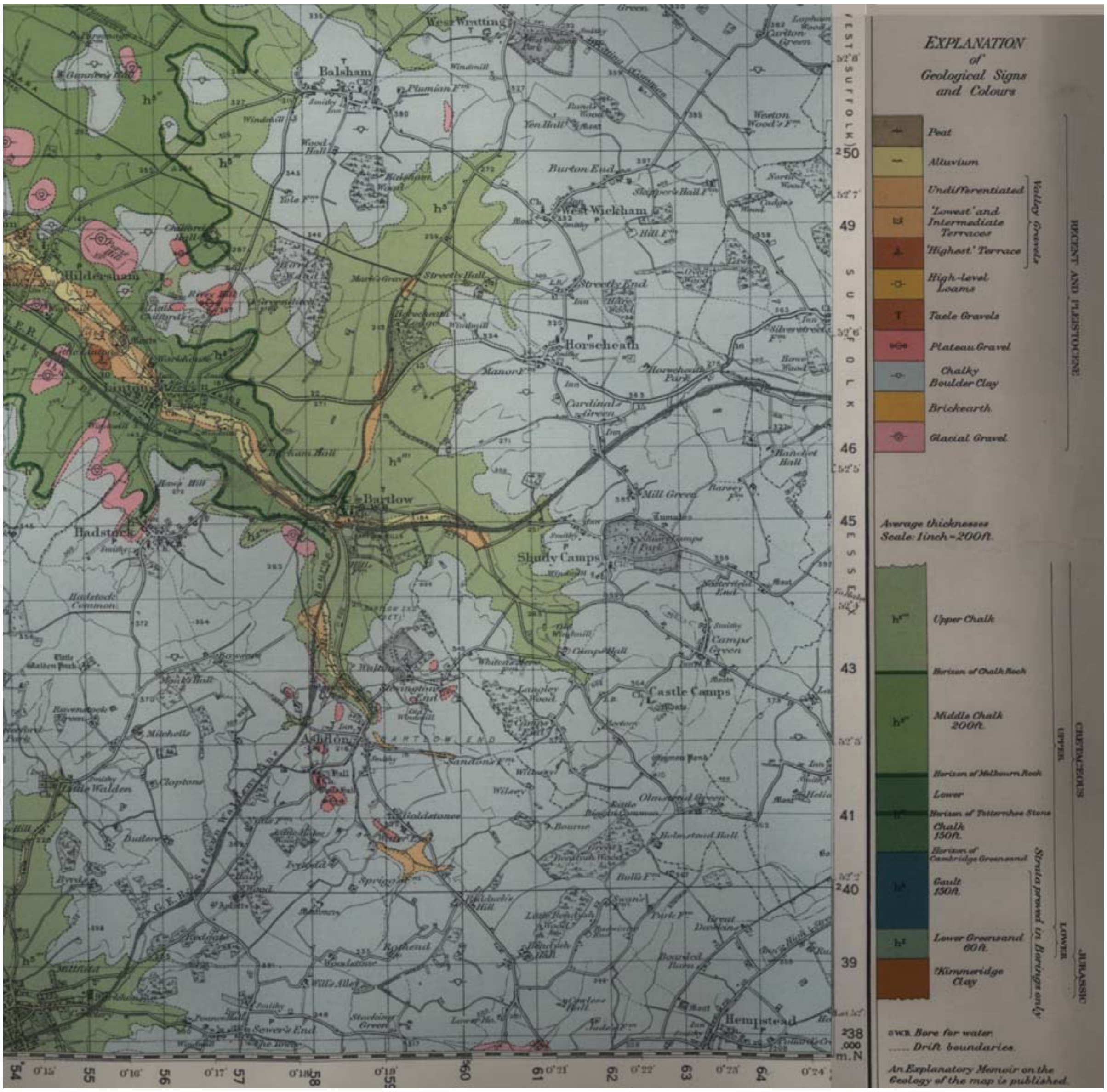

Figure 3.4: Geological Map of the Linton Catchment

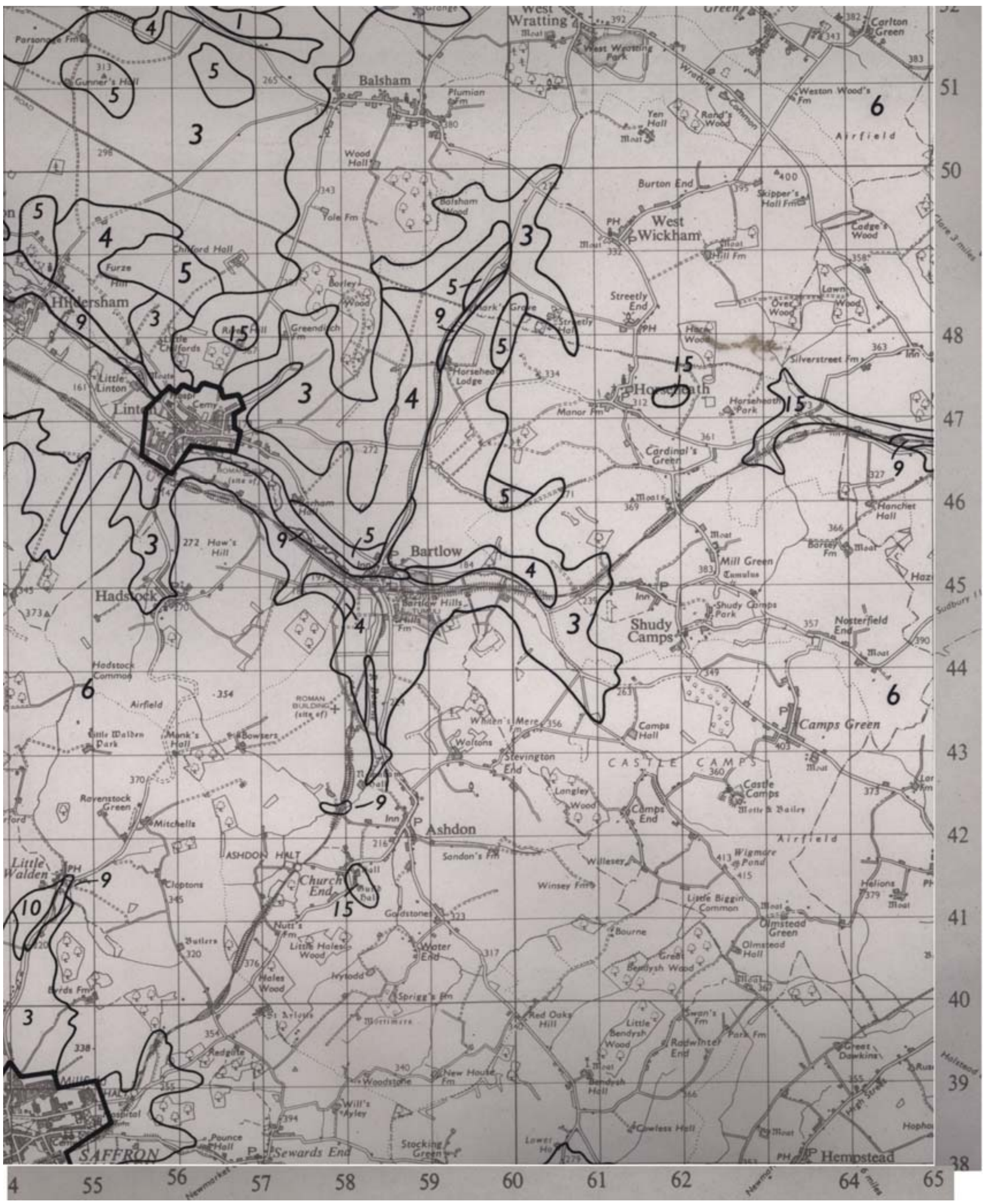

Figure 3.5: Soil Map of the Linton Catchment

Key:

Symbol	**Soil Group**	**Parent Material**
1	Rendzina	Mainly Chalk
3	Brown Calcarous Soil	Loamy, Chalky Drift over Chalk
4	Brown Earth and Brown C. Soil	Sandy, Chalky Drift over Chalk
5	Brown Calcarous Soil	Chalky Boulder Clay over Chalk
6	Calcarous Grey Soil	Chalky Boulder Clay
9	Calcarous Grey Soil	Alluvium, locally overlying Peat
10	Brown Earth	Loamy, Gravelly or Clayey Drift
15	Gleyed Brown Earth	Sandy, Loamy and Gravelly Drift

3.2.2 Catchment Climate

In common with the rest of East Anglia, Cambridgeshire has a climate described as more 'continental' than other parts of the UK. Figure 3.6 illustrates mean temperature, total rainfall and total sunshine by month for the years 1995-2004, in Cambridge. Cool dry winds from the East or North-East can often dominate and a typical yearly pattern is of frosty springs and sunny autumns (Staff, 1946). Precipitation may vary significantly between years (Figure 3.6a) but is typically greater in summer than in winter. However, in summer and early autumn the higher temperatures and longer hours of sunshine (Figures 3.6b and 3.6c) mean that it is usual for evaporation to exceed rainfall and therefore soils to become progressively drier. By autumn it is usual for soil moisture capacity to be around 10 cm below saturation (Barrington Local History and Conservation Society, 1979). This corresponds with measurements at Fleam Dyke, north of Linton, showing very little percolation in summer (Hey and Perrin, 1980). Over a complete year only around 33% of a total of 54 cm of precipitation was found to percolate. This soil state gives a situation where, typically, heavy summer rainfalls have little effect on the water table whereas autumn rainfall produces an immediate sharp rise and rainfall in the winter and spring produce a high and extended annual maximum (Steers, 1965). The increased downflow during the winter is likely to be indicative of fissure flow within the chalk, which occurs when the saturated hydraulic conductivity of the chalk matrix (around 3-5 mm/day) is exceeded (Ragab *et al*., 1997). Considered as a dual-porosity aquifer, the chalk has a mean transmissivity of 110 m^2d^{-1} and a specific yield of 10^{-2} (Muhlherr and Hiscock, 1997).

(a)

(b)

(c)

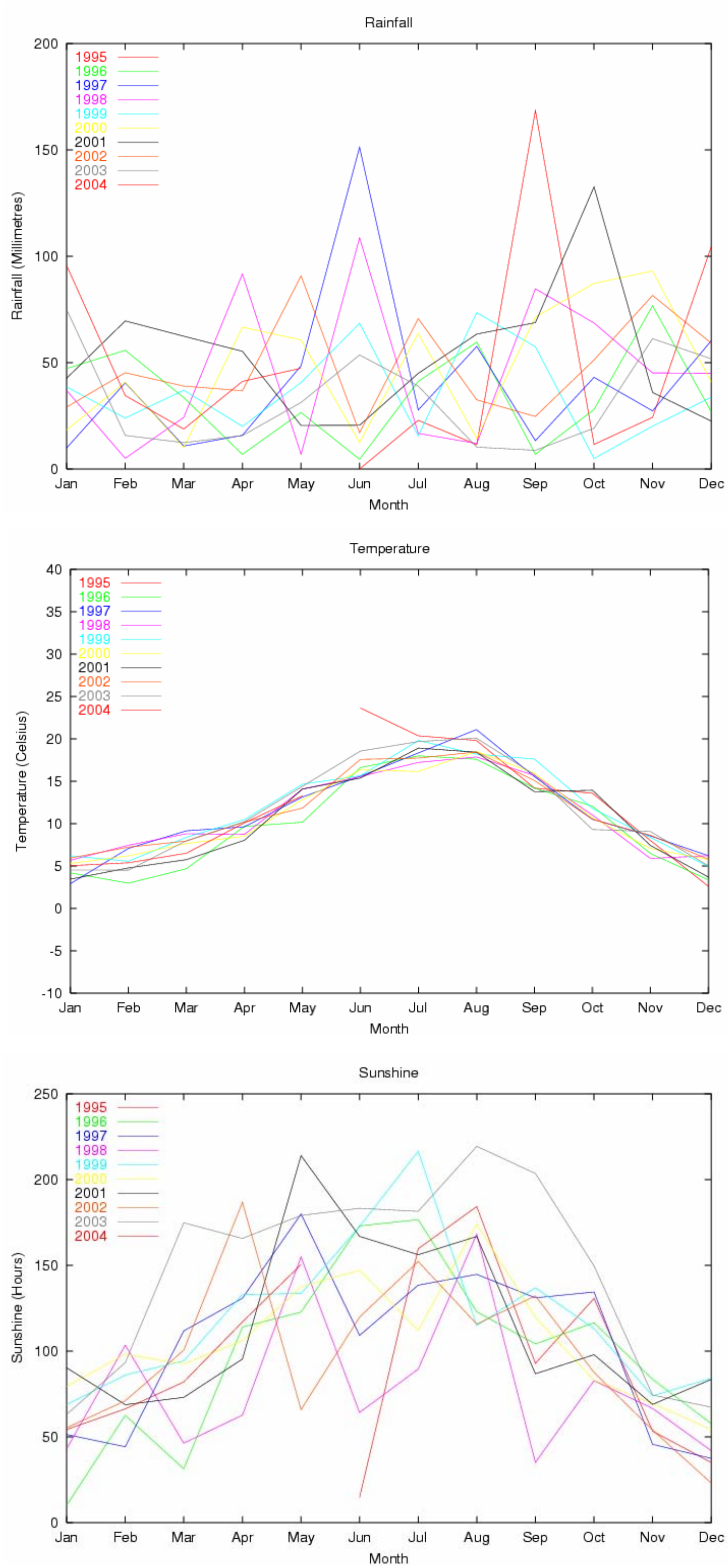

Figure 3.6: Cambridge Climate Statistics. Graphs show (a) Total Rainfall, (b) Mean Temperature and (c) Total Sunshine by month from 1995 – 2004.

Source: http://www.cl.cam.ac.uk/Research/DTG/attarchive/weather/

3.2.3 Vegetation and Land Use

The Granta catchment would originally have been forested; oak woods grew particularly well on the Boulder Clay. The woods would have been interspersed with chalk grasslands on the higher areas. Today little of the forest remains, although isolated patches of oak together with hazel, ash and hawthorn still occur. The influence of the underlying geology is still apparent, however, with trees, hedges and pasture land more plentiful in areas of Boulder Clay. The clay also gives rise to abundant surface water in ponds and small lakes, with accompanying wetland vegetation.

The area has long been used for arable farming: the cold springs are less suitable for fruit crops and long hours of sunshine in the autumns provide good ripening and harvesting conditions. In the 18th century the principle crops were barley and rye; today they include wheat, barley, oats, sugar beet and potatoes. The chalk slopes have unsuitable soils for large scale livestock farming, however mixed farms have been popular with arable on the high ground, stock on the Boulder Clay near the farmstead (Staff, 1946). Although the crops grown have remained similar, the layout and management of the land have changed over time. In the late 18th and early 19th century enclosure took place in the parishes of upland Cambridgeshire, with common fields and pasture being replaced by the familiar large, modern, geometrically shaped fields under the ownership of the larger estates. In Cambridgeshire as a whole, the landcover currently consists of 72.3% arable land, 14.7% grassland (of which 3.5% managed grassland, 5.2% rough grassland and 5.8% calcareous grassland), 7.5% urban and suburban areas and 3.6% woodland (Cambridgeshire County Council, 2005). In the Granta catchment above Linton, arable land (78.6%) and woodland (7.5%) are more dominant; grassland (9.2%) and urban areas (3.1%) occupy a smaller percentage, as shown in Figure 3.7.

Traditionally habitation in the area was relatively scarce, and largely confined to the lower valleys. Few farms were situated on the upper slopes as the dominance of groundwater over surface water transport resulted in a lack of drinking water supply. In modern times however Linton and the surrounding villages have become dormitory towns for Cambridge and other population centres, and the area's population is increasing steadily.

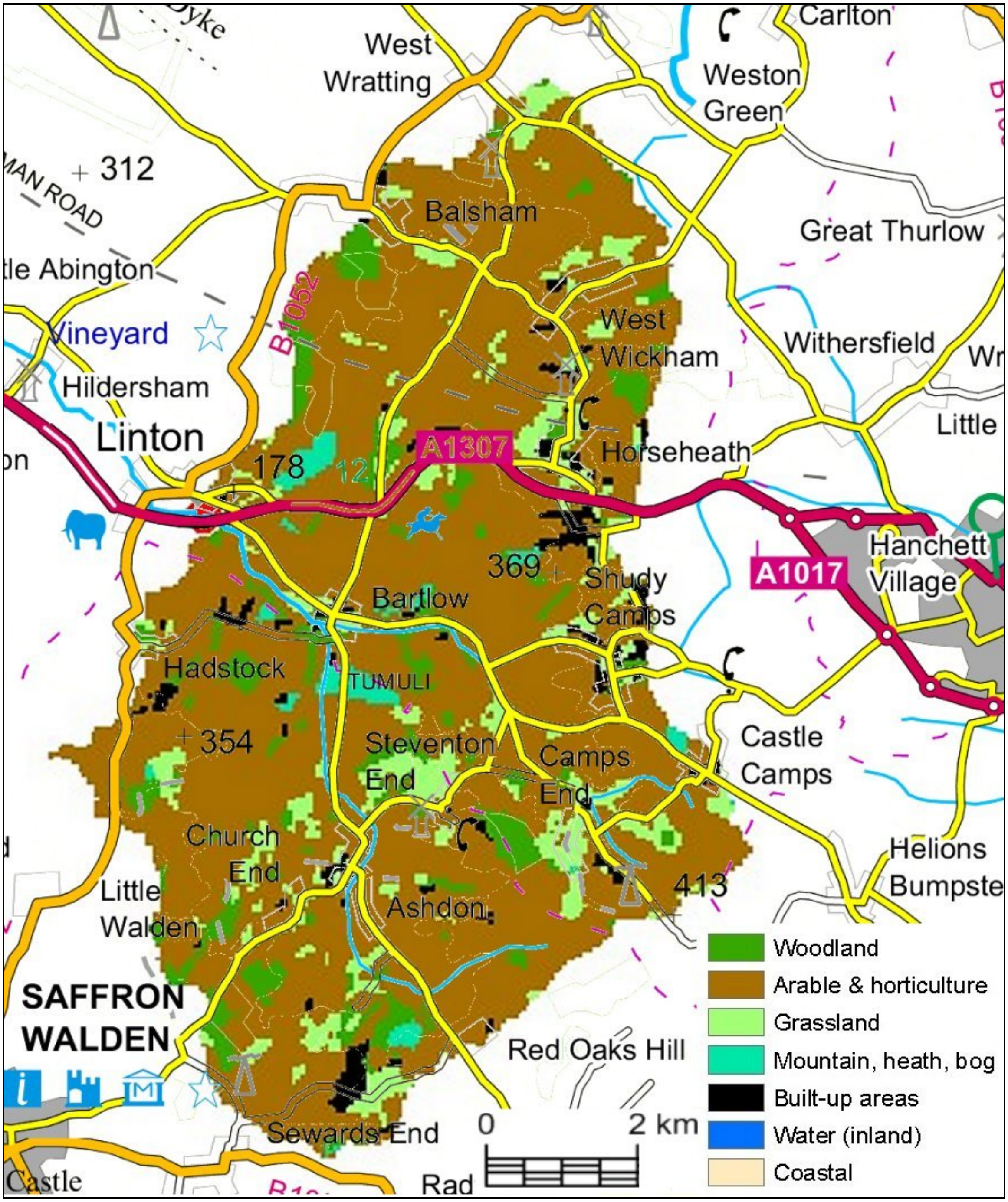

Figure 3.7: Land-Use in the Linton Catchment derived from the Land Cover Map 2000, CEH Monks Wood

Source: http://www.nwl.ac.uk/ih/nrfa/spatialinfo/LandUse/landuse033066.html

3.2.4 Water Management

The flow regime of the Granta is affected by human activity in numerous ways. The high percentage of arable land means that farming has an important influence on water movement. These influences can be categorised as indirect or direct: examples of the former include ploughing which opens macropores encouraging water to infiltrate to deeper levels, and seed drilling which results in more compact soils (Robinson *et al*., 1997). Direct influences include the imposition of artificial drainage on areas of Boulder Clay (Staff, 1946). Field drainage may have the effect of lowering the water table and soil water content in fields, hence reducing groundwater recharge; river flows however may be more sustained by drainage from the top layer of soil. Increases in soil erosion may be another effect of farming, a problem which has intensified since the transition to winter wheats in the 1970s and 1980s which leaves bare ground susceptible to autumn storms after drilling in October. Damaging 'muddy floods' resulting from agricultural runoff have made this a contentious issue sometimes resulting in legal proceedings, and proposed solutions include subsidies for conversion to grassland as well as engineering works to protect property (Boardman, 2003; Boardman *et al*., 1994). In the longer term, erosion may affect both infiltration rates at the surface, and the sediment transfer regime of the catchment.

Intensive farming, in conjunction with a high population, makes requirements for large quantities of water for irrigation and domestic supply respectively. However, Cambridgeshire is one of the driest parts of the country with average annual rainfall of 570 mm (Cambridgeshire County Council, 1998), therefore the demand cannot be met direct from surface rainwater within the catchment. Instead, groundwater abstraction is used with an annual abstraction total of 10^7 m^3 within the county, of which 70% is used for public supply, 30% for industry and agriculture (Cambridgeshire County Council, 1998; Muhlherr and Hiscock, 1997). South Cambridgeshire is supplied almost entirely from chalk groundwater; of the 77 million litres drawn daily by Cambridge Water Company which supplies the area, 97% is drawn from the chalk strata, 3% from greensand and river gravel aquifers (South Cambridgeshire District Council, 2001). Abstraction boreholes that affect the Linton branch of the River Granta are sited at 'Mark's Grave' north of Bartlow, Rivey Hill above Linton, Hildersham and Babraham

(Environment Agency, 1998). The abstracted water is also used to maintain a baseflow level in the summer of 0.04 m^3s^{-1} in the Granta at Linton, preventing the river from drying up as had previously occurred, and was likely to become more frequent as abstraction reduced water table levels (Barrington Local History and Conservation Society, 1979; Staff, 1946).

3.2.5 River Management

As well as human influence on flow paths within the catchment, management of the river channel itself plays an important role in controlling discharge patterns. There are many different reasons why the channel may be modified: to contain the channel or re-route it to somewhere more convenient, to protect or allow the building of near-channel structures, to increase conveyance and provide flood protection. Ancient channel modifications still play an important role, such as the mill pond in Linton linked to the mill construction on what was Linton fen in 1220. Today projects are more likely to have the aim of reversing former changes and returning the channel to its natural state, such as the creation of gravel point bars and riffles in the Granta at Hildersham which are designed to encourage the spawning of wild trout and the growth of aquatic and riparian vegetation (Weightman, 2004; Wood-Gee, 2001).

Where the Granta flows through Linton, more traditional modifications are in evidence. The river has been straightened and its banks reinforced. Weirs have been installed to control the bed gradient and add aeration at low flows. Structures in the channel control its width and depth at certain points such as foot and road bridges, the ford and the mill sluice gates. Vegetation and sediment in the channel are also controlled during routine river maintenance carried out by the Environment Agency in the case of the main river from Linton downstream, and local landowners upstream of this. Weed clearance takes place every year; dredging is carried out at intervals of between 5 and 12 years depending on need, to remove silt which has accumulated in the channel. Dredging of the stream is required in order to maintain flow of water and conveyance capacity and ensure the correct functioning of agricultural drainage systems, and is used especially on steeper sections of topography within the catchment (Dunbar, 2004).

These types of intervention may have far-reaching consequences for the flow regime. The form of the channel is generally simplified, with dredging also restricting the development of channel and bank features (Dunbar, 2004). This is likely to affect rates of process and the extent to which adjustment and dynamism within the channel occur in response to flood peaks (Sear *et al*., 1997). Hydraulic connectivity with the floodplain will also be reduced, with loss of the associated benefits such as flood peak attenuation, sediment storage and nutrient recycling.

3.3 Data Collection

Data collection from the catchment is required for several aspects of the end-to-end modelling process. A long-term rainfall series is required in order to characterise the catchment precipitation regime and build a stochastic rainfall model which can simulate long periods of data. Rainfall, discharge and temperature data are required to calibrate and evaluate a simple rainfall-runoff model to simulate the runoff production and routing processes. Rainfall and discharge data representing subcatchments are also intended to help formulate and guide the rainfall-runoff model structure by improving understanding of spatial variability within different catchment zones. Finally data on inundation extent during the major October 2001 flood event is used to calibrate the floodplain hydraulic model.

3.3.1 Environment Agency Data: Rainfall and Flow

The Environment Agency is able to supply both rainfall and runoff data for the catchment, as detailed below.

(i) Rainfall

Data is available from the following sources close to Linton:

Location	Grid Ref.	Distance from Catchment Centroid	Start Date	End Date	Resolution
Abington Piggot	306445	26.6 km	1/1/1909	31/7/2002	Daily
Cambridge QEW	478558	13.3 km	1/1/1898	31/7/2002	Daily
Little Abington	534495	4.9 km	1/8/1975	31/7/2002	Daily
Linton Chilford	568489	2.6 km	1/1/1976	30/11/2001	Daily
Quy Hall	516612	15.9 km	1/1/1908	31/7/2002	Daily
Bassingbourn	330451	29.3 km	1/8/1999	18/8/2002	15 minute
Bourn	334579	26.4 km	21/10/1991	5/12/2001	15 minute
Burrough Green	641555	11.4 km	1/8/1995	1/1/2002	15 minute
Elmdon	470403	12.9 km	1/8/1991	1/1/2005	15 minute
Fleam Dyke	540549	11.5 km	1/4/1995	18/8/2002	15 minute

Table 3.1: Rainfall gauges close to the Linton catchment, with their corresponding series length and temporal resolution

The location of the gauges is shown in Figure 3.8. The data obtained from the Environment Agency and Meteorological Office raingauges is in either 15 min or daily resolution. Although the closest gauge to the catchment site was of daily resolution and daily data is available for much longer time periods, it was decided that this data did not provide sufficient detail for storm identification, due to the transient nature of much of the rainfall in the Linton area. The 15 min series is therefore be used for profile analysis and modelling. There are three gauges providing 15 min data close to Linton: Burrough Green, Elmdon and Fleam Dyke. A traditional approach would be to construct a synthetic record based on a spatially weighted interpolation of the gauged data; however in this application the use of a single record was felt to be important, to properly characterise storm profiles and other characteristics which would be blurred if average values were taken from a moving storm. The record from Elmdon was therefore used as it provided 13.5 years of data as oppose to the shorter 7 year records from the alternative sites, with relatively few gaps in the data series.

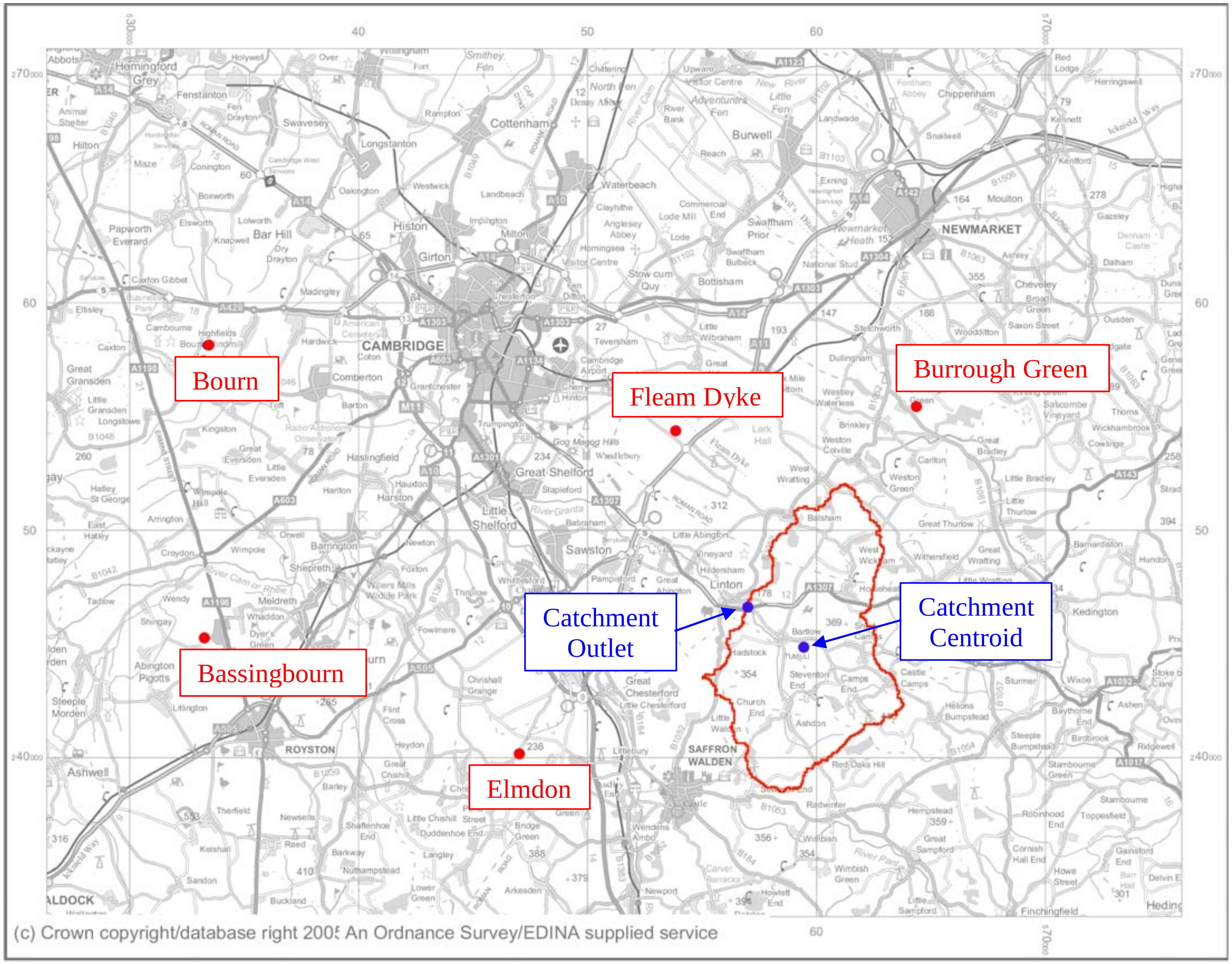

Figure 3.8: Raingauge Locations in the Linton Area

(ii) River Flow

The following table shows river flows measured close to Linton. This study is primarily concerned with those stations on the River Granta.

Location	River	Grid Ref.	Catchment Area (km^2)	Start Date	End Date	Resolution
Linton	Granta	TL 570464	60.0	28/8/1985	1/1/2005	15 min
				2/1/1982	1/8/2002	Daily
Babraham	Granta	TL 510504	98.7	5/1/1979	21/8/2002	15min
				2/12/2000	1/8/2002	Daily
Stapleford	Granta	TL 471515	114.0	5/9/1985	21/8/2002	15min
				1/1/1985	1/8/2002	Daily
Chesterford	Cam	TL 505426	141.0	19/1/1988	21/8/2002	15min
				1/1/1988	1/8/2002	Daily
Dernford	Cam	TL 466506	194.0	2/10/1979	21/8/2002	15min
				1/1/1979	1/8/2002	Daily

Table 3.2: Flow gauges on the Rivers Cam and Granta, with their corresponding series length and temporal resolution

Information on each of the weirs is available through the National River Flow Archive (2002).

Location	Weir Type	Notable Details
Linton	Compound Crump Weir	Structure drowns when water level exceeds 0.46m. River is pump supported to maintain flow of 0.03 m^3s^{-1}. Runoff influenced by abstraction and effluent returns.
Babraham	Triangular profile Flat V Weir	Significant groundwater abstraction. Runoff influenced by abstraction and effluent returns.
Stapleford	Compound Weir with Crump notch	Flow readings can be unreliable. Runoff influenced by abstraction and effluent returns.

Table 3.3: Details of Gauging Stations on the River Granta

3.3.2 Temperature

The rainfall-runoff model, specifically the nonlinear rainfall to effective rainfall transform, requires an estimate for ambient temperature at the time of each sample (Section 5.2). For the period 1/1/1995 – 16/8/2005, temperature data is available at 30 minute intervals (AT&T Laboratories, 2005) and a simple interpolation is used to give 15 minute data. However, for the period 1/1/1991 – 1/1/1995, rainfall and flow data are available at 15 min intervals but temperature data is available only as daily maximum and minimum (BADC, 2005). An algorithm must therefore be used to approximate the daily temperature curve at 15 minute intervals from these data. Downscaling methodologies that have been used in the past range from the simple, e.g. approximation by single sine curve (Allen, 1976; Gelegenis, 1999) through the use of a combination of Fourier harmonics with varying trend (Axelsson, 1998; Vinnikov *et al*., 2004) to the highly complex, such as stochastic weather generators based on GCM output (e.g. Dibike and Coulibaly, 2005).

In this case, the information on the local temperature regime that could be extracted from the 30 minute temperature data was felt to provide the optimal basis for disaggregation. Following Feidas *et al*. (2002) and Peters and Evett (2004), local data from a reference site were used to perform disaggregation based on a single daily measurement. In their study, the reference curve was found as the average of two recorded year-long curves; however the same technique is not suitable for use when taking an average over a large number of years of reference data. There would be an overestimation of temperature variability in the catchment when the average shape of the data was rescaled to reach the maximum and minimum points. Instead, the daily temperature pattern was considered as 3 distinct periods: rise in temperatures from dawn to peak temperature, cooling from peak temperature to sunset, cooling at a separate rate during night hours. The average shape for each period was recorded, and the average time from sunrise to maximum temperature, using data from the period 1/1/1995 – 16/8/2005, enabling an estimated temperature curve to be reconstructed for any given day given knowledge of the maximum and minimum temperature, together with the sunrise and sunset times. This method was then used to reconstruct the 15 minute temperature series for all dates and times when the 30 minute series was not available. A typical example of the results is shown in Figure 3.9, and the complete reconstructed time series in Figure 3.10.

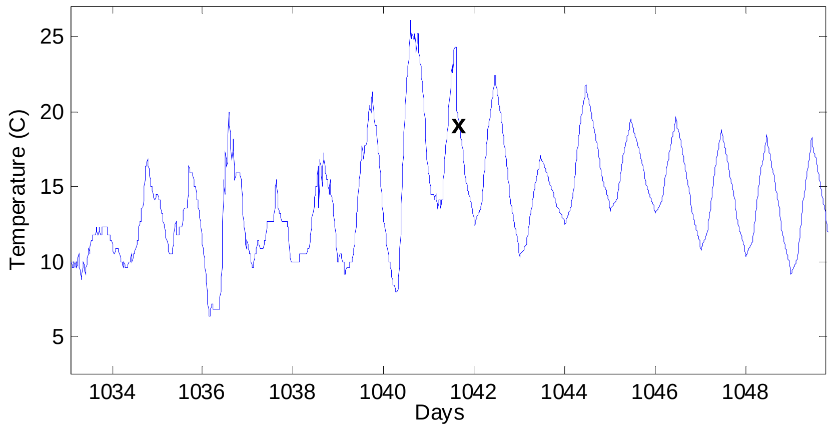

Fig 3.9: Recreation of Temperature Curve. 'x' marks the end of the recorded temperatures and start of the recreated series.

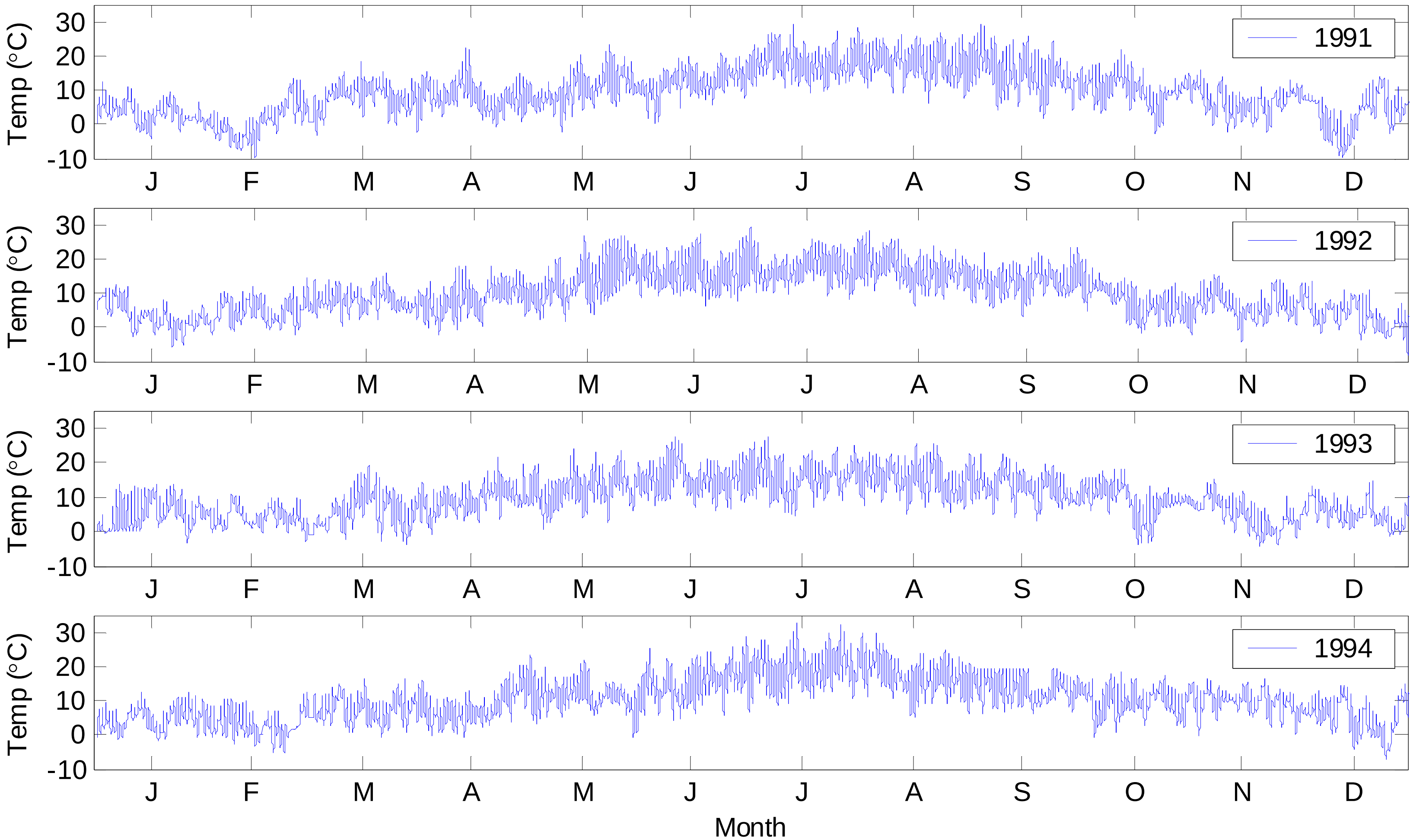

Figure 3.10: Complete Reconstructed Temperature Series for the Years 1991-1994

3.3.3 Tributary Flow Gauging

3.3.3.1 Gauge Details and Location

Environment Agency and Meteorological Office datasets provide historical data for the catchment, but do not provide the local data necessary for detailed modelling of the hydrological regime around Linton. The Environment Agency has responsibility only for the main river downstream of Linton so does not hold information on the upper reaches of the catchment. By a more specific study of the catchment upstream of Linton it was felt that a deeper understanding of the local hydrology would be gained. To achieve this, runoff was monitored on each of the individual subcatchments contributing to the Granta at Linton. This took the form of the use of two velocity/depth gauges placed in the two main tributaries of the Granta which meet at Bartlow (see Table 4 and Figures 3.1, 3.2). There is a small third tributary, however the flows in this are very low due to groundwater abstraction and it was felt that the upper catchment could be adequately represented by knowledge of the two main input flows and the total flow recorded at Linton. The flow gauge to be used is a Starflow Ultrasonic Doppler which is capable of measuring speeds down to 0.021 ms^{-1}, suitable for channels with low flows such as those at Bartlow. The gauge measures the average velocity in a vertical section of water above and in front of the gauge. For use in calculating discharge this measurement must be transformed into average velocity over the cross-section: methods for doing this are described in Section 3.3.3.4. The exact locations of the two gauges are given below, and are illustrated in Section 3.3.3.3.

Location (Grid Ref)	Details
TL 583 449	Bourn tributary flowing through tunnel under disused railway. Regular channel profile, gravel bed.
TL 484 451	Camps tributary flows through bridge under Bartlow-Ashdon road. Regular channel profile, mud bed.

Table 3.4: Details of Flow Gauge Locations

Both the tributaries rise in the high ground south-east of Linton, the Bourn Tributary draining northwards, and the Camps Tributary draining westwards. In order to make a further comparison of the two tributary catchments, statistics for each were obtained using the database included with the Flood Estimation Handbook. Pertinent attributes are given in Table 3.5.

Statistic	Bourn Tributary	Camps Tributary
Area (km^2)	22.25	14.83
Mean Altitude (m)	93	95
Mean Aspect (deg from N)	2	284
Mean Slope (m/km)	37.2	37.3
Longest Drainage Path (km)	9.38	7.98
Mean Distance to Outlet (km)	5.19	4.38
Urban Land Cover 1990 (%)	0.008	0.005

Table 3.5: Tributary Catchment Statistics

The statistics show that the two tributary catchments have very similar topographical character. The Camps Tributary drains approximately two-thirds the area of the Bourn Tributary and has a correspondingly shorter 'longest drainage path' and 'mean distance to catchment outlet'. However, the altitude and slopes of the catchments are very similar and both are predominantly rural. One attribute of the catchments which is not easy to characterise is the extent to which each is influenced by groundwater. This could be in terms of sink points where surface water infiltrates to aquifers, or source points such as springs. This feature may however have significant effects on the hydrological regime of the two catchments, and is considered further in the review of recorded catchment hydrometry (Section 3.4).

3.3.3.2 Discharge Calculation: Method Choice

Two possibilities were considered in order to calculate discharge from the velocity / depth measurements.

1. Stage-Discharge Relation

This method assumes that there is a unique relation between depth and discharge, i.e. that the channel shape will remain constant and that the depth of the river also specifies its average velocity. This assumption is likely to be valid where the riverbed is very stable; the two gauging locations chosen have reasonably stable profiles; however the relationship could be compromised by movement of sediment changing the channel slope. This methodology is also susceptible to hysteretic characteristics in the stage-discharge relation resulting from backwater effects. The validity of the method can be partially tested by plotting velocity-depth relationships for the data to check for a single relationship. It uses only the depth time-series recorded by the Starflow, which has the disadvantage that not all the data available is used; however this could be seen as an advantage given that the velocity measurement of the Starflow was more often subject to error than the depth measurement.

2. Velocity-Area Method

This method would use the both the depth and velocity time series recorded. A survey of the river would be carried out to relate depth to cross-sectional area. The velocity recorded by the Starflow would then be transformed into mean velocity for the cross-section. This would be calculated using analytical calculations of velocity profile within the channel area. Cross-sectional area would then be multiplied by mean velocity to find discharge. The removal of the assumption that the channel has a stable depth:velocity relationship makes this a more robust method; however it restricts the length of time series that are available as both depth and velocity data must be present.

In order to make a decision, depth-velocity curves were plotted for both sites, using the hydrographs for which depth and velocity had been successfully measured by the Starflow (Figure 3.11). Study of the depth-velocity curves show that for a given depth, velocity may vary considerably. The Bourn tributary has the more stable relationship; however use of an averaged depth-velocity curve could typically lead to errors in velocity of up to 30%. The Camps tributary has a less stable relationship and errors could reach 40%. In part this is due to the hysteresis visible in the velocity-depth relationship (e.g. hydrograph 3 of Figure 3.11B). In both cases it was decided that the relationship was not sufficiently well-defined for use of the stage-discharge method and that velocity-area method should be used in preference.

(A)

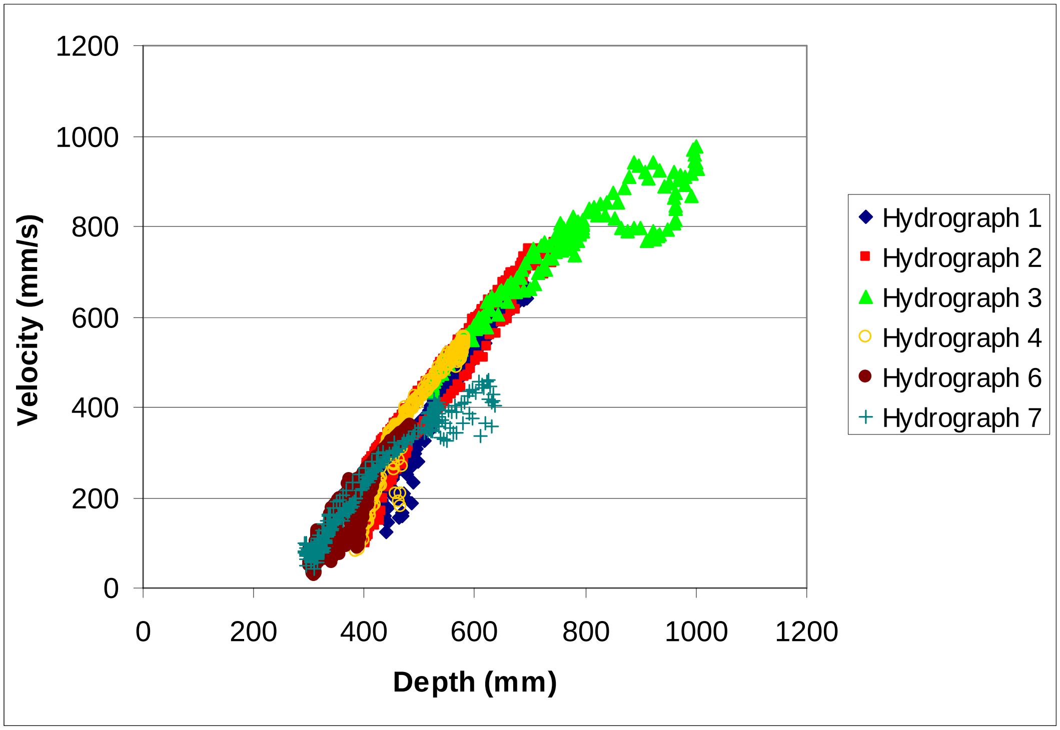

(B)

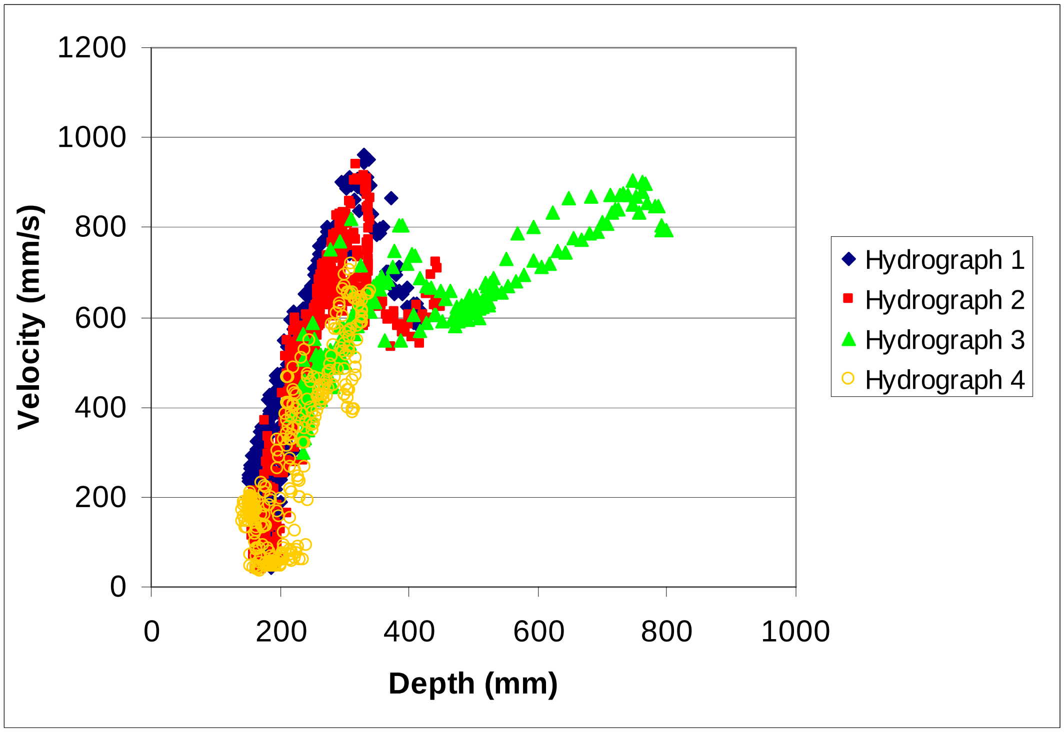

Figure 3.11: Depth-Velocity Curves for individual hydrographs recorded at the (A) Bourn tributary and (B) Camps tributary meeting at Bartlow

3.3.3.3 Discharge Calculation: Channel Survey

In order to calculate the discharge of each channel from measurements of the velocity and depth, the cross-sectional profile of the channel must be known. The gauges were both deliberately placed in locations where the channel was constrained against overbank flow and of a regular shape. In the case of the River Bourn this was inside a tunnel under a disused railway (Figure 3.12), for the Camps tributary it was at one side of a bridge structure (Figure 3.13). By this choice of location, the typical problems of flows outside of the surveyed channel are avoided in all but the most severe floods: during the gauging period the river stayed in-bank throughout.

Figure 3.12: Location of Flow Meter on Bourn Tributary

Figure 3.13: Location of Flow Meter on Camps Tributary

The two channels were surveyed at the locations of the flow meters, and the results are shown in Figure 3.14. The survey was carried out using a telescopic level mounted on a tripod on the riverbank to read the depth of the riverbed below the (arbitrary) survey point using a graduated pole. A Matlab routine was written to convert the depth of water recorded by the Starflow into a cross-sectional area for the river, using linear interpolation between the survey points as shown in the profiles. The relationship is also shown graphically in Figure 3.14.

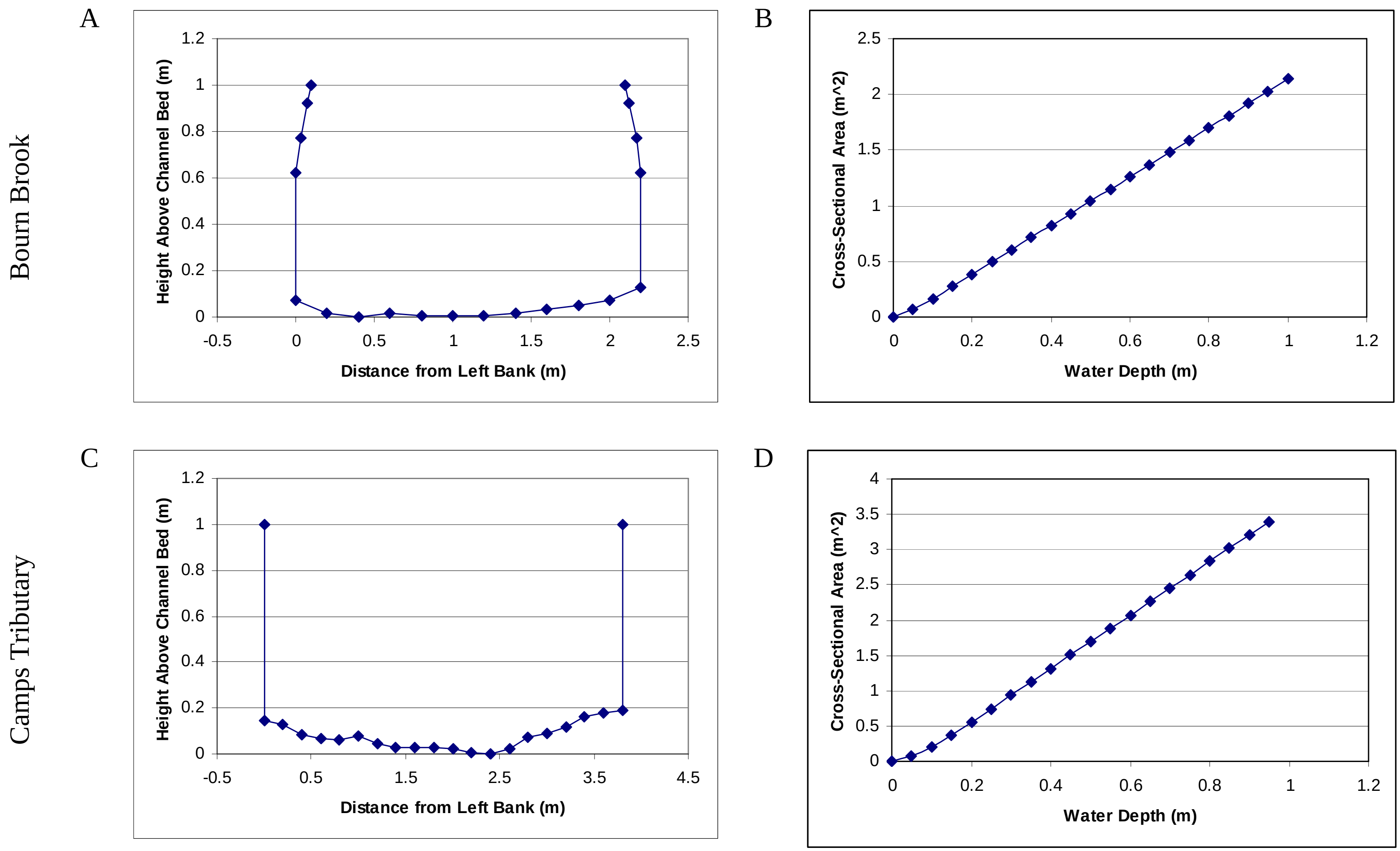

Figure 3.14: Channel Cross Sectional Profiles for (A) Bourn Brook and (C) Camps Tributary. Also depth: cross-sectional area relationships for (B) Bourn Brook and (D) Camps Tributary.

3.3.3.4 Discharge Calculation: Mean Velocity Calculation

In order to calculate discharge, the mean velocity over the channel cross-section must be known. The Starflow records only the mean velocity over a vertical column so a conversion must be found. One possible way to do this is through manual calibration gauging, where a series of velocity measurements are made across the cross-section in order to calculate the total discharge as a sum of discharges between bounding verticals. This method is labour-intensive and relies on the ability to make such measurements during periods of high flow as the velocity : mean velocity relationship may change with depth. It was not found possible to use this method for the Linton tributaries as during the season that the measurements were scheduled, low groundwater levels led to lack of any high flows during fieldwork visits.

Instead, the theory of velocity profiles in open-channel flow may be used to produce an analytical relationship between mean vertical velocity and mean cross-sectional velocity. The theory relies on the Prandtl – von Karman universal velocity distribution law or ‘Law of the Wall’ which states that the velocity distribution in turbulent flow is a logarithmic function of the distance from a solid surface. The law is used by Chow (1959) to perform an integration of resulting velocities within a natural channel of arbitrary shape and hence to derive the mean velocity over the channel. In the case of the two study channels, the cross-sections are such as to allow the shape to be approximated as a rectangle, greatly simplifying the calculations. Using this approximation the mean velocity is found as:

$$\tilde{v} = 2.5 \cdot v_f \cdot \ln\left(\frac{h}{y_0} \cdot \exp\left(-1 - \frac{h}{w} \right) \right) = 2.5 \cdot v_f \cdot \left(\ln\left(\frac{h}{y_0} \right) - \left(1 + \frac{h}{w} \right) \right) \qquad (3.1)$$

where v_f is the shear velocity, h is the depth of water, w is the channel width, and y_0 is a constant which depends on the surface roughness height of the channel bed by the equation:

$$y_0 = m \cdot k \qquad (3.2)$$

where k is the typical roughness height and m is a constant which was found to be equal to approximately 1/30 by experimentation with flow in rough pipes (Nikuradse, 1933).

Using similar methodology, an integration is performed to find the theoretical mean velocity in a vertical column, in terms of the same quantities (all variables as before).

$$\bar{v}\cdot(h-y_0)=\int_{y_0}^{h}2.5\cdot v_f\cdot\ln\left(\frac{y}{y_0}\right)dy$$
$$=\int_{y_0}^{h}2.5\cdot v_f\cdot\ln y\cdot dy-\int_{y_0}^{h}2.5\cdot v_f\cdot\ln y_0\cdot dy$$
$$=2.5\cdot v_f\cdot[y\cdot\ln y-y]_{y_0}^{h}-2.5\cdot v_f\cdot[y\cdot\ln y_0]_{y_0}^{h}$$
$$=2.5\cdot v_f\cdot\left[y\cdot\ln\left(\frac{y}{y_0}\right)-y\right]_{y_0}^{h} \tag{3.3}$$
$$=2.5\cdot v_f\cdot\left[h\cdot\ln\left(\frac{h}{y_0}\right)-h+y_0\right]$$
$$\Rightarrow\bar{v}=2.5\cdot v_f\cdot\left[\frac{h}{h-y_0}\cdot\ln\left(\frac{h}{y_0}\right)-1\right]$$

These two results may then be used to find the theoretical relationship between the mean vertical velocity and the mean channel velocity:

$$\frac{\tilde{v}}{\bar{v}}=\frac{\ln\left(\frac{h}{y_0}\right)-\left(1+\frac{h}{w}\right)}{\left(\frac{h}{h-y_0}\right)\ln\left(\frac{h}{y_0}\right)-1} \tag{3.4}$$

A Matlab routine was written to convert mean vertical velocity recorded by the Starflow into the mean channel velocity, using this equation. The value of k, the roughness height, was estimated as 4 cm, typical of the gravel, brickwork irregularities and small plants found on the channel bed and sides at the flow meter locations. Figure 3.15 shows an example hydrograph reconstructed using a range of values of k, demonstrating that the estimate is relatively insensitive to this parameter.

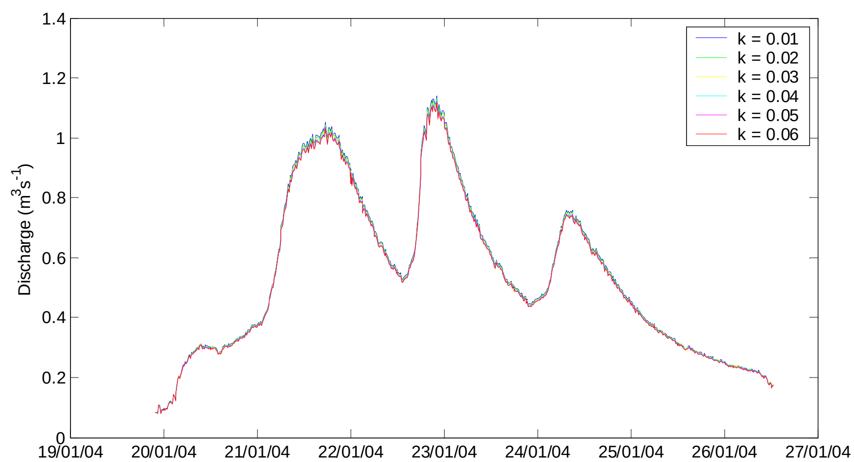

Figure 3.15: Variation of reconstructed discharge according to roughness height

3.3.4 Inundation Data: Residents Survey

Data on the floodplain inundation extent during the 2001 flood is required to evaluate the model performance in terms of both channel and floodplain flow behaviour. Traditionally extent has been captured using remote sensing: reviews of methodology are available in Bates (2004) and earlier Bates *et al*. (1997). Options include photogrammetry (Lane *et al*., 2003), analysis based on a comparison of trash lines with topographic LIDAR data (Lane *et al*., 2003) and, most often used, satellite SAR data (Bates and De Roo, 2000; Oberstadler *et al*., 1997) which can be used in conjunction with image processing methods to identify flood outlines (e.g. Horritt *et al*., 2001). Satellite data are best suited to large catchments with slow response times, as flood outlines are typically recorded to a pixel size of 30 – 50 m, and extended flood peaks give a higher probability of image capture. In order to capture flood depths close to the maximum in Linton in 2001, a satellite image would have needed to be captured within approximately a 4 hour window, and no such image is available. Recent improvement in resolution has come from airborne SAR (Horritt *et al*., 2003) giving pixel sizes of 0.75 – 1.50 m, however this methodology is expensive and data must be acquired on an event-by-event basis.

Instead, the option that was chosen was a survey of affected residents after the event. This type of approach provides an accessible option for flood assessment in small flashy catchments, where the flood peak is not of sufficient duration for other methods to be deployed. It is also a low-cost option that has the potential to be used in a wide variety of applications where there may not be emergency funds available for an immediate response to a flood event. These types of considerations are very important if a flood modelling technique is to be useful in the small, agricultural, lowland catchments that have increasingly been perceived to have been affected by flooding in recent years. The method has been successfully used in the past for model validation (Connell *et al*., 1998; Connell *et al*., 2001).

To implement the survey, questionnaires were sent to each flooded building. This was co-ordinated by members of the Parish Council who were keen to provide accurate data for the current study and who were best able to communicate the requirements to the residents due to their respect within the community. It was also found that homeowners were enthusiastic to provide complete information on their experience of the flood, in the hope that it might be used to improve the response to future events. Information was collected on several aspects of the flood inundation. These included maximum flood depth, timing of maximum water depth and rate of water ingress. The complete data set acquired is presented in Appendix B; Figure 3.16 below shows a summary of the maximum depths recorded at each house for which a survey was returned.

The map of flood depths serves to demonstrate some of the advantages and disadvantages of the method. The collection method is open to bias because it relies on memories and perceptions of the event, and therefore the expected precision of the data is low. It is also possible that worries of insurance blacklisting or concerns to emphasise the major effects of the flood led depths to be under or over-estimated accordingly. The record provides point data only: it is not known whether houses suffered varying depths of flood, and data is not equally spaced in the flooded area. Also, it is not possible to guarantee that houses where no data was recorded were not flooded, as some houses were empty at the time of flooding and neighbours were not able to provide estimates of flood depth. Despite these disadvantages, the approach can capture a much greater depth of information than the simple flood extent recorded when SAR is used, and this extra data can be used to compensate for other omissions. For example, although the data set does not provide definite ‘negatives’ for houses that were not flooded to prevent overestimation of flood envelope, the depths recorded at each house can instead be used to avoid overflooding in the model. Time to peak and timing of flood peak can similarly be used to test the speed and shape of the modelled wetting front in a way that is not possible with instantaneous remote-sensed data. Finally, an attempt was made to validate the accuracy of individual records by comparison with neighbouring houses, and any obvious outliers that could not be caused by underlying terrain were removed.

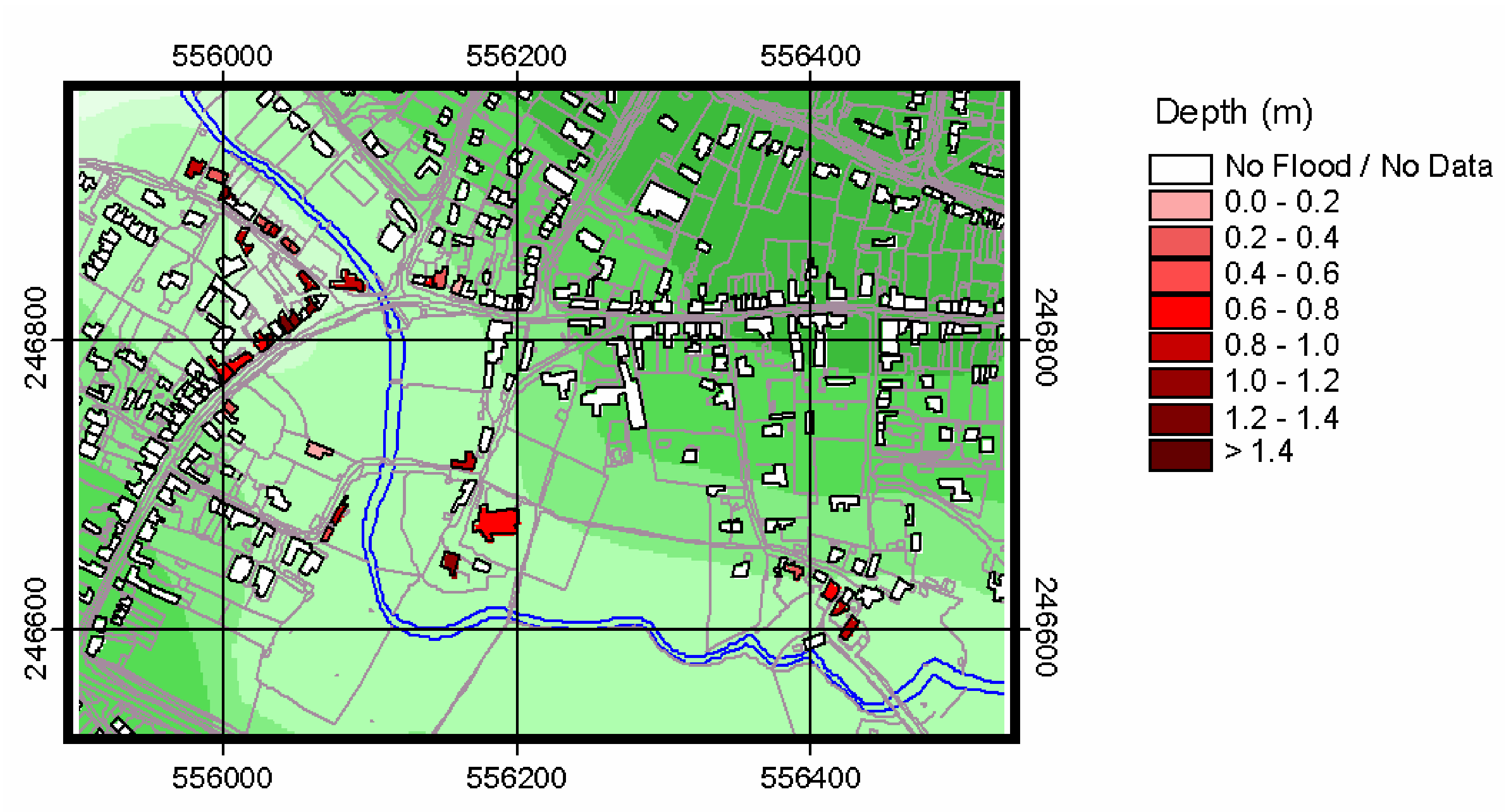

Fig 3.16: Maximum flood depths recorded on 20/21 October 2001, mapped from survey of residents.

3.4 Hydrological Review of Field Site

As discussed in Section 2.2.1, knowledge of the hydrological response characteristics of the catchment should both inform and be informed by modelling methods and results. In part this catchment knowledge derives from field observations and study of the physical form of the catchment, but it is also gained from a study of past response both long-term and to individual rainfall events. In order to take advantage of this information, an investigation was made of catchment behaviour in terms of the data series available for the River Granta. The series used were those to be used in testing the model: the 15 min rainfall series from Elmdon and the discharge series for Linton.

3.4.1 Hydrometeorology

The 15 min rainfall series for Elmdon is shown in Figure 3.17; the gaps present in 1995 and 1999 are due to missing data caused by gauge malfunction. In order to interpret the data in terms of catchment input, the rainfall was summed by month. The totals were recorded for each year, and the minimum, maximum and mean values are shown in Figure 3.18. This demonstrates the characteristic yearly cycle: the rainfall is spread fairly evenly throughout the year with the exception of September and October which are particularly wet. A small peak is also seen in April. The rainfall bounds show that the precipitation can be highly variable between years, with low rainfall totals seen even in winter months. This idea is explored further in Figure 3.19, which shows the seasonal rainfall totals for each year. These provide a visualisation of likely groundwater fluctuations, the winter total being particularly important but also influenced by the summer total controlling the groundwater level at the end of the summer recession.

The monthly totals of rainfall characterise groundwater levels in the catchment; however, as discussed in Section 3.2, flood peaks are generally caused by short duration, high intensity rainfall events when overland flow, soil throughflow and groundwater discharge all contribute to channel flow. The susceptibility of the catchment to this type of event can be visualised by plotting the maximum 24-hour rainfall occurring each month; Figure 3.20 shows the range and mean statistics. The pattern is similar to the monthly total rainfall, with the months September and October showing high 24-hour totals as well as high monthly totals. As recent experience suggests that destructive floods are typically caused by high-volume, high intensity rainstorms on top of high baseflow levels, these two months are a particularly high risk period. The variation in the seasonal 24-hour rainfall maxima over the study period is shown in Figure 3.21. This, together with Figure 3.19 (seasonal rainfall totals), clearly demonstrates the cause of the 2001 floods as the unusually high 24-hour total occurred after an unusually wet summer season and during a winter of medium-high rainfall total.

The rainfall patterns should also be used to guide the choice and structure of rainfall simulation model described in Chapter 4. The difference in total monthly rainfall between consecutive months is relatively small, and even less when the 24-hour maximum is considered. This uniformity signals that it is unlikely to be necessary to consider each month separately in any rainfall simulation; instead it may be sufficient to simply use a wet season including the autumn months, and a dry season.

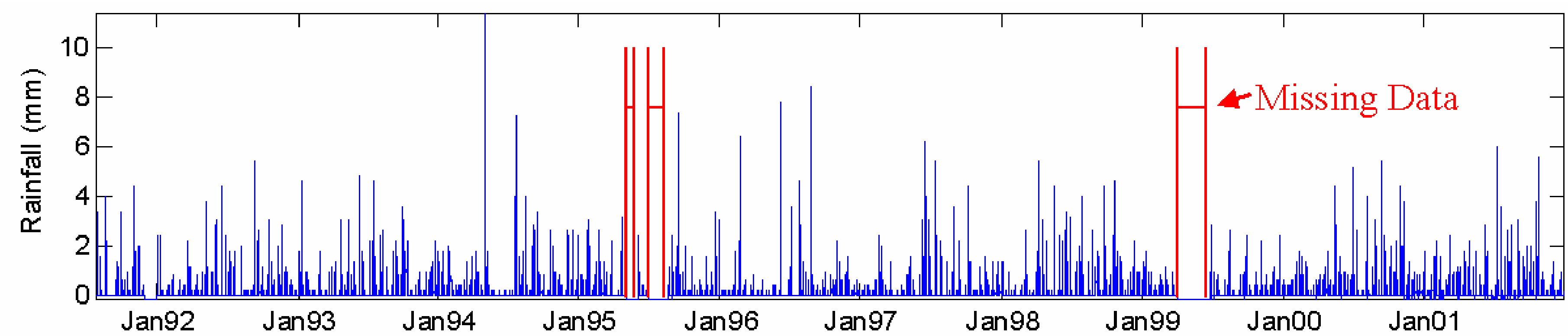

Figure 3.17: 15 min rainfall data from Elmdon

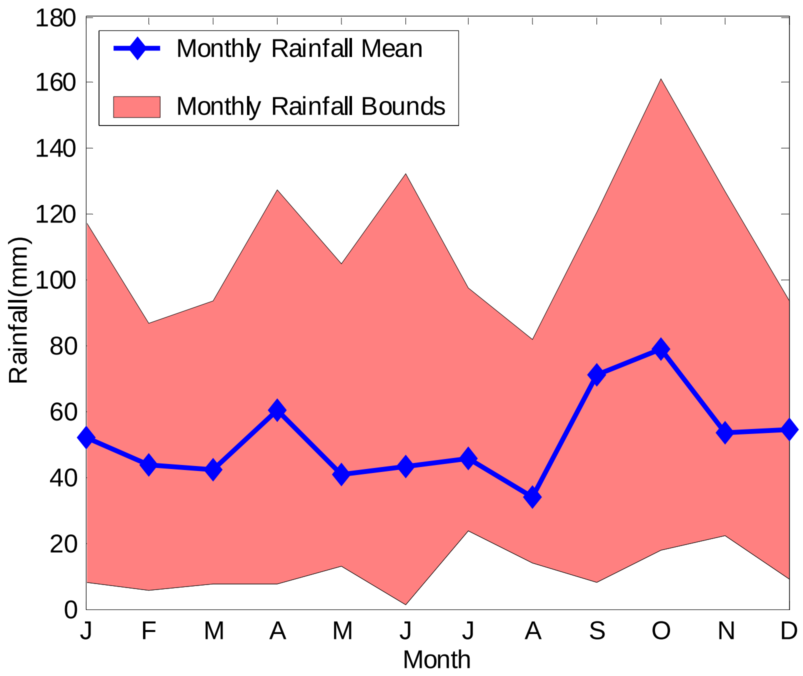

Fig 3.18: Mean and Range of Monthly Rainfall at Elmdon: 1992-2001

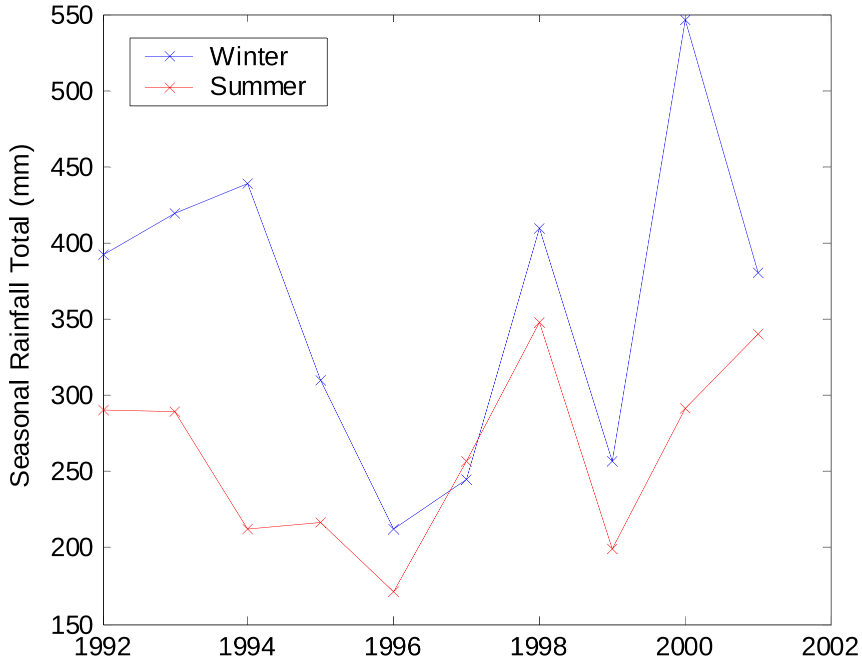

Fig 3.19: Seasonal Rainfall Totals at Elmdon
Winter: September – February
Summer: March - August

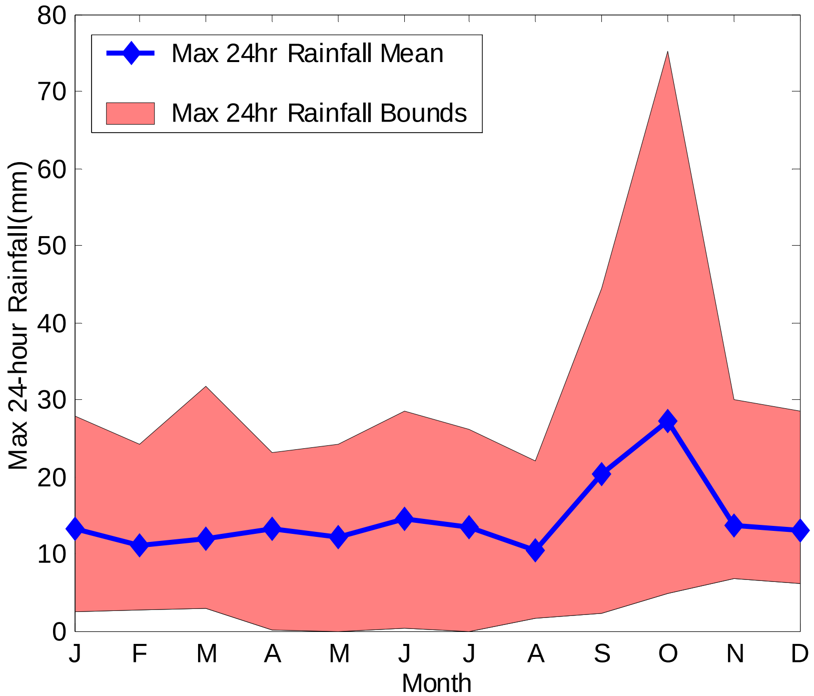

Fig 3.20: Maximum 24hr Rainfall: Mean Value and Bounds by Month

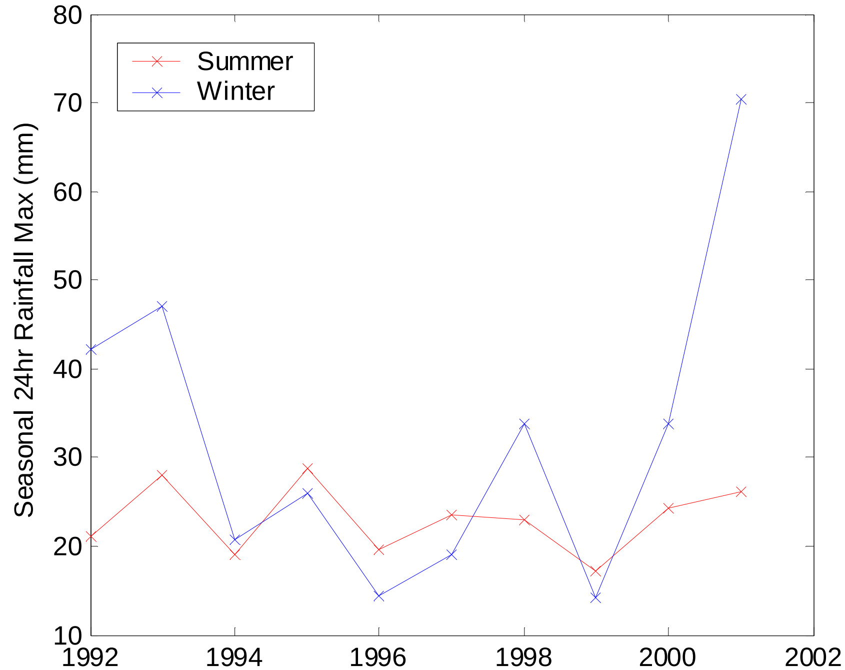

Fig 3.21: Maximum 24hr Rainfall by Season and Year
Winter: September – February
Summer: March - August

3.4.2 *StreamFlow Characteristics*

The flow data from Linton is shown in Figure 3.22 and demonstrates the strong baseflow influence which would be expected from a chalk catchment with high groundwater dependence. Referring back to Figure 3.19 showing the seasonal rainfall totals, the winters of 1996/1997 and 1997/1998 which have low rainfall totals are seen to coincide with low baseflow years, as would be expected. Visual examination suggests a strong link between baseflow level and local flood peaks, suggesting that accurate representation of baseflow will be an important component in any flood simulation or forecasting system for the catchment. One cause of this is likely to be the baseflow level acting as a proxy variable to represent catchment wetness conditions.

When using measured flow data to make inferences about flood characteristics of the Granta, the limitations of the gauging station must be taken into account. The flow gauge on the Granta at Linton is primarily designed for the measurement of low flows, and is drowned when upstream depth relative to the gauge exceeds 0.46 m (National River Flow Archive, 2002). This is demonstrated by considering the flood of 21st October 2001 which provided the inspiration for this project, and comparing it to the less severe flood of 28 November 2000. The 2001 flood caused extensive damage to homes and businesses in the village whereas the 2000 flood caused no damage to property. The flow record (Figure 3.22) shows these floods as having similar maximum flow, however local record documents that the river level was raised by 9 ft during the 2001 flood in comparison to 4.5 ft during the 2000 flood (Linton News, 2000;2001). A report by Halcrow (2004) records evidence from Environment Agency staff that during the 2001 flood, the weir was drowned out and the float to measure level also jammed.

To study broad patterns of baseflow levels in the catchment, the total flows are plotted by month in Figure 3.23. These are also summed into seasonal totals and plotted by year in Figure 3.24. In contrast to monthly rainfall totals which showed a definite peak in September and October, monthly flow totals show a smooth variation through the year, with the September/October rainfall maximum translating into a flow maximum in January. This shows the lag time associated with the filling of groundwater stores and demonstrates again the importance of antecedent conditions and hence long-term rainfall averages in conditioning catchment behaviour. To illustrate this more clearly, Figures

3.27 and 3.28 show water balance characteristics by month in the catchment, in terms of runoff ratio and catchment losses respectively. The runoff ratio is low through the summer as high evapotranspiration means that little water infiltrates to the water table. In September and October, runoff ratio remains low despite lower temperatures and increased rainfall, as rainwater recharges the soil and groundwater stores. This is demonstrated by the peak in catchment losses during these months. The peak runoff ratio comes in January suggesting that during this month the catchment is at its wettest and groundwater stores are at their peak. Even in January, however, the mean monthly flow total does not exceed one third of the mean monthly rainfall total. Water balance figures are also shown on a year-by-year basis (Figure 3.29), showing that catchment losses vary broadly in line with rainfall totals. Runoff ratio does not follow the same pattern, and may be more closely linked to temperature, as shown by the low ratio in the hot, dry year of 1997.

The range of monthly totals and maxima is also shown on the figures. The minimum values must be used with some caution, as low totals can reflect missing data. It is clear, however, that range varies widely across the year, with winter flow values much more variable than their summer counterparts. For rainfall totals the pattern was less pronounced, although it is evident that months with higher mean rainfall also tend to have a greater range. When creating rainfall and flow simulation it may be necessary to model months with high range in greater detail, to capture the full range of extreme behaviour.

Figures 3.25 and 3.26 above are plotted to show the instantaneous flow maxima, both by month and by year. These values are dependant not only on baseflow levels but also on surface runoff caused by heavy rainstorms. Although the flow maxima bounds are constrained by the malfunctioning of the gauge above around 5.5 m^3s^{-1}, it is clear that it is possible for flows in summer to attain high levels, driven by the summer thunderstorms that occur frequently in Cambridgeshire. In general however, the peak flows in the summer months of March – September are lower than in the winter months October – April. In the case of both summer and winter, high peaks do not occur in low-groundwater years, demonstrated by Figure 3.26 in the years 1990, 1996 and 1997.

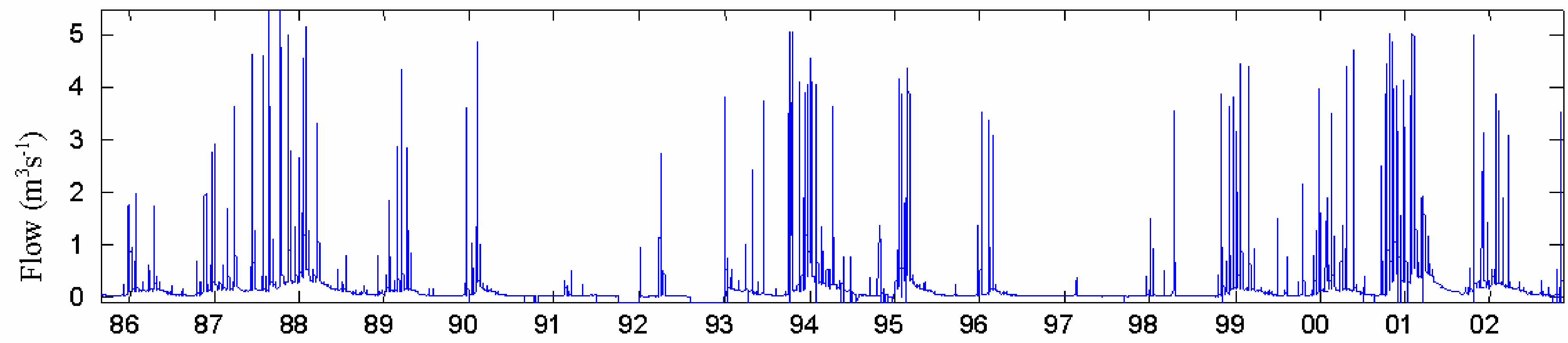

Figure 3.22: 15 min Flow data from Linton

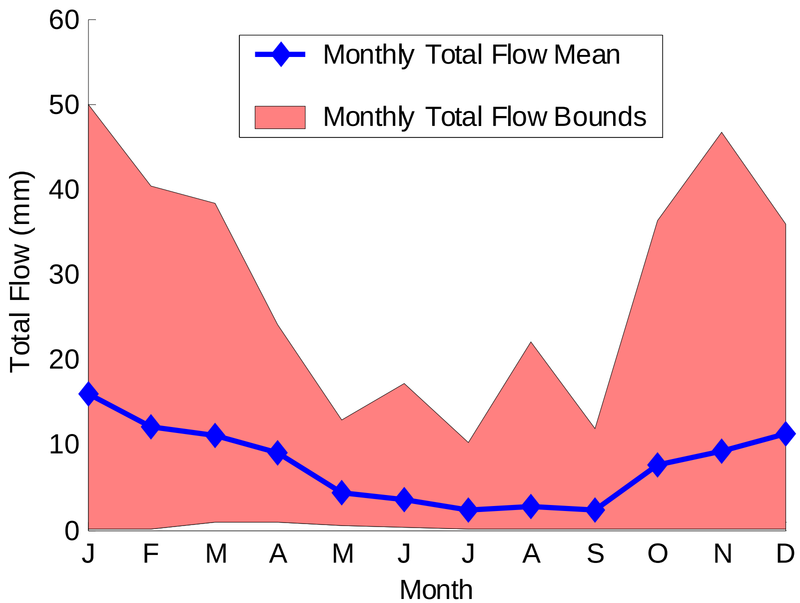

Fig 3.23: Mean and Range of Total Monthly Flow at Linton: 1986-2001

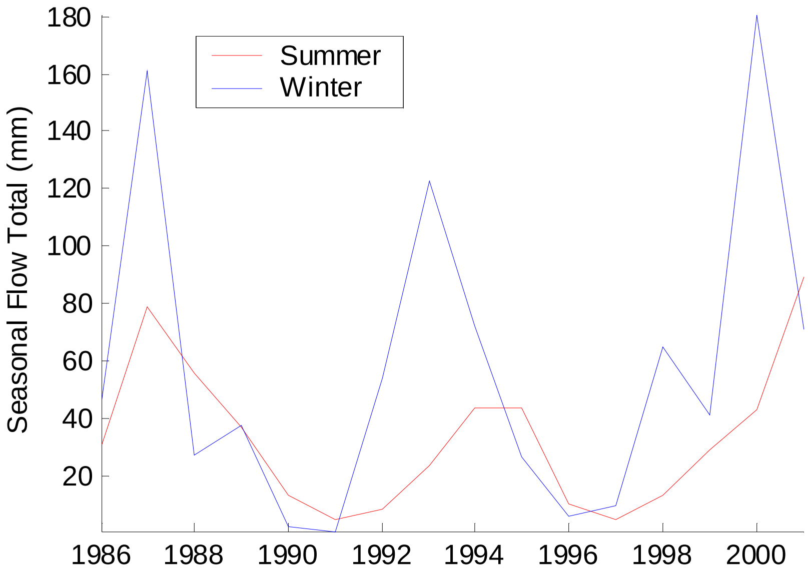

Fig 3.24: Seasonal Flow Totals at Linton
Winter: September – February
Summer: March - August

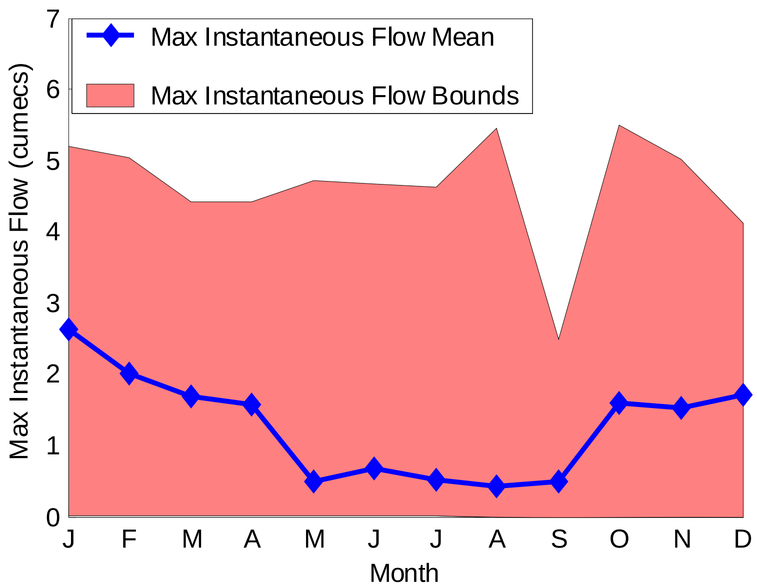

Fig 3.25: Mean and Range of Monthly Instantaneous Flow Maxima at Linton: 1986-2001

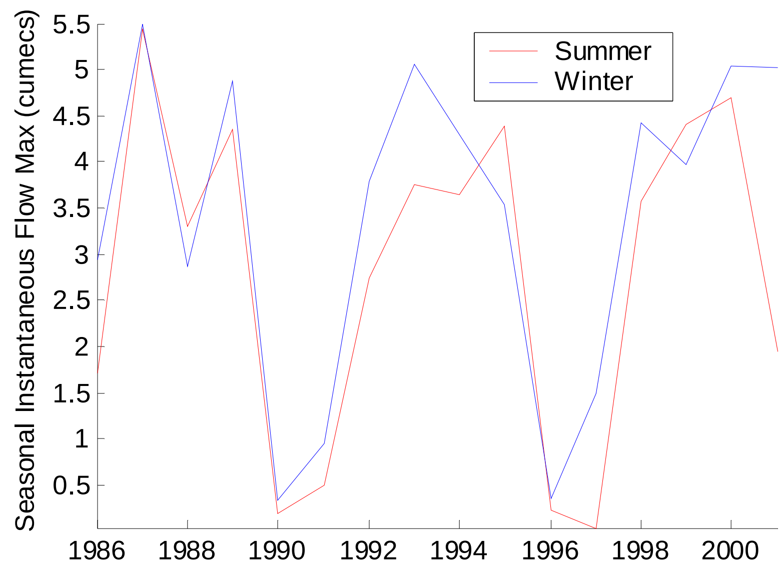

Fig 3.26: Seasonal Instantaneous Flow Maxima at Linton
Winter: September – February
Summer: March - August

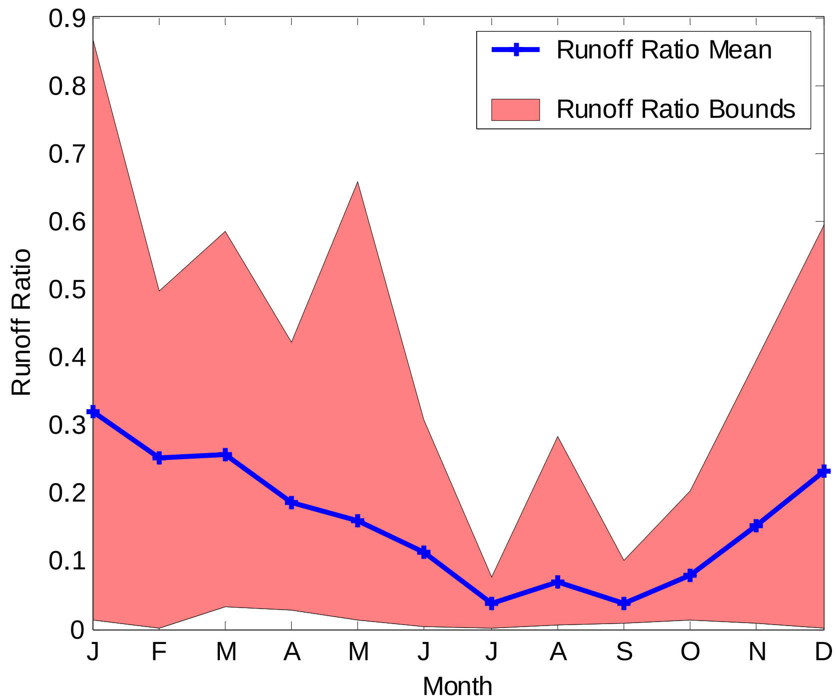

Fig 3.27: Mean and Range of Monthly Runoff Ratio at Linton: 1992-2001

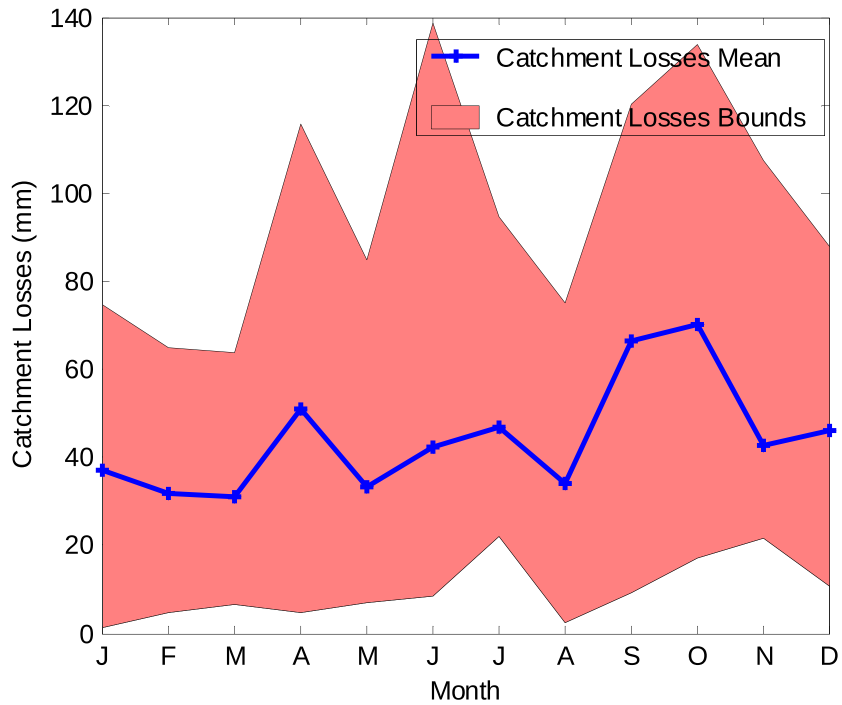

Fig 3.28: Mean and Range of Monthly Catchment Losses at Linton: 1992-2001

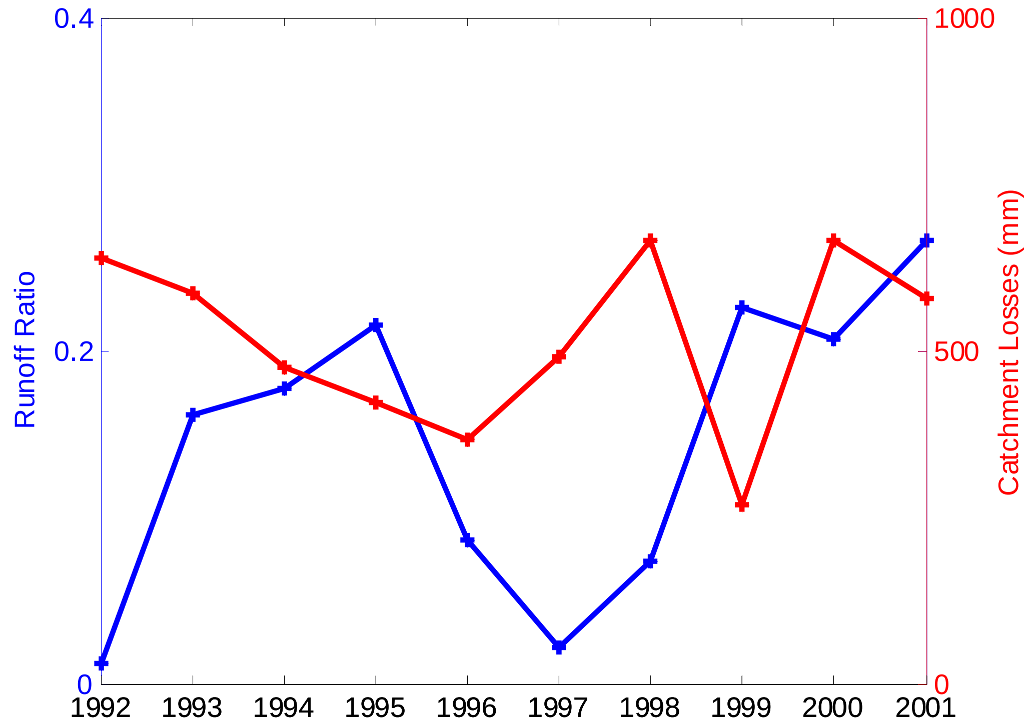

Fig 3.29: Runoff Ratio and Catchment Losses by Year at Linton: 1992-2001

3.4.2.1 Tributary Flow Analysis

Section 3.3.3 explained the gauging and analysis methods used to produce discharge series for the tributaries of the Granta at Bartlow. Here the series are presented in order to assess the contribution of each subcatchment to the flow at Linton. The length of flow series available for analysis was limited by the low flow conditions seen over the 2 year period of fieldwork. This was exacerbated by the poor performance of the Starflow Velocity Meter at low flow depths. In shallow water the recording typically featured high levels of noise, despite being averaged over each 15 minute period. Due to these problems, it was not possible to use continuous velocity measurements, and instead individual hydrographs were extracted from the complete series. For each hydrograph the vertical velocity and depth series are used to calculate the mean cross-sectional velocity and cross-sectional area using the Matlab routines described in Section 3.3.3. These are then combined to give a discharge series; the results are plotted in Figure 3.30. The plots show the discharge for each tributary separately, for the sum of the tributary flows, and the discharge from the Environment Agency gauge downstream at Linton for comparison. The relative areas of the catchment are shown in Table 3.6.

Catchment	Area (km^2)
Bourn Tributary	22.3
Camps Tributary	14.8
Linton	61.6

Table 3.6: Relative Catchment Areas

The two tributaries typically have very similar discharges, especially during flow events, despite the larger catchment area of the Bourn tributary. However the elongated recession period of the Bourn tributary suggests that this subcatchment has a greater storage capacity. The timings of the flood peaks in the two catchments are also similar, although this can vary by storm. The lower peak flow : area ratio of the Bourn and the more sustained recession suggests that groundwater interactions are more significant in this tributary catchment.

The combined discharge of the two tributary catchments is also compared to the discharge recorded at Linton. Again this relationship shows variability between storms. In hydrographs 1 – 3 of Figure 3.30 it is observed that during the wetting-up and recession periods, there is little additional flow added between the confluence of the tributaries and the Linton gauge, despite the additional 24.5 km^2 of catchment area; however during the flow peak there is significant flow added in this reach. This may provide some evidence for the observation that there is a third small tributary which is generally dry due to abstraction but shows ephemeral flow during storms. It may also reflect surface runoff flowing laterally into the main channel. In hydrographs 4 and 5 of Figure 3.30, the recession flows at the confluence are markedly lower than at Linton; this typically coincides with low flows in the Camps tributary, however the cause for this change in behaviour is not clear.

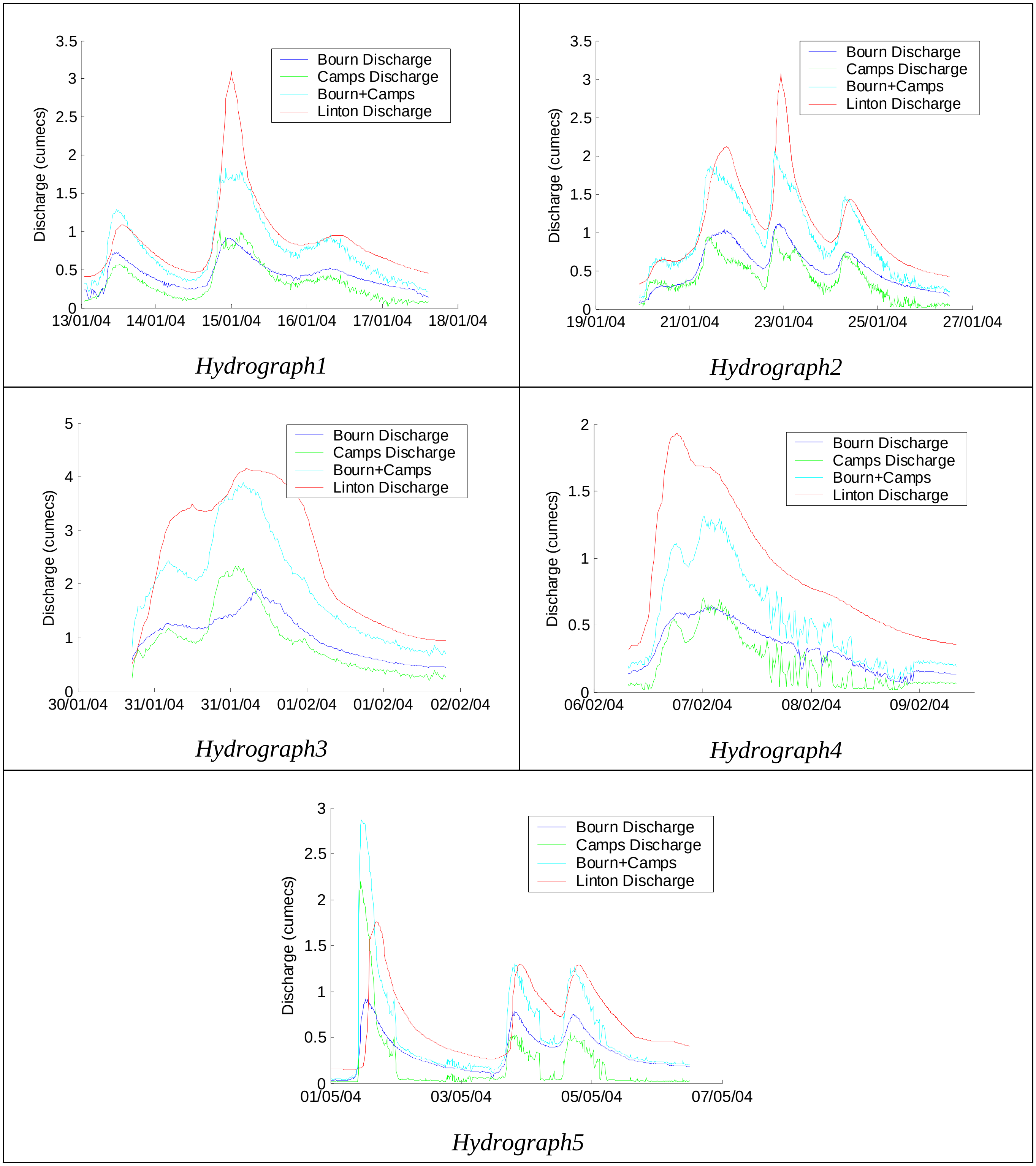

Figure 3.30: Comparison of discharges in the Bourn and Camps tributaries, and at Linton, for 5 hydrographs during the gauging period

3.4.3 Trends in Rainfall and Flow

As well as patterns across each year, a short investigation was made into the trends in rainfall and flow during the study period, and the correlations between them.

3.4.3.1 Annual Totals

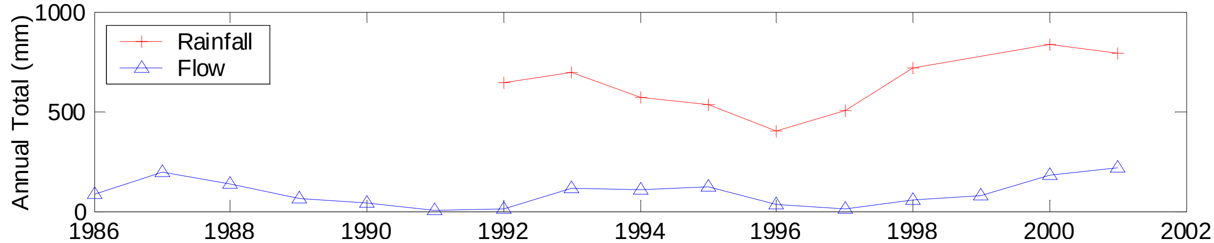

Figure 3.31: Annual total Rainfall and Flow

Comparison of annual totals of rainfall and flow (Figure 3.31) shows that from 1992 to 2001, the average percentage of rainfall that leaves the catchment as river flow is 14.0%. The high percentage loss is due to a number of reasons including groundwater abstraction, water flow out of the catchment through bedrock and soil, and evaporation.

The record is not sufficiently long to detect any linear trend in the annual total for rainfall or flow; however over this short timescale there appears to be a cycle of length around 6 years occurring in the flow data. Although the cycle here cannot be attributed to a specific cause, cycles of length 4-8 years are often found to be linked to the North Atlantic Oscillation and associated weather patterns.

3.4.3.2 Annual Maxima

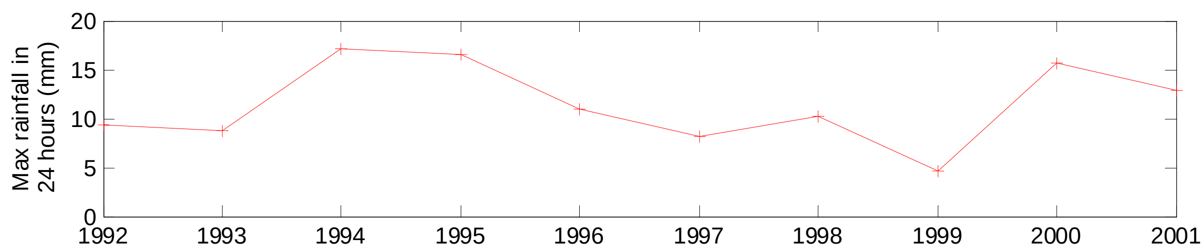

Figure 3.32: Annual maxima for 24 hour rainfall depth

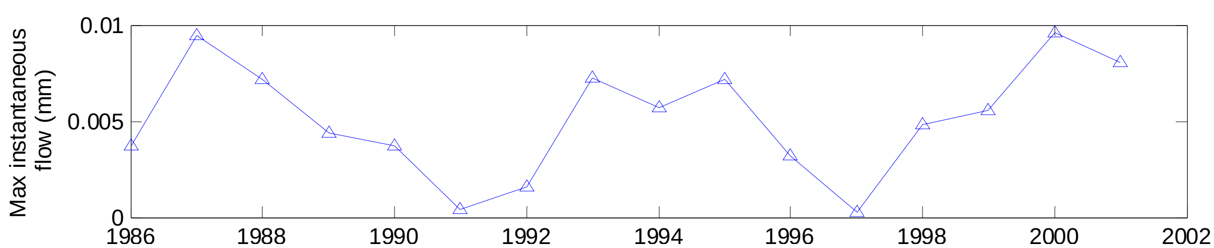

Figure 3.33: Annual flow maxima

The pattern in annual flow maxima shown in Figure 3.33 mirrors closely that shown in the annual flow total (Figure 3.31). This provides further evidence for the suggestion in Section 3.4.1 that catchment wetness conditions play a major role in controlling flood flows. For example, the effect of low winter rainfalls of 1996/1997 can be seen particularly clearly. For the same reasons, the fact that the maximum 24-hour rainfall total (Figure 3.32) does not seem to correlate with the flow maximum suggests that intense short term rainfall can only be a contributing factor to high flows, not the sole cause.

3.4.3.3 Events over Threshold

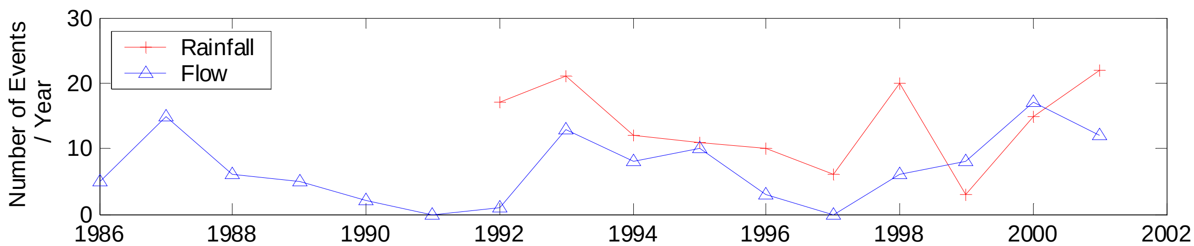

Figure 3.34: Events per year over fixed thresholds: Flow: 1.5 m^3s^{-1}, Rainfall: 4 mm/day

The ‘events over threshold’ statistic shows the frequency of medium-high rainfall and flow events. Flow events are defined as independent, and hence contribute to the total, where they are separated by a 24 hour period for which the flow is under the threshold. The rainfall data shows simply the number of calendar days for which rainfall is greater than 4 mm. This does not guarantee independence, however as only 4% of rainstorms last for 25 hours or longer then no more than two days of high rainfall should be recorded for the same storm in the majority of cases. It should also be noted that some of the totals are artificially low due to missing data: this applies to 1991/1992 for flow data and 1999 for rainfall data.

Excluding the 1999 data, the rainfall and flow sequences show a correlation coefficient of 0.48 suggesting a weak positive correlation, confirming that seen by eye. Reasons for the lack of a stronger correlation include the dependence of flow on antecedent conditions and duration of rainfall event. Although the years 2001 and 2002 show higher than average number of rainfall and flow events, there is no evidence from this plot of a sustained linear trend in event frequency.

3.4.4 Meteorology of the October 2001 storm

The flooding of Linton in October 2001 was caused by a slow moving front over the east of the UK which brought prolonged heavy rainfall (Met Office, 2006). 70.2 mm of rain fell at Linton; other parts of the county had even higher totals, such as Cambridge which recorded 90.4 mm, the highest total in a 24 hour period since records began in 1900. Figure 3.35 shows the synoptic chart for 12:00, 20th October 2001, Figure 3.36 the rainfall radar images for 00:00 21st October 2001 – 00:00 22nd October 2001 and Figure 3.37 the resulting rainfall totals in the period 09:00 20th October – 09:00 22nd October. The high rainfall totals, shown in Figure 3.37 to be centred over the Cambridgeshire region, demonstrate the short-term cause of the flood event. However, the unusually wet summer and early autumn preceding this event were instrumental in providing the long-term cause, as discussed in Section 3.4.1.

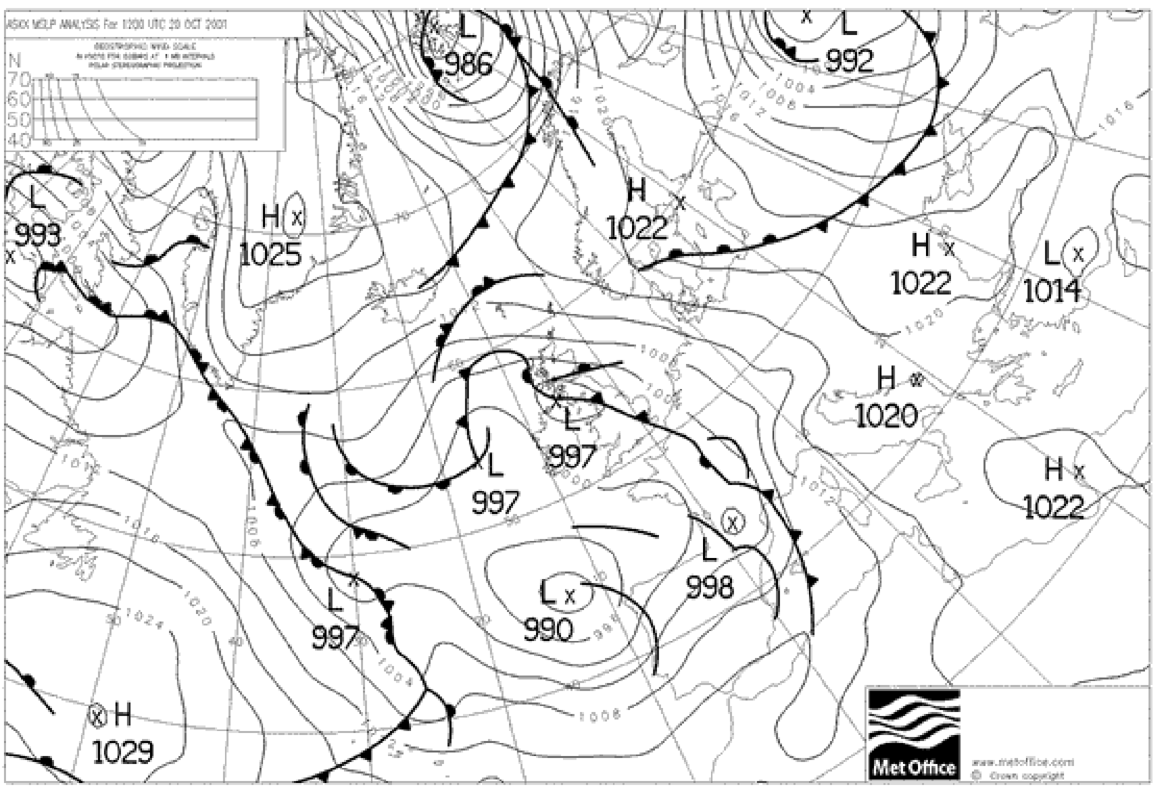

Figure 3.35: Synoptic chart from 20 October 2001 showing the cold front which caused heavy rainfall and flooding in Linton

Source: http://www.met-office.gov.uk/climate/uk/interesting/images/asxx20thoct01.gif

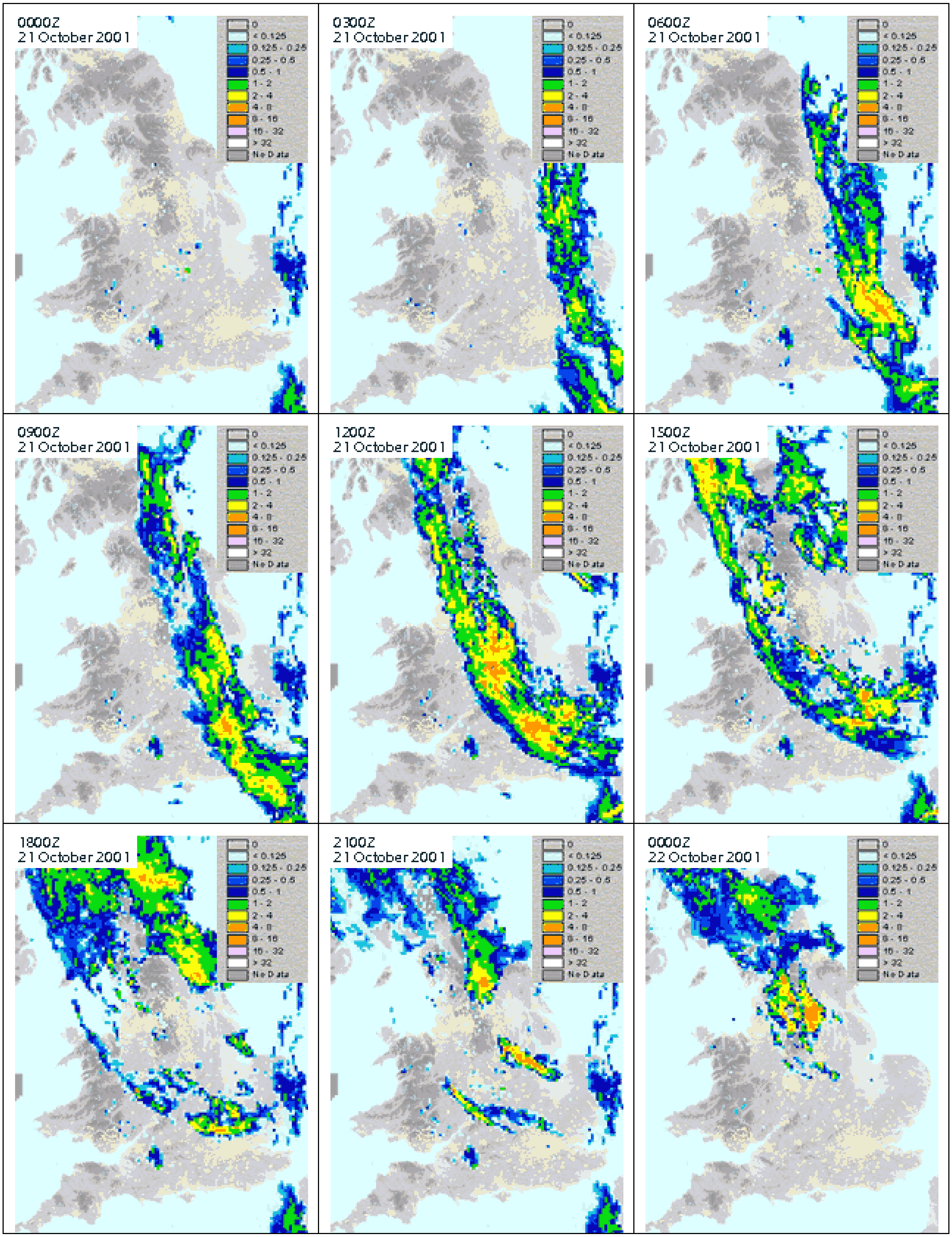

Figure 3.36: Rainfall Radar images at 3-hourly intervals from 00:00 21st October 2001 – 00:00 22nd October 2001.

Source::http://www.metoffice.gov.uk/climate/uk/interesting/oct2001rain2.html

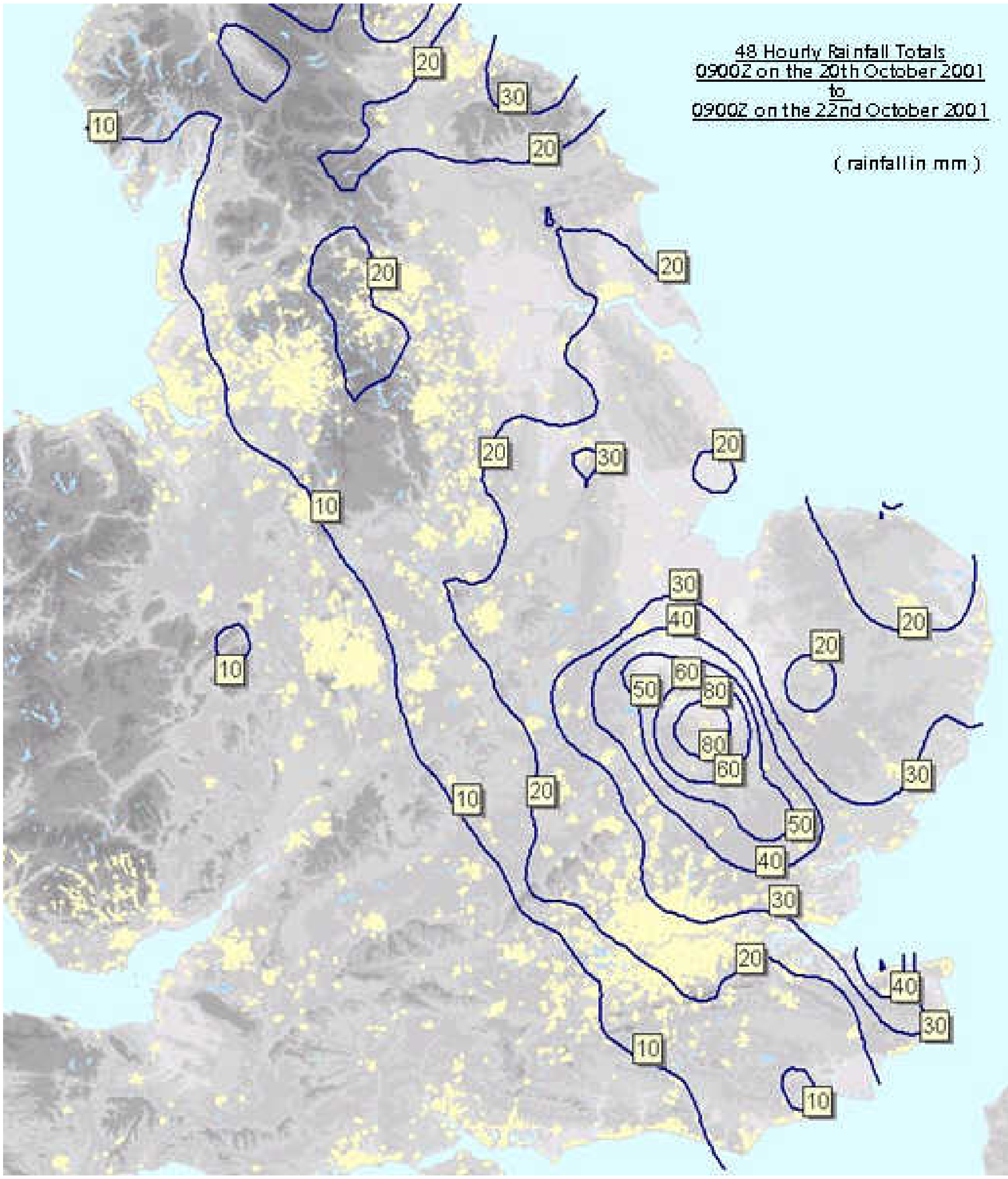

Figure 3.37: Rainfall totals (mm) in the period 9am 20th October – 9am 22nd October

Source: http://www.met-office.gov.uk/climate/uk/interesting/oct2001rain2.html

3.5 Historical Rainfall-Runoff and Flood Risk Modelling

3.5.1 Introduction to the Study

The Environment Agency is responsible for maintenance and flood management of the River Granta where it is identified as ‘Main River’. This designation includes the river from the gauging station just upstream of Linton, downstream to the Cam confluence. Linton is one of several sites along the river which has been identified as at risk of flooding, in response to both the October 2001 floods which inundated 150 houses, and the historical flood record. As a result of the risk, the Environment Agency is responsible for carrying out periodic reports into the Standard of Protection provided for residents in case of flood. The most recent modelling and analysis was originally carried out by Bullen Consultants (2002). The model was later audited by Halcrow (2003) who identified a number of deficiencies in the assumptions made regarding the model structure, input data, and hydraulic regime, and therefore updated the model and published the new conclusions in their final report (Halcrow, 2004). This report remains the current Environment Agency position with respect to the Granta valley, and the conclusions were used as the basis for a cost-benefit analysis for floodplain improvement works.

The methodology used is typical of that employed in flood defence applications, and represents a standard technique recommended by the Environment Agency (see Section 1.3.3 for an overview discussion of these techniques). In brief, the methods detailed in the Flood Estimation Handbook (FEH) are used for upstream flow estimation. This includes both statistical methods and those using a rainfall-runoff model. The flow is then routed along the channel and overbank using a hydraulic model created using the iSIS modelling software (Wallingford Software Ltd, 2006). The report provides a good demonstration of the implementation procedure, together with some of its advantages and disadvantages. Insight into the technique allows a later comparison with the execution of and conclusions from the continuous simulation methods proposed in this study. An overview of the report methods and findings is therefore presented below.

3.5.2 Methods used in the Study

3.5.2.1 Estimation of Flow Regime

Unlike the 2D raster floodplain proposed in this thesis, which allows flow contributions along the model boundary and additional runoff contributions, this model uses a single hydrograph at the upstream boundary point of the channel. In this case, Bartlow was used as the boundary point to enable modelling of a potential storage reservoir upstream of Linton. The prediction was made using a combination of statistical and rainfall-runoff approaches. The statistical methodology used the historical record of annual maximum flows at sites along the Granta to construct flood frequency curves. For stations without a sufficiently long historical record, a 'pooling group analysis' is undertaken which uses supplementary data for other catchments in the UK with similar hydrological attributes to extend the flow record. Priority is given to catchments close to the study site. In the case of Linton, 17 other sites were used, giving a combined total of 486 years of record. Using this extended data set, the flood frequency curve was constructed using the median annual flood and growth curve produced by fitting a Generalised Linear Distribution to the data.

In addition to the statistical flow analysis, a rainfall-runoff model was constructed for the catchments upstream of each flow gauge on the Granta. Five flood events during the period 2000-2001 were used to estimate parameters which control the shape of the hydrograph for each catchment. These parameters were standard percentage runoff (SPR), baseflow (BF) and time-to-peak (Tp). The baseflow parameter was however adjusted to take account of the raised groundwater levels during the study period. The rainfall-runoff model was then used to produce a revised flood-frequency curve by processing the long rainfall series available for the catchments. Finally, the parameters and scaling factors obtained were transferred from the gauging station locations to the relevant upstream subcatchments where the input flow series is required. Differences in area, land-use etc. were adjusted for during the process.

The two flood frequency curves were then compared, to ensure that the predictions from the rainfall-runoff model lie within the confidence limits of the statistical analysis. Where this is not the case, a scaling factor is applied to reconcile the data sets. In the case of Linton, a factor of 1.54 was required, at Babraham the factor was 0.85.

3.5.2.2 Formulation and Calibration of Hydraulic Model

Having estimated the upstream flow conditions, a hydraulic model was used to simulate the flood propagation along the channel and surrounding floodplain areas. iSIS is a 1d channel model which is designed to include structures within the channel and out-of-channel storage zones. It is based on cross-sectional channel data and details of within-channel structures; cross-sections were surveyed at 200 m intervals and at every structure location. LIDAR data were available for the river corridor and were used to extend cross-sections further into the floodplain to allow for overbank flows up to the indicative flood outlines suggested by the Environment Agency, and to simulate static floodplain storage capacity. This required manual editing to remove inconsistencies from the LIDAR DEM. Manning's *n* must be specified for the model and was chosen as 0.035 $m^{-1/3}s$ for inbank flows and 0.05 $m^{-1/3}s$ for out-of-bank flows, after a field visit and consultation of recommended values provided by Chow (1959).

The combined rainfall-runoff and hydraulic models were then tested on the Granta between Linton and Stapleford by simulating three observed flood events; those of October 2000, February 2001 and October 2001. Modifications were made to the hydrograph time-to-peak parameter to improve the model fit, as the model was found to be relatively insensitive to Manning's *n*. After these modifications, the model was deemed to provide satisfactory simulations of gauged flow hydrographs. In addition to testing against individual hydrographs, the model was also tested in its ability to reproduce the flood frequency characteristics of the sites. Using a design rainfall simulation representing the 100-year event, the results were compared against the 100-year flow event taken from the statistical analysis. Again agreement was found to be acceptable.

3.5.3 Results of the Study

The results from the statistical analysis are given in Table 3.6 for the three gauging stations on the Granta of Linton, Babraham and Stapleford. The 100-year pooled flows were used to calibrate the rainfall-runoff model.

Return Period (yrs)	Design Peak Discharge (m^3s^{-1})					
	Linton		Babraham		Stapleford	
	Single Site	Pooling	Single Site	Pooling	Single Site	Pooling
2	4.43	4.43	4.10	4.10	3.89	3.89
5	5.44	6.18	5.75	5.66	4.45	5.31
10	5.85	7.21	6.73	6.59	4.67	6.14
25	6.23	8.44	7.93	7.72	4.86	7.15
50	6.45	9.33	8.81	8.55	4.95	7.89
100	6.61	10.22	9.69	9.38	5.03	8.62

Table 3.6: Design Peak Flows from Statistical Analysis

The model was run for design events with return periods of 2, 10, 25, 50, 100 and 200 years. For each event the number of properties within the projected flood envelope was calculated. At Linton, no properties were at risk below the 100-year return period, 11 at risk for the 100-year flood, a further 4 in the 150-year flood and again a further 4 in the 200-year flood. The properties were situated on the High Street and Church Lane; the majority of flooding was confined to recreation grounds and fields. A map of the results is shown in Figure 3.38, and for comparison, the 100-year flood envelope from the Environment Agency indicative floodplain map. It is interesting to note that of the two, the Halcrow iSIS study predicts a significantly reduced area to be flooded during the 100-year event. This may in part be due to inadequacies in the gauged record, as discussed in Section 3.4.2.

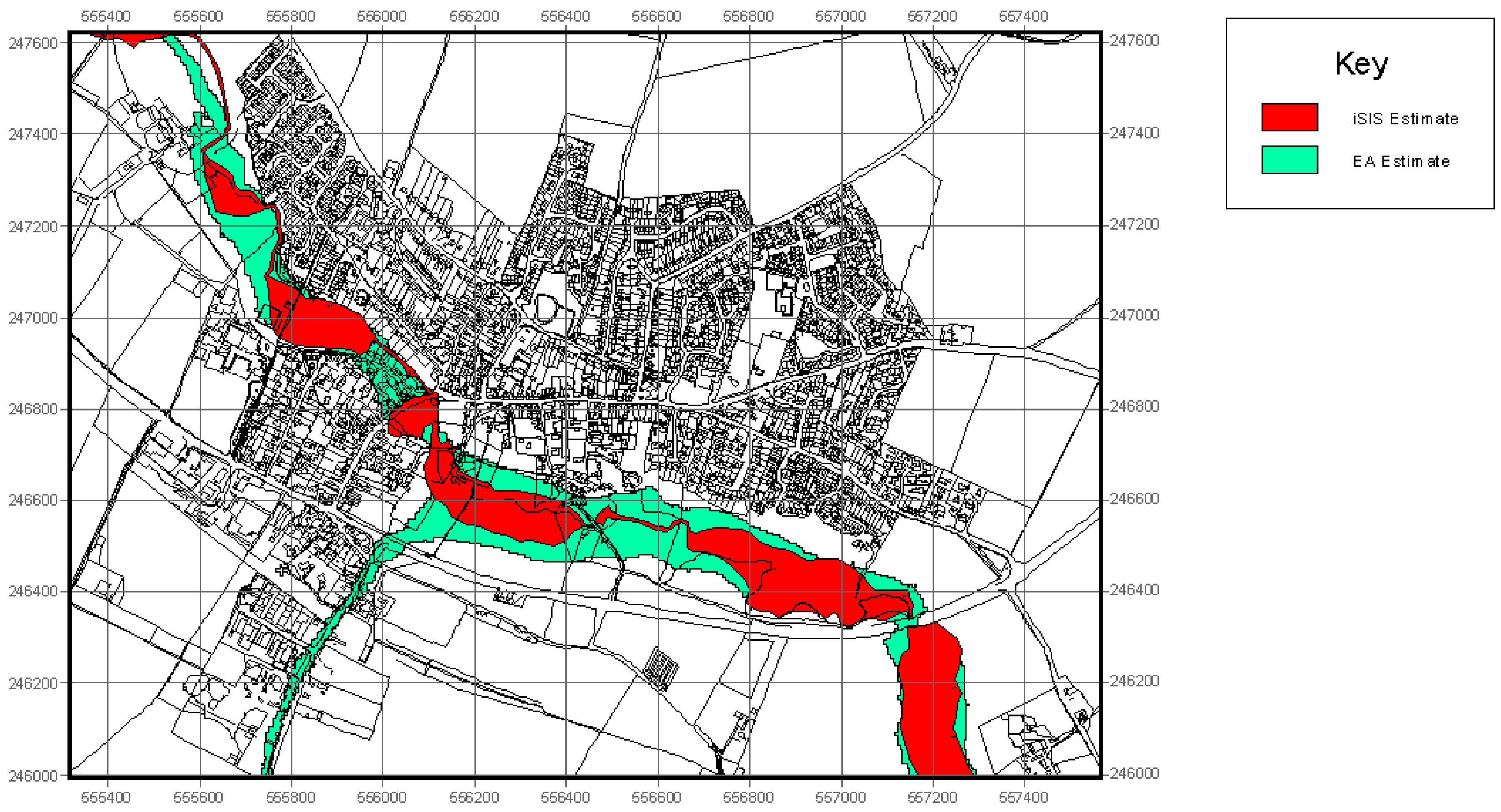

Figure 3.38: !00-yr Flood Outline Estimates from

(a) iSIS model and (b) Environment Agency indicative floodplain map

3.5.4 Comment on the Method and Conclusions

There are several assumptions made during the modelling methodology that may affect the results of the study. Firstly both the rainfall-runoff and hydraulic models used are relatively simple models which may not reflect the full non-linearity and complexity of catchment behaviour. For example, the rainfall-runoff model employs a linear hydrograph formulation which does not account for antecedent wetness conditions, likely to be very important in a groundwater-dominated catchment such at that of the Upper Granta.

Another simplification is the use of a 1d hydraulic model which cannot fully simulate 2d routing of water over the floodplain. iSIS allows simple floodplain flow routing along predetermined pathways, however the capacity was not used here. Instead, the assumption is made that the floodplain provides static storage areas but does not provide downstream conveyance capacity.

Another assumption is that the annual maxima series from the gauged records at Linton and Babraham can be used directly within the statistical analysis. This does not take account of the fact that Linton weir is known to drown at levels exceeding 0.46 m, and that Babraham station is also known to be bypassed at high flows. Therefore neither station may record the true magnitude of large events. For the October 2001 event in particular, the report notes that Environment Agency staff stated that the float at Linton gauging station jammed (therefore the high levels were not properly recorded). At Babraham the October 2001 annual maximum recorded is also incorrect; the value given is 6.71 m^3s^{-1} compared with the 20.5 m^3s^{-1} recorded in the 15-minute series used elsewhere in the report. Although the effect of such errors may be reduced by the use of pooling group data, they would still have a significant effect on the design flows produced which would be smaller than those actually occurring in the catchment. This may have important knock-on effects in the provision of flood protection measures in the catchment, which may be considered uneconomic in a cost-benefit analysis using the reduced design flows.

3.6 Conclusion

The need for any model building exercise to be underpinned by practical application and testing, in a study catchment representative of the locations of the intended future use of the model, was emphasised in Section 2.1. This chapter therefore introduced the catchment which was used throughout the thesis to provide a testing ground for the end-to-end modelling framework as it is developed.

Section 3.1 explained the choice of catchment. The Granta above Linton is representative of a problematic class of catchments where the speed of response hinders the use of traditional upstream monitoring to aid real-time forecasting and warning systems, but in which an ‘end-to-end’ forecasting system based on precipitation forecasts may provide a solution. Section 3.2 then provided further information on the geology, soils, climate, land-use and management of the catchment. The geology of the area plays a major role in controlling catchment response to climate, the jointed nature of the chalk bedrock giving rise to significant groundwater contributions to river flows.

The data collection undertaken was described in Section 3.3. The Environment Agency provided rainfall and flow records, and temperature data was reconstructed using interpolation and reference curve techniques. In addition, velocity/depth gauges were installed in the two main tributaries of the Granta upstream of Linton; discharge was then reconstruction from the measured data (Section 3.3.3). Data on flood extent during the 2001 flood was collected using a survey of affected residents (Section 3.3.4). Using the collected data, a hydrological review of the study catchment was undertaken in Section 3.4. Monthly and annual rain and flow statistics were used to analyse the catchment water balance characteristics. The tributary flow records were also used to assess the spatial variability of catchment response. Further to this, the meteorological conditions leading to the flood event of October 2001 were presented in Section 3.4.4.

Finally, a review of previous flood risk modelling carried out in the catchment was presented in Section 3.5. A study was undertaken in 2004 using the statistical and rainfall-runoff techniques recommended in the FEH to estimate upstream hydrographs for design flood events. The flood wave was then routed downstream using a 1d model. The results of the study were presented and a critical assessment of the methods was made.

Part II

COMPONENT MODEL DEVELOPMENT

Chapter 4

STOCHASTIC RAINFALL GENERATION

Abstract

This chapter describes the stochastic rainfall generation component of the flood risk assessment framework. A review of stochastic rainfall generation methodology is undertaken, and two candidate profile-based model structures are put forward for testing in the study catchment.

The modelling methodology is described in detail. The rainfall record is segmented into single storms, using stipulated storm identification criteria. A database of storm characteristics is thus created; interdependence and seasonality of variables is considered at this stage. The database is used to estimate the empirical distribution of each storm characteristic. The first candidate model uses these distributions directly; the second extends the intensity distribution with an extrapolated upper tail. Finally, samples from the distributions are used to create synthetic rainfall series.

The methods for model performance evaluation are discussed in relation to the objectives of the study. The two candidate models are assessed in their ability to reproduce observed rainfall maxima for durations ranging from 1 hour to 28 days, long term averages being particularly important in the groundwater-dominated study catchment. The empirical model without extrapolated upper tail was found to achieve the better results, and was therefore chosen for use in future simulations.

4.1 Introduction

The first step in developing an end-to-end modelling scheme for the Granta is to specify the rainfall input. As described in Section 1.5.3, the concept of a single design storm, that can embody the complex causative relationships between rainfall, antecedent catchment wetness conditions and the range of flood characteristics that cause destructive flooding, is increasingly being rejected. As Cameron *et al.* (1999) suggest, to identify one combination of storm depth, duration, profile and antecedent conditions that constitutes the 'most damaging' storm, is to simplify the pre-storm catchment state, even where the complete hydrograph of a storm is specified rather than purely the peak value. Wheater (2002) focuses on a variety of storm characteristics that control the flood hydrograph and may be important depending on the intended application. For example, the storm volume may be required when planning storage reservoirs, or the volume over a threshold level may determine the quantity of water overtopping existing defences.

To address the deficiencies of the 'design storm' approach, the use of continuous simulation of rainfall and flow is becoming increasingly popular. This method involves the use of long-duration rainfall series, either observed or stochastically simulated, as input data to a rainfall-runoff model. The corresponding discharge simulations can then be sampled directly to obtain the desired statistics of the flow regime. The use of long flow series removes the need for statistical extrapolation of flow characteristics to higher return periods, a practice which may introduce additional uncertainty in the choice of distribution used for extrapolation (Beven, 2000). As Lamb (1999) comments, this method provides considerable advantages in representing the dynamic features affecting runoff production. Continuous soil moisture accounting gives implicit consideration of antecedent wetness conditions and estimation of baseflow. Although the method is more computationally intensive than previous approaches such as that of Eagleson (1972) who analytically described the relationships between rainstorm and flood frequency characteristics, recent advances in computing resources have made the technique of continuous simulation a practical method in flood hydrology (Beven, 2000).

In order to use this technique within the end-to-end modelling framework, long periods of rainfall data are required to estimate flow characteristics for the desirable extreme return periods. Observed rainfall series at 15 minute resolution are only available for 15 years and therefore a stochastic rainfall generator must be constructed and tested. The function of the generator is to extract information from the rainfall series, and use it to build a statistical characterisation of the rainfall regime. This characterisation would typically contain information on the distributions of storm intensity, duration and inter-storm periods. The aim is to use the information collected to enable the generation of stochastic simulations of catchment rainfall over arbitrarily long periods.

4.2 Review of Stochastic Rainfall Generation Methodology

A variety of stochastic rainfall generation models have been developed, all relying on an initial decomposition of regional empirical rainfall records to identify frequency characteristics of storm data (e.g. depth, duration and intensity). These characteristics are then used to parameterise the rainfall generator. This simulation approach has the advantage that a relatively short period of calibration data can to be used to generate long-term simulations of rainfall and catchment wetness which may incorporate extreme conditions. Such extremes may arise simply from the particular combination of storm characteristics (e.g. long duration with high intensity) or from more complex behaviour such as clustering of high magnitude events or the superposition of severe events on already wet catchments. However, for simulation of truly extreme intensity, depth or duration beyond empirical experience, the derived frequency characteristics used to parameterise the model must be re-estimated through further distribution fitting. While possible using standard techniques, such extrapolation is difficult to validate and likely to be associated with significant uncertainty.

Previous studies in continuous rainfall-runoff simulation have employed a variety of different rainfall models. The main distinction is between storm profile-based methods and pulse-based methods (Cameron *et al.*, 2000). Profile-based methods split the total storm depth into time-step depths by using a profile or mass curve, whereas pulse-based methods use statistical distributions to model the arrival time and characteristics of rain pulses within the storm period.

4.2.1 Profile-Based Models

Eagleson (1972) first proposed the use of stochastic rainfall simulation for flood frequency assessment. The stochastic rainfall model he employed used a relatively simple event-based, derived-distribution approach, with storms characterised by point rainstorm intensity and point rainstorm duration. Intensity and duration were measured from an observed timeseries and frequency parameters fitted using independent exponential distributions.

This principle has been used extensively in later studies (Cadavid *et al.*, 1991; Diaz-Granados *et al.*, 1984; Hebson and Wood, 1982) and extended by Loukas (2002) to incorporate spatially variable rainfall data. While the event-based approach is computationally simple, coupling to rainfall-runoff models requires the use of simplifying assumptions about antecedent catchment wetness which may bias the resulting runoff characteristics. With advances in computer power, this restriction can now be relaxed, and recent studies incorporating Eagleson's model have increasingly used continuous rainfall series, with soil moisture accounting models implicitly providing catchment wetness information (Beven, 1987; Blazkova and Beven, 2000). An additional requirement of this approach is the accurate estimation of extra parameter(s) to simulate the inter-arrival times of storms. Blazkova and Beven (2000) used an exponential distribution to model inter-arrival time, normalized to preserve seasonal rainfall totals, while Cameron *et al.* (1999) found empirical distributions of inter-arrival time, intensity and duration to be uncorrelated and modelled them independently.

Recent improvements have been made by relaxing the assumptions associated with simple distribution models. For example Cernesson *et al.* (1996) and Arnaud and Lavabre (1999) both showed that extreme events follow an 'over-exponential' distribution, and Moughamian *et al.* (1987) showed that the exponential fit performed poorly when compared to a Gumbel (EV 1) distribution. Cameron *et al.* (1999; 2000) noted that inflexibility in the tail of an exponential probability density function (pdf) could lead to bias in the representation of the mean storm intensity of extreme rainfalls and suggested that more flexible models such as the Generalised Pareto Distribution (GPD) should be used in preference.

A further key assumption of Eagleson's model is the independence of storm intensity and duration. This restrictive simplification was relaxed by Cameron *et al.* (1999) who developed the 'Cumulative Density Function and Generalised Pareto Distribution Model' (CDFGPDM) which allows for such correlation by segmenting the intensity into seven duration classes. When compared to the MEEM (Modified Eagleson Exponential Model), this model performed significantly better in the simulation of extreme statistics and the improvement was attributed to the independence assumption of the MEEM (Cameron *et al.*, 2000). An alternative approach was also adopted by Kurothe *et al.* (1997) who used a joint pdf to represent the negative correlation between intensity and duration, and Goel *et al.* (2000) who further extended this to allow for either positive or negative correlation.

One of the major tasks in defining a storm-based model involves the identification of storms within the observed rainfall timeseries. The most common criteria are a lower bound for the duration of storm, lower bound(s) for the intensity of the storm averaged over set period(s) and a lower bound for the separation time between storms. These criteria must reflect the governing hydrometeorology and the percentage of the series that the modeller intends to classify as storm rainfall, and may vary greatly. Cameron *et al.* (1999), for example, classified 99% of rainfall in their empirical timeseries as event rainfall, whereas Blazkova and Beven (2000) isolated only the highest intensity events. Cameron *et al.* (1999) defined a storm as having a minimum intensity of 0.1 mm/hr, a minimum duration of 1 hour and a minimum separation time of 1 hour. A different set of criteria were used by Koutsoyiannis and Mamassis (2001), who employed rules that a storm should have minimum hourly intensity of 5 mm or daily intensity of 15 mm, and minimum separation time of 6 hours. These are however just examples, and a wide variety of definitions have been used to suit particular demands and specific data resolutions.

Storms may also be separated into categories which may have different identification criteria. The most commonly adopted segmentation procedure is to split events by season, where the definition of season may be data or objective dependent. For example, Blazkova and Beven (2000) used four unequal seasons of November – April, May, June – August, September – October to reflect the main changes in rainfall through the year found at their study site in the Czech Republic. Walshaw (1994), by contrast, used 12 equal length seasons as a compromise between continual seasonal change and the need to retain sufficient observational data within each season. As well as a split by season, Blazkova and Beven (2000) also divided storms into high and low intensity events, in order to distinguish convective and frontal rainfall. An additional criterion they adopted was that the intensity should not drop below 6 mm/hr.

Splitting events into separate categories permits a more flexible approach to statistical fitting as distribution types or parameters may be allowed to vary between categories.

This approach does, however, increase the number of parameters to be identified from the (possibly limited) data available, and Walshaw (1994) suggests that homogeneities across seasons should be exploited by fitting a constant shape parameter across seasons where this is appropriate to the distribution type.

4.2.2 Pulse Models

Pulse-based models characterize inter-arrival time and storm duration in a similar way to profile-based models, however instead of using an empirical storm profile, the storm is modelled as a series of randomly-generated raincells. One of the first pulse models to be used was the 'Poisson Model with Rectangular Pulses' (Rodriguez-Iturbe *et al*., 1984; Rodriguez-Iturbe *et al*., 1987) in which each point of a Poisson process represents a rain pulse with random intensity and duration. The intensity and duration are typically selected from exponential distributions, however if longer-term effects are to be studied then a longer-tailed Pareto distribution may be substituted.

A common problem with Poisson models is their failure to transcend temporal aggregation scales effectively, so that their application is limited by the resolution of the calibration data (Rodriguez-Iturbe *et al*., 1987). This is a significant drawback if the model is to be used to study long-term processes such as extended wet or dry spells. To this end, cluster-based models such as the Neyman-Scott model or the Bartlett-Lewis models were introduced (Rodriguez-Iturbe *et al*., 1987). In these models, a rain pulse is associated with each point of a clustered point process rather than a Poisson process. Storm origins arrive as a Poisson process, then a random number of raincells from a Poisson or geometric distribution are attached to the origin of each new event. In the Neyman-Scott model, the positions of these cells are independent identically distributed random variables (IIDRVs), whereas in the Bartlett-Lewis the intervals between cells are independent identically distributed (IID). Again, the exponential distribution is most commonly employed. The Neyman-Scott model therefore tends to give rainfall clustered towards the beginning of the storm, which may be more realistic from a physical standpoint where rainfall is associated with an initial frontal system (Cowpertwait, 1994). These models have been demonstrated to be much more successful in reproducing the physical rainfall process and the multifractal scaling properties associated with true rainfall series (Islam *et al*., 1990; Olsson and Burlando, 2002).

These models have been significantly developed and improved since they were first introduced. Both models were initially shown to overestimate the probability of long dry periods (with aggregated surface runoff therefore showing an error of up to 20%). Rodriguez-Iturbe *et al.* (1988) therefore modified the Bartlett-Lewis model, so that instead of selecting storm durations from the static distribution exp(η), η should be drawn each time from a γ distribution. Entekhabi *et al.* (1989) suggested a similar improvement to the Neyman-Scott model. Questions were later raised as to whether the extra parameters produced improvements in the fit to historical rainfall series. Burlando and Rosso (1991) and Velghe *et al.* (1994) found that, in the modified Bartlett-Lewis model especially, the greater parameter complexity leads to high sensitivity to the parameter estimation method used. Calenda and Napolitano (1999) suggested an alternative to the usual method of moments for parameter estimation (Onof and Wheater, 1993), which attempts to alleviate this problem.

Onof and Wheater (1993) tested the modified model and found that it was successful in reproducing proportions of dry time periods at a variety of scales. However there were still problems in replicating the extreme values of the depth distribution. This was mitigated (Onof and Wheater, 1994) by using a γ variable to replace the exponential distribution of pulse intensity. A jitter process was also superimposed on each rainfall pulse to avoid the overestimation of daily auto-correlation. Verhoest *et al.* (1997) compared the three versions of the Bartlett-Lewis model (original, modified and modified gamma) against 27 years of test data and found that the modified model was most successful, while the modified gamma failed to produce the expected improvements in representation of extreme events. They suggested that this could be due to the clustering of rainfall events, which gives rise to design storms of shorter duration than those in observed series.

Further developments to the Neyman-Scott model include its generalisation to a 2D model by Cowpertwait (1995) such that rain cells occur as discs on the x-y plane, and the inclusion of multiple classes of raincell type to allow, for example, heavy convective raincells (Cowpertwait and O'Connell, 1997).

4.3 Methods

4.3.1 Method Choice

The choice was made to use a profile-based model for the current application. The storm characteristics required for each simulated storm produced by the model are mean storm intensity, storm duration, storm profile (mass curve) and storm inter-arrival time. The profile model was chosen over the pulse model both for its simplicity and ease of implementation; but also through a desire to use a 'data-based' model as described by Cameron *et al.* (2000) whose characteristics can be determined directly from the rainfall series without the need for parameterisation. For the same reason the storm characteristics are sampled directly from the empirical distributions rather than from a standard distribution fitted to the empirical histogram. This method is suitable where there is a sufficiently long rainfall record at high resolution to characterise the empirical distributions, and removes the need to choose and parameterise a standard distribution that may not reflect the full complexity of catchment behaviour. It also eliminates the uncertainty introduced during distribution fitting.

It is, however, possible that the 15 year rainfall record available for the catchment may not be sufficiently long to capture the full range of rainfall behaviour in the catchment. Although the stochasticity of the model allows combinations of storm characteristics not seen in the record, in the long term there may be storm characteristics more extreme than any recorded, which would not therefore be reproduced. The characteristics considered are storm intensity, duration and inter-arrival time. On inspection of the rainfall characteristics, it was felt that the duration and inter-arrival time were sufficiently well captured by the empirical record. In the case of inter-arrival times, extreme values were obtained during the drought period of 1996-1997 and are therefore thought to be adequately represented. Long storm durations are also present in the record due to the occurrence of low intensity, long duration events. However, the same argument does not hold true for storm intensities, especially since intensity is considered by duration class as described in the following sections. The possibility for short-duration, high intensity events in the record to create long-duration, high intensity events in a simulated series is therefore removed, and a reduced number of storms in each class diminishes the likelihood of extreme events appearing in the record. Instead, in order to introduce these into the simulated rainfall sequence, a tail can be appended to the empirical intensity density estimate. Theory predicts the form that this tail should take given that under reasonable assumptions the data points can be considered independent identically distributed random variables (IIDRVs): see Section 4.3.4.1 for further details. This method was therefore considered in addition to sampling from the unaltered empirical distribution, as a compromise between reducing needless parameterisation and predicting the complete range of rainfall behaviour.

The structure of the method involves several components which are outlined in the following sections. Briefly, the approach first involves the segmentation of the record into single storms, and then using this to create a database of storm characteristics. If appropriate, the database should be divided into different classes of storm, for example by seasonality or storm intensity. Second, the database must be used to estimate the empirical distribution of each storm characteristic, and then finally, parameterisations of the extrapolated upper tail should be considered to create an extended sampling procedure. The data to be used in the model is the 15-year record of 15-minute data available from the Elmdon raingauge; this choice was made for reasons of proximity to the catchment and length of record. In order to accurately capture the characteristics of the catchment rainfall, it was felt to be important both to use a single rather than spatially averaged record, and to use a record local to the catchment. The possibility of supplementing the record with others close to Linton was also rejected as this would mean that storms were double-counted and hence would give lower than expected variability in storm characteristics. For further details and summary statistics of the rainfall data, refer to Sections 3.3.1 and 3.4 respectively.

4.3.2 Storm Identification and Sampling

4.3.2.1 Storm Identification Criteria

The storm identification criteria must ultimately reflect the goals of the modelling study. The study catchment of the Granta has been identified as groundwater-dominated due to the underlying chalk aquifer. A strongly non-linear runoff response is therefore expected, in which long-term rainfall volumes are of equal importance to short-term storms in controlling flood behaviour. An analysis of storm volumes demonstrates that contributions to total rainfall volume are evenly spread between storms of different volumes (Figure 4.1). As such, it is important that the storm identification criteria incorporate the majority of small rainfall events as well as severe storms.

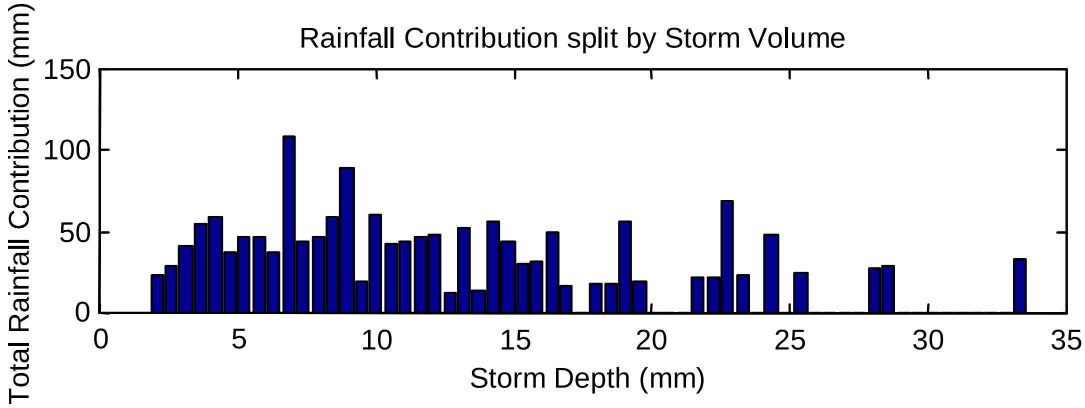

Figure 4.1: Rainfall contribution split by storm volume for the Elmdon rainfall series 1991-2005

The choice of parameters should be such that rainfall is correctly grouped according to storm body, and such that very minor events which do not have representative storm profiles are excluded. On the basis of initial analysis, the following identification parameters were chosen:

Parameter	Condition
Minimum Storm Duration	6 hours
Minimum Termination Time	6 hours
Minimum Intensity	1 mm hourly or 6 mm daily

Table 4.1: Initial Storm Identification Parameters

Similar parameters have also been used in other studies (e.g. Koutsoyiannis and Mamassis, 2001). An experimental trial was undertaken, applying these criteria to a section of the rainfall series, and then inspecting sections of data to check the quality of storm identification. The results showed that the algorithm successfully identified most of the storms, including longer-duration, lower-intensity events. However, there were notable periods of rainfall which were not classified, including short, high intensity events. This type of rainfall pattern appears frequently within the rainfall sequence and makes an important contribution towards the overall rainfall depth, so must be included as a storm period. Subsequent experimentation with the storm identification parameters, in particular the minimum duration and minimum intensity was then used to determine the combination of conditions which optimally characterised rainfall events as storm periods. Minimum termination time was left unchanged as it was felt that the method adopted by Cameron *et al.* (1999) who used a termination time of 1 hour would fail to group events caused by the same storm body. The final parameters selected are shown in Table 4.2; the notable change being in the definition of storm duration criterion in order to reflect the frequent occurrence of short duration storms.

Parameter	**Condition**
Minimum Storm Duration	1 hours
Minimum Termination Time	6 hours
Minimum Intensity	0.4 mm hourly or 3 mm daily

Table 4.2: Storm identification parameters refined after initial experimentation.

The new algorithm was again tested against a rainfall sequence, and the results inspected to check quality of storm identification. The use of the updated parameters was found to produce a satisfactory result which identified all major storm events, identifying 93% of total rainfall depth as storm rainfall. A typical section is shown in Figure 4.2 with the start and end points of each storm identified marked in green and red.

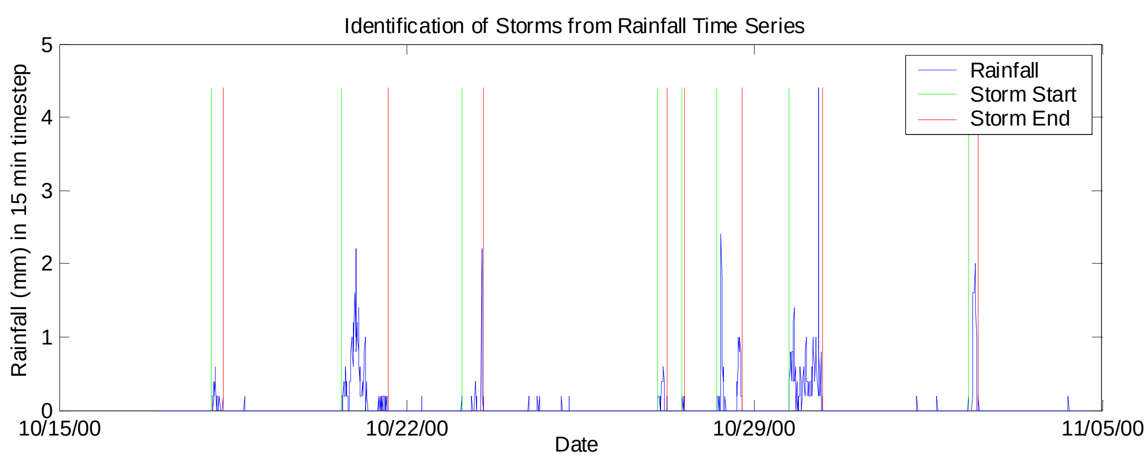

Figure 4.2: Identification of storms from rainfall sequence, sample period.

4.3.2.2 Dependence of Intensity upon Duration

As noted in Section 4.2.1, models which assume that mean storm intensity is independent of storm duration have been shown to perform less well than those which allow for such dependence. In order to evaluate the importance of this dependency within the local rainfall data, the empirical relationship between duration and mean intensity was constructed (Figure 4.3). The plot below was re-drawn from a wireframe mesh constructed from a 2D histogram. This plot was created using the complete rainfall series for Elmdon.

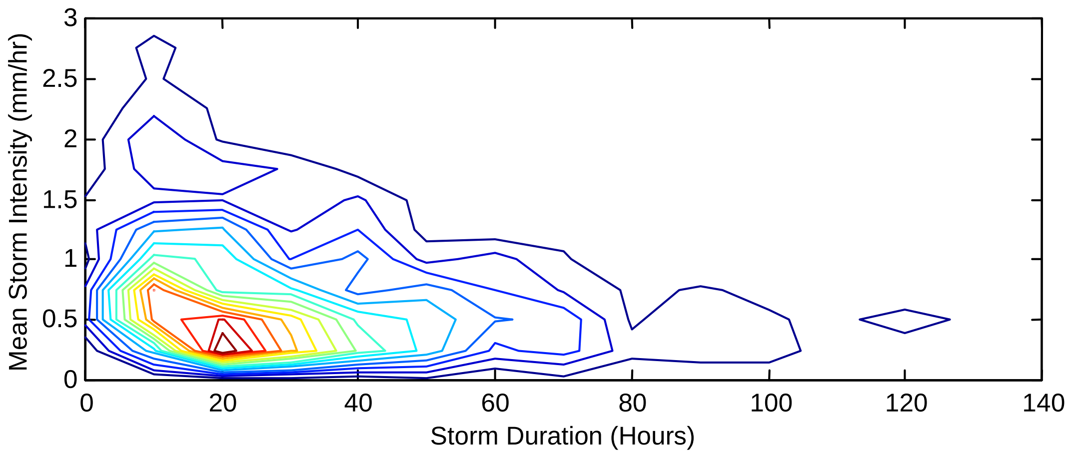

Figure 4.3: Relationship between Storm Duration and Mean Intensity

Although this plot reveals that there is negative correlation between intensity and duration, there are no clear cut-offs between duration bands with 'similar mean storm intensities' as found by Cameron *et al.* (1999).

Two possible approaches for allowing dependence between duration and mean intensity were considered. The first was to define a series of duration categories and to consider the distribution of storm intensity within each one. One method considered for defining the duration categories was such that each contained the same number of storms in the historical test sequence used. However it was found that unless a very large number of categories was used, there was insufficient discretisation for higher-duration storms. Instead, class boundaries were equally spaced (to nearest hour) along a log-transformed scale. Five categories were used to give a compromise between sufficient number of storms per class and small class widths.

The classes were therefore defined as follows:

Duration Class (Hours)	Number of Storms in Class
1 – 2	108
2 – 5	246
5 – 11	334
11 – 25	219
25 +	38

Table 4.3: Duration Classes with Number of Storms in Each Class

The second approach considered was to use an empirical estimate of the full bivariate distribution of duration and mean intensity, based on a smoothed 2D histogram. This method is covered in more detail when methods of empirical density estimation are considered in Section 4.3.3.

4.3.2.3 Seasonality

In the rainfall series used here, as in most environmental time series, seasonal variation is apparent. A plot of the average monthly rainfall shows that most rainfall occurs in the months September to January, which reinforces the empirical observation that most floods occur in the autumn (although this is also driven by evaporation rates).

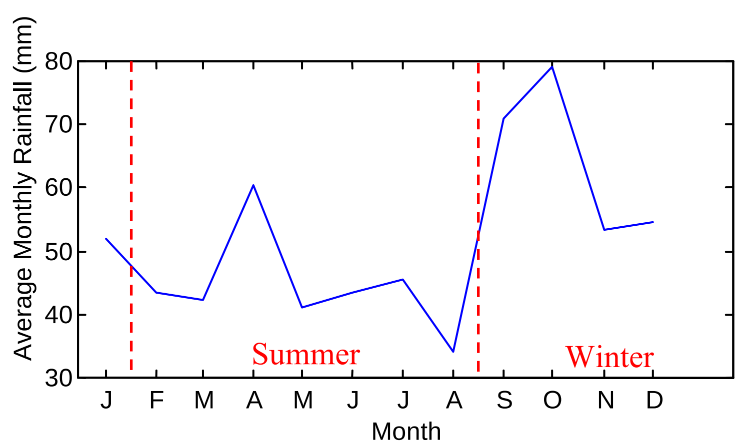

Figure 4.4: Rainfall totals by month showing rainfall seasonality.

In the past, modellers have used several different methods of accounting for seasonality in the data. It is possible to remove known seasonal components to create a stationary series (Walshaw, 1994), however the components which affect the upper tails of the distributions may not be known (Davison and Smith, 1990). Some models have parameters that can be continuously varied to mimic seasonality (e.g. Guenni *et al.*, 1996). Some modellers have felt able to ignore seasonal effects for their particular site, (e.g. Cameron *et al.*, 1999), but in general the favoured approach is to fit separate models to each of a chosen number of seasons. The number of seasons is chosen as a compromise, with more seasons giving improved representation of data but decreasing the amount of data available in each season, hence increasing the uncertainty within the model (Cameron *et al.*, 2000). In general, the number of seasons used has been either two (winter and summer) where data has been limited (e.g. Cameron *et al.*, 2000) or twelve (monthly) where data is more abundant (e.g. Onof and Wheater, 1993; Walshaw, 1994). In this study, the greatest consideration was that sufficient data should be available within each season, and so just two seasons were used. The choice of these was based on Figure 4.4 above, and is September – January and February – August. Although the winter season is shorter, this is ameliorated by an increased concentration of storms during these months.

4.3.2.4 Sampling Methodology

To build a database of empirical distributions of storm characteristics, storms are identified and characterised from a historical record. As explained above (Section 4.3.1), the record from Elmdon was used for this purpose. The empirical distributions which are sampled from the results for each season are as follows: storm duration, storm intensity for the five separate duration classes, storm inter-arrival time. For histograms of the distributions, see Section 4.3.3. The profile of each storm is also recorded; these are later scaled to give simulated storms.

4.3.3 Empirical Density Estimation

4.3.3.1 Theoretical Background

When the database of storm characteristics is complete, it must then be used to estimate and provide samples from the underlying distributions. The values of each sampled storm characteristic can be considered as observations from a distribution with unknown density function $f(x)$. To enable efficient modelling, an estimate $\hat{f}(x)$ of the density function is required. Ideally, a nonparametric density estimation method should be employed for this purpose in order to reduce the number of assumptions made about the form of the underlying density. The simplest method of nonparametric density estimation is the histogram; however this gives rise to a non-differentiable form which cannot adequately represent the continuous nature of characteristics such as storm duration. Generalization of histograms by spline curve fitting could be used to interpolate between the data points, however the form of the resulting function remains potentially biased by the limited sample size and so a smoothing technique rather than an interpolation would provide a more robust generalization tool.

The standard smoothing technique for density functions is kernel density estimation, which produces a smooth density function using weighted local averaging. A detailed explanation of kernel methodology is given by Silverman (1982; 1986), where it is also shown that the Gaussian kernel density estimator can be implemented using a Fast Fourier Transform. Antoniadis (1995) implemented this method for Matlab and this procedure was adopted for this study. Many extensions to Silverman's methodology have been suggested, such as that of Marchette *et al.* (1996) who allow the Gaussian kernel to have multiple bandwidths, however such additional complexity may be unwarranted for rainfall modelling. The choice of a Gaussian kernel is also one option among many, however Marron and Nolan (1988) demonstrate that kernel functions can be rescaled such that the difference between two kernel density estimates using two different kernels is almost negligible, and thus the choice of scaling parameters is far more influential.

4.3.3.2 Parameter and Transformation Choice

In implementing the Gaussian kernel density estimator, the smoothness of the resulting density is determined by the bandwidth of the kernel. There are many methods of choosing this smoothing parameter, (eg. Silverman, 1986; Hardle, 1991; Park and Turlach, 1992), which vary in their complexity. At the simplest, the choice can be made by eye from suitable plots of the output density. Alternatively, the following 'rule of thumb' can be used:

$$\text{Bandwidth} = k_1.\sigma_x.n^{k2} \qquad \textit{(4.1)}$$

where x is the input sample, σ_x is the sample standard deviation and n is the sample size. Different suggestions have been made for the values of the constants (e.g. Silverman, 1986; Scott, 1992). It has been demonstrated that if the empirical data had a normal distribution, the ideal window width would have $k_1 = 1.06$, $k_2 = -0.2$, however by reducing the parameter k_1 to 0.9 the results can be improved for skew distributions (which applies to the distributions being modelled in this study). Silverman (1986) showed that the results could be improved still further by using a more robust measure of spread instead of the standard deviation:

$$A = \min(\sigma_x, \text{IQ range}(x)/1.34) \qquad \textit{(4.2)}$$

The parameter can also be drawn from the data, using the method of ‘cross-validation’ (Silverman, 1986). This entails omitting each data point in turn from the calculation, and then maximising a suitable long-likelihood function. However, the discretization of the data points inherent in the Fourier Transform methodology (even on a fine grid) can lead to poor results when using cross-validation.

A further issue which is important when modelling rainfall characteristic distributions is that of discontinuous distributions. Due to the way in which storms have been defined, i.e. by minimum intensity, duration and inter-arrival time specifications, the densities of the duration and inter-arrival time variables must vanish for values less than the specified minimum (this does not apply to intensity as the distribution of mean storm intensity rather than point intensity is used). Although one option would be to compute the density as normal, truncate it for the appropriate value, and scale to produce a density (integrating to 1) this would give disproportionately small weighting to points near the discontinuity (Silverman, 1986). Instead, the suggestion is made that the empirical distribution could be reflected around the discontinuity point before smoothing, then double the calculated density for points above the minimum would be used. This is similar to the method suggested by Scott (1992) using a one-sided kernel. By using this method, the difficulties of a skewed distribution are also avoided as the distribution to be fitted is symmetrical.

The density estimation methods used in this study are therefore summarised as follows. The mean storm intensity has a skewed distribution but no discontinuity at a positive minimum value, so is log-transformed before fitting. The storm duration and inter-arrival time both have discontinuous distributions so the distributions are reflected around the discontinuity before fitting. All three densities are then estimated using a Gaussian kernel with bandwidth chosen using the improved Silverman ‘Rule of Thumb’ method.

4.3.3.3 Fit of Smoothed Distributions

The following diagrams (Figures 4.5 and 4.6) show the results of smoothing the histograms to produce empirical distributions for the winter and summer season although, as noted in the next section, these distributions are not required explicitly.

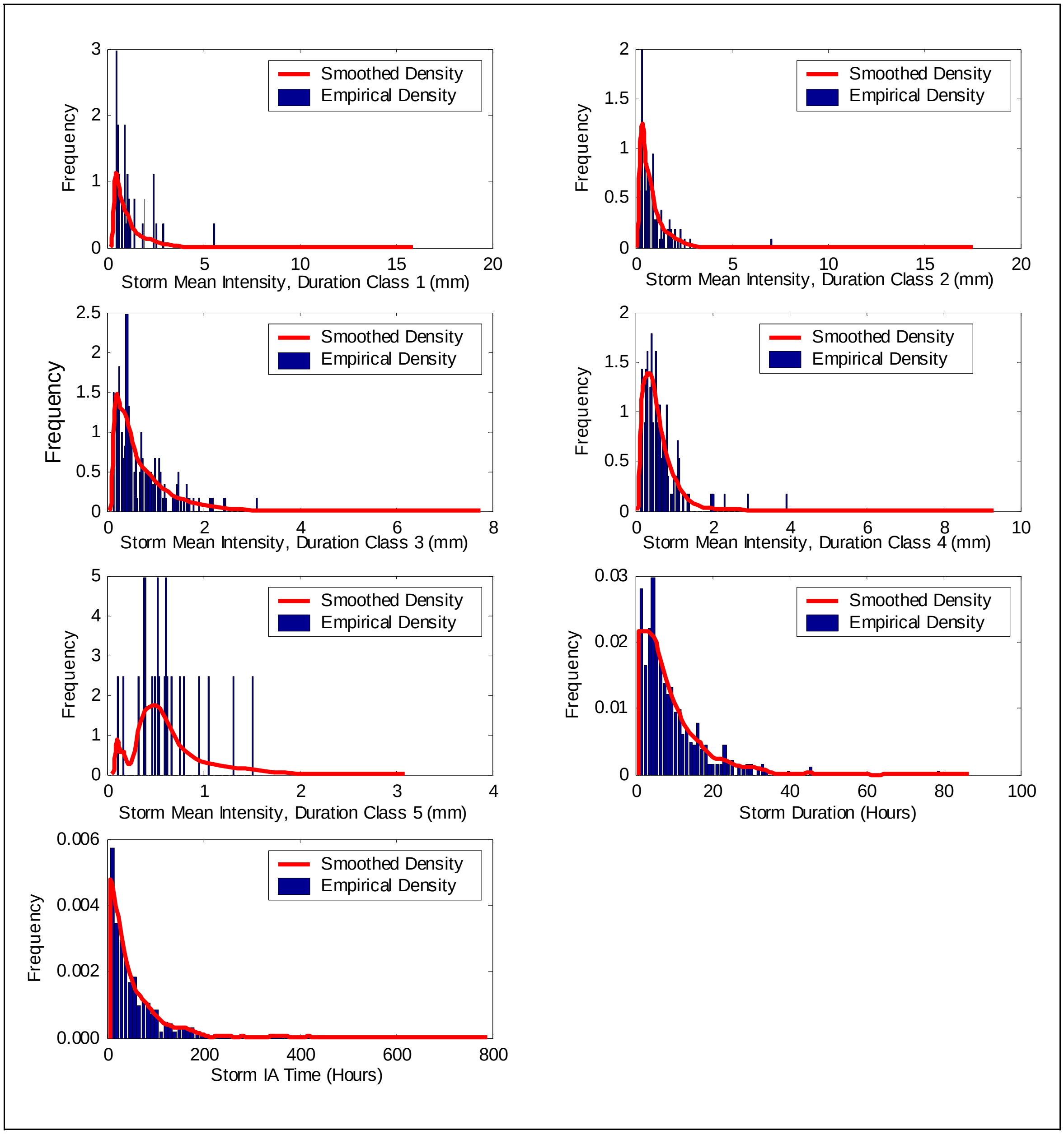

Figure 4.5: Histograms and Smoothed Density Estimates of each Parameter for the Winter Season

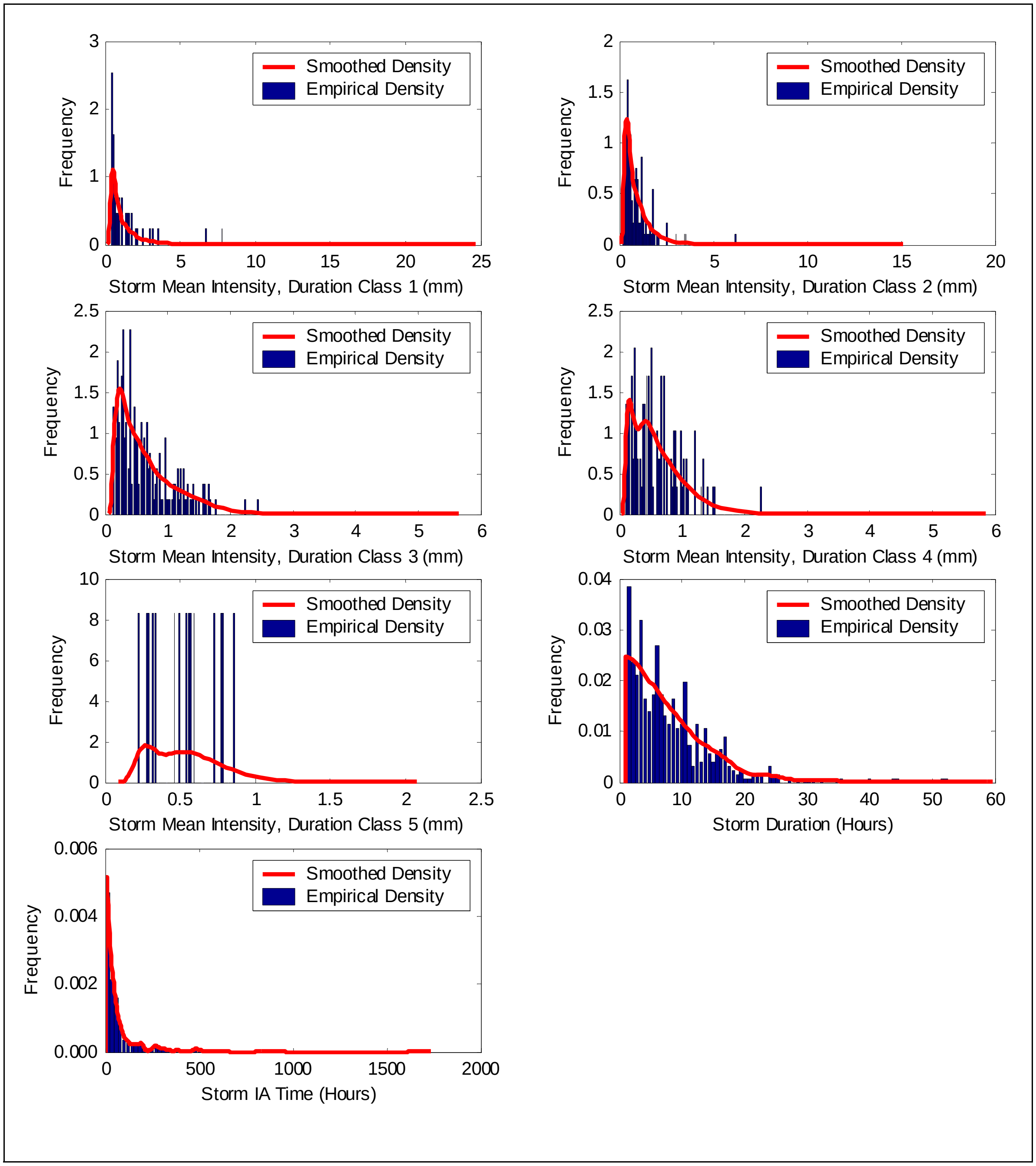

Figure 4.6: Histograms and Smoothed Density Estimates of each Parameter for the Summer Season

4.3.3.4 *Sampling from the Smoothed Distribution*

In order to draw a random sample from the smoothed distribution, it is not necessary to find this distribution explicitly (Silverman, 1986). Instead the following procedure can be used: choose sample X randomly from the observations recorded. Then generate ε to have pdf that of kernel K (in this case the normal density N(0,1)). The random sample from the distribution is then $Y = X + h\varepsilon$ where h is the bandwidth. Where a reflected distribution is used, samples are reflected about the discontinuity as appropriate. The procedure is slightly different in the case where smoothing is applied to the log distribution, here instead $Y = Xe^{h\varepsilon}$.

4.3.3.5 *Use of Multivariate Density for Duration and Intensity*

The kernel method of Section 4.3.3.1 can be directly extended to higher dimensions (Silverman, 1986), in this case the bivariate density of duration and mean intensity. The kernel used is the bivariate normal, with bandwidth = $k_1 * \mathbf{A} * n^{-1/6}$. As before, the optimal value of k_1 can be found for normal data, this is 0.96. The same scaling ratio is used as for one dimension to give $k_1 = 0.82$ to allow for skew distributions. **A** is again taken as min(σ_x, IQ range(x)/1.34) (where **A** is now a vector to allow for different scaling for each variable). To draw observations from the smoothed density, a bivariate version of the method of Section 4.3.3.4 is used:

$$\begin{bmatrix} Y_1 \\ Y_2 \end{bmatrix} = \begin{bmatrix} X_1 \\ X_2 \end{bmatrix} + \begin{bmatrix} h_1 & h_2 \end{bmatrix} \cdot \begin{bmatrix} \varepsilon_1 \\ \varepsilon_2 \end{bmatrix} \qquad (4.3)$$

with a vector bandwidth h used to give different smoothing parameters in the two dimensions.

4.3.4 *Empirical Density Estimation with Fitted Tail*

4.3.4.1 *Predicting the shape of the intensity tail*

Cox *et al.* (2002) provide a review of the probability theory of extreme values, as applied to stationary processes, and its applicability to flood frequency estimation. They demonstrate that, when considering the limiting form of the cumulative distribution function (cdf) of the maximum of a series of IIDRVs, there are only three possible solutions. These are the Gumbel, Frechet and Weibull distributions, particular cases of the generalised extreme-value (GEV) distribution. The distribution cdfs are shown here:

$$H_1(x) = \exp\left(-e^{-x}\right) \quad -\infty < x < \infty \qquad \textit{Gumbel} \qquad (4.4)$$

$$\begin{array}{llll} H_2(x) = \exp(-x^{-\alpha}) & x \geq 0 & H_2(x) = 0 \quad \textit{otherwise} & \textit{Frechet} \\ H_3(x) = \exp\left(-(-x)^{\alpha}\right) & x \leq 0 & H_3(x) = 1 \quad \textit{otherwise} & \textit{Weibull} \end{array} \qquad (4.5)$$

The Weibull is of less interest as it applies where the random variables have an upper bound. The Gumbel holds when the distribution reaches its limiting value (1) at least exponentially fast; the Frechet when a power law rate applies. A popular approach is to model extreme value series using the Gumbel rather than the inclusive GEV distribution; however Coles *et al.* (2003) highlight the dangers of underprediction of both extreme values and the associated uncertainties when using this restricted method.

We may wish to characterise the sequence not only by its maximum, but also by the number and magnitude of peaks over a threshold u_n. Madsen *et al.* (1997) showed that using this 'partial duration series' is a more efficient technique than using the annual maximum series. Assuming that the mean number of exceedances $n(1-F(u_n))$ tends to a limit v, then these exceedances form a Poisson process, with the probability of non-exceedance tending to e^{-v} for large n.

Given that there is an exceedance, the size $Z = X-u_n$ has the cdf $F(z+u_n)/(1-F(u_n))$. In the limiting form this has the generalised Pareto distribution (GPD).

$$G_P(z) = \begin{cases} 1-(1+\frac{k}{\sigma}z)^{-1/k} & k \neq 0 \quad \textit{Frechet / Weibull} \qquad (4.7) \\ 1-\exp(-z) & k = 0 \qquad \textit{Gumbel} \qquad (4.8) \end{cases}$$

Here the parameter σ provides simple scaling, whereas the parameter k controls the shape of the distribution, k < -0.5 giving a concave plot, k = -0.5 a linear plot, -0.5<k<0 a bounded convex plot, k = 0.5 an exponential 'thin tailed' unbounded convex plot and k > 0.5 a 'heavy tailed' unbounded convex plot with infinite moments for orders > 1/k (Katz, 2002). The majority of studies have found that maximum rainfall within a set time period has a heavy tail (e.g. Egozcue and Ramis, 2001; Smith, 1999; Smith, 2001) however Cameron *et al.* (1999) argue that for the British climate there are probable upper bounds to rainfall intensities, suggesting that a bounded distribution with $k < 0$ should be used. The upper bound is often referred to as the 'probable maximum precipitation' and may be quantified by the maximisation of the physical factors that control the precipitation evolution (Collier and Hardaker, 1996).

4.3.4.2 Parameter estimation technique

Several methods can be used for the estimation of the GPD parameters, the most popular being maximum likelihood estimation (ML), probability weighted moments method (PWM) and Pickand's estimator. The ML method is preferred for its simplicity and applicability to structured models (Coles, 2001). It has been suggested that the PWM method is superior to the ML method for small sample sizes: Katz (2002) and Hosking *et al.* (1985) give examples of gross overestimation of the shape parameter when ML estimation is used. The investigations of Coles and Dixon (1999) suggest however that the superiority of the PWM is due to the imposed constraint $k < 1$ inherent in this method, and that if this same constraint is applied to the ML method, similarly good results would be found.

In order to modify the ML method to impose bounds on k, two different methods have been suggested. Cameron *et al.* (1999) introduced the dependence $k = -\sigma(b-u)$ where b is the upper bound postulated for the data, which enforces a distribution also bounded at b. Coles and Dixon (1999) use an alternative method, that of penalised maximum likelihood estimation (PML) which imposes a penalty function for values of k not in the required range. This can be seen as analogous to Bayesian methods using a prior distribution (e.g. Martins and Stedinger, 2000) which allow recent measurements to be combined with historical knowledge (Jin and Stedinger, 1989). In this study, the PML method is used as it is felt that this allows the structure of the data to impose the upper bound rather than using a predefined limit.

The ML estimation technique selects distribution parameters such that the probability of obtaining the observed data is maximised. Grimshaw (1993) gives a comprehensive algorithm for the implementation of this method in the GPD case. Grimshaw's method was implemented for Matlab by Brodtkorb *et al.* (2000) and a modified version of their algorithm was used here. Their implementation of the PWM method was also used in those cases where the ML estimates do not exist (e.g. when k < -1).

The main modification made to the method was an implementation of the PML method. The penalty function used is that recommended by Coles and Dixon (1999), with the form:

$$P(k) = \begin{cases} 1 & k \le 0 \\ \exp\left(\frac{k}{k-1}\right) & 0 \le k \le 1 \\ 0 & k \ge 1 \end{cases} \qquad (4.9)$$

The corresponding penalized likelihood function is then:

$$L_{Pen}(\sigma, k) = L(\sigma, k) \cdot P(k) \qquad (4.10)$$

This function penalizes all unbounded distributions (k >0) with the penalty increasing as lower order moments become infinite. No distributions with infinite mean (k>1) are accepted.

Using the parameter estimation technique outlined, a GPD distribution was fitted to the upper third of intensity values within each duration class. The parameters for each distribution are given in Table 4.4 below.

Intensity Class	1		2		3		4		5	
Season	W	S	W	S	W	S	W	S	W	S
Shape	-0.0153	0.3197	0.1484	0.1411	-0.1112	-0.2743	0.2285	-0.0981	-0.1462	-1.1135
Scale	0.2828	0.2162	0.1594	0.1646	0.1520	0.1497	0.0931	0.0953	0.1083	0.0965

Table 4.4: Penalized Maximum Likelihood Estimates for GPD Parameters

In order to draw a sample from the distribution with upper tail, the sample is first classed as either belonging to the empirical part of the distribution, or the upper tail, using a uniform random variable to ensure the correct proportion of samples lie in each part. In the former case, the sample is made using the technique described in Section 4.3.3.4; in the latter it is drawn from the GPD distribution using a sampling function created by Brodtkorb *et al.* (2000).

4.4 Model Performance Evaluation

4.4.1 Evaluation Methods

In order to evaluate stochastic rainfall models, a set of numerical or qualitative criteria must be designed. As models are not designed to reproduce specific rainfall series, but rather to reproduce the dynamic behaviour of natural weather patterns, evaluation criteria should reflect key statistical characteristics of the series. Importantly, such characteristics must also reflect the hydrologist's perception of the model qualities which are important to the specific application. Some of the possible objectives of model evaluation are outlined here.

1. Representation of extreme statistics. Cameron *et al.* (1999), following Onof and Wheater (1993), tested their models against annual maximum rainfalls of periods of 1, 2, 6, 8, 12 and 24 hours, whereas Smithers *et al.* (2002) used 10 different durations and Cameron *et al.* (2000) restricted themselves to just the 1 and 24 hour maxima which were found to be independent, and used the seasonal rather than annual maxima. Recognising the restrictions of judging seasonal maxima against only one observed series realisation, Cameron *et al.* (2000) calculated confidence limits for quantiles of a fitted GEV distribution, and judged a model as behavioural if was bracketed by the 2.5% and 97.5% simulations.

2. Representation of dry periods. As well as flood peaks, the model should also be able to reproduce droughts. The proportion of dry intervals, with the mean and standard deviation of their length, have been used for this purpose (Cameron *et al*., 2000).

3. Representation of storm characteristics. Koutsoyiannis and Mamassis (2001) ensured that storm character was adequately reproduced by their model by plotting total storm depth and incremental storm depth against duration for each duration class, together with respective standard deviation and autocorrelation. The mean and standard deviation of storm duration can also be used.

4. Representation of long-term rainfall averages. This measure would use essentially the same method as that used when evaluating representation of flood peaks (Point 1).

However, longer durations (e.g. months) would allow comparison of long-term averages against observed data.

In order to produce rainfall simulations to enable a flood frequency analysis for Linton, the relevant objectives of model evaluation were felt to be the accurate representation of rainfall maxima at a range of durations, to represent the range of causes of flooding from short-term, high intensity events, through prolonged but lower-intensity rainfall events, to longer-term rainfall averages. These evaluations should be split by season as summer and winter rainfall patterns differ considerably, as discussed in Section 4.3.2.3. The performance of the rainfall model was therefore tested by extracting seasonal maximum rainfalls of durations 1 hour, 24 hours, 7 days and 28 days from simulated rainfall sequences of the same duration as the observed sequence, and comparing these to the true seasonal maxima. This contrasts with previous studies which have in general only tested rainfall maxima for durations of less than 24 hours. By extending the duration, a more comprehensive evaluation of the model is made, and the longer-term rainfall volumes which are particularly important in a groundwater-dominated catchment such as Linton are included in the validation exercise. In order to account for the inherent variability in stochastic simulation, 100 sequences were created and used to obtain these statistics. The range of values was then plotted to ensure that the observed values fall within this envelope. When validating the simulated extremes, it is important to recognise the inherent difficulty associated with the treatment of observed extremes as 'true' data against which the model should be compared. Although the observed data provide the best information available on catchment behaviour, the rainfall record represents only a single sample from the range of possible records, and is therefore prone to sampling bias. This is especially relevant given the short length of rainfall data available, and should therefore be taken into consideration during the validation procedure.

4.4.2 Evaluation of Empirical Density Model: Results

As described above, for winter and summer the derived statistics from 100 simulations are plotted together with the observed values (Figures 4.7 and 4.8). The results show that for each duration, the true maxima are bracketed by the model simulations, demonstrating that the model is adequately reproducing the rainfall characteristics of the catchment in terms of seasonal extremes.

It is interesting to note that for the 7 day and 28 day totals, the true maxima are approximately central to the multiple model simulations, however for the 1 and 24 hour totals the model simulations tend to over-predict the rainfall total, especially for the winter season. One possible cause for this finding is that the duration classes chosen were too wide, meaning that the intensity and profile shape of storms was not matched to their duration with sufficient accuracy. For example an 11-hour storm could be given a higher intensity or flatter profile sampled from a 5-hour storm, giving an unrealistically high 24-hour total. Over longer time periods this effect would be less noticeable as high within-storm totals would be counterbalanced by the assumption that no rain falls without storm periods.

To test this theory, the methodology suggested in Section 4.3.3.5 was implemented, namely to use a bivariate distribution for duration and intensity, smoothed using a bivariate normal kernel. Surprisingly, this did not improve the results, with the seasonal maxima for 24 hour duration still proving over-predicted. The methodology did not, however, address the similar problem in profile choice, although it is not clear how to smooth the array of profile shapes as they cannot obviously be ordered. One possibility is to make a random choice from existing profile shapes and then to add noise. However, it was felt that by tying the intensity and/or profile shapes more closely to the sampled duration, the model is limited in the choice of storms and may not address the assumption that the observed storms do not encompass the full range of possible storms.

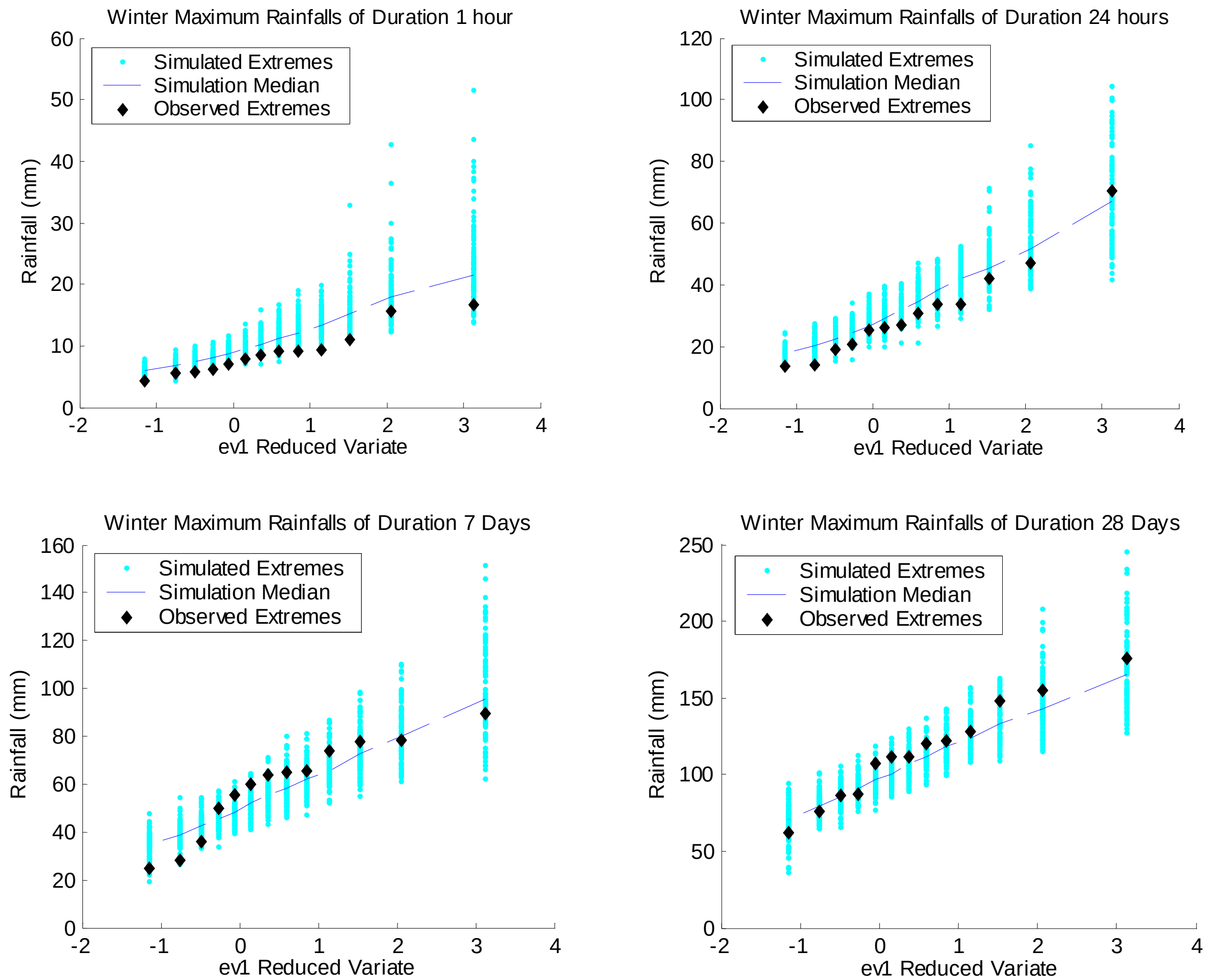

Figure 4.7: Observed Maximum Winter Rainfalls compared with 100 Simulated Realisations, for Durations 1hr, 24hr, 7 day, 28 day.

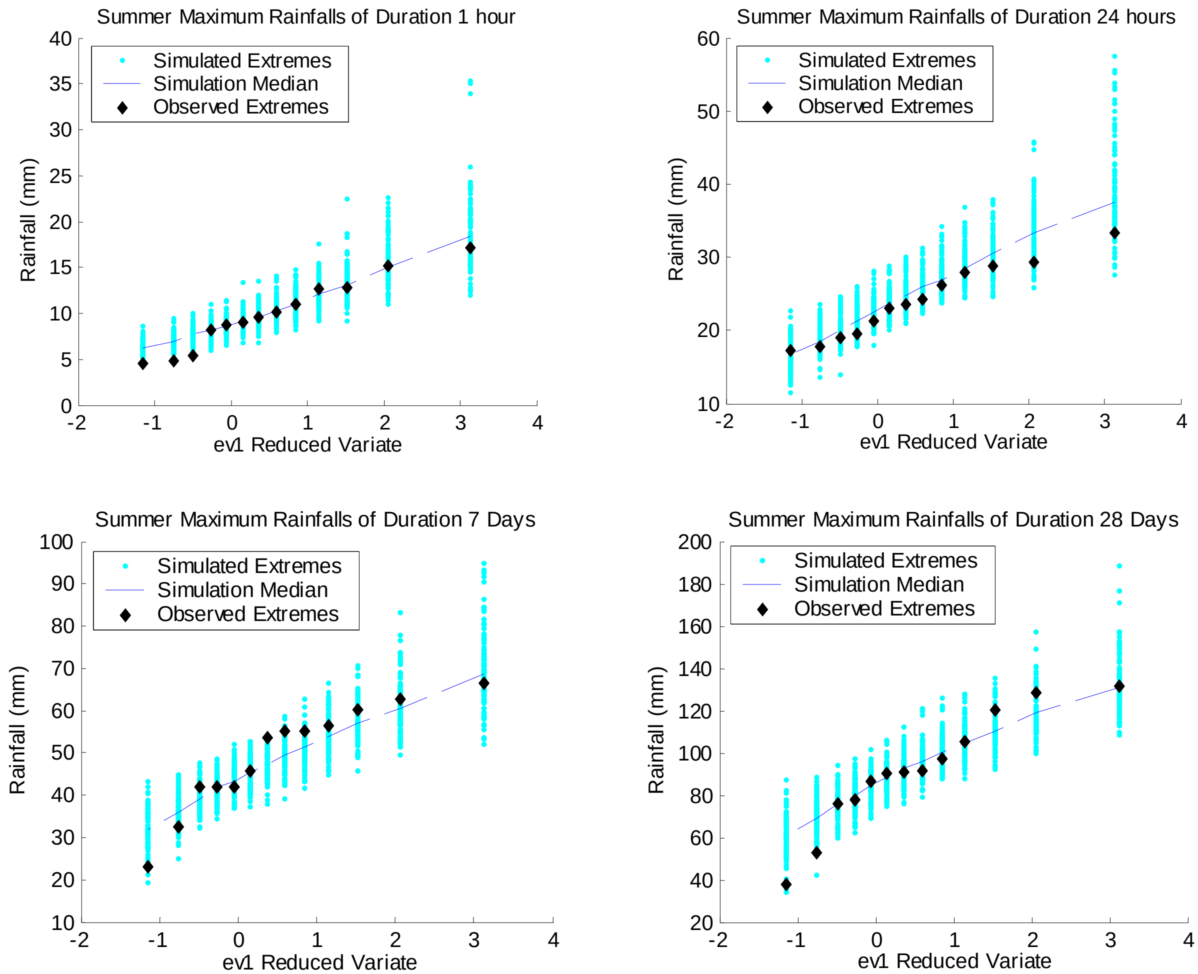

Figure 4.8: Observed Maximum Summer Rainfalls compared with 100 Simulated Realisations, for Durations 1hr, 24hr, 7 day, 28 day.

4.4.3 Evaluation of Empirical Density Model with Fitted Tail: Results

As with the original simulation model, the performance of the extended model was tested by plotting the seasonal maxima at durations of 1hour, 24 hours, 7 day and 28 days. The plots are shown in Figures 4.9 and 4.10 for the winter and summer seasons respectively. It is clear that these predictions produce a much poorer fit than the original model without GPD tail added, with the simulations overestimating the observed maximum flows in almost all cases. This was to be expected given that the original model tended to produce an overestimation, and this problem has been exacerbated by the possible inclusion of storms of higher intensity than that observed.

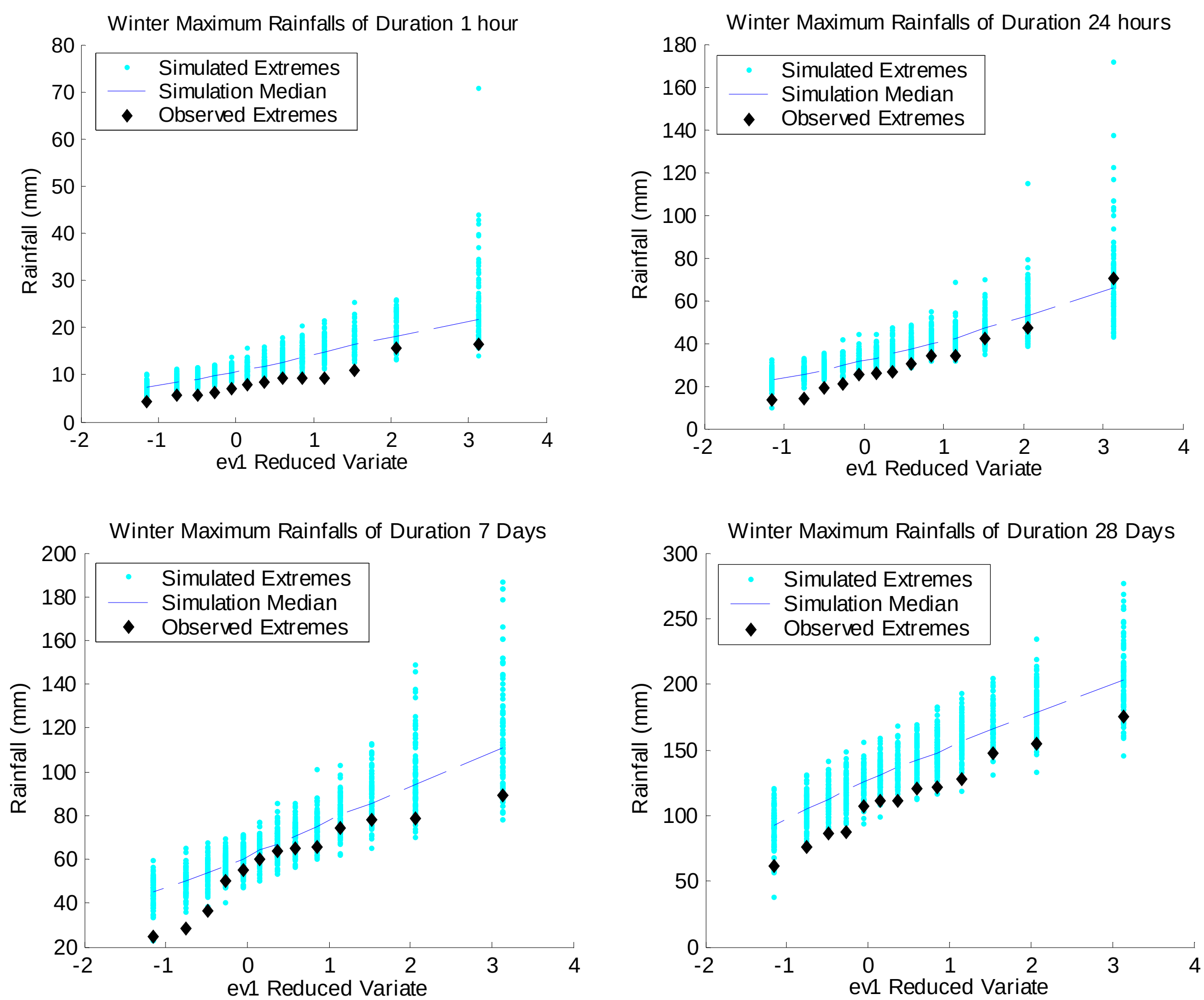

Figure 4.9: Observed Maximum Seasonal Rainfalls compared with 50 Simulated Realisations using model with GPD tail, for Durations 1hr, 24hr, 7 day, 28 day.

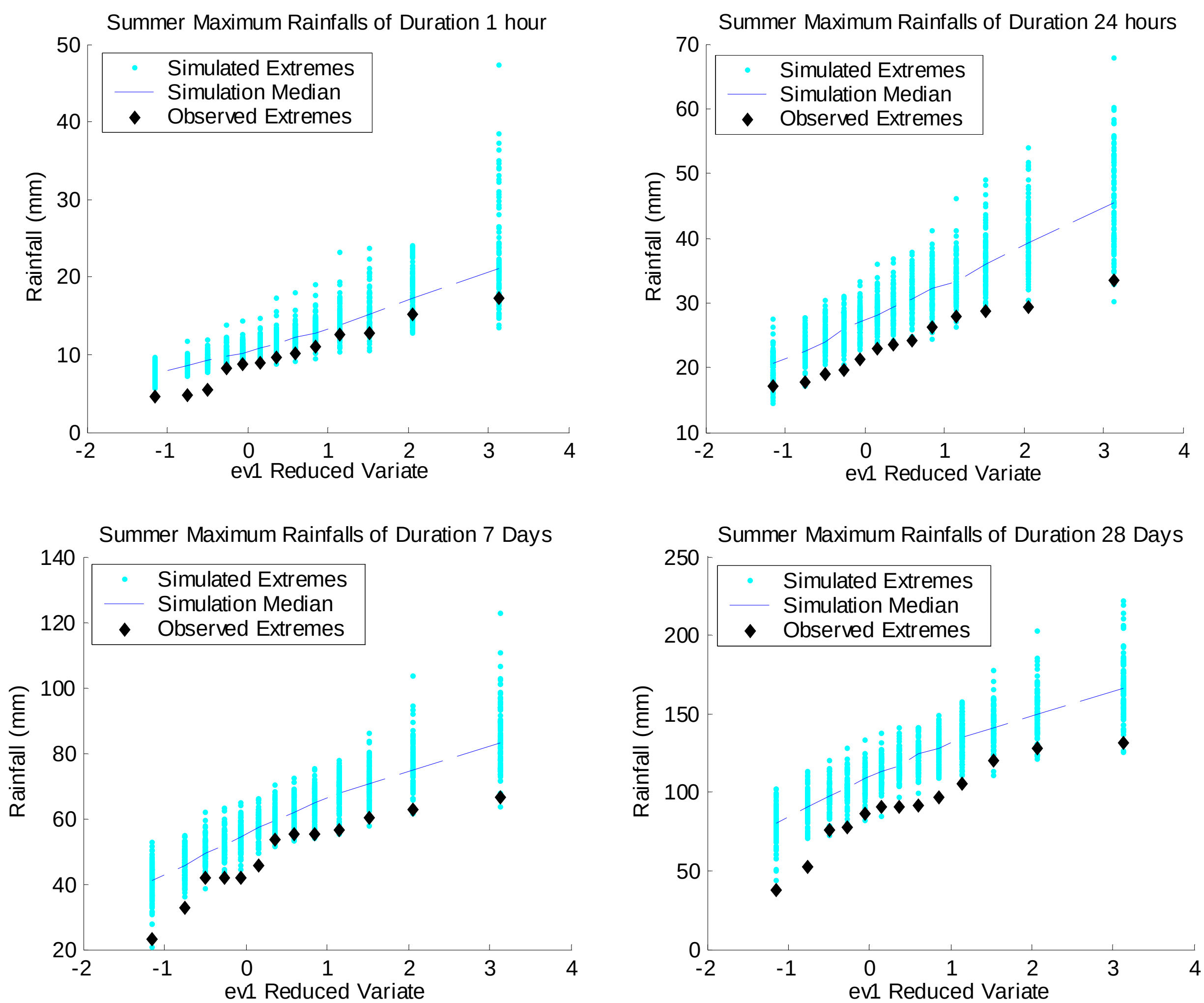

Figure 4.10: Observed Maximum Summer Rainfalls compared with 100 Simulated Realisations using model with GPD tail, for Durations 1hr, 24hr, 7 day, 28 day.

4.4.4 Discussion

The results of the model evaluation with respect to reproduction of extreme rainfall statistics show that the empirical model, without extension by mean of an upper intensity tail, produces simulation results which bracket the observed extremes. In contrast, when a tail is added to the intensity distribution the model shows marked overestimation of the rainfall extremes.

It could be argued that due to the relatively short sequence of validation data available, the latter set of simulations provide an equally valid prediction of future behaviour and indicate that much higher rainfall totals than those observed could be expected. However the model choice must be made with regard for the meteorological and hydrological behaviour of the catchment of interest. If we are to accept that higher intensities of storms should be included in the model despite lack of empirical evidence, in fact with a reduction of fit quality, we must be certain both that such storm intensities are likely to occur, albeit with low probability, and that the storms so produced would have important effects on the flood regime of the catchment that could be observed during a long measurement period but are not already achieved through use of the empirical model. In respect of the first point, the concept of *'probable maximum precipitation'*, that there is an upper bound on intensity given a specified duration, location and season, is widely used. The calculation of such a figure would be based on critical meteorological conditions of raindrop size and frequency. This concept is in conflict with the assumptions behind the addition of an infinite tail to the intensity distribution, although even if accepted it cannot be used to draw conclusions on whether the intensity spectrum is fully represented by the empirical data.

Secondly, consideration must be given to the critical processes governing discharge generation within the particular catchment of interest. Summer storms are known to generate high intensity, short duration rainfall in the Linton catchment, yet there are no corresponding records of damaging flood peaks during the summer months. Instead, flood events are generally autumn or winter phenomena, caused only when rainstorms occur in times of high antecedent groundwater levels. The stochastic rainfall model would replicate such conditions through unusual clustering of rainfall events (i.e. a series of low inter-arrival times), contributing to an extreme value of long-term rainfall total. This type of pattern is possible through use of the empirical model, and does not depend on high intensity rainfall during individual storms. Given this assessment, the empirical model (without intensity tail) was chosen to be used in future simulations.

4.5 Conclusion

The stochastic rainfall model has been shown to provide an efficient and accurate characterisation of the rainfall regime recorded by the Elmdon gauge. Using kernel-based smoothing of the empirical distributions of storm characteristics, the rainfall series has been used to determine the model behaviour without additional parameterisation. Storms have been separated by season of occurrence, to allow for different meteorological behaviour during winter and summer seasons. Storms were also grouped according to intensity to account for the correlation between duration and intensity. In addition to the purely empirical model, a second model was created which allows for the possibility of storms with higher intensity than that measured during the calibration period. This is done by using a parameterisation of an extreme value distribution to fit an upper tail to the intensity distribution, while retaining the empirical distribution for lower intensities.

The two models were tested by comparing the observed rainfall maxima over periods from 1 hour to 28 days with the corresponding maxima from a suite of simulated series. This tested both the short and long term rainfall response characteristics. The results suggest that the first empirical model provides an accurate simulation of the observed maxima, with the range of simulation maxima bracketing these for each test. The second model with an extended upper tail performed less well, with a tendency to overestimate maxima, and was therefore rejected in favour of the purely empirical model. The finding that a restriction of the intensity distribution to empirical pdf alone does not prevent realistic simulation of extremes follows the conclusions of Cameron *et al.* (2000) who did not use an upper tail for high duration intensity classes. The decision was also validated by a consideration of the controlling processes of flood generation in the Linton catchment, demonstrating the importance of a model tailored to the individual site characteristics.

Finally, the processes described above of storm identification, separation by season and duration, density estimation, sampling and production of stochastic rainfall sequences, were all automated as Matlab scripts, such that arbitrarily long series may be generated to form the input for a rainfall-runoff model.

Chapter 5

RAINFALL-RUNOFF MODELLING

Abstract

This chapter describes the structural choice, parameterisation, application and testing of the rainfall-runoff model component of the flood risk assessment framework. A transfer function model is used, consisting of a nonlinear module to represent runoff generation and a linear module to represent runoff routing. This class of model allows the incorporation of some information on catchment structure, while retaining the benefits of a lumped model.

The model algorithms are defined, and through consideration of catchment characteristics and gauged flow data available from the river tributaries, two candidate model structures are put forward. These are tested using a restricted search of the parameter space to find optimal parameter sets for each structure. The simpler model is found to be preferable, providing improved parameter identifiability while achieving similar predictive performance to the more complex model.

The rainfall-runoff model is tested using an application to the Linton catchment of the River Granta. The GLUE methodology for uncertainty estimation is used, which rejects the premise of an optimal model parameterisation and instead allows many different parameter sets to contribute to the model prediction. The model is validated in terms of its predictive capacity for hydrograph simulation and annual maxima statistics. The performance of the model is found to be satisfactory, and to allow prediction of extreme discharges even where flow records are incomplete due to gauge malfunction.

5.1 Introduction

Within the end-to-end modelling scheme, the rainfall-runoff model is required to represent the transition of water from rainfall over the catchment area to channel discharge upstream of Linton. The hydrological processes that the model must represent include interception and evapotranspiration, overland flow and infiltration, soil storage and subsurface flow and routing. The methods available to simulate these functions range from explicit process representation in physically-based mechanistic models to empirical 'black-box' models. A physically-based model is structured to represent the scientist's perceptual model of the system and is based on hydrological principles. Such mechanistic models are often large and complex with many parameters, reflecting the perceived complexity of the underlying system (Young, 1993). At the other end of the scale are empirical models where the model structure and parameter values are inferred from the experimental data available and no prior knowledge of the system is assumed. Most models lie somewhere between these two extremes, and the choice of model must be made with respect to the project goals. In particular, the outputs required from the model must be considered; these could range from the simple, e.g. a single hydrograph, through to the very complex, e.g. distributed mapping of soil moisture.

In this study, the primary function of the model is to make an accurate prediction of discharge given information on rainfall. No other information is required on catchment state or water table levels, and no validation datasets on this type of variable are available. This fits with the consideration that the model chosen must be suitable for parameterisation with limited quantities of observational data. These points led to the conclusion that a lumped model would be most suitable for this application. There is, however, a requirement that some information on catchment structure can be incorporated into the model, as data is available for separate tributaries within the catchment. A popular class of models that have the ability to include this type of structural information are the *Transfer Function* models. These models originated from unit hydrograph theory and the Nash Cascade (Nash, 1959), which represent the catchment as a linear system. The conventional model structure is detailed in Section 5.2.2, and allows the catchment to be modelled as a combination of interconnected flow pathways. The structure has been widely tested, and comprehensively reviewed by Young (2003). Two methods of using this basic approach have emerged: the first is referred to by Wheater *et al.* (1993) as a 'hybrid metric-conceptual model' and uses an *a priori* identification of model structure based on the hydrologist's knowledge of the catchment. Parameters of this model are then optimised using the data available. This approach is used in the popular IHACRES model of Jakeman *et al.* (1990). The second has been termed 'Data-based Mechanistic Modelling' by its developers (Young and Beven, 1991; Young and Beven, 1994) and uses an *a posteriori* model identification approach using statistical estimation procedures, based on the philosophy that the data itself should be allowed to suggest the model structure.

Transfer functions in themselves are not sufficient to map rainfall to stream discharge, due to the nonlinearity of the system. Antecedent conditions in the catchment, together with storm profile and intensity, affect the relationship between the measured rainfall and the 'effective rainfall' – the fraction of the rainfall that is routed into the channel system – in a nonlinear way. The transfer function module must therefore be augmented with a nonlinear module which seeks to represent this complexity. Again several options have been developed, ranging from conceptual catchment moisture deficit accounting schemes (Croke and Jakeman, 2004; Evans and Jakeman, 1998) through those which seek to provide a simple conceptualisation of soil storage behaviour (e.g. Jakeman and Hornberger, 1993; Post and Jakeman, 1996; Sefton and Howarth, 1998) to those which allow the data to suggest the filter form (Young and Beven, 1991; Young and Beven, 1994). Chapman (1996) evaluated four loss models including that of the IHACRES model of Jakeman *et al.* (1990) and the 'Time Compression Approximation' of Reeves and Miller (1975). He found that the optimal algorithm varies between catchments, but that increasing the complexity of the module does not necessarily improve the results.

5.2 Model Definition

Transfer function methodology was used in this study to provide the rainfall-runoff model component. As outlined above, the model consists of a nonlinear rainfall transform module that controls the fraction of the rainfall available as runoff (the *Effective Rainfall*), followed by a linear routing module controlling the characteristics of the runoff pathways. The combination of serial and parallel linear pathways may be chosen by the hydrologist; a simple example using two parallel pathways is illustrated in Figure 5.1.

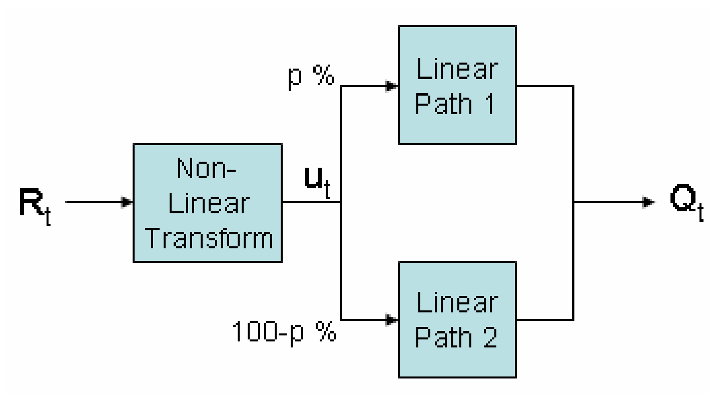

Figure 5.1: Example Transfer Model Structure with two parallel linear pathways
R_t = Rainfall, u_t = Effective Rainfall, Q_t = Discharge

The following sections describe the algorithms used for the nonlinear and linear transforms, and the choice of linear pathway structure.

5.2.1 Non-Linear Rainfall Transform

The nonlinear rainfall to effective rainfall transform used in the model is set out below (Equations 5.1 – 5.3). This version of soil storage representation was applied by Sefton and Howarth (1998) in their version of IHACRES. It is, in turn, a generalisation of the 'Antecedent Precipitation Index' concept which provides a representation of current soil wetness (Ye *et al*., 1998).

$$u_t = R_t\left(S_t + S_{t-1}\right)/2 \qquad (5.1)$$

$$S_t = cR_t + \left[1 - \frac{1}{\tau\left(T_i\right)}\right]S_{t-1} \qquad (5.2)$$

$$\tau\left(T_i\right) = \tau_w \cdot \exp\left(20f - T_i f\right) \qquad (5.3)$$

Here u_t is the volume of effective rainfall at time t resulting from input rainfall R_t. S_t represents the catchment storage index at time t, $\tau(T_i)$ is the recession rate of S_t at temperature T_i which depends on the recession rate at 20ºC, τ_w. The parameter c is used to ensure that the volume of effective rainfall equals the volume of runoff (requiring that catchment storage is similar at the start and end of the modelling period, usually achieved by modelling between two times of low flow). The parameter f modulates evapotranspiration with temperature. The model therefore requires a temperature series for the period of interest, and the use of calibration techniques to identify parameters c, τ_w and f for each model application.

The form of the non-linear function implies assumptions about the hydrological response of the catchment which reflect the beliefs of the modeller (Young and Beven, 1994). Some features of the catchment are constrained in their ability to affect the catchment response to rainfall, for example seasonal vegetation effects may only be represented through the temperature parameter f (Ye *et al.*, 1998).

5.2.2 Linear Routing Transfer Function

The linear routing module of the rainfall-runoff model is provided by the use of a transfer function to convert effective rainfall u_t into flow Q_t. A generalised higher-order transfer function has the form shown in Equation 5.4.

$$Q_t = \frac{b_0 + b_1 \cdot z^{-1} + \cdots + b_m \cdot z^{-m}}{1 - a_1 \cdot z^{-1} - \cdots - a_n \cdot z^{-n}} \cdot u_{t-\delta} \qquad (5.4)$$

Where z^{-1} is the backward shift operator, i.e. $z^{-1}Q_t = Q_{t-1}$. The notation [m n δ] is used to refer to a transfer function of this order; i.e. where the numerator has order m, the denominator has order n, and the pure time delay is δ.

In cases where the denominator polynomial has real roots, this form is equivalent to a linear combination of first order transfer functions of the form shown in Equation 5.5.

$$Q_t = \frac{b}{1 - az^{-1}} \cdot u_{t-\delta} \qquad (5.5)$$

Each such transfer function represents a single flow pathway where $Q_t = aQ_{t-1} + bu_{t-\delta}$. A higher order transfer function may therefore be designed to represent any combination of flow pathways within the catchment which exist in series or parallel.

The most usual form of transfer function to be specified for small catchments is that of two parallel pathways representing quickflow and slowflow. This structure has been used in many applications, with possible interpretations of the two pathways being that they represent surface and subsurface flow, or old and new water. Although in cases of low noise it has been shown that a model with three components is often identifiable (Jakeman and Hornberger, 1993), this structure has less often been used in hydrological applications. In some applications a single component may be preferable, such as those where data is scarce (McMillan, 2002), or in ephemeral catchments without significant baseflow (Ye *et al*., 1997a; Ye *et al*., 1998).

In the case of the catchment of the Granta to Linton, the choice of model structure was made in relation to both knowledge of physical catchment characteristics and gauging carried out in the field, as described in Chapter 3. The chalk aquifer underlying the catchment is known to give significant baseflow and therefore flows are expected to have a component pathway with a slow time constant relating to this groundwater contribution. This suggests that a one-component model is unlikely to be a suitable candidate structure as it would be unable to reproduce both the baseflow and flood peaks caused by runoff from the boulder clay surface cover. A two-component model may provide sufficient scope for representation of the catchment behaviour; however it is also possible that a three-component model would be more suitable to allow the simulation of a shallow subsurface flow in addition to the deep aquifer flow.

Parallel pathways within the catchment may also be used to represent different geographical areas of the catchment which may have different physical characteristics or different precipitation regimes. This type of structure could also be used to allow scenario modelling, for example by examining effects of land-use change in individual subcatchments. It was thought possible that such a model might prove necessary in the Linton catchment, as the three tributaries meeting at Bartlow drain areas with varying topography and which frequently receive markedly different rainfall totals during storm events. The component hydrographs reconstructed using gauged data from Bartlow were therefore consulted. Figure 5.2 shows a typical result, reprinted from Chapter 3.

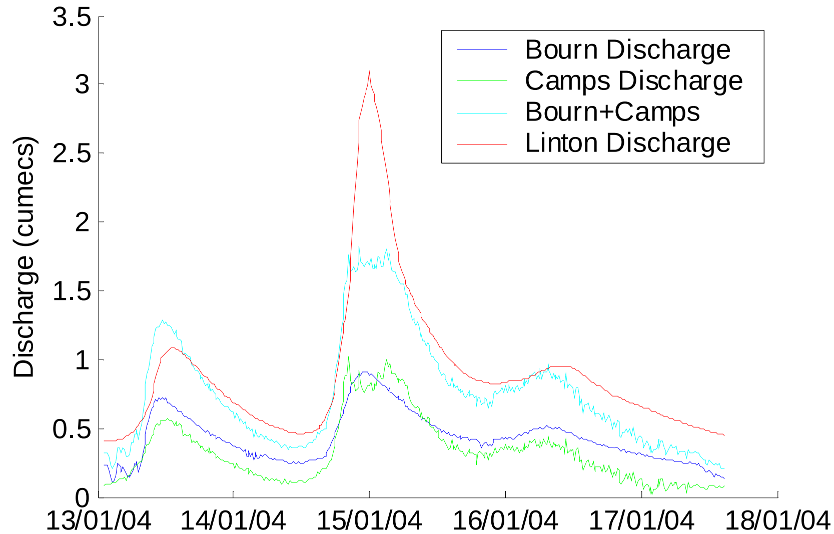

Figure 5.2: Comparison of Discharges from the tributaries of the Granta, and that recorded at Linton, for a single hydrograph.

The two major tributaries (Bourn and Camps tributaries) were found to have very similar hydrograph forms, although the Bourn tributary may have a slightly slower recession. This suggests that the two tributaries do not need to be represented as separate flow pathways, and could more parsimoniously be considered as a combined source. As described above, this source is expected to require representation by at least two parallel pathways to include the known groundwater component. However, it appears from the sample hydrograph that an additional flow pathway may be activated in times of high flow, increasing the flow peak between Bartlow and Linton. This is postulated to be a result of overland or near-surface flow directly into the river channel rather than through tributary streams, as a result of the less complex topography close to Linton. This result is not however seen in all the sample hydrographs.

Two different model structures were therefore developed for testing. The first comprised two parallel pathways, under the assumption that additional flow between Bartlow and Linton may be represented by an additional volume entering the same pathway structure as that of the upper catchment. The second adds an additional pathway, expected to have a shorter time constant and therefore be activated mainly during flood events, which allows for a different underlying mechanism of water transport in the lower part of the catchment. Results from the tests are allowed to determine the final choice of structure. This method follows the philosophy of data-based mechanistic modelling, allowing the data to determine model structure.

The two structures to be used are therefore as follows:

$$Q_t = \frac{b_0 + b_1 \cdot z^{-1}}{1 - a_1 \cdot z^{-1} - a_2 \cdot z^{-2}} \cdot u_{t-\delta} = \left[\frac{\beta_q}{1 - \alpha_q \cdot z^{-1}} + \frac{\beta_s}{1 - \alpha_s \cdot z^{-1}} \right] \cdot u_{t-\delta}$$

Equation 5.6: Two-component transfer function structure

$$Q_t = \frac{b_0 + b_1 \cdot z^{-1} + b_2 \cdot z^{-2}}{1 - a_1 \cdot z^{-1} - a_2 \cdot z^{-2} - a_3 \cdot z^{-3}} \cdot u_{t-\delta} = \left[\frac{\beta_q}{1 - \alpha_q \cdot z^{-1}} + \frac{\beta_s}{1 - \alpha_s \cdot z^{-1}} + \frac{\beta_{xs}}{1 - \alpha_{xs} \cdot z^{-1}} \right] \cdot u_{t-\delta}$$

Equation 5.7: Three-component transfer function structure

The model structures are shown in diagrammatic form in Figures 5.3 and 5.4. The parameters that must be estimated for the two component model are β_q, β_s, α_q, α_s, δ (where suffix q represents quickflow parameters, s represents slowflow parameters), given calibration data consisting of effective rainfalls $\{u_t\}$ and flows $\{Q_t\}$. For the three component model there are additional parameters β_{xs}, α_{xs} representing the extra store. However, there is an additional constraint that water volume must be conserved within the model, as we assume that all effective rainfall becomes discharge. In order to satisfy this constraint, it is easier to consider the parameters in terms of proportion of flow p_q and p_s (and p_{xs} for three stores) entering each of the pathways, with the corresponding recession time constants τ_q and τ_s (and τ_{xs}). The constraints then become:

$p_s = 1 - p_q$ *(5.8: Two components)*

$p_{xs} = 1 - p_q - p_s$ *(5.9: Three components)*

The new parameters are related to the original parameters by the following equations:

$$\tau_q = \frac{\Delta}{\ln(\alpha_q)} \qquad \tau_s = \frac{\Delta}{\ln(\alpha_s)} \qquad \tau_{xs} = \frac{\Delta}{\ln(\alpha_{xs})} \tag{5.10}$$

$$p_q = G_q = \frac{\beta_q}{1-\alpha_q} \qquad p_s = G_s = \frac{\beta_s}{1-\alpha_s} \qquad p_{xs} = G_{xs} = \frac{\beta_{xs}}{1-\alpha_{xs}} \qquad (5.11)$$

Where G_q, G_s and G_{xs} are the steady state gains of the first order components.

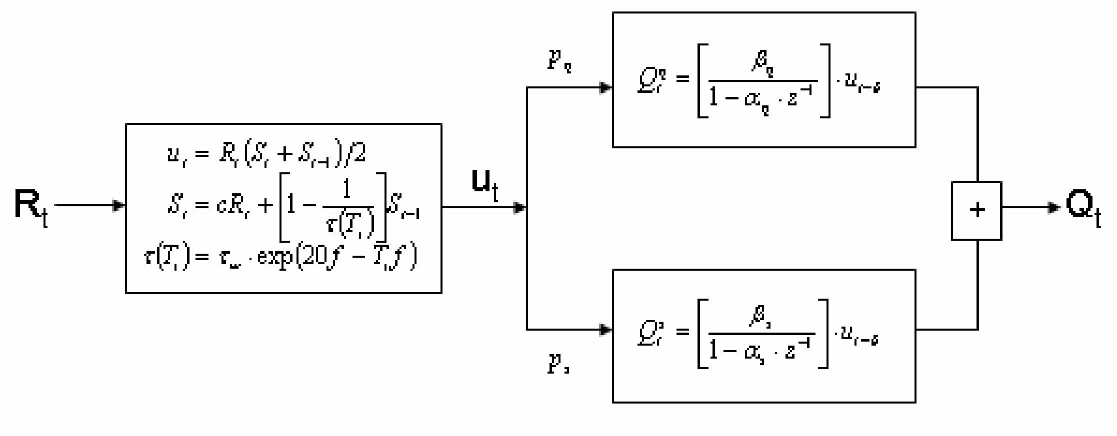

Figure 5.3: Schematic diagram of two-component rainfall-runoff model structure.

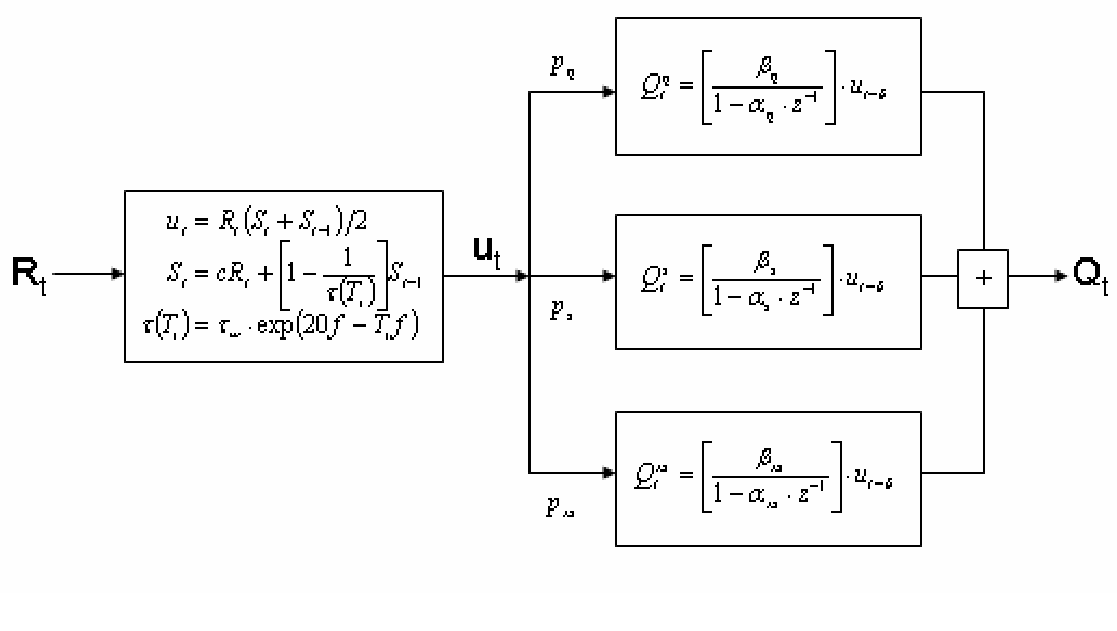

Figure 5.4: Schematic diagram of three-component rainfall-runoff model structure

5.3 Model Calibration Techniques

5.3.1 Calibration Strategies

In order to make predictions of discharge from the rainfall hyetograph, values for the parameters c, τ_w and *f* in the non-linear module, and τ_q, τ_s and p_q (also τ_{xs} and p_s for the three-component model) in the linear module must be found. There are numerous techniques available to choose these values. The first decision that must be made is whether the hydrologist believes that an 'optimal' parameter set exists to be found, or whether it is believed that many parameter sets may produce similarly good results.

In the former case a number of automatic optimisation techniques may be used. In many studies using transfer function models, the Simplified Refined Instrumental Variable (SRIV) technique (Young, 1984; Young and Jakeman, 1980) and its corresponding continuous time form are used (e.g. Jakeman *et al*., 1990; Ye *et al*., 1998). However many other techniques are available from basic hill-climbing algorithms, to simulated annealing and genetic algorithms. A discussion of various methods is given in Sorooshian and Gupta (1995). When optimum parameters have been identified, they may in turn be used to inform our knowledge of catchment dynamics (Hansen *et al*., 1997).

In the latter case, it is accepted that in trying to model any hydrological regime, there may be no optimum parameter set, nor indeed any optimal model structure. Instead, given a set of observed data and a particular model structure, many different parameter sets from different regions of the parameter space may give similarly good predictions, judged in terms of some objective function. Instead of a peak in the response surface of the objective function, a plateau may be found, with the value of the objective function limited by errors in observed data or by constraints imposed by the model structure. This type of response has been described by the term 'equifinality' (Beven, 1996; Beven and Binley, 1992), and demands new methods of model calibration together with an acceptance of the uncertainty within the modelling procedure

5.3.2 GLUE

5.3.2.1 Philosophy

The Generalised Likelihood Uncertainty Estimation (GLUE) methodology, proposed by Beven and Binley (1992), is premised on the concept of equifinality and allows many different model realisations to contribute towards an estimation of hydrological response and, integrally, the associated uncertainty.

Based on principles from Bayesian statistics, the technique relies on the computation of a 'likelihood' measure, which represents an estimate of how likely the model is to produce acceptable simulations based on its performance tested against some observed data. The idea of a likelihood measure is adapted from traditional statistical theory, where it measures the probability of the observational errors giving rise to the measured data, assuming that the given model structure is correct. In a hydrological context, the choice of the likelihood measure rests with the modeller and is a subjective choice, as the model structure and parameterisation are being tested for suitability in a particular context rather than absolute accuracy. Assumptions that errors are independent or conform to given distributions are also rejected. The only constraints on the likelihood measure are that it should be zero for models which are considered ‘non-behavioural’ (i.e. produce results too poor to contribute to the final prediction), and that it should increase monotonically with perceived ‘goodness-of-fit’ to the calibration data. The method can easily be extended to a multicriterion calibration by amending the likelihood measure accordingly (Gupta and Sorooshian, 1998).

The model is then run many times using many different parameter sets (Monte Carlo simulations), and the likelihood value calculated for each one. These likelihood values are then normalised such that the sum of all the likelihood values calculated is unity. Finally the predictions of each behavioural model are weighted using the normalised likelihood value. A cumulative distribution can then be calculated for each prediction variable at each timestep, and hence quantiles as required (Equation 5.12).

$$P(Q_t < q) = \sum_{i \in X} L(\Theta_i) \text{ where } X = \left\{ i \mid Q_t^i < q \right\} \qquad (5.12)$$

Where Q_t is the predicted flow (or other variable) at time t, q is the observed flow, Θ_i is the i^{th} set of parameters for the model, $L(\Theta_i)$ is the likelihood value obtained when the model is run using these parameters, and Q_t^i is the predicted flow at time t using these parameters. The empirical nature of the GLUE method allows the calculation of such quantiles despite the typically non-normal distribution of the set of flow predictions.

The success of the methodology may be tested against the calibration data (or separate validation data in the case of split-sample testing) by plotting both the recorded flow, and quantiles at typically 90% or 95% certainty from the GLUE procedure. Where further calibration data are available, either from a different time period or from the measurement of an alternative variable, a test may be carried out to determine whether the uncertainty in the response would be constrained by use of the additional data. By repeating the methodology with a likelihood measure that combines the two sets of data, the updated prediction bounds may be plotted. A narrowing of the bounds represents an improved constraint of response, however this does not always occur, for example Lamb *et al*. (1998) found little improvement when using borehole data in addition to discharge data.

5.3.2.2 Feasible Parameter Ranges

A number of decisions must be made when carrying out the GLUE analysis. Assuming that the model structure has been fixed, feasible ranges must be identified for each model parameter, beyond which the parameter will not be tested. These should generally be set more widely than hydrological experience with the given parameter might suggest, as previous studies have found high likelihood values even with extreme parameter values (e.g. Beven and Freer, 2001; Duan *et al*., 1992) and the choice of narrow ranges may represent an unwarranted restriction of the search space (Xiong and O'Connor, 2000).

5.3.2.3 Parameter Space Sampling Strategy

Further to the definition of the bounds of the parameter space, the methodology to be used to sample this space must be decided. The most basic method is to use a uniform sampling strategy for each parameter independently. This strategy has been used in the majority of applications of the procedure to date due to its simplicity; however it may be inefficient if there are large parts of the parameter space which do not produce any behavioural simulations. This could occur if the feasible parameter ranges have been set too wide, or could be due to interactions between the parameters. This inefficiency has led to various attempts to improve the sampling strategy, generally by using some prior information about the parameter space. This information could be in the form of mechanistic arguments, past experience of the model, or more commonly using an adaptive sampling strategy based on previous samples or an initial trial set of samples. Examples of this are the tree-structured strategy of Spear *et al*. (1994), the Guided Monte Carlo algorithm (Chen *et al*., 1997; Shorter and Rabitz, 1997), various methods of Markov Chain Monte Carlo e.g. the Shuffled Complex Evolution Metropolis algorithm (Vrugt *et al*., 2003), and the stochastic response surface method of Hossain *et al*. (2004). Marshall *et al*. (2004) provide a comparison of four different methods.

5.3.2.4 Likelihood Measures

Once samples have been taken from the parameter space, the model is run using each parameter set in turn. Outputs should then be made from the model to allow a comparison with the observed data available. Typically for a rainfall-runoff model this consists of simulated channel discharge. A method must then be chosen to compare the observed and simulated discharges and produce the monotonically increasing likelihood measure required by the GLUE method.

Probably the most widely used likelihood measure is the R^2 efficiency measure of Nash and Sutcliffe (1970)

$$E = 1 - \frac{\sigma_e^2}{\sigma_o^2} \qquad (5.13)$$

Where σ_e^2 is the sum of squared errors (error variance) and σ_o^2 is the variance of the observations (here observed discharges). E has the value 1 for a perfect fit, 0 for a fit no better than a straight line fit through the mean of the data, and should be set to 0 for even worse fits where a negative value is produced.

Although the sum of squared errors is a standard metric in statistics, it can have disadvantages in a hydrological setting. In particular, it only gives unbiased estimates of the parameters if errors are independently identically distributed as $N(0,\sigma^2)$. This is a particular problem if errors are due to timing errors where hydrograph lag is incorrectly estimated: in this case errors will be correlated and very poor values of E may be found even if hydrograph shape is correct (Troutman, 1985). The sum of squared errors measure also biases the likelihood measure towards high flow periods where error variance is expected to be higher. This may be an advantage if peak flows are of particular interest to the modeller, however Sorooshian and Gupta (1995) proposed an alternative in the form of a 'Heteroscedastic Maximum Likelihood Estimator' which allows for changing error variance. It is also possible to bias the likelihood measure towards particular parts of the hydrograph by using transformations of the likelihood measure such as taking logs to accentuate recession periods, or using powers to increase the focus on flow peaks. Maximum likelihood estimators may also be developed for autocorrelated Gaussian error (Beven, 2001b; Sorooshian and Dracup, 1980).

The choice of likelihood function is not limited to statistical measures such as those described above. It may instead be chosen to reflect the modeller's perception of the importance of error form. An example of this is in the use of fuzzy measures, based on ideas from fuzzy set theory, which are particularly appropriate when observational data is scarce or uncertain. The measures are essentially a simple function of the error between observed and simulated data (this may be done separately for each timestep, with values then combined to give a likelihood measure for the whole series) and have been used in various hydrological applications (e.g. Aronica *et al*., 1998; Franks *et al*., 1998; Freer *et al*., 2004; Wealands *et al*., 2005).

5.4 Calibration and Validation

5.4.1 Data

The data available for the calibration of the rainfall-runoff model consists of rainfall and flow data from the Environment Agency, as detailed in Chapter 3. During the period 1991-2005, 15-minute rainfall data is available from Elmdon, and 15-minute flow data is available from Linton. Both these records, however, contain extended periods of missing or corrupt data, unsuitable for use during calibration. The series were therefore processed to obtain four continuous and error-free sections of data which could be used for model calibration (Table 5.1).

Series	Start Month	End Month	Length
1	Feb 1993	Jun 1994	1 Year 5 Months
2	Jan 1995	Apr 1995	4 Months
3	Nov 1995	Mar 1999	3 Years 5 Months
4	Jul 1999	Aug 2005	6 Years 2 Months

Table 5.1: Error-free periods of rainfall and flow data.

In total there are 11 years and 4 months of data series available for calibration. The length of series required to effectively calibrate a model depends both on the complexity of the model (number of parameters and sensitivity of these parameters) and on the seasonal variability of the catchment response. Beven (2001b) suggests that for a simple 5-parameter model, 15-20 hydrographs are typically required for a robust calibration. Others have found that a longer series was required, for example Ye *et al*. (1997b) deemed 2-3 years of data adequate; Hornberger *et al*. (1985) found 18 months of data insufficient to record the full range of catchment behaviour. In this case, the 2-store model requires 7 parameters, the 3-store model 9 parameters, and it is concluded that the length of data available is sufficient.

Due to the strong seasonal baseflow signal in the flow data, it is important that the model is calibrated using continuous series of data covering multiple years of record, to allow the model solutions to reflect the seasonal catchment response in addition to the flashy stormflow response. This is achieved within the chosen model structure by a correct parameterisation of the f and τ_w parameters which control the response of the soil moisture store, together with correct distribution of water volumes between quickflow and slowflow stores. Each of the four data sets are therefore input into the model as a whole, in preference to treating the individual seasons separately. The two longer datasets of three and six years respectively are particularly valuable in achieving this aim.

5.4.2 Methodology

5.4.2.1 Model Structure Identification

A primary analysis involves the consideration of the model structure, with the aim of deciding the minimum complexity required. In the Linton catchment two structures were evaluated: the two-store and three-store transfer function models. The evaluation consisted of an initial period of testing to determine which structure was able to reproduce the catchment behaviour to the fullest extent within a well-conditioned framework. Standard methodology for using the IHACRES model suggests that a full parameter space search should be made for the f and τ_w parameters only, with the remaining parameters defined by an optimisation search method. This method greatly reduces the computational effort required as the search space is reduced from six dimensions to two. This technique would not be suitable for the current application as it does not recognise equifinality of solutions across transfer function parameters, which is important in capturing uncertainty in the model predictions; however the method can be used to give an overview of typical model success. For each of the two model structures, wide limits were initially chosen for the f and τ_w parameters (Table 5.2) in order to fully capture model response.

Parameter	Min	Max
f	0	0.5
τ_w (days)	0.5	150

Table 5.2: Initial parameter ranges.

This 2d parameter space was then fully searched using the *rivid* function of the Captain Toolbox (Young *et al*., 2004) to produce an optimised solution for each (f, τ_w) pair. This function uses the Refined Instrumental Variable algorithm which provides robust, unbiased estimation of multivariate transfer function models. The optimisation algorithm was run once for a [2 2 d] model structure and once for a [3 3 d] model structure (refer to

Section 5.2.2 for explanation of notation). Where the denominator polynomial has real roots, these correspond to the 2 and 3-store models. The pure time delay d was allowed to vary between 0 and 12 hours. The solutions were then assessed for goodness-of-fit using the R^2 efficiency measure. As explained previously, four data series of varied length are available for calibration; the results for each series are plotted in Figure 5.5.

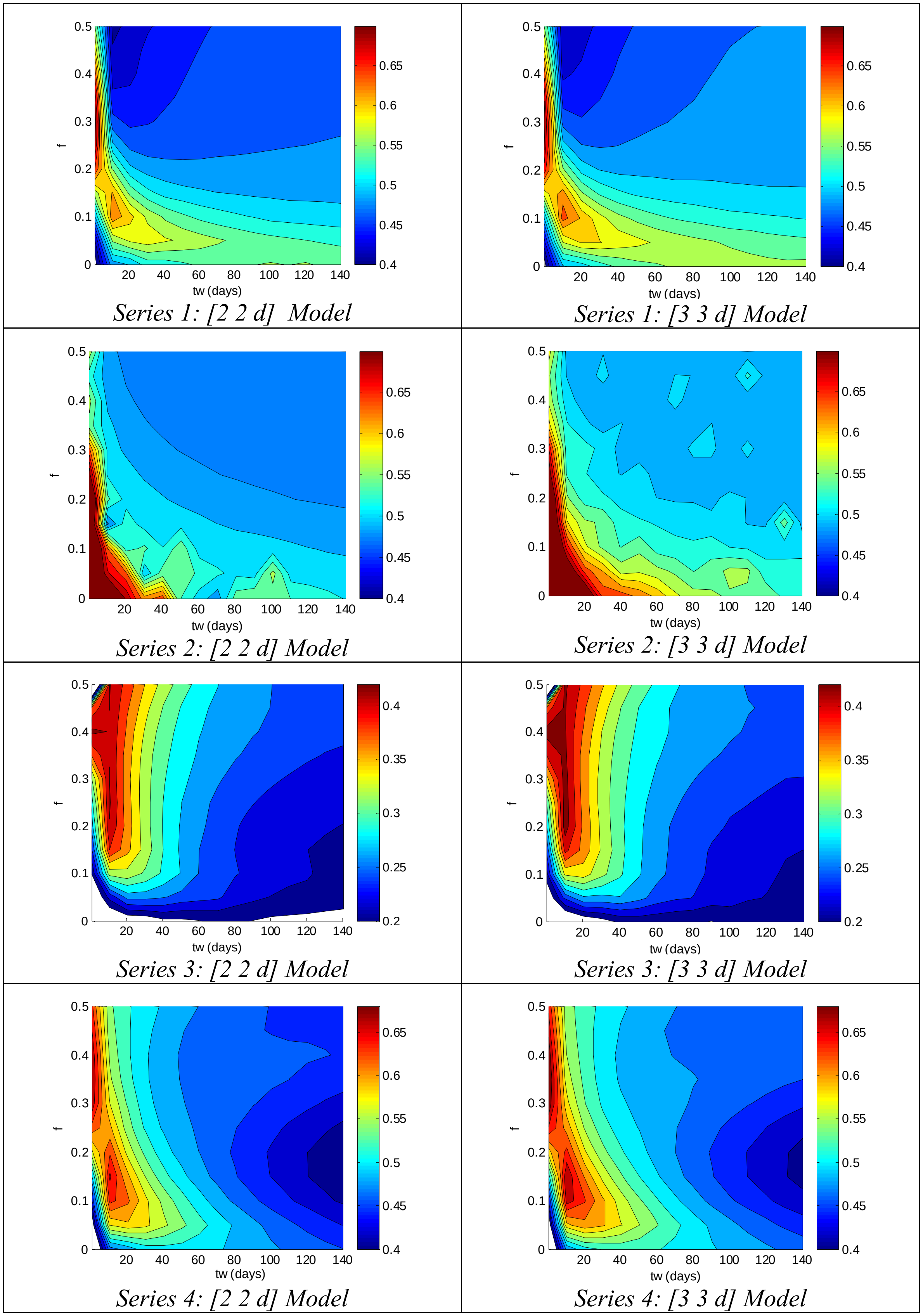

Series 1: [2 2 d] Model

Series 1: [3 3 d] Model

Series 2: [2 2 d] Model

Series 2: [3 3 d] Model

Series 3: [2 2 d] Model

Series 3: [3 3 d] Model

Series 4: [2 2 d] Model

Series 4: [3 3 d] Model

Fig 5.5: Optimised R^2 values from a parameter search of f-t_w space, using each of the four time series of data, fitted using the two-store [2 2 d] and three-store [3 3 d] models.

It is clear that there are significant differences in optimal parameterisation between the data series. In particular it proved difficult to find a satisfactory parameterisation for Series 3; note that the colour scale is adjusted for this series in Figure 5.5 above. Series 3 spans the years 1996-1999, notable for extremely dry conditions. During the 1996-1997 period particularly, flow seldom exceeded the 0.04 m^3s^{-1} pump-supported level. The model struggled to simulate the lack of response to the limited winter rainfall; this is conjectured to be partly due to abstraction within the catchment which is not represented by the model. Although the parameter sets above consider each series separately, the model is designed to process multiple years of simulated rainfall, and therefore parameterisations must be found which are applicable across all series. This presents a more difficult problem, and highlights the difficulties of model selection within a catchment showing strong seasonal variation such as the Linton catchment.

The differences in performance between the two-store and three-store models were compared using the graphs above. Use of the additional store does produce an improvement in optimum fit, however the increase in R^2 value is typically small. In order to consider the improvement in the light of the parameterisation aims, i.e. to find parameterisations suitable for all series, the improvement in the average R^2 across series by adding the third store is shown below in Figure 5.6.

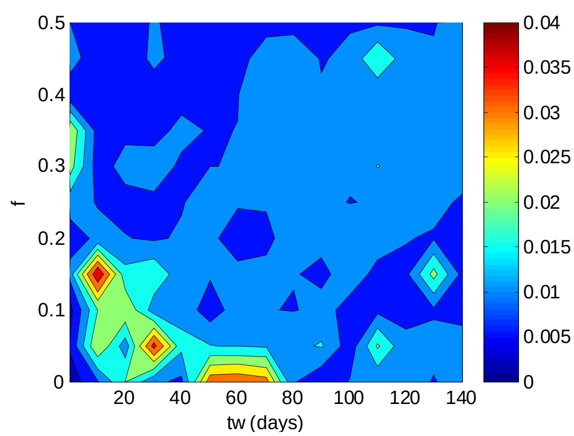

Fig 5.6: Improvement in average R^2 value using [3 3 d] model.

The improvement in R^2 of between 0.01 and 0.04 in the regions of interest was not felt to be sufficient justification for the addition of the extra parameters required for the three-store model. Over-parameterisation is an ever-present danger in hydrological modelling, often resulting in ill-conditioned models which fail to extract the information present in the data series available. This leads to a lack of stability in the model, typically resulting in poorer validation results despite better calibration performance in models with larger numbers of parameters (Perrin *et al*., 2001). This response is well demonstrated by an attempt to identify the pure time delay parameter in a trial application of the GLUE procedure in the Linton catchment. For the two and three store models, parameter sets are randomly sampled and tested against the data series available. For each set with an R^2 value greater than 0.6, the parameter d is plotted against the R^2 value (for further details on this procedure, refer to Section 5.4.3.1). The results are shown in Figures 5.7 and 5.8.

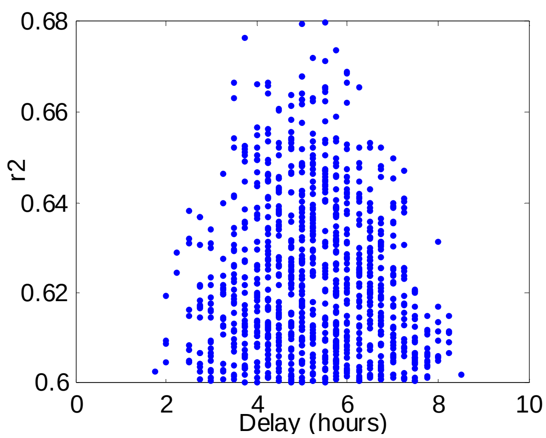

Figure 5.7: Delay identification using the 2 store model

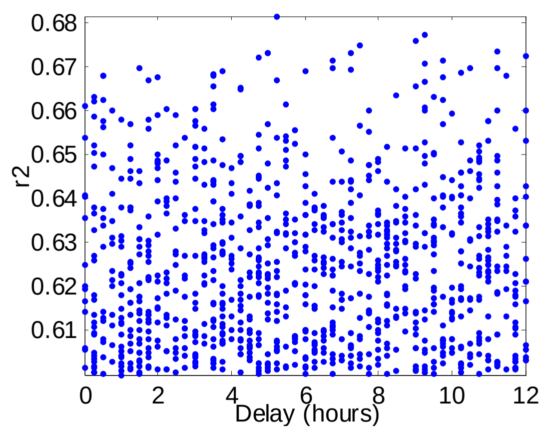

Figure 5.8: Delay identification using the 3 store model

Figure 5.7 shows that using the 2-store model, the pure time delay is identified from the calibration data to within a range of around 4 hours. Although there is uncertainty within this range, information from the data series has been used to constrain the value within these bounds. The 3-store model has failed to identify such a constraint, and good fits are found up to the edge of the parameter space. This would typically be caused by other parameters compensating for poor values of delay, suggesting ill-conditioning of the model.

In order to understand why the three-store model did not produce an obviously improved fit to the data over the two-store model, the contribution of each of the stores to the total discharge over a period of several months was considered. For each model structure, a parameter set producing a high value of R^2 was chosen, with similar value of shared parameters, and the model output as a combination of three flow sources was plotted against the recorded discharge (Figures 5.9 and 5.10). The plots show that the two-store model has been able to replicate the behaviour of the three-store model. This has been done by using a slow flow pathway with a smaller time constant, and redistributing the percentage of flow in each pathway. The reduced number of parameters has not prevented the model from representing both flood peaks and the seasonal cycle in baseflow, caused in the Linton catchment by variations in discharge from aquifers underlying the catchment. The result suggests that the flow processes throughout the catchment are homogeneous, and the data available does not justify separate representation of subcatchment areas.

The two-store model is therefore be used for all further simulations in the catchment, as it provides similar predictive performance to the three-store model in a well-conditioned model structure.

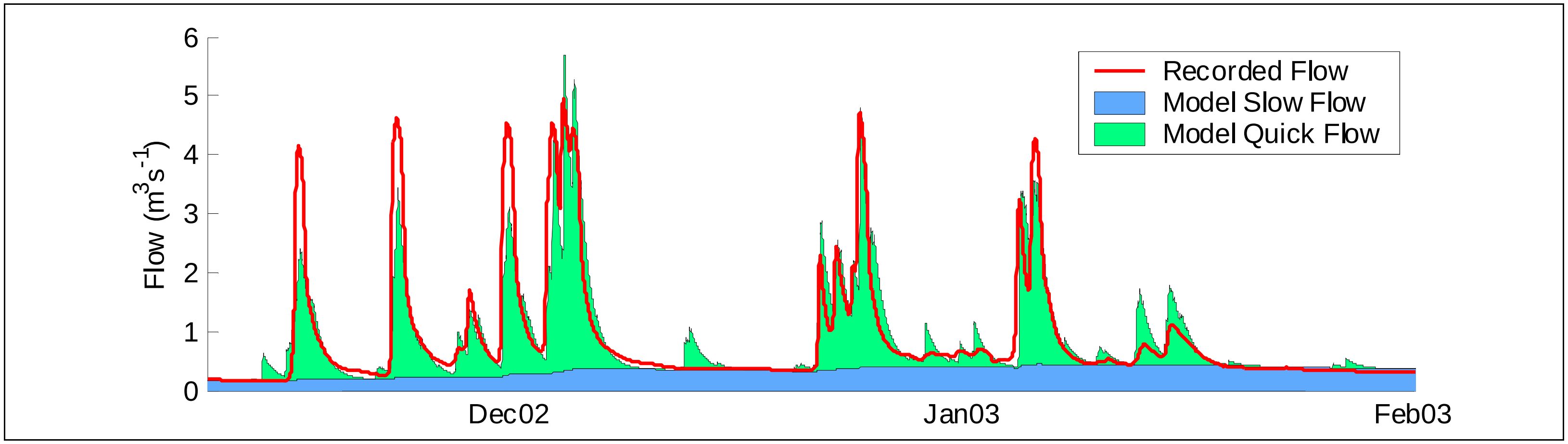

Figure 5.9: Discharge separated by flow path for 3-month example period: Two-store model.

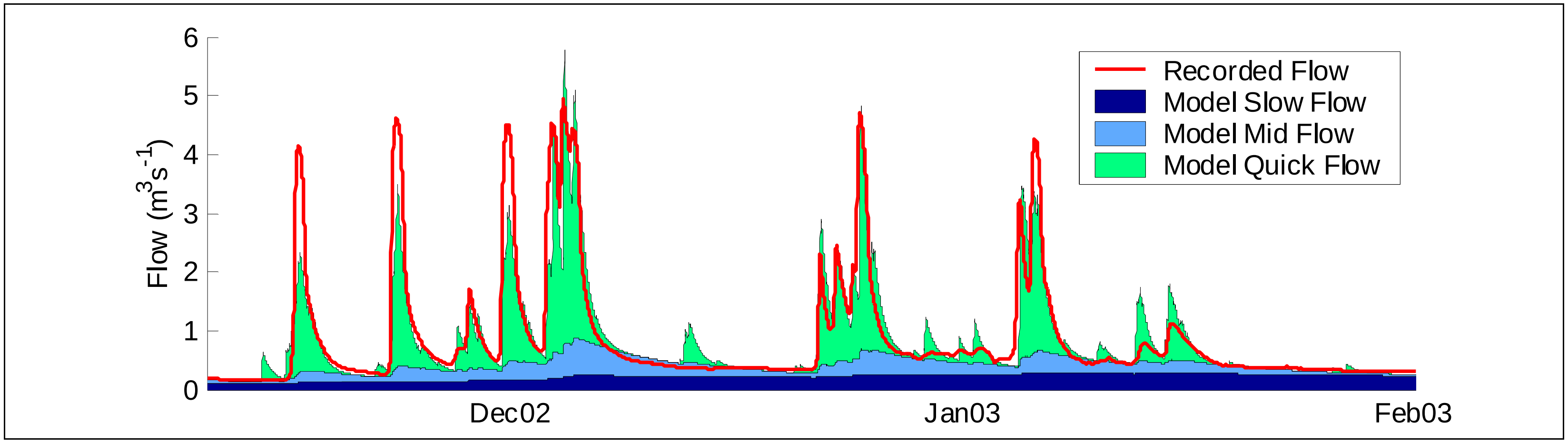

Figure 5.10: Discharge separated by flow path for 3-month example period: Three-store model.

5.4.2.2 *Production of Behavioural Parameter Sets*

With the choice of model structure made, parameter values to control the rainfall-runoff model must next be identified. In order to capture the range of possible catchment behaviours identifiable from the rainfall-flow record, 1000 independently sampled parameter sets for the model were used. Each was required to produce a reasonable simulation of the flow record given the input rainfall record, and the level of similarity achieved was rated using a likelihood measure.

The following procedure was used to produce the parameter sets. First, 1000 parameter sets were sampled according to the chosen feasible parameter ranges and sampling strategy. Any sets which did not meet specified criteria for parameter interaction were discarded. Each set was then used to reproduce a flow record for each of the rainfall records available. The chosen likelihood measure was then calculated to rank the performance (combined across record periods) for each parameter set. Any sets not achieving a reasonable standard were discarded; the remainder were recorded along with the likelihood value. This process was then repeated until 1000 parameter sets were retained and recorded. Each step of this process is explained in further detail below.

5.4.2.3 *Parameter Ranges and Sampling Strategy*

As detailed in Section 5.2, the two-store rainfall-runoff model has 7 parameters to be identified: c, f and τ_w for the non-linear rainfall transform, τ_q and τ_s the time constants for the fast and slow flow pathways in the routing transfer function, p_q the proportion of flow in the fast pathway, and δ the pure time delay. In order to choose the initial parameter space for the parameters, a combination of knowledge of the model and catchment gained through the optimisation exercise undertaken in Section 5.4.2.1 was used.

The parameters f and τ_w were subject to a full parameter space search during the trials to determine model structure. Although the initial ranges were chosen deliberately to be wide, in many cases good results were found up to the boundaries of the parameter space, as has been observed elsewhere in model calibration studies (Beven, 2001b). It was therefore decided to retain the original bounds, as there is no physical basis on which to restrict parameter values. The trial sampling procedure above may also be used to inform the choice of ranges for the parameter c controlling the nonlinear store, and the parameters of the linear routing module. Knowledge of the optimised parameter values found for each (f, τ_w) pair provides some information on typical parameter values, although it is important to note that these records do not give us any information on the range of behavioural parameter values within a single (f, τ_w) pair. By considering the ranges observed in the trial procedure, and widening them to account for within-pair variability, the ranges were chosen as shown in Table 5.3.

Parameter	Minimum	Maximum
f	0	0.5
τ_w	0.5 days	140 days
c	1 mm	4000 mm
p_q	0	1
τ_q	0 hours	20 hours
τ_s	0.5 days	80 days
d	0 hours	15 hours

Table 5.3: Initial parameter ranges

5.4.2.4 Likelihood Measure

In order to associate each parameter set with a 'degree-of-belief' or likelihood measure, a comparison is made between the flow series predicted by the model using that parameter set, and the measured flow series. Given the wide range of options available in choosing a likelihood measure, it is essential to consider the aspects of fit which are most important for the purpose of the particular model application. Here, the aim of creating the rainfall-runoff model is to provide long-term simulations of flow behaviour in response to rainfall, in order to consider the relationship between return period and flood magnitude in the Linton catchment. The likelihood measure chosen should therefore be biased towards a validation of model fit during high flow periods. This aim is achieved in two ways. First, the comparison between observed and predicted series is made only during the winter months October-March of each year of simulation. This measure was implemented in response to model trials which showed that due to the highly non-linear behaviour of the system between seasons, a likelihood measure that gave equal weight to summer and winter performance lead to optimal parameterisations which gave relatively poor performance in winter months. By biasing the validations towards high-flow periods, significant improvements in winter flow fitting are achieved, and therefore significant improvements in annual flood peak estimation are made. Increased errors during summer periods as a result of this choice will not adversely affect high flow predictions as they were not found to cause erroneous simulation of significant flood peaks. It is also important to note that there is no conflict between this choice of likelihood measure and the crucial ability of the model to simulate inter-annual variability of baseflow levels, as the model is still parameterised using data series lasting multiple years, and is therefore tested in its ability to predict winter flows conditioned on summer rainfall totals.

The second method by which model fit is biased towards correct prediction of flood peaks is in the choice of the Nash-Sutcliffe efficiency, R^2 (as described in Section 5.3.2.4) to give a likelihood value for each winter season. As previously described, this measure is biased towards high flow periods as these are likely to contain the greatest error magnitudes.

The likelihood value for each series must then be combined to give a single likelihood value for the parameter set. The values are combined by a weighted average to give greater weighting to the longer data series. The weighted mean efficiency is preferred here over the commonly-used Bayes equation for updating likelihood measures, as this would bias the resulting likelihood value towards those of later series over those of earlier series. Although this can be a desirable characteristic when modelling catchments which show dynamic behaviour, here the system is not considered to have changed significantly during the period of the flow record. Although land-use changes and climate change could act to alter the catchment response, they are unlikely to produce important effects within the relatively short period of twelve years.

If a particular parameter set performs poorly in predicting the recorded data, it should be classed as 'non-behavioural' and not used in future predictions. This is equivalent to setting the likelihood measure to zero. A cut-off value for the likelihood measure is therefore defined, and only models achieving better than this are retained. The requirement for specification of this threshold value has been seen has a weakness in the calibration structure as it requires a subjective decision which may influence the range of behaviour produced by the model. The value chosen depends on both the accuracy required in the model, and the difficulty of the task in reproducing the recorded values. Typically rainfall-runoff models predicting complete years of data in a flashy upland catchment would be expected to achieve values of around 0.5-0.7. In this case the more difficult task of achieving good predictions in a groundwater-dominated catchment is balanced against the decision to validate on winter periods only; a mid range value of 0.6 is therefore used.

5.4.3 Results

5.4.3.1 Parameter Ranges

The parameter ranges required for the model were found using an iterative method. The initial ranges specified in Section 5.4.2.3 were used to produce the first batch of parameter sets. These sets were then used to predict the flow response for each of the data series, and the likelihood measure was then calculated by comparing each response with the recorded flow series. Only those series with a likelihood measure greater than 0.6 were retained. The sensitivity of the model to each parameter was then visualised using a 'dotty plot': a one-dimensional representation of the response surface. Each simulation is represented by one dot on a graph showing the likelihood value against the parameter of interest (for examples see Figure 5.11). Where the parameter range has been set unnecessarily wide, no high values of the likelihood function will be found at the margins of the plot. In most cases however, high likelihood values will be found throughout the parameter range. This may be an indication that the parameter range is too narrow, or it may reflect interdependence between parameters; knowledge of the model must be used to determine the cause. The dotty plot visualisation was used to adjust the parameter ranges before resampling, so that further parameter sets were sampled from the portion of the parameter space showing behavioural results. The updated parameter ranges are shown in Table 5.4.

Parameter	Minimum	Maximum
f	0	0.5
τ_w	0.5 days	150 days
c	1 mm	2500 mm
p_q	0	1
τ_q	10 hours	20 hours
τ_s	0.5 days	80 days
d	0 hours	10 hours

Table 5.4: Final parameter ranges.

When 1000 behavioural samples had been retained (from an original sample size of 200,000), these were again visualised using dotty plots (Figure 5.11). The dotty plots show behaviour typical of GLUE samples, with limited parameter sensitivity for the ranges sampled. The parameters f, τ_w and τ_s show little sensitivity with good values of R^2 throughout the parameter ranges. Parameter p_q is constrained to the upper part of the range, showing that the model simulates the catchment behaviour well with a high proportion of flow in the quickflow pathway, despite the strong baseflow influence known to exist in the catchment. This is a surprising finding and may reflect the insensitivity of the R^2 performance measure to errors in recession periods, together with the bias of the objective function towards winter periods when the baseflow component plays a less defining role. The quickflow time constant τ_q is also constrained to the higher values in its range. Parameter d, the pure time delay, is constrained to the central part of the range, showing high model sensitivity to this parameter. This may be expected as errors in time delay would cause autocorrelated timing errors in hydrograph predictions, which would lead to high error totals.

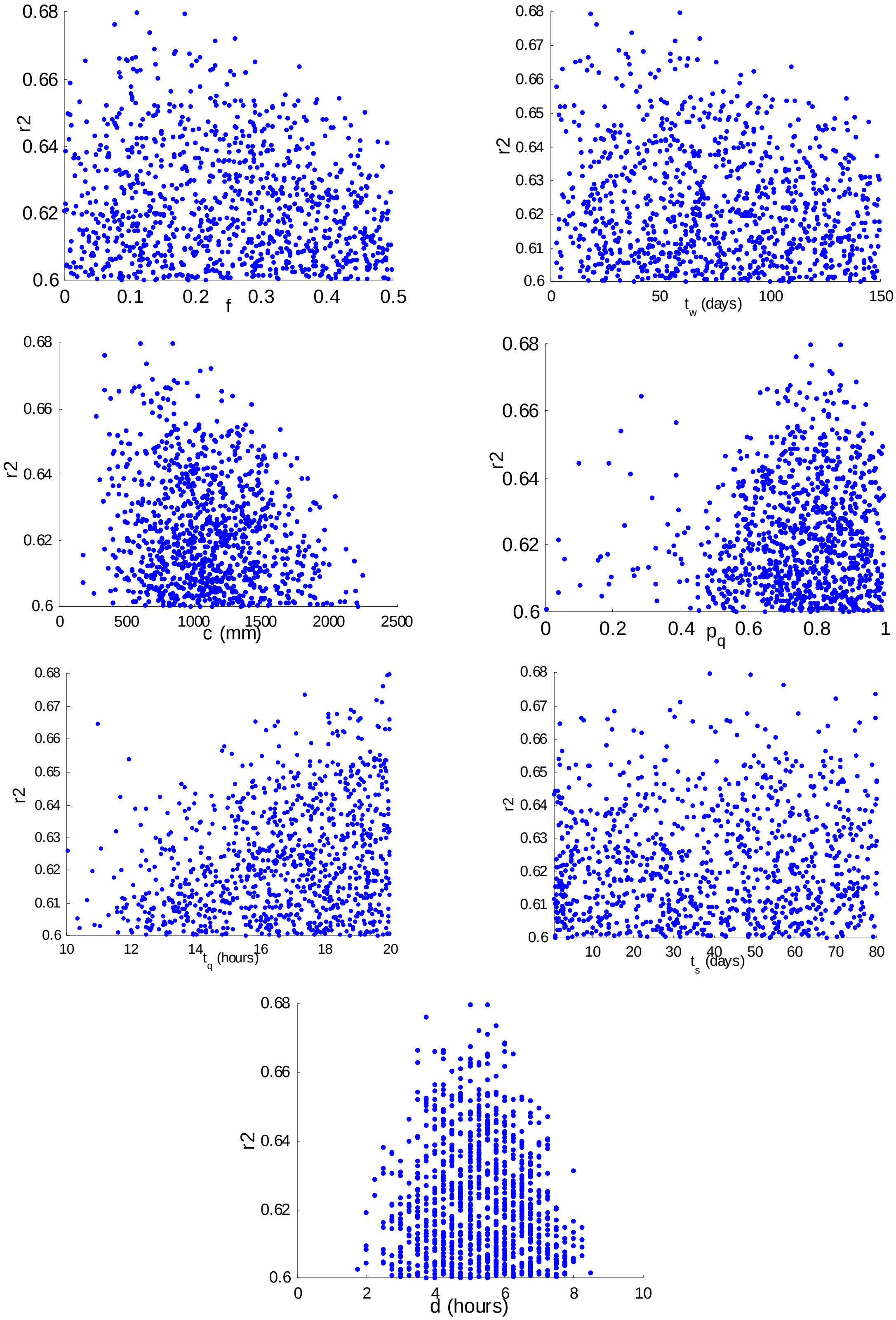

Figure 5.11: Dotty plots of 1000 behavioural parameter values vs R^2

5.4.3.2 Output Hydrographs

The 1000 behavioural parameter sets, weighted by likelihood measure, were used to make discharge predictions in response to input rainfall series. At each timestep, the weighted cumulative distribution of discharge magnitude is found, and this is used to determine the upper and lower probability limits. The standard probability points of 0.05 and 0.95 were used. Examples of the limits obtained are shown below in Figures 5.12 to 5.14.

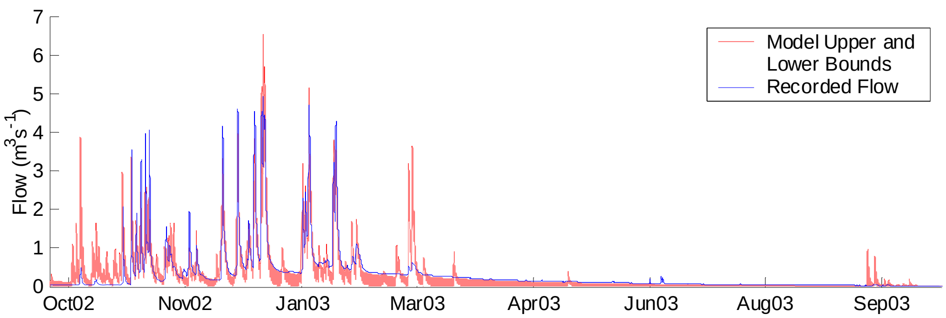

Figure 5.12: GLUE bounds for 2002/2003 hydrological year.

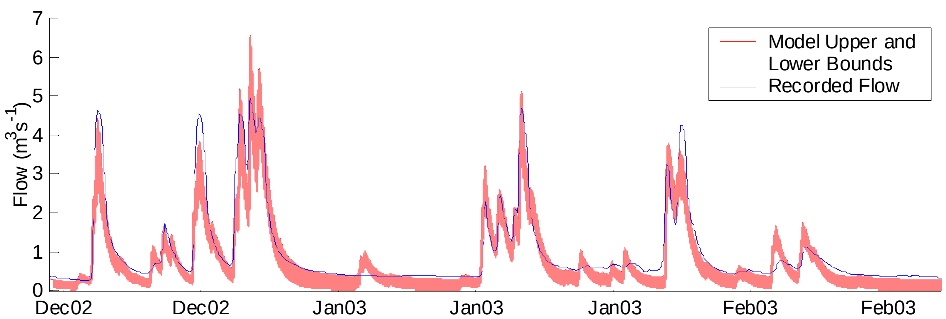

Figure 5.13: GLUE bounds for Winter 2002/2003 detail.

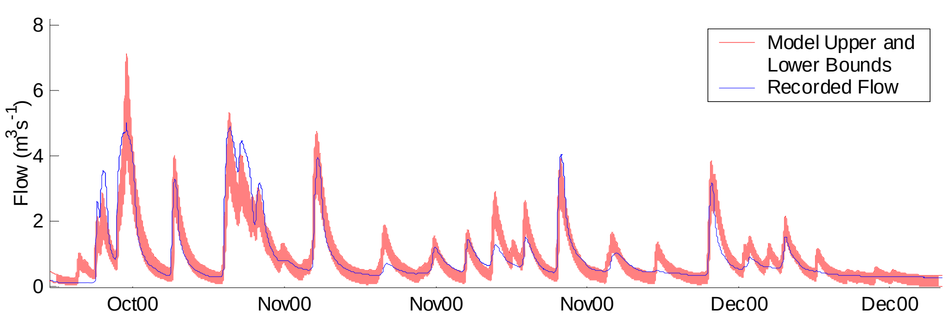

Figure 5.14: GLUE bounds for Winter 2000/2001 detail.

Figure 5.12 demonstrates the fit during a complete year. In general the fit is good, although the 5% and 95% bounds bracket the data better during the winter than during the summer; in recession periods the model predictions are generally slightly too low. This is likely to be due to the calibration strategy which was weighted towards high winter flows in response to the intended use of the model for flood peak prediction. There are also discrepancies at the start and end of the winter season where some realisations of the model predict high flows that did not occur. This would typically be due to incorrect soil moisture status within the model; these parameter sets predict quicker wetting up or slower drying out of the soil matrix than actually occurred, and demonstrate the difficulty of consistently good discharge prediction in catchments displaying a highly non-linear response to rainfall.

Figure 5.13 shows a close-up of the 2002/2003 year described above, in order that the hydrograph fit can be examined in more detail. Although the model bounds bracket the data for much of the series, the predictions are generally low compared with the recorded flow, in both recession and peak periods. This suggests that the models are not predicting sufficiently high soil moisture levels during the particular season. To verify this, detail from an alternative winter season where the catchment was much wetter (2000/2001) is plotted in Figure 5.14. In this, model predictions show improved accuracy in both high and low flow periods, suggesting that the model has been able to make an accurate prediction of seasonal wetness conditions. It is promising to note that in both cases, the highest flood peak was predicted well by the model ensemble, as it is the annual maximum from each year that is used in further statistical analysis.

5.4.3.3 Prediction of annual maxima

In the light of the intended model use, for predicting the frequency of occurrence of floods of different magnitudes over long simulation periods, it is important to validate the model in terms of reproduction of discharge extremes in addition to the prediction of hydrographs. As noted in the previous paragraph, yearly extremes appear to be bracketed well by the discharge uncertainty bounds. However, this method of plotting the flows does not show the cumulative distribution of annual maxima when individual series are considered separately; previous studies suggest that different model parameterisations often record maxima from different rainfall events (Lamb, 1999). The model performance was therefore tested by comparing observed annual extremes with the uncertainty bounds of modelled annual extremes (Figure 5.15). This comparison is necessarily limited by the short period of data available, however it affords a simple but useful check on model behaviour.

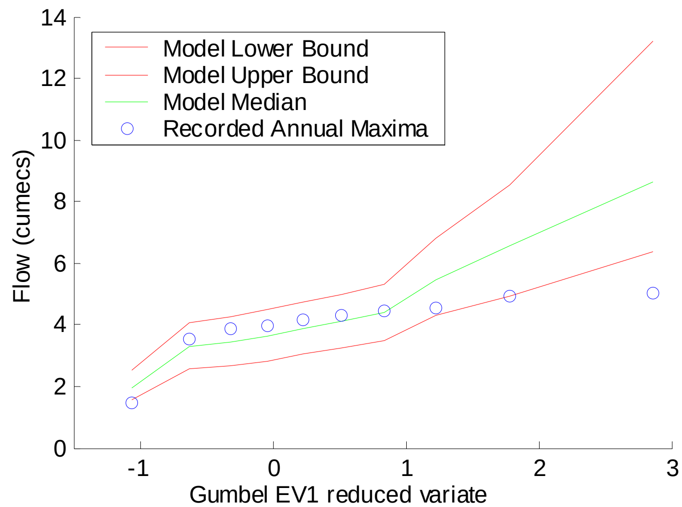

Figure 5.15: Comparison of observed and modelled annual flow maxima, using 10 years of gauged flow data.

Figure 5.15 shows that the model performs well in comparison to the observed extremes for the lower return periods, with observations correctly bracketed by the uncertainty bounds of the model. However for higher return periods, the model predicts higher discharges than those present in the record. This is not unexpected, and in fact is an encouraging result because the gauge at Linton is known to drown at water levels above 0.46 m, and therefore records high flows inaccurately, typically recording flows no higher than 5 m^3s^{-1} even during extreme events. Figure 5.16 below demonstrates the response during a flood peak; the model is able to predict the extreme discharge despite missing data where the gauge malfunctioned. Given the knowledge of this problem with the gauged flows, the model performance is accepted as satisfactory.

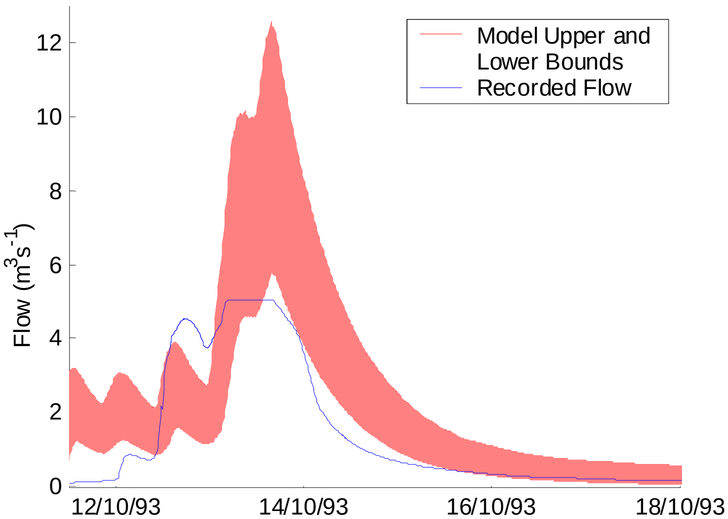

Figure 5.16: GLUE bounds during event with overtopped gauge

5.5 Discussion and Conclusions

This chapter has described the largely successful application and testing of a rainfall-runoff model for the Linton catchment, while raising many issues relating to the choice and calibration of the model. The existence of equifinality in model structure and parameterisations was considered, together with the extent to which it can be efficiently incorporated within an inclusive modelling method. The succession of choices that must necessarily be made during a modelling procedure each have their own influence on the final result and introduce bias tied to the modeller's understanding of the catchment. Above all, the method has emphasised that there are no right answers in model choice, and decisions must be made in relation to the aims and objectives of the study.

From the start, the presumption of an optimum model structure and parameter set was rejected in favour of an acceptance of equifinality. The decision was felt necessary due to the conscious simplifications made in representing the layers of complexity present in the true catchment by a model designed to reproduce only stream discharge. Proxy representations of unmodelled processes and effective parameters acting at scales far removed from those measured remove the possibility of model parameterisation direct from physical catchment characteristics. There are, however, limits to the number of possible catchment representations that can be efficiently included within the GLUE method for investigating and integrating equifinality. As each uncertainty in model structure and parameterisation adds another dimension to the search space, computational effort required to evaluate the model predictions increases exponentially. After investigation of model results using two different model structures representing different conceptualisations of dominant processes, the decision was therefore made to fix structure within the procedure, and to consider only the parameterisation of the model as subject to equifinality. The need to accept multiple parameter sets was highlighted by the wide range of parameter values producing high quality model simulations, as evidenced by visualisations of the behavioural subset of the parameter space using dotty plots. The practical need to restrict application of uncertainty estimation within computational limits is an ever-present consideration and a subject that is returned to in the Chapter 7.

The dependence of the modelling results on the multitude of choices made during model development brought to attention the judgements which must be made based on the hydrologist's experience and the aims of the study; and hence the importance of catchment knowledge and process understanding in order to optimise results. The threshold level at which simulations are considered behavioural has no grounding in any physical cut-off point and yet has a controlling effect on the range of behaviour considered possible within the catchment. The choice of likelihood measure again is subjective and yet essential in differentiating behavioural from non-behavioural simulations. This may be perceived as an advantage in allowing the hydrologist to tailor the model behaviour to the aims of the application, however it may introduce bias into the extent to which different processes are properly represented by the model. The difficulty of making these decisions was highlighted by Beven (1987) who found that different modelling objectives - continuous simulations versus flood peak estimation - led to different parameter choices and differing parameter sensitivity. Although Cameron *et al*. (2000) showed that by accepting equifinality, multiple objectives may be met simultaneously, there remain many viable models of the catchment which are excluded.

In the current study, such choices were typified by the decision to bias the model parameterisations towards the winter periods where it was considered most important to achieve correct simulation of flood peaks. This inevitably led to compromises in model accuracy during the remainder of the yearly cycle; in particular irregularities were found during the wetting up and drying out periods in early autumn and spring respectively. This finding reflects results in other studies of continuous simulation. Cameron *et al*. (2000) found difficulties in parameterisation of TOPMODEL such that flood peaks which followed a prolonged dry spell were properly simulated; similar results were also indicated by Brasington and Richards (1998) and Lamb (1999).

In the Linton catchment, the problems of modelling groundwater-dominated river discharges were felt to make such choices particularly important. Other studies (e.g. Lamb, 1999) have commented on the difficultly of representing such hydrological regimes, and the need for manual adjustment of parameters in addition to standard optimisation techniques to reflect the hydrologist's perception of model success. Errors were postulated to be due to inaccurate representation of the dynamics of recharge to the slow-flow store; made more probable in the Linton catchment due to known abstractions of groundwater for drinking water, a process not included in the model. While it would be possible to introduce extra components into the model in an attempt to represent this process (and the many others ignored as a result of the simple model structure) there is a danger that the resulting additional parameters would cause the model to become ill-conditioned. This was demonstrated when the addition of two extra parameters during the trial of the three-store model caused reduced identifiability of model parameters.

The above discussion has emphasised the restrictions that must be placed upon uncertainty estimation, and gone some way to demonstrating the ambitious nature of an attempt to represent equifinality within an end-to-end modelling structure. It has also given an example the uniqueness of any individual catchment and model application, and the need therefore to be prepared to adapt standard techniques of modelling and likelihood evaluation in response. Despite these considerations, it was found possible to produce a catchment model that was well-conditioned and able to reproduce catchment responses in terms of both hydrograph simulation and flood frequency estimation, while including the perceived dominant sources of uncertainty.

Chapter 6

URBAN FLOODPLAIN INUNDATION MODELLING

Abstract

A Floodplain inundation model is required as part of the end-to-end flood risk assessment framework in order to translate upstream discharge predictions into simulations of flood wave progression along the channel and associated inundation patterns along the river corridor including urbanised areas. This chapter describes the formulation of the inundation model and its application to the study reach at Linton on the River Granta.

This application reflects the wider expectations of recent years that floodplain inundation models should be able to provide simulations of flood events over complex urban terrain. The data to parameterise the complex topography of such landscapes is now frequently available through airborne LIDAR scanning which can be used to produce DEMs of resolution 1 m or better. However, computational constraints often preclude model applications at such high resolution. This chapter therefore explores two strategies that attempt to address this mismatch between model and data resolution in an effort to improve urban flood forecasts. The first explores the use of high resolution data directly within a reduced-complexity model structure which couples a 1d channel model to an efficient 2d raster storage cell floodplain representation. The second approach seeks to further reduce the computational overhead of this raster method by employing a sub-grid parameterisation to represent the effect of buildings and micro-relief on flow pathways and floodplain storage, while allowing model application at coarse spatial resolution.

The two strategies are tested through a reconstruction of the October 2001 flood event in Linton. Results from both approaches are encouraging, with the spatial pattern of inundation and flood wave propagation matching observations well. The sub-grid parameterisation is shown to achieve accuracy close to that of a full high resolution implementation, while reducing model run-times by an order of magnitude.

6.1 Introduction

A Floodplain inundation model forms the final link in the chain of coupled models used to simulate the propagation of floodwater through the Linton catchment. It is required in order to translate discharge predictions at the gauging site upstream of the town into simulations of flood wave progression along the channel and associated inundation patterns along the river corridor and within the urbanised area.

Significant recent advances in floodplain inundation modelling have been achieved by directly coupling 1d channel hydraulic models with 2d raster storage cell approximation for floodplain flows (e.g., Bates and De Roo, 2000). The strengths of this reduced-complexity model structure derive from its explicit dependence on a regular gridded digital elevation model (DEM) to parameterise flows through riparian areas. This approach offers order of magnitude gains in computational efficiency over more complex finite element and volume codes, and so enables a more critical examination of parameter and structural model sensitivities and predictive uncertainty using Monte Carlo methods (Aronica, *et al*., 2002).

Previous applications of this reduced-complexity framework have generally used mid-range grid scales of 25 – 250 m, with the aim of simulating flood wave propagation and inundation over long (10^1-10^2 km) river reaches (Bates and De Roo, 2000; Horritt and Bates, 2001b). These grid scales enable the use of medium-resolution digital elevation data from digitised contour data, air stereo-photogrammetry or other sources. However, results from models run at such coarse resolution may suffer from inaccuracies due to the umodelled effects of detailed floodplain geometry below the grid scale. Large cell sizes have forced the use of weakly constrained floodplain roughness parameters as a substitute for the combined effects of vegetation and structures (Bates *et al*., 1998; Horritt, 2000; Horritt and Bates, 2001b; Mason *et al*., 2003). Although computational constraints have previously limited model resolutions to these mid-range scales, continuing advances in computer resources now offer the potential to apply such models at finer spatial scales where the geometrical complexity of the built environment may be explicitly modelled. If successful, this would enable an extension of the 2d modelling approach to urban landscapes where buildings may play a large part in constricting and directing water movement, and where flood risk is most acutely realized.

Until recently, application of high resolution models at the floodplain scale was also limited by the lack of quality survey data. Increasingly, however, airborne laser altimetry (LIDAR) is being used to provide DEMs at very high spatial resolutions (0.5 – 2 m) with precision of around 0.1 m. Although this data source has been used for rainfall-runoff modelling (Lane *et al*., 2004), and coarse-scale flood inundation modelling with finite-element schemes (Bates *et al*., 2003; French, 2003; Marks and Bates, 2000; Mason *et al*., 2003), it has yet to be used within a reduced-complexity raster scheme to allow representation of urban topography at the smallest grid scales. Building on the opportunities presented by this emerging data source, this chapter explores two contrasting approaches to modelling urban flood hydraulics using reduced complexity methods parameterised with airborne LIDAR (see Sections 6.1.1 and 6.1.2). The two modelling methods are tested through application to the Linton catchment in the context of a reconstruction of the flood of October 2001. Validation is carried out using hydrograph records and distributed inundation depth data within a multi-criteria approach, to allow verification of estimated channel wave attenuation and flood outline. Comparisons are made of the running times and accuracy achieved in each case. The final aim of the chapter is to make an informed choice of the most suitable model structure, scale and parameterisation for use within the end-to-end modelling framework.

6.1.1 Reduced Complexity Modelling

The first model developed here uses the simple combined 1d channel and 2d raster scheme at a 2 m grid resolution, which allows explicit representation of buildings in the topographic boundary condition. Application of the raster method at this scale requires a number of modifications to existing approaches (e.g., Bates and Horritt, 2000), including a new channel-floodplain cell mapping routine, revised and improved stability procedures, and adaptive time-stepping. When applying the model at this resolution, two particular aspects of its performance should be considered. First, an assessment must be made of the model success in representation of the governing physics. The computational gains in raster modelling arise largely by adopting a uniform flow approximation for floodplain flows in which gravity and frictional forces are assumed to dominate the momentum balance. While this may be reasonable for slow flows over smooth, low gradient rural floodplains, complex urban flows are likely to comprise unsteady and rapidly varying regions. It is therefore possible that neglecting the pressure and inertial terms of the momentum equation may lead to erroneous flow paths, velocity and depth distributions, and so model ability to reproduce inundation behaviour must be verified. Second, the operational efficiency of the model should be assessed when it is applied at high resolutions to large model domains which may contain upwards of 10^6-10^7 cells.

6.1.2 Sub-Grid Scale Modelling

The wealth of terrain information contained within a LIDAR scan of a river reach brings into focus a situation increasingly being found in hydrological modelling: the availability of parameterisation data of smaller scale and larger extent than it is computationally feasible to include in a simulation. This may be contrasted with the historical situation where model complexity was often limited by the data available. In response to this reversal, methods of sub-grid parameterisation are becoming increasingly popular; Chapter 2 explored their potential ability to improve the behaviourability of model response. Although traditionally any treatment of sub-grid variability might have been considered as a method of compensating for unmeasured local heterogeneity, it may instead be viewed as an opportunity to include additional observed data into the model structure in an efficient way. Sub-grid methods have been applied in various forms, for example to resolve issues in partially-wet cells at the inundation edge zone (Bates and Hervouet, 1999; Defina, 2000; Defina *et al*., 1994; Hervouet and Janin, 1994); to identify vegetation and include the information through a frictional coefficient (Mason *et al*., 2003); or as part of a more complex scheme to modify the full shallow water equations to take into account small-scale ground irregularities (Defina, 2000).

Following this approach, the second model developed here uses the concept of 'cell porosity' to allow the use of sub-grid topographic information within a coarse resolution model. The porosity function quantifies the percentage of the assumed cell volume that is available for water storage after accounting for sub-grid features; similarly modified values of cell boundary cross-section area and wetted perimeter are also defined. By using this information to adjust the continuity and momentum equations, it may be used to inform model behaviour in terms of preferential flow directions and flow volumes in a way that is not possible using a simple roughness coefficient. The method is designed to reflect the first order controls on flow conveyance while enabling simulations to be carried out at a computationally efficient resolution. Yu and Lane (2006b) demonstrated the potential of the porosity concept by using sub-grid scale information at a resolution half that of the model. By allowing more extensive porosity information to be included, this paper shows that a detailed representation of structures on the floodplain can be incorporated within a model running at an efficient scale

6.2 Modelling and Methods

6.2.1 Developing the Raster Storage Cell Approximation

6.2.1.1 Channel Wave Treatment

The basic reduced complexity model used here couples a 1d channel model with a 2d floodplain model. The channel model uses the kinematic approximation to the Saint-Venant equations, which describe one-dimensional unsteady open channel flow. They consist of a continuity equation and a momentum equation, both partial differential equations written below in their Conservation form (Equations 6.1 and 6.2). Variables used are: Q, flow; A, cross-sectional area; t, time; x, horizontal position; y, vertical position; g, gravity; S_0, bed slope; S_f, friction slope.

Continuity Equation: $$\frac{\partial Q}{\partial x} + \frac{\partial A}{\partial t} = 0 \qquad (6.1)$$

Momentum Equation: $$\underbrace{\frac{1}{A}\cdot\frac{\partial Q}{\partial t}}_{\substack{Local\\Acceleration\\Term}} + \underbrace{\frac{1}{A}\cdot\frac{\partial}{\partial x}\left(\frac{Q^2}{A}\right)}_{\substack{Convective\\Acceleration\\Term}} + \underbrace{g\frac{\partial y}{\partial x}}_{\substack{Pressure\\Force\\Term}} \underbrace{-g(S_0}_{\substack{Gravity\\Force\\Term}} \underbrace{-S_f)}_{\substack{Friction\\Force\\Term}} = 0 \qquad (6.2)$$

The equations can be simplified by using the full continuity equation, but a reduced form of the momentum equation. The kinematic approximation uses only the gravity and friction force terms, neglecting pressure and acceleration terms. This simplification therefore represents flow controlled by opposing gravitational and frictional forces, and does not allow backwater effects where level or velocity changes may propagate upstream.

The kinematic wave equations may be solved analytically for inbank flows, however when overbank flow occurs an analytic solution is no longer possible. Instead, a numerical solution is used, applying the finite difference form of the equations (Chow *et al*., 1988). This is achieved by combining the continuity and momentum equation to produce a single equation with Q as the only dependant variable. By using Manning's Equation to relate S_0 to Q and A, Equation 6.3 can be derived. In the equation, n is

Manning's roughness, P is the wetted perimeter and q is the lateral flow between the channel and the floodplain.

$$\frac{\partial Q}{\partial x} + \left(\frac{nP^{2/3}}{S_0^{1/2}}\right)^{3/5} \cdot \frac{3}{5} \cdot Q^{-2/5}\left(\frac{\partial Q}{\partial t}\right) = q$$

Equation 6.3: Kinematic Wave Expressed as Single Equation

This equation may then be solved numerically to find Q(x,t) for each value of x (horizontal distance along the channel) and t (time). The data requirements for this channel model are channel slope, channel width and channel depth, provided at each increment of horizontal distance along the channel.

6.2.1.2 Floodplain Storage Cell Methodology

The floodplain model uses a raster cell approach that has been popularised by Bates and De Roo (2000) and De Roo *et al*. (2000) with their model LISFLOOD-FP; similar ideas have also been used by Estrela and Quintas (1994) and Romanowicz *et al*. (1996), all building on methods suggested by Cunge *et al*. (1976). This type of model has been shown to be useful in practical scenarios (for example land-use change predictions: De Roo *et al*., 2001; De Roo *et al*., 2003), and is particularly prized for its ability to produce inundation predictions at a similar level of accuracy to finite element codes while running an order of magnitude more quickly (Aronica *et al*., 2002; Horritt and Bates, 2001b).

The floodplain model uses numerical discretisation in space and time, as with the channel model. The floodplain is treated as a grid of square cells, with flow allowed between 4-connected cells at each time step. As in the channel model, continuity and momentum equations are solved to calculate the flow rate. The continuity equation relates flow across cell boundaries to the volume stored in the cell (Equation 6.4); the momentum equation uses Manning's Law to relate flux to surface slope and hydraulic radius (Equation 6.5).

Continuity Equation: $$\frac{\partial h^{i,j}}{\partial t} = \frac{Q_x^{i-1,j} - Q_x^{i,j} + Q_y^{i,j-1} - Q_y^{i,j}}{\Delta x \Delta y} \qquad (6.4)$$

Momentum Equation: $$Q_x^{i,j} = \frac{h_{flow}^{5/3}}{n}\left(\frac{h^{i-1,j} - h^{i,j}}{\Delta x}\right)\Delta y \qquad (6.5)$$

Where $h^{i,j}$ is water depth at cell (i,j), h_{flow} is free water depth between two cells, Δx and Δy are the cell dimensions, n is Manning's friction coefficient, and Q_x and Q_y are the flow rates in two directions between cells. The flow between two adjacent cells is illustrated in Figure 6.1.

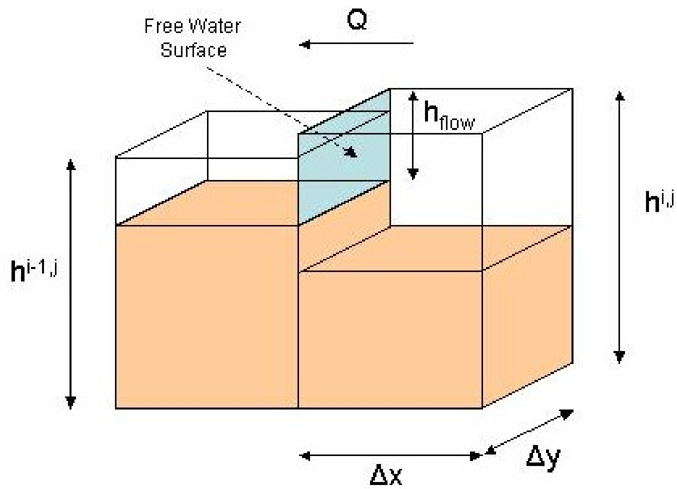

Figure 6.1: Variables for calculation of flow between adjacent floodplain cells

In order to implement these equations within the model, the volume of water stored in each cell is recorded at a given time step. The momentum equation is then used to calculate flow between each two adjacent cells. The continuity equation uses these flow values to update the volume of each cell in preparation for the next time step. Where a floodplain cell contains a channel boundary, this is included as an extra term in the continuity equation, with flow controlled by the same momentum equation.

6.2.1.3 Improving Model Function and Stability

The numerical approximations to the differential equations used in the raster cell approach make the model vulnerable to errors caused by discretisation of the processes in time. Theoretical flow magnitudes are calculated at the start of each time step and assumed to be constant over the time step. In practice this is not always a good assumption, especially in areas of steep gradient or high water depth where flow rate is high. In these cases, flow rate would decrease rapidly during the time step as surface gradient decreased. One result of the simplification is that during the drying process, more water may be calculated to leave a cell than was originally contained within it. In order to prevent this, flows are scaled down appropriately.

Another manifestation of the same overprediction of flow is that when flux between floodplain cells is controlled only by the momentum equation above, instabilities occur in areas of high water depth. This is due to excessive flow volumes which lead to a surface slope which reverses at each time step, creating unstable oscillations in water depth and a characteristic ‘chequerboard’ pattern visible on the simulated floodplain. Several solutions have been proposed to this problem. In the version of LISFLOOD-FP described by Bates and De Roo (2000), a flow limiter was implemented to curb oscillations between neighbouring cells. This was achieved by restricting the change in depth of a cell such that no flow directions would be reversed in the following time step, using the following restriction to the flow calculated using Manning’s Equation:

$$\hat{Q}_x^{i,j} = \min\left\{Q_x^{i,j}, \frac{\Delta x \Delta y\left(h^{i,j} - h^{i-1,j}\right)}{8\Delta t}\right\} \qquad (6.6)$$

Hunter *et al*. (2004) report anecdotal evidence from authors of other storage cell codes that such a flow limiter is generally required to prevent numerical instability.

Application of a flow limiter has, however, been shown to give rise to auxillary complications, as demonstrated by Hunter *et al*. (2004) who showed that it caused underprediction of inundation front velocity and flood volume, and inaccuracies in shape of wetting front. Bradbrook *et al*. (2004) proposed an alternative solution by controlling time steps using a Courant-Friedrichs-Levy (CFL) condition applied over the whole floodplain. The CFL condition requires that the model time step be less than the time required for a wave to travel the length of one grid cell, and is used, usually in the context of channel flow, to improve stability by prevent erroneous accumulation of water within a cell. However, the condition does not ensure stability and despite this measure oscillations still occurred in areas of deep water and in areas of shallow surface slope. In a similar vein, Hunter *et al*. (2004) define time-steps based on a stability analysis of a simplification of the continuity and momentum equations, and combine this with a linear scheme for near-zero free surface gradients. This method was shown to greatly improve inundation and drying behaviours, however it resulted in extremely small time steps; a condition which could prove a severe complication for the high resolution applications proposed here.

A new solution is therefore sought, which would reduce problems with inundation front behaviour while retaining the model efficiency which is seen as one of the most important properties of the storage cell methodology. This solution is implemented as a combination of several methods. Most importantly, the flow limiter is improved to consider multiple outflows from a single cell to several neighbouring cells as dependant processes. By coupling the flow directions, the flow limiter can be applied in a more realistic way which recognises the interaction of flow paths by proportional scaling of each flow direction. The cell outflow limit is calculated such that in no direction will the flow be reversed in the following time step. However, where previous methods applied an equal upper limit in each direction, the maximum total outflow is instead imposed using individual limits scaled according to relative flow volumes in each direction. This condition was subject to a modification introduced to avoid neighbouring cells in equilibrium preventing flow in a perpendicular direction, by removing equilibrium pairs from the calculation of minimum slope. The additional condition that the volume of water leaving any cell must be no greater than the volume of water stored in the cell is also retained.

$$Q_x^{i,j} = \min\left\{ Q_x^{i,j},\ \underbrace{\left(\frac{Q_x^{i,j}}{Q_x^{i,j}+Q_x^{i-1,j}+Q_y^{i,j}+Q_y^{1,j-1}}\right)}_{Proportion \cdot of \cdot flow} \cdot \underbrace{\left(\frac{\min\left\{H_x^{i,j}, H_x^{i-1,j}, H_y^{i,j}, H_y^{i-1,j}\right\}\Delta x \Delta y}{1+1/(Number \cdot of \cdot Outflows)}\right)}_{\substack{Max \cdot total \cdot outflow \cdot before \cdot surface \cdot \\ gradient \cdot is \cdot reversed}},\ \underbrace{\left(\frac{Q_x^{i,j} \cdot h^{i,j} \cdot \Delta x \Delta y}{(Q_x^{i,j}+Q_x^{i-1,j}+Q_y^{i,j}+Q_y^{1,j-1}) \cdot \delta t}\right)}_{\substack{Outflow \cdot required \cdot \\ to \cdot empty \cdot cell}} \right\} \qquad (6.7)$$

Where $H_x^{i,j}$ = water surface elevation change between neighbouring cells in x-direction.

In tests, the use of this limiter was found to ensure model stability while retaining behavioural flow routing. It is important, however, that the limiter is not used to force stability when inappropriately long time steps are used. Therefore a complementary measure is to replace the fixed time step used by Bates and De Roo (2000) by one calculated by applying the CFL condition to channel flow. This does not ensure unconditional stability (i.e. in the case where floodplain flow celerity might exceed that of the channel peak), but by linking the time step to channel flows, it provides major computational efficiencies by avoiding a search of the entire floodplain. This represents a significant saving when the model is applied to large model domains. The method improves stability during the flood peak by constraining the time step to the region of typically highest velocities, but allows for extended time steps during low flows. Figure 6.2 illustrates the typical pattern of changing time step obtained through this simple procedure in a flood hydrograph.

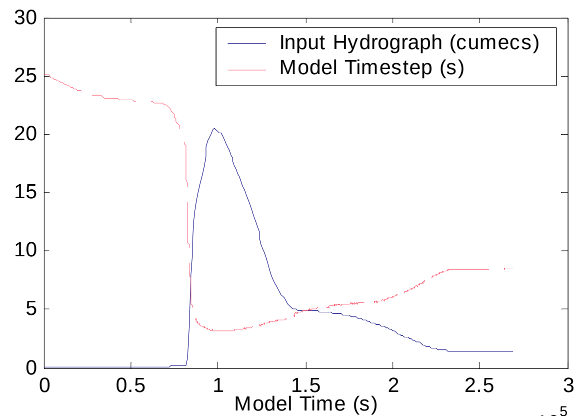

Figure 6.2: Adaptive time-stepping through a flood hydrograph simulation by applying the CFL condition to channel flows.

A final improvement is to the drying treatment: using the original LISFLOOD-FP code, water continues to advance rather than recede during the drying phase (Hunter *et al*., 2004). To counter this, the start of a drying phase is imposed on edge cells which are identified by a threshold depth and inflow/outflow paths as being in the transitional flow reversal stage. Taken together, these changes to the model are intended to produce improvements in dynamic behaviour without compromising efficiency.

The steps described above represent solutions which enforce stability in a model which would otherwise show numerical instability. Although the intention is only that unwanted numerical artefacts are removed from model results, the reality is that the exact form of flow limiter used can have an important impact on model predictions due to effects such as altered shape of wetting front. Trials carried out using alternative forms of flow limiter demonstrated that the choice of limiter acts in the same way as an additional parameter of the model, reducing or increasing the flood envelope. Different methods of coupling the perpendicular flows within the limiter also had the potential to change the flow paths predicted by the model. This extra 'parameter' additionally interacted with the other model parameters; thus if the limiter was changed, the channel friction value required for optimum predictions might also need to be changed. Although the choice of the limiter has traditionally been treated as a minor part of 2d raster storage cell modelling, often unreported in journal articles describing model developments and applications, these results highlight its fundamental role in the model.

6.2.1.4 Floodplain: Channel Coupling

Running the model at high resolution may also necessitate an updating of the treatment of the relationship between channel and floodplain. Previous applications of the raster cell code have generally used cell sizes of similar width to the channel, and therefore defined the channel as a chain of cells. The extreme case of channel width much smaller than grid spacing was considered by the 'Near Channel Floodplain Storage' model of Hall *et al*. (2005), however their representation is only appropriate where the channel width is negligible compared to cell width. Using a high resolution model on a headwater catchment with a narrow channel brings the possibility of channel width significantly smaller or greater than cell width, without being negligible. Two versions of the model were therefore developed. The first uses a channel width smaller than cell width, and records a series of floodplain cells that contain channel sections (Figure 6.3). In each of these cells, the percentage of the cell that is occupied by the channel is used to define a volume:depth ratio as water enters the cell.

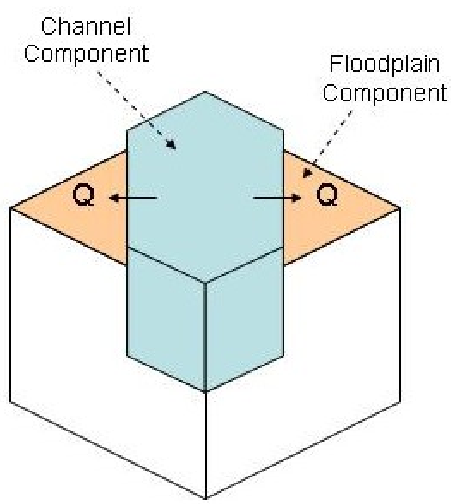

Figure 6.3: Floodplain Cell Containing Channel Section. Arrows demonstrate flow between floodplain and embedded channel.

In the second version, the channel width is greater than the cell width, and the channel is defined by a matrix of cells. Each cell in the outer channel is mapped to a channel centreline cell (Figure 6.4) which is used to route flow along the channel, and to hold a depth value for water in the channel. Flow between channel and floodplain can take place at any boundary between the two cell types.

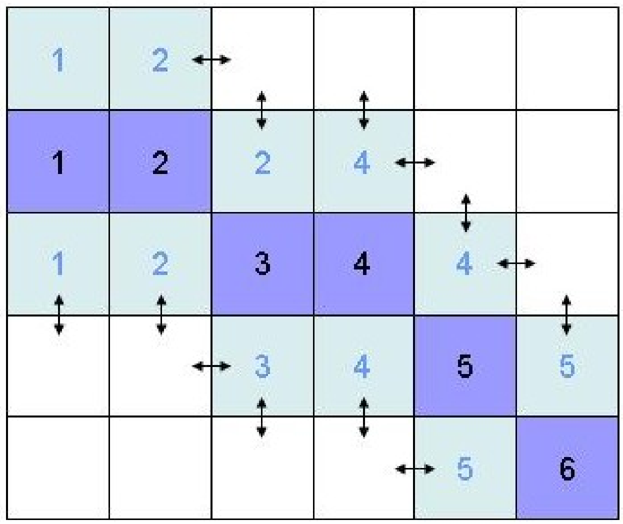

Figure 6.4: Mapping channel-floodplain boundary cells to channel centreline. Arrows represent flow between channel and floodplain

6.2.2 Model using Sub-Grid Scale Porosity Information

Section 6.2.1.1 above describes the way in which cells interact during the flood process, dependant on the water surface slope and depth of free water surface. Previously the model has been run using terrain elevation values from a bare-earth DEM at typical grid-scales of 10^1 – 10^2 m. High resolution modelling at scales of 10^0 m provides the opportunity to use a DEM which explicitly includes floodplain structures represented as elevated grid cells, but incurs a penalty in terms of model running time. The reason for the increase is twofold: not only is the number of active gridcells increased, but also the model time step must be decreased for a smaller grid size as prescribed by the CFL Condition. The second aim of the model development process was therefore to extend the basic model structure to allow sub-grid scale information to be used in an efficient and meaningful way within a model with coarser grid spacing. This would allow the important effects of terrain complexity and structures within the cell to be represented without the corresponding increase in running time. Figure 6.5 shows the typical information available from within a grid cell, here assuming that DEM information at a 2 m scale is used within a 10 m grid cell, although this methodology would be suitable for any combination of values.

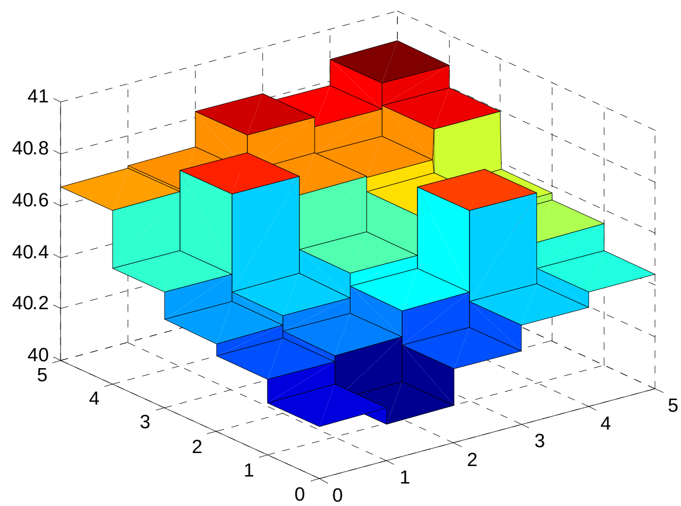

Figure 6.5: Schematic representation of micro-topography within a coarse model grid cell.

The model attempts to use the sub-grid scale information to improve the flow routing behaviour. Avoiding the complexity of analytical solutions of flow around topographical features (e.g. Bradford and Sanders, 2002; Shige-Eda and Akiyama, 2003), the objective is to modify only the two main controls: direction and rate of flow between cells. Rate of flow is controlled by the absolute and relative depths of water in neighbouring cells, which in turn can be calculated more accurately the more information is available on the cell microtopography. The 2 m DEM is used to specify the lowest point in each cell, at which water begins to enter the cell. Above that, a volume:depth relationship is created based on the percentage of the cell volume which is above ground surface and hence available for water storage. This percentage is termed the cell ‘porosity’; note that it is a function of the water depth in the cell as at higher depths the blocking effect of the cell microtopography is reduced. Figures 6.6 and 6.7 below demonstrate the pattern of flooding in a simple porous cell with grid size 2 m and topographical information at 1 m scale.

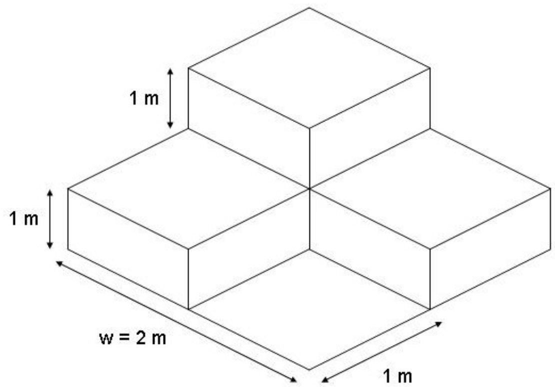

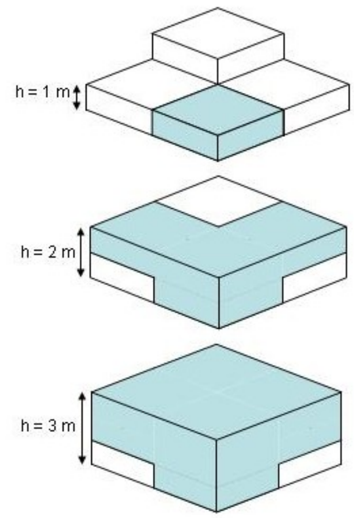

Figure 6.6: Simple example of 2 m cell with nested 1 m micro-DEM

Figure 6.7: Schematic representation of progressive inundation

The volume:depth relationship is created using linear interpolation between values calculated at discrete depth values. The relationship for the example cell constructed in Figure 6.6 is shown graphically in Figure 6.8 below. In order to use the relationship within the model, the porosity value for each cell is calculated at a range of depths and stored in a lookup table.

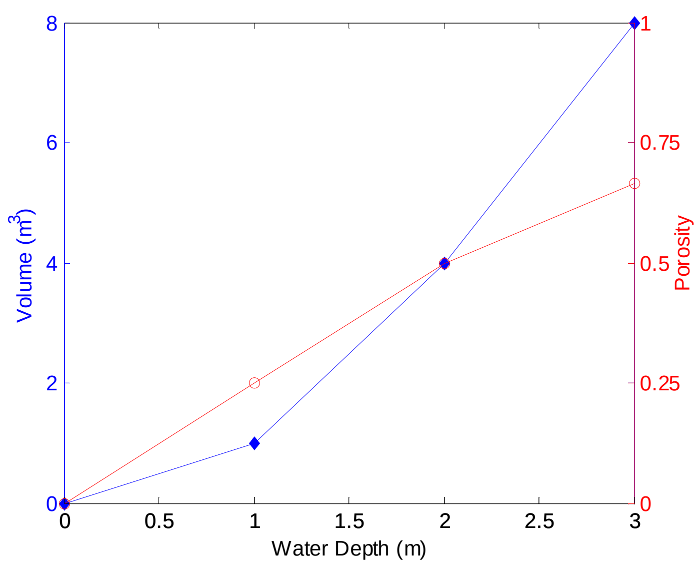

Figure 6.8: Volume:Depth and Porosity:Depth relationships for example cell of Figure 6.6

The changing volume:depth relationship as water moves between cells also requires a corresponding revision of the flow limiter described in Equation 6.7, to give:

$$Q_x^{i,j} = \min\left\{ \begin{array}{l} Q_x^{i,j}, \underbrace{\left(\frac{Q_x^{i,j}}{Q_x^{i,j} + Q_x^{i-1,j} + Q_y^{i,j} + Q_y^{1,j-1}} \right)}_{\mathrm{Pr}oportion \cdot of \cdot flow} \cdot \underbrace{\left(\min_{i,j}\left\{ \frac{H_x^{i,j}}{\frac{1}{P_C} + \frac{1}{Num.Flows * P_O}} \right\} \Delta x \Delta y \right)}_{Max \cdot total \cdot outflow \cdot before \cdot surface \cdot gradient \cdot is \cdot reversed}, \\ \underbrace{\left(\frac{Q_x^{i,j} \cdot h^{i,j} \cdot \Delta x \Delta y}{(Q_x^{i,j} + Q_x^{i-1,j} + Q_y^{i,j} + Q_y^{1,j-1}) \cdot \delta t} \right)}_{Outflow \cdot required \cdot to \cdot empty \cdot cell} \end{array} \right\} \quad (6.8)$$

Where P_C and P_O are the porosities at the current depth for the central and outflow cells, and $H^{i,j}$ is water surface height difference between central cell and outflow cell. The formula uses the approximation that cell porosity remains constant during the time step, i.e. that insufficient depth change occurs to significantly alter porosity.

With more accurate depth knowledge, the direction in which water flows can also be controlled by the sub-grid parameterisation. A clear example of this would occur in a sloping cell, where shallow water depths allow flow over only the lowest boundaries (Figure 6.9).

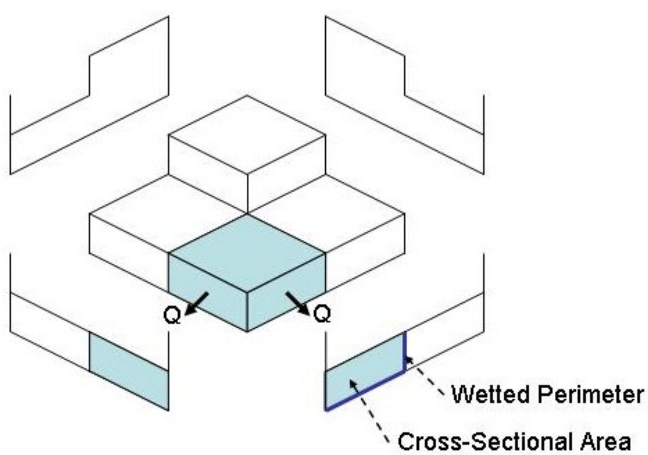

Figure 6.9: Example Part-Flooded Cell with Boundary Cross-Sections Illustrated

The momentum equation for flow between cells requires the cross-sectional area and wetted perimeter of each boundary. Two methods of providing this information were investigated. The first was to use a look-up table approach, as for the porosity values, where the two values are each specified for a range of depths. The second was a simplified approach, designed to remove the need to store multiple large arrays of values by using porosity as a proxy variable for cross-sectional area and wetted perimeter. The porosity was used to estimate the number of sub-cells providing no water storage volume, i.e. those that represent a structure on the floodplain. All other sub-cells are assumed empty. The ‘full’ sub-cells are then assumed to have a random distribution within the grid cell, and the average values for cross-sectional area and wetted perimeter are calculated. To test the validity of the simplifying assumptions, the method was used to calculate these values, and they were compared against the true values for each cell (Figures 6.10 and 6.11).

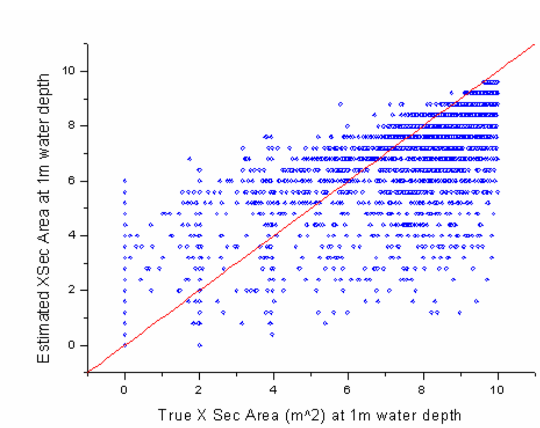

Figure 6.10: Comparison of True and Estimated Cross-Sectional Area

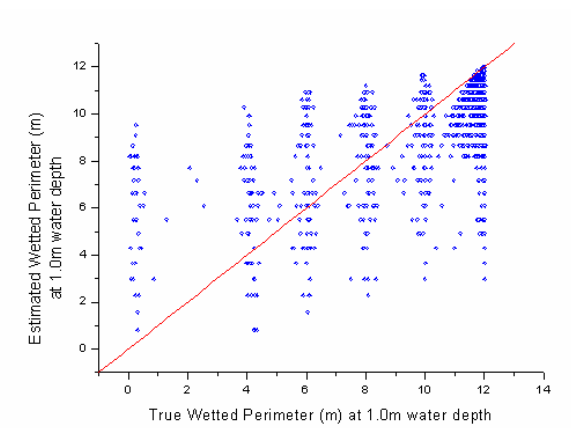

Figure 6.11: Comparison of True and Estimated Wetted Perimeter

The graphs show a weak correlation between true and estimated values of cross-sectional area and wetted perimeter. However, due to wide spread of values around the 1:1 line, the simplification was not felt to be sufficiently accurate for use within the model. The full look-up tables were therefore stored for each parameter.

6.3 Data Collection and Processing for Test Applications

6.3.1 Upper Granta Catchment

In order to explore the two approaches to urban flood simulation, a series of numerical experiments were undertaken, based on a reconstruction of the October 2001 flood event on the River Granta study site (Chapter 3). In order to perform multiple simulations for calibration and validation, it is important to reduce the model running time as far as possible, and therefore a relatively short reach of approximately 2 km is used. An aerial photograph and map of buildings and features on the floodplain are shown in Figures 6.15 and 6.16. The following sections describe the collection and processing of the input data required for the model, including topographical information, channel structure description and flow boundary conditions. The collection of calibration and validation data in the form of observed hydrographs from the Linton and Babraham flow gauging stations, and inundation extent and depth data from a residents' survey, is described in full in Chapter 3.

6.3.2 Topographical Data

6.3.2.1 Bare-Earth Elevation Model

An airborne LIDAR survey acquired in 2000 by the UK Environment Agency was used to derive both a 2 m DSM (Digital Surface Model) and a 10 m bare earth DEM as the boundary conditions for the high resolution and porosity models respectively. The 2 m resolution of the DSM was chosen to enable accurate representation of the urban area at a practical, if time-consuming, resolution for simulation. Using a 10 m grid scale, the 'porosity' model offers a more efficient representation, but at the expense of detail which must be recaptured from the sub-grid parameterisation. A model at 10 m grid resolution without sub-grid scale information is also used as a control to test against the models using high-resolution information.

The resolution of the raw point cloud is suitable to produce a digital elevation model of grid sizes 1 m upwards. However, the complex urban terrain is not well represented by an interpolation direct from the raw points, particularly due to the lack of differentiation between permeable areas of tall vegetation and impermeable buildings, as shown in Figure 6.12.

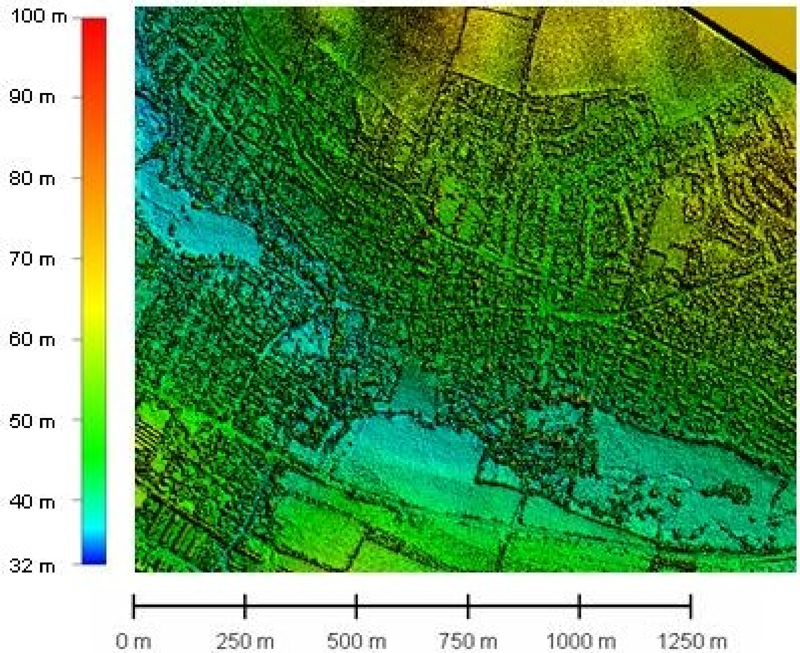

Figure 6.12: Raw LIDAR image of the Linton Area

Surface models were therefore derived by first processing the raw points to produce a bare-earth model, and then superimposing known floodplain structures onto this (Section 6.3.2.2). In order to create the bare-earth model, the point cloud was processed to remove all objects from the floodplain. This can often be achieved by using only the last-return points from the LIDAR data set which represent reflections from the ground surface rather than elevated objects. However in this case only single-return data was available, and hence a filtering algorithm was used as an alternative.

The algorithm first interpolates between recorded points to produce an elevation grid. Each grid cell is then considered as the centre of a moving window of grid cells. The average elevation value for the window is calculated, and if the central cell elevation exceeds this value by more than a specified threshold, any points within the cell are deleted. In the case of large structures, the algorithm will only remove edge cells and must therefore be iterated until the whole structure has been erased. Figure 6.13 shows the removal of a structure using a sequence of iterations.

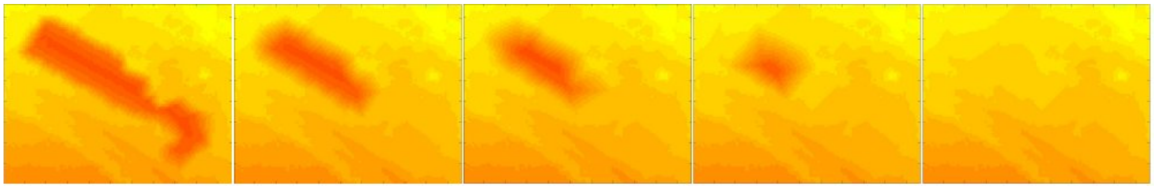

Figure 6.13: Removal of a floodplain structure through iterative filtering: Five successive iterations showing the interpolated gridded DSM at each stage.

When the iteration process is complete, the final set of LIDAR points is interpolated using local cubic splines to give regular elevation grids at the 2 m and 10 m scales required. An image of the resulting bare-earth terrain model is shown below in Figure 6.14. Slight 'blockiness' can be seen in some parts of the landscape, especially within the urban area, due to interpolation between sparse point returns from the ground surface. However, in general the method was successful in returning an accurate bare-earth terrain model.

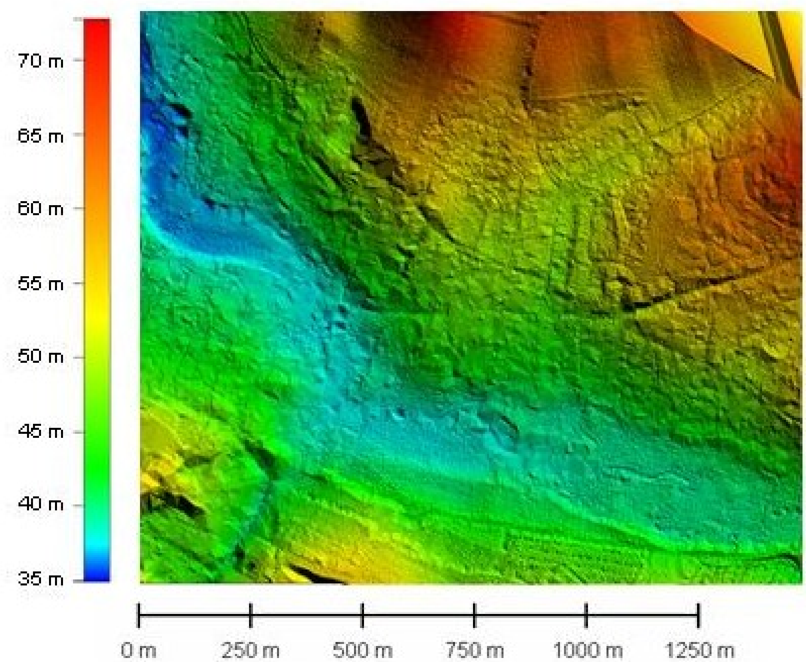

Figure 6.14: Filtered LIDAR image of the Linton area

6.3.2.2 Floodplain Structures

The 2 m DSM requires that structures on the floodplain should be superimposed onto the bare-earth model (this step is not required for the 10 m model where the porosity methodology is be used as an alternative). This method allows improved surface representation over use of the raw LIDAR points as only impermeable structures that have the effect of blocking flow pathways are considered. Data is available from the 1:2500 vector street plans taken from the UK Ordnance Survey Land-Line.Plus data set: detailed digitalised surveys of natural and man-made features. The Land-Line map, together with the corresponding area as an aerial photograph, are shown in Figures 6.15 and 6.16.

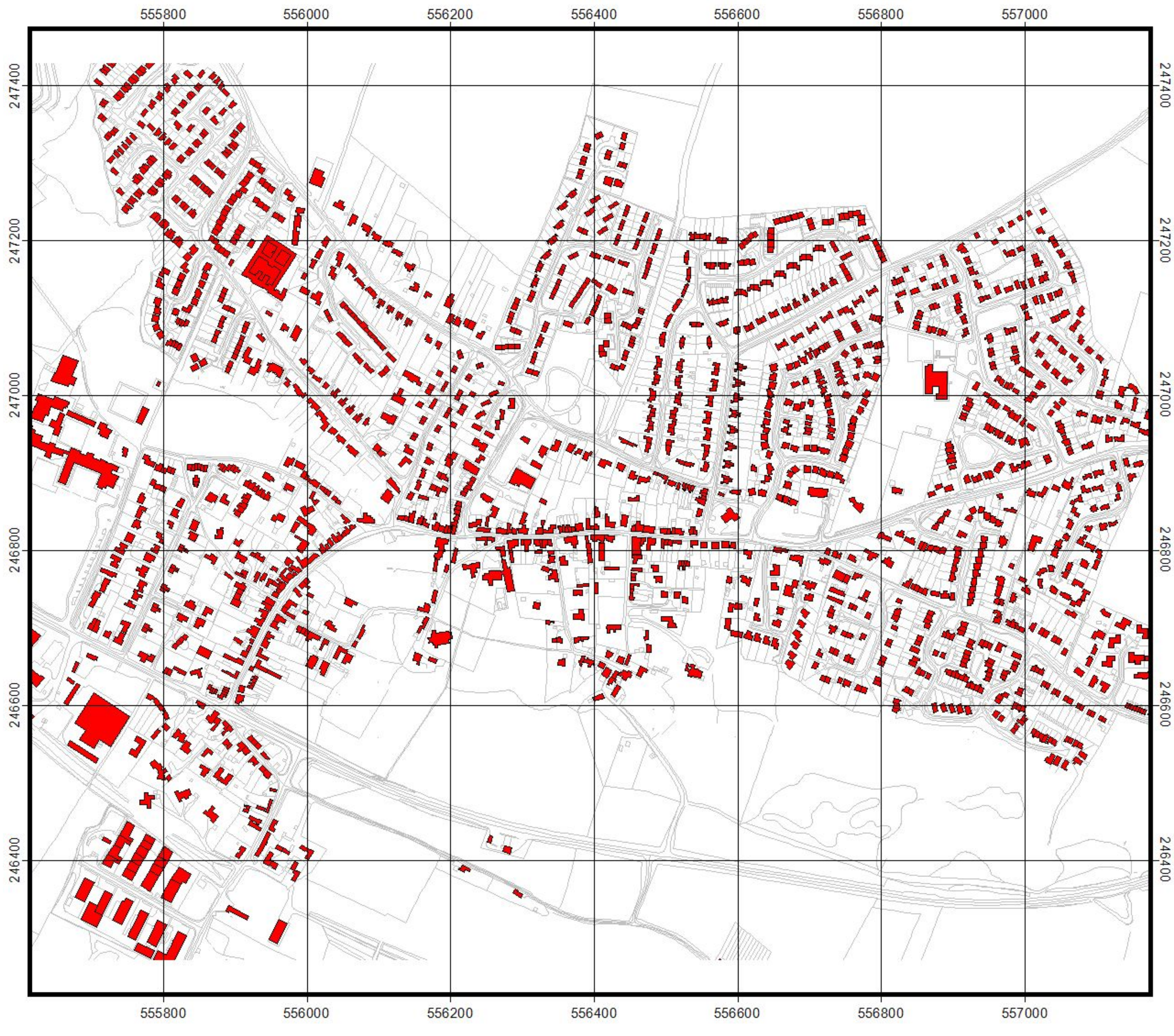

Figure 6.15: Land-Line.Plus surveyed data for Linton, buildings extracted as polygons

Figure 6.16: Aerial Photograph of Linton

Building outlines were extracted from the Land-Line map, and these were used to build polygon features in ArcView (Figure 6.15). In turn these were transformed into a grid with the required cell size. Grid cells containing a building were given an arbitrary height value of 10 m; exact height data was not required as simulated floods do not overtop buildings. However if necessary for future applications, building heights could be extracted by resampling the original LIDAR point cloud. Other cells were given a height of zero. The building grid was then added to the terrain grid to form the topographical boundary condition for the model, as shown in Figure 6.17:

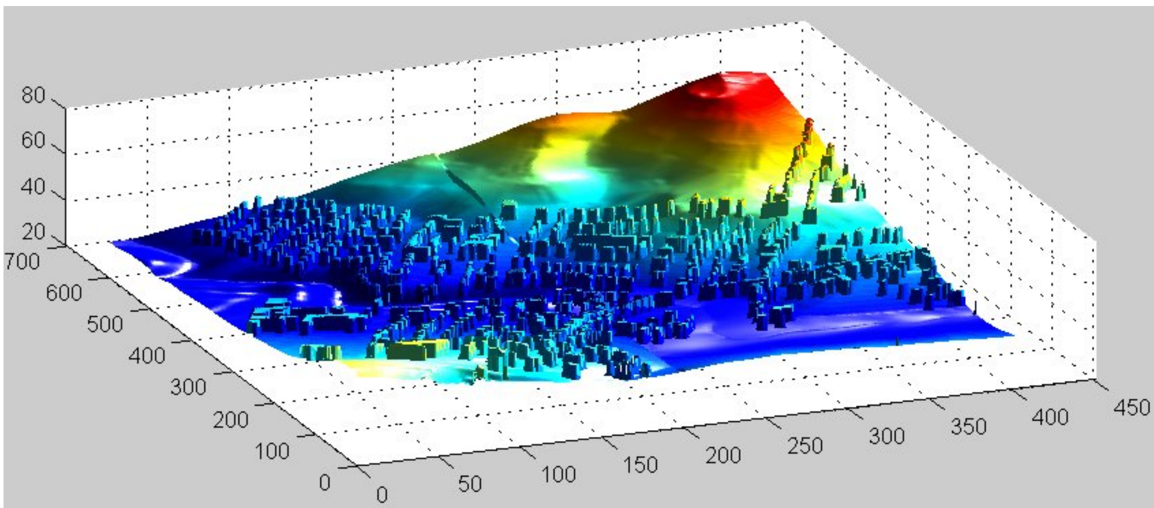

Figure 6.17: Topographical Model Boundary Condition, with 10x Vertical Exaggeration

6.3.2.3 *Porosity Information*

For the model implementation at 10 m scale using the porosity treatment, the DEM at 2 m scale is used in conjunction with that at 10 m to calculate the sub-grid scale information look-up tables for porosity, cross-sectional area and wetted perimeter, for each cell and boundary, at the following sequence of depths (all in metres):

[0, 0.25, 0.5, 0.75, 1, 1.5, 2, 2.5, 3, 4, 5, 6, 7, 8, 9, 10, 11, 12]

Depth intervals are smaller at lower depths in order to allow sufficient representation of topographical complexity. At higher depths porosity is influenced mainly by the presence or absence of man-made structures and hence shows less variation with height, allowing wider depth intervals. This pattern is illustrated in Figure 6.18, which shows porosity values mapped over the study area at a range of depths. At low depths, porosity is controlled by ground surface topography, demonstrated by the distinctive pale signature of the smoother land of the floodplain, the rougher land though the built-up area showing as darker tones. At high depths, the influence of the ground surface shape is reduced, and only buildings are apparent in the porosity map.

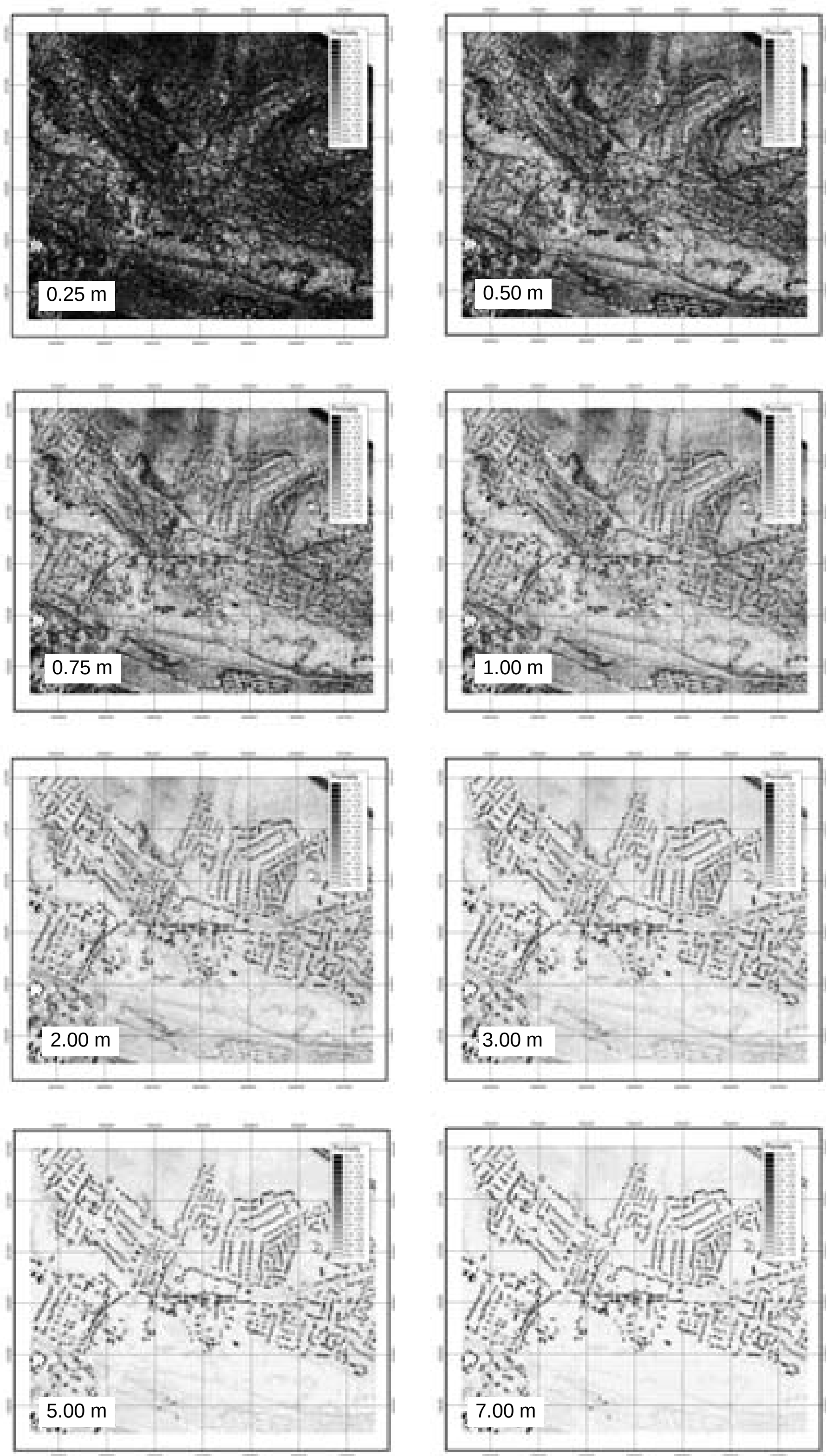

Figure 6.18: Porosity values over the model domain mapped at increasing depth.

6.3.3 *Channel Structure*

The model requires specification of channel width and bankfull depth. The Land-Line.Plus maps include vector data for both banks of the channel and were therefore used to specify channel width. This analysis was carried out in ArcView by creating a sequence of points along the channel centreline and then associating these with the shortest distance to each of the bank lines. The width vector interpolated to the 2 m grid is plotted in Figure 6.19, the 10 m vector was created similarly.

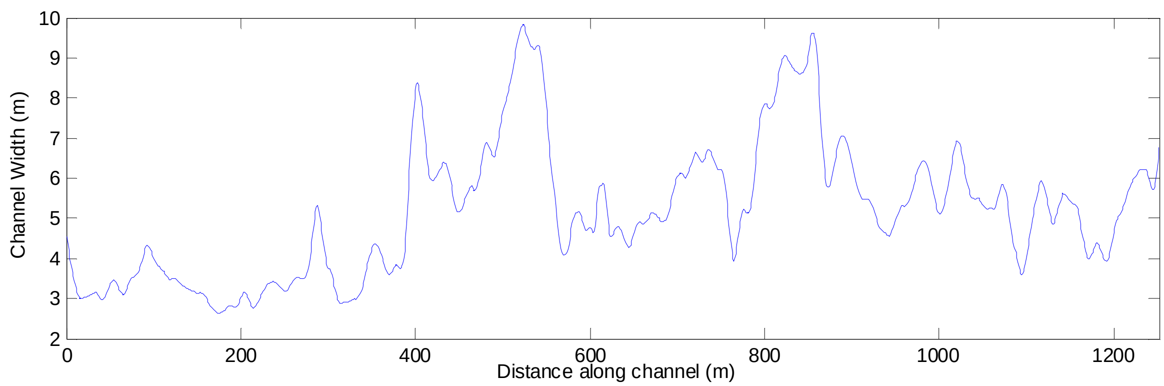

Figure 6.19: Channel width

Channel bankfull depths were available from surveyed cross sections taken at 200 m or better intervals, including sections at all channel structures e.g. bridges, fords. Bankfull depths are interpolated between these points to give values for each channel cell (Figure 6.20).

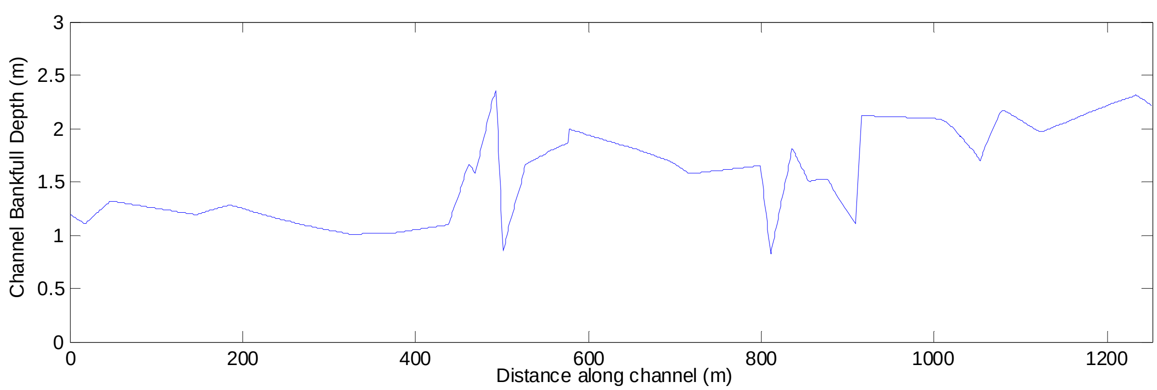

Figure 6.20: Channel bankfull depth

6.3.4 Channel Boundary Flow Conditions

Flow data is available at the upper and lower points of a 10 km reach surrounding Linton, from the Environment Agency gauging stations at Linton and Babraham. Stage and discharge are recorded at a 15 minute time step. This reach is too long to be modelled efficiently at the high resolutions considered in this study, a common problem when undertaking complex urban applications of flow models. To overcome this, a one-way nested catchment method is used, with a low-resolution model application at the reach scale producing channel flow records which serve as boundary conditions for an inner high-resolution application. This one-way nesting methodology is commonly used in distributed hydrological models which require meteorological boundary conditions, (e.g. Kleinn *et al*., 2005; Wood *et al*., 2004) or regional climate models set within a general circulation model (e.g. Cocke and LaRow, 2000; Leung and Ghan, 1999). It can also be used when sensitivity analysis shows that particular regions of the model area are important to model results and therefore warrant more detailed treatment (Hall *et al*., 2005).

The nested catchments areas are shown in Figure 6.21 below. The map shows that in this case, the upstream limit of the inner model area coincides with that of the outer. Therefore the outer model is required to provide the downstream boundary condition only.

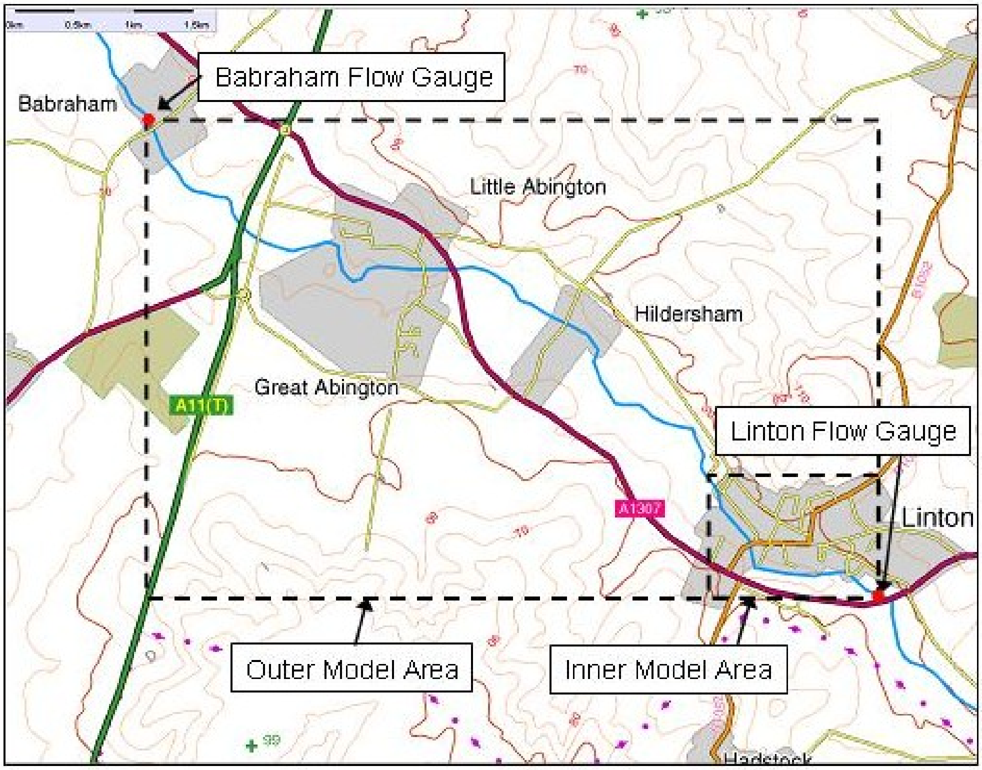

Figure 6.21: Nested Flow Modelling Areas

The values of the roughness parameters for channel and floodplain areas are not known and these were therefore treated as calibration coefficients, a methodology used by Horritt and Bates (2001b). The outer model was calibrated with respect to the downstream hydrograph only; this is considered sufficient as the only output required from this model application is the channel flow at the downstream point of the urban area.

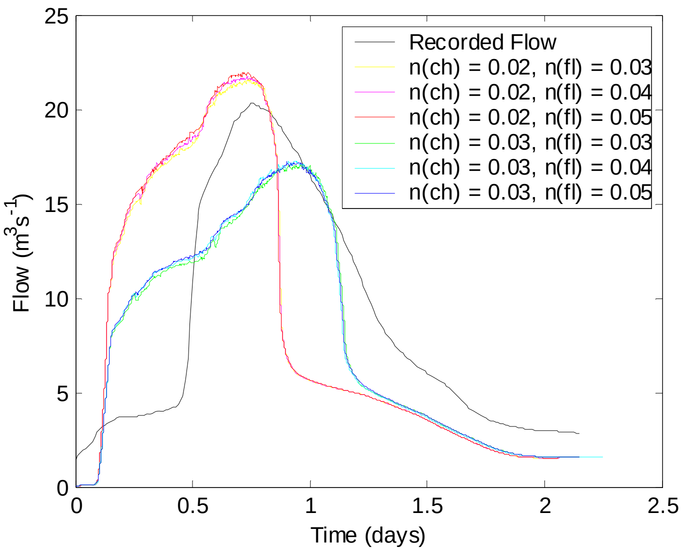

Figure 6.22: Comparison of modelled hydrographs, using a range of channel (n(ch)) and floodplain (n(fl)) friction coefficients (Manning's n, $m^{-1/3}s$), demonstrates the insensitivity of the model to floodplain friction

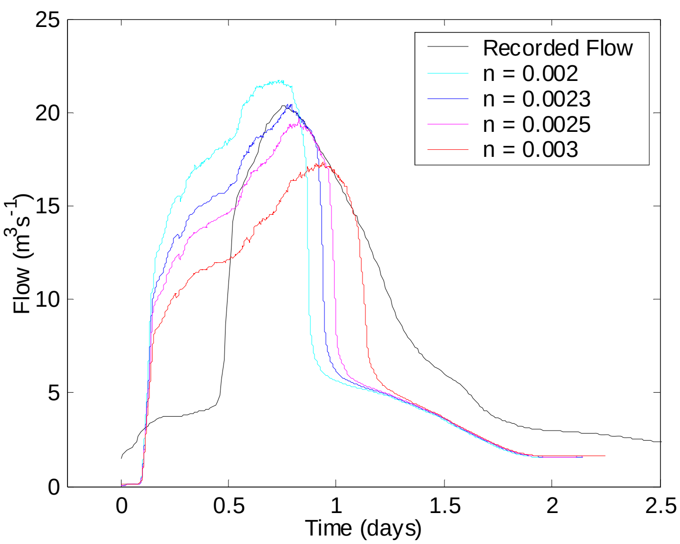

Figure 6.23: Calibration of the channel friction coefficient (Manning's n, $m^{-1/3}s$) by matching observed and modelled flood wave propagation at the reach scale

The model was found to be insensitive to floodplain friction (Figure 6.22), an effect which is conjectured to be due to the flow limiter required (Hunter *et al*., 2004) and is common in storage cells schemes (Hall *et al*., 2005; Romanowicz and Beven, 2003). Models which do not use this limiter are generally responsive to the friction coefficient, but may still find issues of equifinality during calibration (Pappenberger *et al*., 2005). The model was therefore calibrated using the channel friction parameter alone. If the optimal value is chosen using the R^2 measure, the accuracy of prediction of peak discharge and lag may be compromised in order to minimise errors in the shape of the rising and falling limbs of the hydrograph. In this study, the importance of prediction of peak magnitude and timing was felt to override that of hydrograph shape; therefore a performance measure based only on success in prediction of the flood peak is used. This type of approach was suggested by Lamb (1999), who experimented with measures based on both peak magnitude and lag error, and on magnitude error only. Here, the performance measure chosen was based on both magnitude and lag, as both are felt to be important in the context of flood warning provision; however it is clear from Figure 6.23 that optimal performance in both is achieved simultaneously using $n = 0.023\ m^{-1/3}s$. Channel flow at the downstream boundary of the inner model area was duly recorded to provide the boundary condition for the inner model, this is shown in Figure 6.24. A worthwhile extension of the current work would be to include uncertainty bounds on the boundary condition calculated from the reach-scale model.

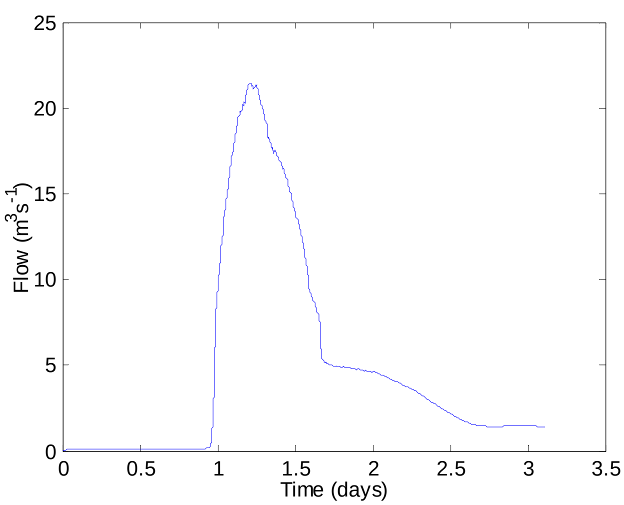

Figure 6.24: Channel Flow Lower Boundary Condition for the Inner Model

6.3.5 Non-Channel Boundaries

Boundary conditions must also be imposed for those parts of the floodplain not designated as channel cells. Previous studies have used various methods to do this, a popular solution being to use the no-flow (free-slip) boundary condition at all points except the prescribed channel (Vionnet *et al*., 2004). This however can lead to pooling at the downstream boundary of the modelled area, and various alternatives have been used such as imposition of water surface elevation (Hardy *et al*., 2000; Horritt and Bates, 2002), use of coupled models along the reach (Tucciarelli and Termini, 2000), or first order (or higher) extrapolation from neighbouring cells (Beffa and Connell, 2001). The last method, using first-order extrapolation, was chosen for the application to Linton.

When the floodplain is near the headwaters of the catchment, the contribution of lateral inflow into the channel is significant compared to the channel input, even when there are no major tributaries in the reach. The model caters for this by allowing a source term at each channel cell. In the absence of any other information, the flow rate for each cell is calibrated from the volume change between upstream and downstream hydrographs, distributed evenly along the channel during the main flood peak. Trials were carried out into the effects of allowing variable lateral flows, however no significant effects on simulation predictions were found. The lateral inflow rate hence becomes the final boundary condition for the model.

6.4 Model Testing and Results

Using the boundary conditions described above, three versions of the model were tested in their ability to simulate urban flooding in Linton. In addition to the 2 m DSM and 10 m porosity models, this included a further, baseline, model run at a 10 m resolution using a bare earth DEM with no porosity information. The details of the model and simulation characteristics are given in Table 6.1.

Model Type	Grid Scale (m)	Sub-grid Parameterisation	Grid Size (x,y)
Baseline	10	No	144 x 120
Porosity	10	Yes	144 x 120
Urban DSM	2	No	720 x 600

Table 6.1: Details of the three model structures and applications

6.4.1 Validation Methodology and Statistics

Validation studies of floodplain inundation models have highlighted the importance of evaluating model response in terms of both the dynamics of flood wave propagation and the spatially distributed pattern of inundation. For this study, only one key sensitive parameter was explored, the channel friction coefficient. For a range of values of this parameter, the predictive performance of the model was therefore evaluated in terms of downstream hydrograph fit, the spatial pattern of inundation and additionally by a metric which combines these two characteristics.

6.4.1.1 Validation by inundation extent and depth

Conventionally, the accuracy of predicted inundation extent is measured through a comparison of mapped and modelled flood boundaries (e.g. Bates and De Roo, 2000; Bradbrook *et al*., 2004). In effect this is a binary validation, as accuracy in flood depth prediction is not considered. In this study, such a binary analysis could be carried out by comparing those houses reported flooded compared to those that the simulation suggested would flood. However, because the observations are limited to the ‘flooded’ observed condition, this would lead to a maximally wet simulation being preferred. Instead, it is possible to take advantage of the extra information gathered during the survey of residents by validating on depth of flooding as well as extent. Although this could be achieved using a traditional least squares analysis, it was felt to be important to recognise that when using data points based on a questionnaire to residents, there is significant scope for errors in estimation/memory of flood depth. A technique designed to incorporate this uncertainty is the use of a fuzzy goodness of fit measure (Freer *et al*., 2004; Seibert and McDonnell, 2002). Each flooded building is given a score between 0 and 1 depending on quality of fit between simulated maximum flood depth adjacent to each building and reported flood depth. 1 indicates a perfect fit; here this was taken to be within 10 cm of reported flood level. This then decreases linearly down to 0 for an incorrect fit, here taken to be more than 50 cm discrepancy in flood levels (Figure 6.25). Finally, the mean of the individual fuzzy scores was taken to give the overall score.

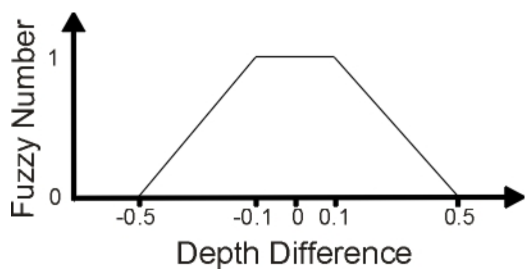

Figure 6.25: Fuzzy Performance Measure for Inundation Depths

When validating model results by inundation extent and depth, all simulation results should be expressed at the highest resolution grid scale. Horritt and Bates (2001a) found, in an application of LISFLOOD-FP to a reach of the River Severn, that model predictions were near identical at all grid scales under 250 m when the simulated water surface was mapped back over a high resolution terrain model. This result is thought to be less likely to reoccur at higher resolutions where small-scale terrain features such as levees have an enhanced influence on the model; however it should not be dismissed. Therefore in order to test all three model implementations against the same criteria, the simulated water levels from the two 10 m models (with and without porosity information) were mapped onto the 2 m DSM, using bilinear interpolation incorporating additional edge treatments to produce smooth water surfaces. It was then these high-resolution water depth matrices that were compared with the observed depths to produce the validation score.

6.4.1.2 Validation on Downstream Hydrograph

The Nash-Sutcliffe R^2 measure was initially considered for validation of the downstream hydrograph, however it was found to be unsuccessful in differentiating hydrograph fit based on a single storm, particularly due to autocorrelation of errors. Instead, benefiting from the observation that the simulated hydrographs have a consistent form, a linear combination of peak magnitude and lag errors (shown in Figure 6.26) is used to give an intuitive goodness-of-fit measure.

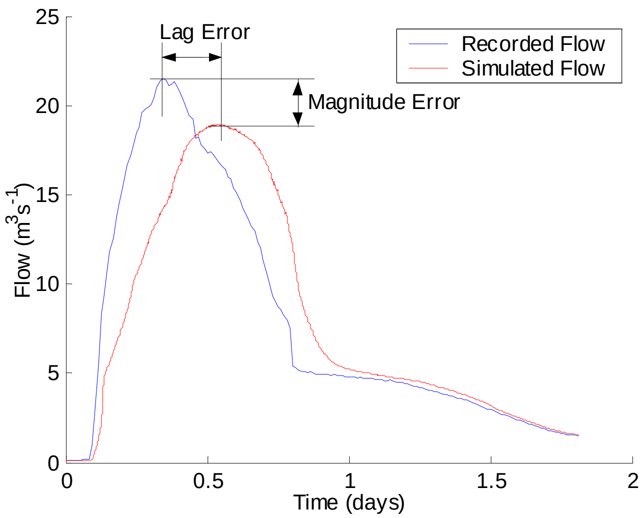

Figure 6.26: Example of Magnitude and Lag Errors

First, absolute peak and lag errors are independently linearly rescaled to lie within the interval [0,1] such that 0 indicates the worst result from the sets of simulations, 1 the best. These two rescaled values are then combined to give a hydrograph validation score:

$$\text{Validation Score} = 0.5 * (\text{Magnitude}' + \text{Lag}') \qquad (6.9)$$

6.4.1.3 Multi-criteria Validation

The final objective is to combine validation measures for model performance in simulating inundation and downstream hydrograph. This enables the models to be judged according to their ability to represent the whole floodplain process correctly and therefore to score highly against multiple validation criteria simultaneously, without needing to be recalibrated separately according to the particular flood characteristics to be modelled.

Any dual calibration is likely to be a trade-off between different responses, as demonstrated by the 'Pareto Set' concept of Gupta *et al*. (1998), but can, in some cases, improve the identifiability of model parameters (Kuczera and Mroczkowski, 1998). To try and make some comparison between different members of the Pareto Set, one option is to combine the validation criteria into a single goodness-of-fit index (Beven, 1993; Beven, 2000) for example using Bayesian updating, weighted mean or fuzzy set operations. Here a linear mapping of the response spaces is used for a comparison of available parameter sets with hydrograph and inundation data given equal weight. The general formula for k criteria is shown below, for this application k=2.

$$L\left(\Theta \middle| \underline{Y}_1 \ldots \underline{Y}_k\right) = \frac{1}{k} \cdot \sum_k \frac{L\left(\Theta \middle| \underline{Y}_k\right) - \min_{i,j} L\left(\Theta_i \middle| \underline{Y}_j\right)}{\max_{i,j} L\left(\Theta_i \middle| \underline{Y}_j\right) - \min_{i,j} L\left(\Theta_i \middle| \underline{Y}_j\right)} \qquad \textit{(6.10)}$$

with data sets $\underline{Y}_k$, parameter sets Θ , likelihood L()

This formula was used to combine the fuzzy measure for performance in simulating inundation extent and depth, and the combined measure for performance in simulating hydrograph peak magnitude and timing.

6.4.2 *Results*

6.4.2.1 *Validation by inundation extent and depth*

Model simulations were carried out for the channel friction coefficient, Manning's n, over the range 0.02-0.06 $m^{-1/3}s$. Plots showing the maximum flood extent for each case are shown in Figure 6.27. A preliminary comparison of the performance across model type and channel friction parameter is made by plotting modelled against reported flood depth for each inundated buildings (Figure 6.28).

Visual inspection shows that the best results are obtained for values of n around 0.05/0.06 $m^{-1/3}s$, higher than field observations for a fine gravel, low sinuosity, relatively clean channel might suggest (Chow *et al*., 1988). This may reflect a combination of factors including error in upstream hydrograph record, alternative flow sources such as overland flow, groundwater breach of cellars, as well as model process error leading to channel roughness parameterisation compensating for unmodelled processes. First impressions also suggest that the models run at 2 m and 10 m with porosity information are less prone to outliers than the baseline 10 m model. To make a structured comparison, the fuzzy scores for inundation validation, outlined in section 6.4.1.1, are plotted in Figure 6.29. This comparison shows that fit improves with channel roughness for all three models, with the scores from the baseline 10 m model dropping below those of the models using high resolution data for the higher values of the channel friction parameter. This drop in performance is due to overflooding in some areas, demonstrated in the outlying points in Figure 6.29(C). The houses represented by these outliers are circled in the Figure 6.30, which shows the wider flood envelope associated with the baseline 10 m model compared to the 10 m porosity model. The wider and smoother outline reflects increased volumes of water on the floodplain, and a loss of the boundary detail achieved in the 10 m porosity model due to the improved specification of flow pathways and preferential flow directions.

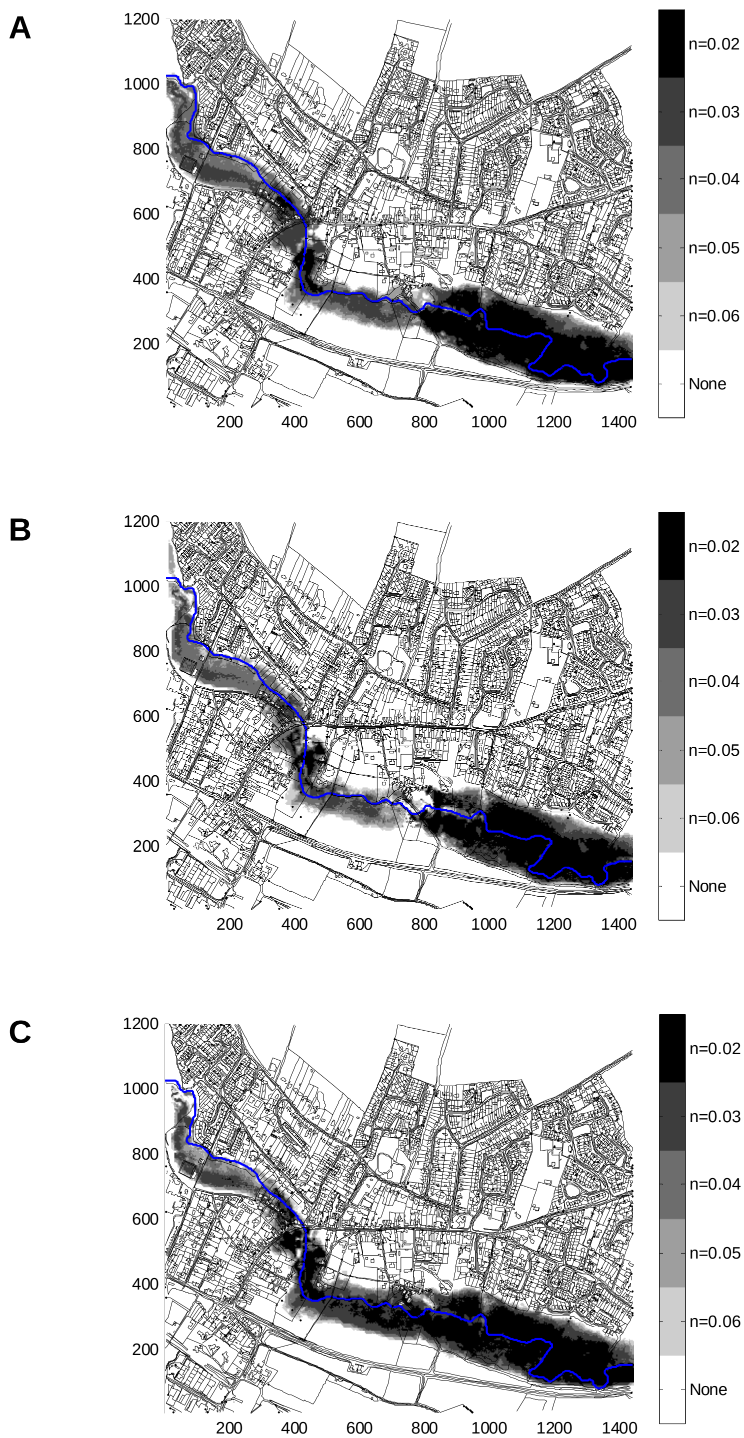

Figure 6.27: Floodplain Inundation in the urban model domain around Linton. Figures show results for the three model structures; A) High resolution 2 m model; B) 10 m model with porosity treatment; C) 10 m model without porosity

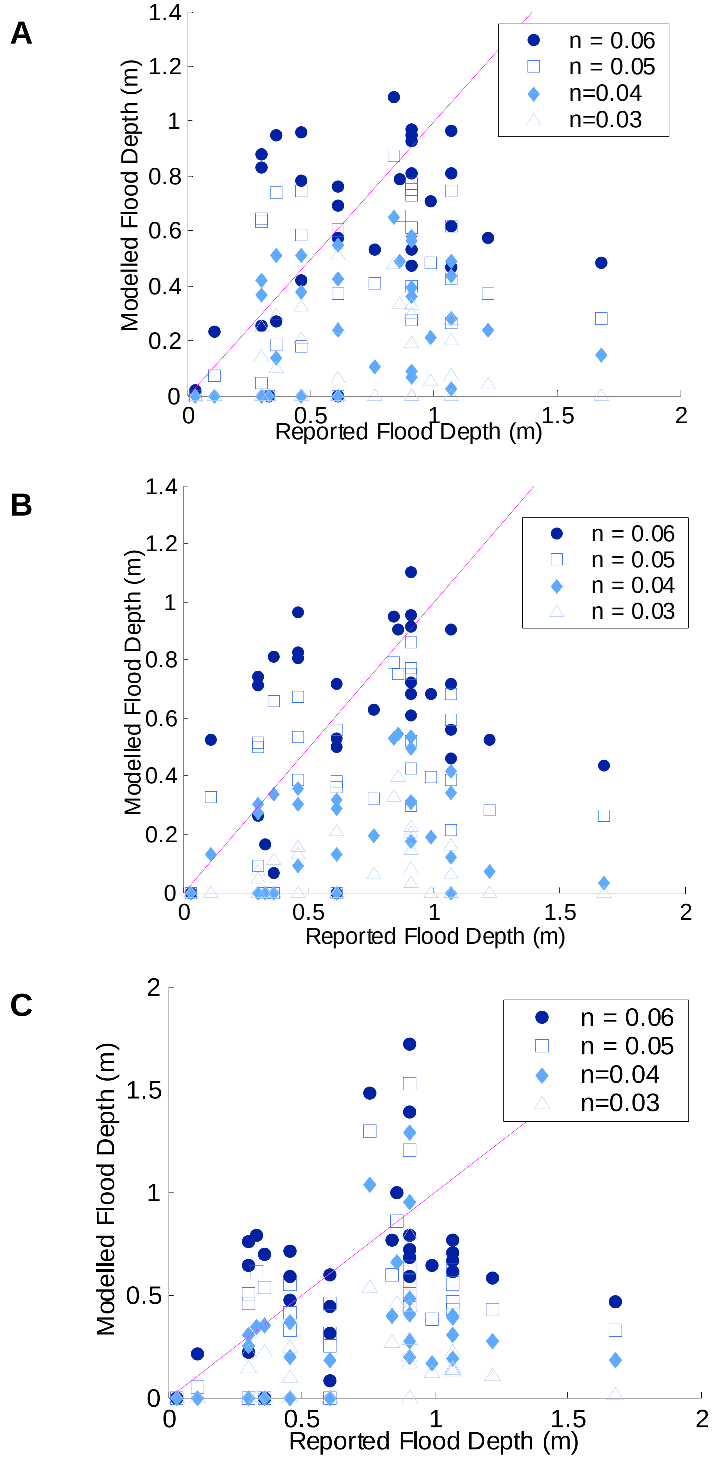

Figure 6.28: Observed and predicted maximum flood depths in reporting households, conducted for channel Manning's n between 0.03-0.06 $m^{-1/3}s$. Results are presented for the three model structures; A) High resolution 2 m model; B) 10 m model with porosity treatment; C) 10 m model without porosity.

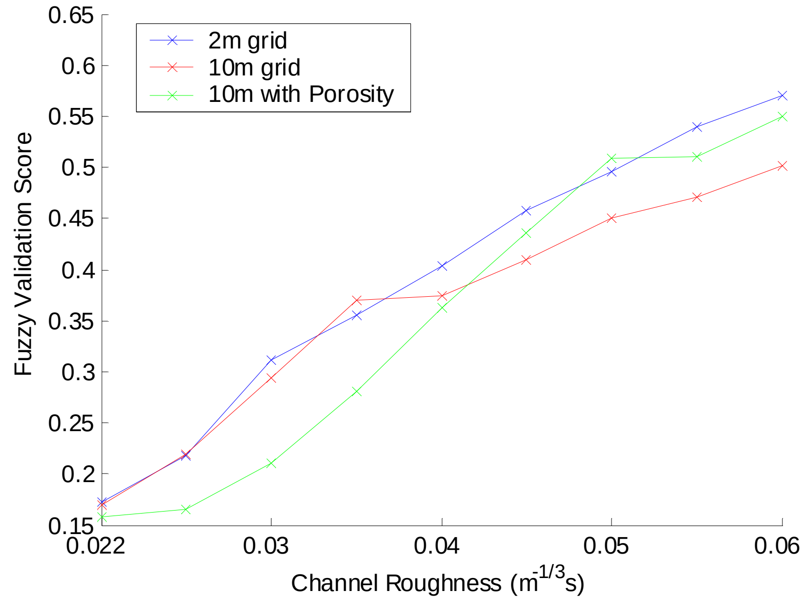

Fig 6.29: Fuzzy validation score for the three model structures varying with channel roughness

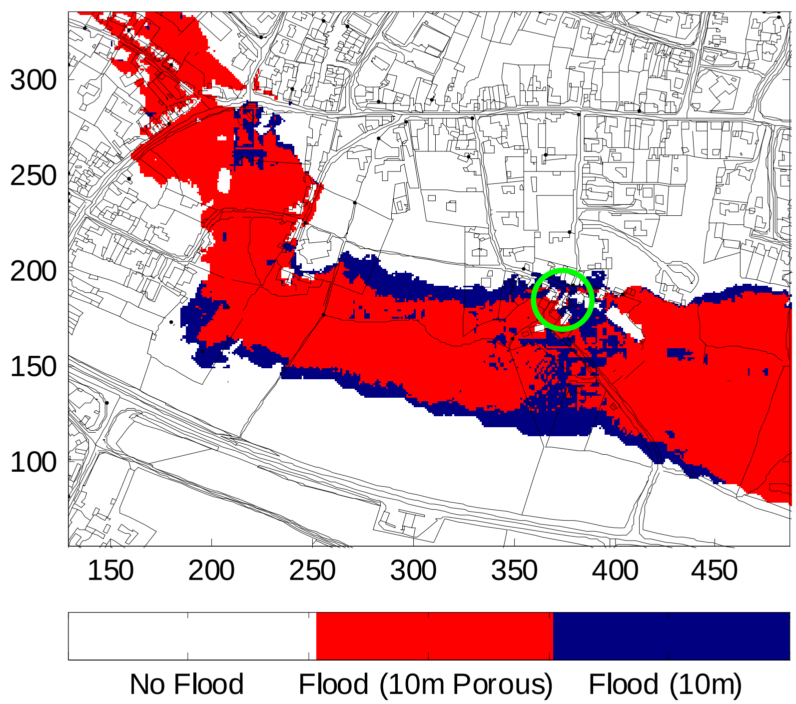

Fig 6.30: Maximum flood envelopes predicted for the two 10 m models, with and without porosity information. Circle shows properties where depth is severely overestimated in the latter case.

6.4.2.2 Validation on Downstream Hydrograph

The model is also calibrated on downstream hydrograph data. Figure 6.31 shows the simulated hydrographs for the three model structures run with channel roughness values from n = 0.02 $m^{-1/3}s$ to n = 0.06 $m^{-1/3}s$. In each case the downstream boundary condition derived from the outer model is plotted for comparison. The optimum value of channel friction to achieve a good fit to the downstream hydrograph varies with the model structure, but is always in the range n = 0.02 $m^{-1/3}s$ to n = 0.04 $m^{-1/3}s$. At higher values of n, all models overestimate the lag time, however while the '2 m' and '10 m with porosity' models achieve a reasonable representation of hydrograph shape and magnitude, the baseline 10 m model greatly overestimates the attenuation occurring in the reach.

The hydrograph validation scores (described in Section 6.4.1.2) are plotted in Figure 6.32. The 2 m model and the 10 m model with porosity are both able to achieve high scores across a wide range of channel friction coefficients; however the baseline 10 m model is unable to make good predictions for higher values of n due to over-attenuation of the flood wave, and hence has a much more restricted behavioural parameter space. The over-attenuated hydrograph indicates that excess water is being routed onto the floodplain, as shown by the spatial model responses discussed above. This again demonstrates the importance of porosity information in restricting and directing flow. An examination of the evolving channel breach points showed that these were very similar with or without porosity information; however the volumes able to flow through the breach points were much greater when porosity information was not used. Figure 6.33 shows typical differences in flood volumes when porosity information is introduced into the model, through a series of snapshots of flood depth during rising limb, flood and recession.

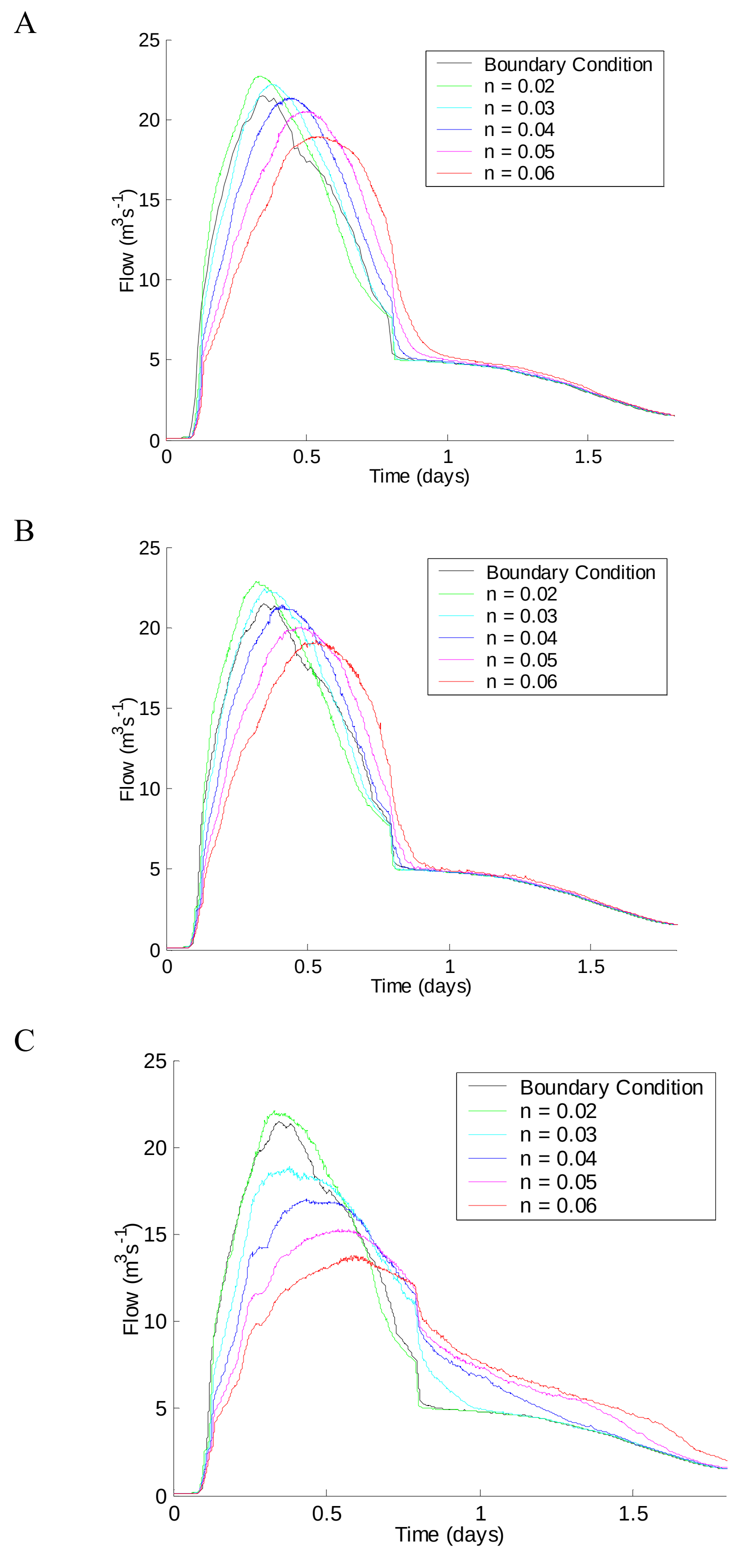

Fig 6.31: Flood wave routing performance, shown for Manning's $n = 0.02 – 0.06\ m^{-1/3}s$. Results are presented for the three model structures: A) High resolution 2 m model, B) 10 m model with porosity treatment, C) 10 m model without porosity.

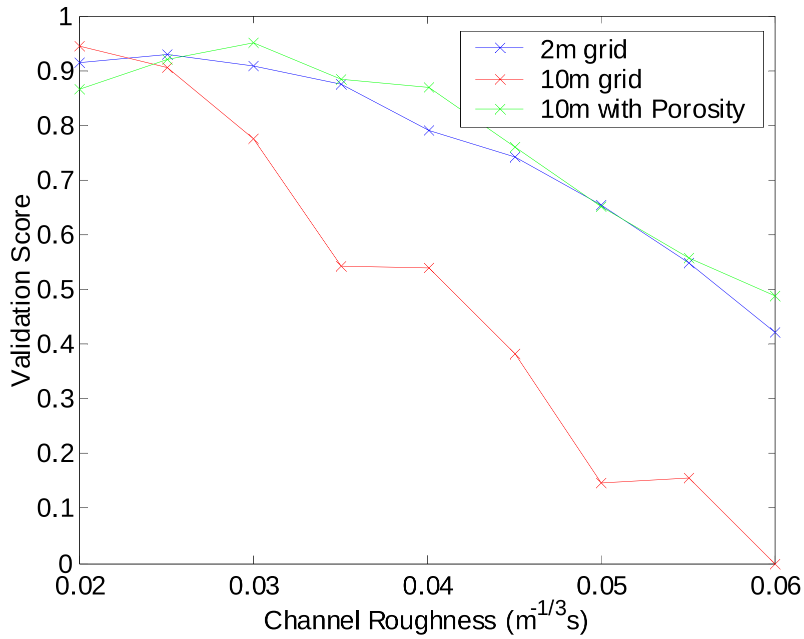

Fig 6.32: Validation using Combined Peak/Lag Hydrograph Measure

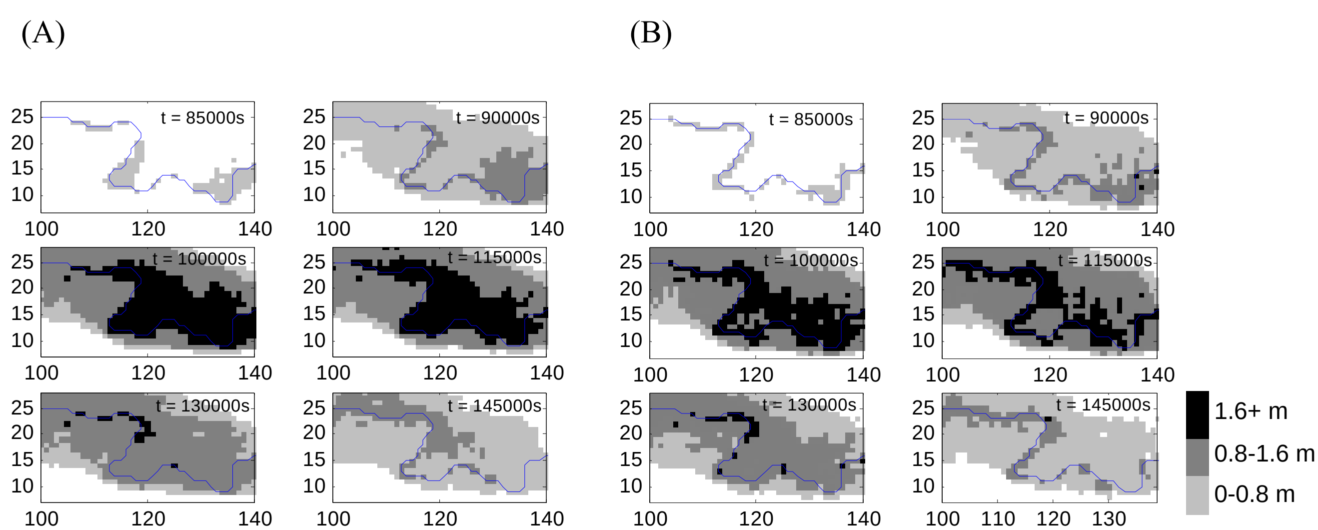

Figure 6.33: Snapshots of the inundation pattern predicted by the 10 m codes, without (A) and with (B) porosity information. The 'blocking' effect of sub-grid topography is shown in the discontinuous and irregular pattern of floodplain depths. Inundation depths are references to the attached greyscale legend.

6.4.2.3 Multi-criteria Validation

The combined likelihood measure, incorporating both aspects of predictive performance (Section 6.4.1.3), is plotted against the channel roughness parameter for each of the three models (Figure 6.34).

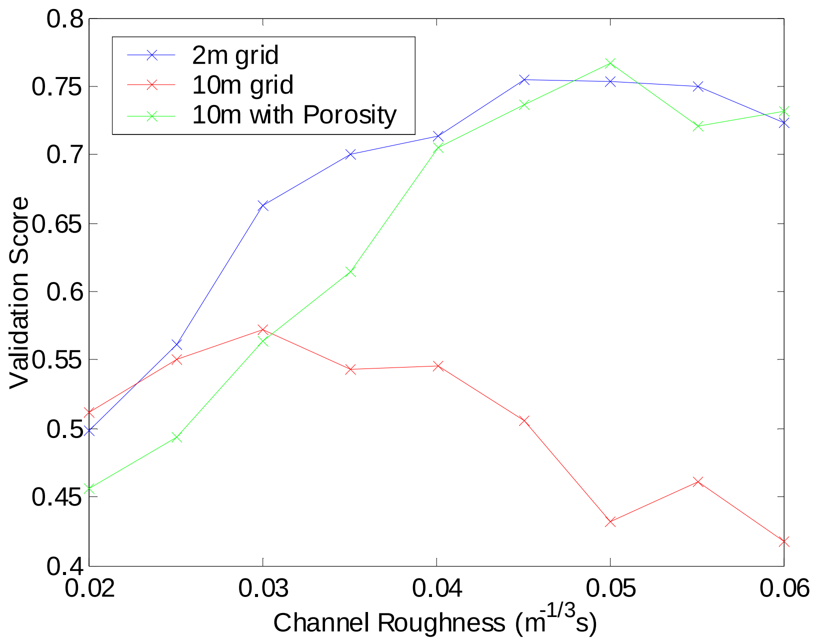

Fig 6.34: Validation using Combination of Fuzzy Inundation measure and Peak/Lag Hydrograph Measure

Such a comparison suggests that the 2 m and 10 m porosity models give a similarly good fit to recorded inundation levels using channel roughness of around 0.05 $m^{-1/3}s$, while the baseline 10 m model gives a poorer fit peaking at channel roughness 0.03 $m^{-1/3}s$. This reflects the inability of the 10 m model to produce realistic predictions for both downstream hydrograph and inundation extent for the same value of the channel friction parameter.

6.5 Discussion

This case study has established the potential of including explicit porosity information as an alternative to full high-resolution topographical data within a raster storage cell floodplain inundation model. In tests against the baseline 10 m model, the full 2 m implementation and the 10 m model with porosity information were found to behave very similarly, and with greater predictive power and robustness. The downstream hydrographs derived from the two models were almost identical, and the distributions of depths were also very similar. The main differences were found for low values of channel friction where the 10m model with porosity gave lower water depths.

A study of the improvements in performance when using high-resolution data is therefore made for the two models together. First, improvements in inundation prediction are considered. It was found to be important to validate on depth as well as inundation extent, as although flood outlines from the baseline 10 m model were approximately correct, the model made significant overprediction of flood depth in some places, where the models with high-resolution topography were able to provide accurate simulations. A similar finding has been made in several other studies. Bates and De Roo (2000) used the LISFLOOD_FP model to simulate a flood event on the River Meuse at resolutions of 25 m, 50 m and 100 m. They found that at the lowest resolution, flood depths were significantly overestimated, and suggested that this was due to the smoothing out of levee structures which allowed more water onto the floodplain. Yu and Lane (2006a) also found an increase in flood extent and depth with grid size, using the JFLOW model, and associated this with the smoothing effect of mesh coarsening together with poorer representation of surface routing processes. Tarrant *et al*. (2005) compared models run at three scales and found more complex behaviour, concluding that individual flow pathways may open or close depending on the particular choice of grid size. In this study, depth overestimation associated with larger grid size was found to particularly affect houses near to the inundation boundary. This finding adds increased weight to the suggestion by Hunter *et al*. (2004) that model conditioning on flood outline only may not be sufficient to fully capture the model's ability to replicate the flood event.

Improvements in inundation prediction are linked directly to improvements in downstream hydrograph prediction, as the impeded inundation on the floodplain prevents excess water leaving the channel and therefore provides an accurate estimation of within-channel flow. When a multi-criteria validation is carried out, the results suggest that different model implementations may require substantially different channel roughness coefficients to provide the optimal fit: the 10 m baseline model peaks at n = 0.03 $m^{-1/3}s$, while the high-resolution models peak at n = 0.05 $m^{-1/3}s$. This change in model behaviour according to grid size, and subsequent need for re-calibration, has been recognised in several other studies and, in addition to the effects of coarsened DEM representation described in the previous paragraph, has also been attributed to the fact that a finer grid size leads to an increase in channel flow velocities (Connell *et al*., 1998; Nicholas and Mitchell, 2003).

In the light of these findings, it is reasonable to compare the ‘best’ result in terms of goodness-of-fit measure for the three implementations, and recognise that roughness coefficients may not be transferable because they are ‘effective’ parameters designed to represent a model characteristic at the grid scale, and not absolute quantities. They may also compensate for other inadequacies in the model and therefore represent the combined behaviour of several aspects of the conceptual floodplain model. However, it remains clear that by including high-resolution topographical information, the model’s performance in terms of the combined validation measure is much improved, demonstrating an enhanced ability to make simultaneous accurate predictions of downstream hydrograph and floodplain inundation. The baseline 10 m model is unable to do this due to over-attenuation of channel hydrograph at high values of Manning’s n.

These results help to explain the similarity of results from the 2 m model and the 10 m model with porosity information. The improvement in performance may be considered in terms of flow pathway definition. Inclusion of information on the porosity of each cell allows flow volume and direction to be controlled in a manner similar to that allowed in the higher resolution implementation. This is the concept referred to by Lane (2005) as flow ‘blockage’. Models including porosity information are therefore able to provide a much more realistic simulation of flood extent evolution, and therefore also improve accuracy of in-channel floodwave attenuation by improving estimation of the volume of water stored on the floodplain. This finding agrees with that of Yu and Lane (2006b) who demonstrate the effects of flowpath blockage in reducing the speed of inundation and maximum inundated area in a simulation of the November 2000 flood event on the River Ouse in Yorkshire.

This is a very encouraging result, as by using a 10 m model resolution with porosity information instead of the full 2 m DEM, the model running time is reduced to approximately 1/38 of its former value. Model running times using the optimal channel friction n = 0.05 $m^{-1/3}s$ are shown in Table 6.2. This saving has been made without significant loss of accuracy when simulating flood propagation through complex natural and urban terrain.

Model Type	**Running Time (mins)**
10 m grid	80.4
10 m with Porosity	235.0
2 m grid	9016.3

Table 6.2: Execution times for the three model structures, benchmarked on a Pentium 4, 3.2 MHz PC with 1.5GB RAM, based on simulations with the optimal channel friction coefficient, n = 0.05 $m^{-1/3}s$.

6.6 Conclusion

This chapter presents new approaches to the use of high-resolution calibration data within a 2d floodplain inundation model. Increasingly, airborne mapping of floodplain topography produces DEMs at a higher resolution than computational resources allow to be used in typical current model structures. A solution is therefore sought in the use of reduced-complexity modelling. The data was used in two ways: firstly through a full high-resolution implementation, and secondly by inclusion as porosity information within a model running at a lower resolution. The porosity information was used via calibrated relationships between water depth in each cell and values of parameters describing cell porosity, boundary cross-sectional area and wetted perimeter.

This methodology was included in a model built to provide a compromise between performance and stability. Model time step was controlled by the use of the CFL condition applied to the channel cells where water velocity is expected to be fastest, and a 2d coupled flow limiter was used to prevent instability. The model was then applied to a section of the River Granta, where the town of Linton is surrounded by a largely rural floodplain with rolling topography.

Applications of the model to the urban area demonstrated the potential of including explicit porosity information within a raster storage cell floodplain inundation model. A model run at 10 m grid scale with porosity information derived from a 2 m DEM is able to mimic the inundation and flow characteristics shown by a full application of the model at 2 m resolution, while decreasing model simulation time to approximately 1/38 of the original. This is in contrast to the 10 m model without porosity information which shows a much poorer performance when validated against downstream hydrograph and inundation data. The successful application of the porosity model is particularly encouraging in that it offers scope to improve flood forecasts in urban areas by simply accounting for the effects of flow blocking on conveyance, without the need to incorporate more complex non-linear terms in the momentum equation. The 10 m model with porosity was therefore chosen for further use in the end-to-end flood risk assessment framework.

Part III

END-TO-END FLOOD RISK ASSESSMENT WITH UNCERTAINTY ESTIMATION

Chapter 7

AN END-TO-END FLOOD RISK ASSESSMENT FRAMEWORK

Abstract

In Chapter 1 the case was presented for an 'End-to-End' modelling strategy: the creation of a coupled system of models to allow continuous simulation methodology to be used to predict the magnitude and simulate the effects of high return period flood events. This chapter brings together the rainfall, rainfall-runoff and hydraulic models described in the previous three chapters to create such a system. It is then tested through an application to the catchment of the River Granta upstream and including the small town of Linton (UK National Grid Ref. TL 560469).

The model chain is subject to stochasticity and parameter uncertainty, and hence the variables used to pass data between models are also uncertain. Therefore in order to produce robust estimates of flood risk, uncertainties must be propagated through the model chain. It is also important that their effects be quantified in terms of variables relevant to the end user such as spatial inundation extent or number of properties flooded. Methods to allow the propagation and quantification of uncertainty within a computationally efficient framework are established and applied to the Granta catchment.

Results are considered in terms of their implications for successful floodplain management, and compared against the deterministic methodology more commonly in use for flood risk assessment applications. The provenance of predictive uncertainty is also considered in order to identify those areas where future effort in terms of data collection or model refinement might best be directed in order to narrow the prediction bounds and produce a more precise forecast.

7.1 Introduction

In order to provide the long-term flood frequency prediction capabilities required for strategic planning applications, the rainfall simulation, rainfall-runoff and floodplain hydraulics models described in the preceding chapters are coupled together to form a model chain. This chain allows the simulation of catchment rainfall to be transformed into runoff series and then statistically decomposed. Relevant characteristics are used to prescribe input into the floodplain hydraulic model to simulate inundation response. As described in Chapter 1, continuous simulation provides a powerful new approach for flood frequency estimation, which has only recently become practical for widespread application as a result of recent improvements in computing power. The benefits achieved by removing the simplifying assumptions of the alternative design event or derived distribution approaches have led to its increasingly uptake as a standard technique in flood risk analysis applications (Lamb, 1999).

The hydrological literature contains many examples of the use of continuous simulation. Boughton and Droop (2003) provide a review of its application in design flood estimation, and reflect the majority of studies which restrict model coupling to rainfall and rainfall-runoff models. These studies divide into those which use observed rainfall data (e.g. Chetty and Smithers, 2005; Maskey et al., 2004; Pandit and Gopalakrishnan, 1996) and those which use a stochastic simulation of rainfall input (e.g. Franchini et al., 2000; Hashemi et al., 2000; Onof et al., 1996). Applications which go further to couple hydraulic models are rarer but include applications to design of structural floodplain defence measures (Hsieh et al., 2006) and flood mapping studies (Faulkner and Wass, 2005). Typically, simple coupling takes place in terms of channel discharge, but this has been extended to include full hillslope-floodplain coupling (Charlton, 1999).

As equifinality of model structures and parameters has become accepted in hydrological modelling, applications of continuous simulation have reflected this in regular inclusion of uncertainty analyses carried out using Monte Carlo simulation. There have been extensive studies using stochastic rainfall simulations linked to TOPMODEL (Blazkova and Beven, 2002; Blazkova and Beven, 2004; Cameron et al., 2000) although a variety of other rainfall runoff models have also been used (Kuchment and Gelfan, 2002; Lamb, 1999). Uncertainty estimation for predictions in ungauged catchments has also been carried out (Lamb and Kay, 2004).

The potential for the use of coupled models in event-based simulation is also significant, both in terms of hindcasting historical flood events and in operational forecasting to improve lead times by using meteorological forecasts. Numerical weather prediction (NWP) models have now also been used to provide ensemble forecasts to drive rainfall-runoff and hydraulic models. In this case, uncertainty is typically considered only in the weather prediction models (Bartholmes and Todini, 2005; Gouweleeuw et al., 2005), reflecting a perception that errors in these models dominate over errors in the structure or parameterisation of the coupled catchment models (Jasper et al., 2002). This is often due to a failure to resolve convective cells at resolutions comparable with rainfall-runoff models.

The European Flood Forecasting System (De Roo et al., 2003) aims to provide a structure within which different combinations of models can be used to provide probabilistic forecasts in response to medium-range weather forecasts. This system has trialled the feasibility of including uncertainty estimation in such forecasts; early applications limited uncertainty modelling to the NWP models for efficiency reasons (Pappenberger et al., 1999), but noted that “a major research challenge should be the development of computationally tractable techniques to analyse how uncertainties cascade through a chain of linked non-linear models” (De Roo et al., 2003). Despite the simplification, these studies found that computational limits imposed a necessarily small ensemble of precipitation inputs. Efforts were made to choose those ensemble members “most significant” for the prediction using a measure of distance in the parameter space (Sattler and Feddersen, 1999), and again to constrain numbers of simulations required by grouping similar hydrographs (Pappenberger et al., 1999). More recent work has succeeded in considering uncertainty in NWP, rainfall-runoff and inundation models within a GLUE framework, again using concepts of functional similarity in parameter sets to reduce the number of simulations required (Pappenberger et al., 2005). Nonetheless, this study found computer power to form the major limiting factor preventing a full uncertainty analysis.

This chapter outlines an extension of the continuous simulation methodology used in previous studies, designed to consider the impact of predictive uncertainty directly on the pattern and probability of floodplain inundation. GLUE is used to cascade uncertainties through this non-linear system, considering at each model stage the dominant uncertainties in model parameterisation, initial conditions, boundary conditions or observed data and therefore the key uncertainties in model function. Experimentation is used to identify components of the system which are particular subject to associated uncertainty and therefore towards which future effort might best be directed in order to tighten uncertainty bounds.

Using this technique, a framework is created which allows knowledge of model shortcomings and associated equifinality to be assimilated into a practical flood risk assessment method. Particular importance is placed on the need to integrate uncertainty estimates into easily understandable model predictions, useful to the end-user communities such as planning authorities, engineers and the general public.

7.2 A Flood Magnitude and Inundation Frequency Analysis for Linton

This section sets out an application of the end-to-end forecasting methodology. An efficient system for model coupling and uncertainty propagation is established, and then used to analyse of the frequency characteristics of the discharge of the River Granta at Linton. These are then extended to evaluate the concomitant patterns of flood routing and inundation distribution.

7.2.1 Using GLUE in End-to-End Hydrological Modelling

The GLUE technique was introduced in Chapter 5 as a tool for investigation of model response and associated uncertainty, when equifinality of model structure or parameterisation is likely to be significant. The advantages of the technique lie in the ability to make predictions of uncertainties in highly non-linear systems where the assumptions of traditional statistical techniques prove too restrictive. By using Monte Carlo sampling of the model structure and/or parameter space, rejecting non-behavioural simulations, and rating behavioural simulations by using an objective measure of fit with respect to some validation data, quantiles of the model output variables may be produced. Generally, upper and lower confidence bounds at the 90% or 95% level would be used to specify the predicted model output.

It is important to note that when estimating the upper (and similarly lower) confidence limits using GLUE, the discharge predictions at each timestep do not simply relate to a single set of parameter values and cannot therefore be related to a single model realisation. This implies that when applying GLUE to two or more coupled models, uncertainty bounds cannot be cascaded through the model series by treating uncertainty bounds for output timeseries as a prediction relating to a single parameter set that may be input into the following model. Instead, results relating to each parameter set must be propagated through the model chain individually to produce frequency distributions for parameters of interest.

7.2.2 Efficiency in End-to-End modelling

As discussed in the introduction, the computational demands of applying GLUE to a chain of coupled models present serious constraints on the number of dimensions over which uncertainty can be considered. Decisions therefore had to be made in order to restrict the scope of the analysis, balancing the efficiency of the system against the extent and accuracy of the results.

7.2.2.1 Length of Simulations

Beven (2000) suggests that, ideally, a T-year event should be estimated using a period of data 10T years in length to ensure robust identification. In practice, much shorter series are considered sufficient or used out of expediency: the Flood Estimation Handbook (Robson and Reed, 1999) recommends a series of length 2T years or greater. The aim here is to produce predictions at a range of return periods applicable to typical flood risk planning studies. In particular, estimation of the return period of the 2001 event would be useful, as such key recent historical events have formed the basis of planning policy. Initial estimates of this figure vary wildly from 50-100 years suggested by local residents in response to collective memory of past catchment behaviour, to 400 years suggested by a study commissioned by the Environment Agency (Halcrow, 2004). The simulation period was therefore chosen to be 1000 years, sufficient for a reasonably robust estimate of floods up to a 400-year return period, and allowing tentative estimation of the magnitude of a 1000-year flood.

7.2.2.2 Coupling of Rainfall and Rainfall-Runoff Models

The rainfall simulation model has been derived using empirical data rather than fitted parameters, and therefore parameter uncertainty is not present within the model. Instead, the perceived uncertainty in a 1000-year simulation of catchment rainfall relates to the inherent stochasticity of the model. One realisation of a 1000-year series represents only a single possible outcome: other realisations may yield different estimates of flood magnitudes relating to return periods of interest. However, as no judgement is made as to which realisation may most accurately represent future conditions, each simulation is assigned the same weight in the uncertainty estimation procedure. In choosing the method of coupling the rainfall and rainfall-runoff methods, two sources of uncertainty are therefore considered: the uncertainty in realisation of rainfall series, and the uncertainty of choice of rainfall-runoff model parameters.

The most comprehensive approach to uncertainty estimation would be to consider these two sources of uncertainty as a two-dimensional parameter space and searching systematically, i.e. every rainfall realisation coupled with every parameter set. This strategy would, however, lead to 10^6 model simulations each of 1000 years, and thus be extreme costly in computational terms. An alternative approach, used by Cameron et al. (1999), considers the rainfall realisation and rainfall-runoff model parameter sets together, and creates a joint set of Monte Carlo samples which contain independent random selections. This results in less dense sampling of the parameter space, but reduces the computational overhead by a factor of 1000. Cumulative distribution functions of variables sampled from the output runoff series are still specified by a 1000-point curve (i.e. 1000 independent realisations) using this methodology, which is deemed to provide sufficiently accurate representation to justify interpolation between points of the curve. The joint Monte Carlo sample must be assigned a performance weighting in order to create the required distributions: the weighting associated with the rainfall-runoff model parameter set are used for this purpose since the weightings of the rainfall simulations are deemed to be equal.

7.2.2.3 Coupling of Rainfall-Runoff and Floodplain Hydraulic Models

The rainfall-runoff model is used to process each series of simulated rainfall to yield an estimate of the associated channel discharge at the gauging station upstream of Linton which forms the upstream boundary of the inundation model. The rainfall-runoff and inundation models must be coupled in such a way as to allow the uncertainty associated with the multiple realisations of the discharge series to be represented in the input to the floodplain hydraulic model.

This decision must be made in terms of the specific requirements of the analysis. Here the aim is to use the hydraulic model to extend the flood frequency analysis to include inundation extent estimation at various return periods, which specify the uncertainty associated with the predictions. The most complete technique for estimating uncertainty in inundation predictions would be to route the discharge predicted by each rainfall simulation / rainfall-runoff model combination through the floodplain hydraulic model. This would allow the creation of frequency distributions for inundation at each grid cell. Unfortunately this is clearly not a practical proposition since the floodplain hydraulic model typically has a running time of around one hour per day of simulated time at a gridscale of 10 m, longer for higher resolutions (see Section 6.5).

However, by careful choice of assumptions with regard to the flow behaviour at the site, efficient methods for estimation of inundation frequency are possible. Here, an approach based on three key assumptions is proposed.

- First, it is assumed that the inundation extent related to a particular flow event is independent of flow conditions prior to the time at which out-of-bank flow began. This means that no consideration is given to conditions where standing water relating to a previous extent affects the capacity of the floodplain to store or transport floodwater from the current event. However, this assumption is justified as temporal juxtaposition of out-of-bank events is relatively rare within the catchment. By making this simplification, continuous simulation of the floodplain behaviour is no longer required and flood events may be modelled individually, thereby significantly reducing the computational overhead.

- Second, the assumption was made that the frequency distribution of inundation extent could be characterised using an annual maximum series for flow events. This reduces the analysis time required over that for a peaks-over-threshold (POT) analysis. Although a POT analysis gives a more complete picture of catchment behaviour, the same advantage can typically be acquired by using one additional year of annual maximum data (Robson and Reed, 1999). Given the long simulated data series, it is therefore not considered necessary.

- A third assumption is made that the event in each year which causes the greatest inundation is that which has the greatest instantaneous peak discharge. This is based on the premise that the magnitude of an event is a good indication of other damaging attributes of a flood such as over-bank volume or duration. Such an assumption is considered reasonable in a small headwater catchment such as that at Linton where long, lower-volume events resulting from delayed subcatchment response are unlikely, and no major control structures (e.g. dams) exist. This assumption is key to reducing time spent processing rainfall-runoff data as the storm with maximum discharge in each hydrological year can be easily identified. In contrast, identifying the storm causing most inundation from a flow series would be a challenging and time-consuming task, and might not be possible without carrying out the inundation simulation in full.

The magnitude of the discharge annual maximum is therefore collected for each year of the 1000-year flow series. In turn this can be used to give an estimate of peak flow for any given return period. In order to use the peak flow estimate to produce simulations of associated inundation, a hydrograph must be associated with the peak flow. The simplest method of achieving this would be to run the model to steady state, i.e. the hydrograph increases from typical baseflow levels to a steady flow at the peak value. However the inundation forecast produced from such a hydrograph would only be a true representation of catchment conditions if the assumption that the catchment reaches steady state is valid. This is not thought to be true in the Linton catchment where the flashy response to flood peaks gives insufficient time for steady state to occur. An estimate of the hydrograph shape is therefore required. Typically, flood hydrographs may be approximated as a triangle, as recession tails are less important to inundation estimation. Houghton-Carr (1999) gives examples of techniques for estimation of the shape from gauged records or catchment descriptors. In this study, a simple measure of hydrograph volume is required that may be used for comparison across storms. The measure chosen was the length of time before and after the flood peak at which the discharge remained above 3.5 m^3s^{-1}. This threshold value was chosen after initial tests to identify correct volume estimation of the hydrograph. It must also be a compromise between capturing the complete hydrograph above bankfull level (calculated as between 4 and 5 m^3s^{-1} through the centre of Linton using Manning’s formula to relate depth to discharge) and achieving adequate separation of neighbouring peaks. This measure is computationally efficient in terms of data requirements and provides the opportunity to produce frequency distributions of hydrograph volume in addition to peak value. To ensure that the triangular hydrographs produced represented an accurate representation of true hydrograph volumes, a set of sample annual maximum hydrographs were saved and their volume compared with the triangle estimation (Figure 7.1 below).

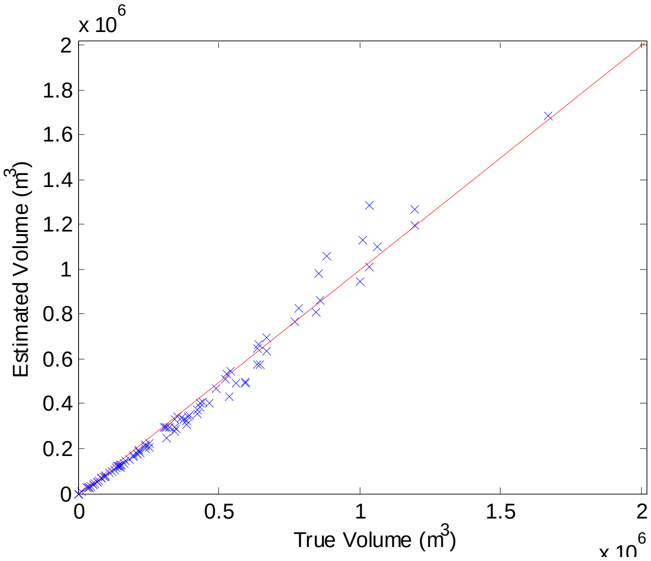

Figure 7.1: Validation of the Hydrograph Volume Estimation Technique

By storing the two threshold measures of the hydrograph in addition to the peak discharge, an estimation of the hydrograph shape may therefore be reconstructed for each flood event. This reconstruction can be used as input into the floodplain hydraulic model.

A final decision was taken that uncertainty in calibration of the floodplain model, i.e. value of Manning's n for channel friction, would not be part of the coupled uncertainty analysis. If this were to be undertaken, then for each return period of interest, the design event corresponding to each of the 1000 discharge series realisations would have to be propagated through the inundation model with each possible value of channel friction, giving rise to tens of thousands of simulations. This is not computationally feasible given that each inundation simulation takes several hours to perform. Instead, by considering only the uncertainty from the rainfall and rainfall-runoff models, the confidence bounds on the design event magnitude may be translated directly into confidence bounds on inundation extent. A limited sensitivity analysis of the model response to uncertainty in channel friction is, however, undertaken to provide a gauge of its relative effects on the inundation predictions. There is clear scope for this additional uncertainty source to be more fully considered in future applications when computational restrictions may have been lessened, however at present this simplified analysis is thought reasonable as unlike the strongly equifinal behaviour of the rainfall-runoff model (Chapter 5), the hydraulic model calibration (Chapter 6) gave a unimodal performance distribution with a single optimal value.

7.2.3 Data Preparation and Processing

7.2.3.1 Creation of Rainfall Series and Rainfall-Runoff Parameter Sets

Simulated rainfall series were produced using the methodology described in Chapter 4. Using the empirical distributions of each characteristic of the rainfall record, simulated storms were ascribed a mean intensity, duration, profile shape and inter-arrival time. For each hydrological year (1 September – 31 August) storms were created separately for the summer and winter seasons to allow for differences in precipitation patterns, and then concatenated to yield complete timeseries. As stated in Section 7.2.2.2 above, series of 1000 years duration were produced. One series was randomly generated to correspond to each rainfall-runoff model parameter sample, 1000 in all.

The rainfall-runoff model parameter sets used were those created using the process described in Chapter 5. They parameterise a transfer function model consisting of a non-linear rainfall transformation and two parallel linear runoff routing pathways. The retained parameter sets are those which achieve a performance, measured by the R^2 criterion, greater than the required threshold of 0.6. The discharge predictions produced by each set are weighted by this performance value.

7.2.3.2 Creation of Temperature Series

In order to respond to simulated series of rainfall input, the rainfall-runoff model also needs a temperature input at each 15-minute interval. This input is not measurable since the series are simulated rather than observed, and hence it must also be simulated. Temperature may be considered either as a predictable quantity that can be modelled as an average of observed records, or as a stochastic process which should include random fluctuation. In the case of the present application, temperature is required as a controlling process on the soil moisture recession curve within the catchment. As previously demonstrated, this recession is a slow process with characteristic timescales of several months. The short-term fluctuations in temperature are therefore less important; instead the requirement is to represent correctly the average temperatures on a monthly scale.

Plotting average monthly temperatures at Linton over the historical record showed relatively small variation between years, and therefore it was concluded that an average yearly temperature would be suitable for use in the simulations. The average temperature for each month was found from the historical record, and these points fitted by a sine curve as shown in Figure 7.2 below.

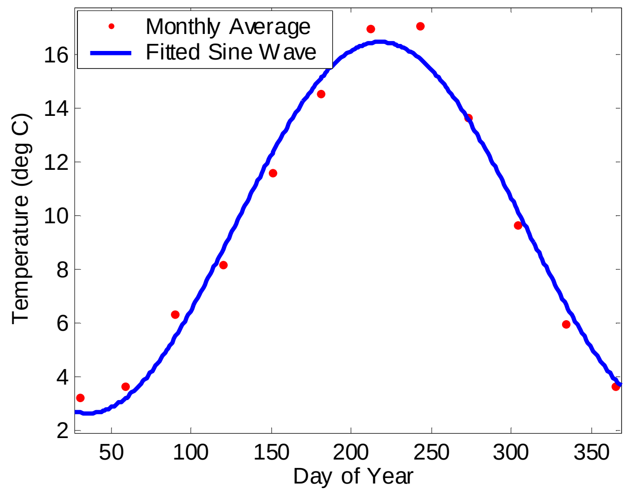

Figure 7.2: Average Yearly Temperature Curve Fitting by Sine Wave

A daily temperature curve was superimposed on the yearly curve. The curve was created using the average maximum deviations from the mean during each month of the year. Positive and negative deviations were considered separately as their magnitudes were often significantly different. The diurnal curve created in Section 3.3.2 was then fitted to these maxima and minima. Superimposing the two curves gave an average temperature value for every 15-minute period during the year.

7.2.3.3 Process Methodology

The method by which the rainfall series were created and processed using the rainfall-runoff model and characteristics of the discharge series saved, had to be carefully designed to minimise memory and storage requirements. The 1000-year rainfall series were too large to be held in memory complete (each consists of 1000 * 365 * 24 * 4 = 3.5 * 10^7 points), so were split into 100-year sections that could be processed separately and then stitched together, saving final conditions at the end of each partition to become antecedent conditions to the next section. In order to ensure that the prescribed initial conditions of catchment storage did not contribute to the model behaviour, the model was run for a period of 5 years as a warm-up before the start of the 1000-year period. Due to storage considerations, each 1000-year series was created on the fly and processed using the rainfall-runoff model before being deleted immediately. In turn, the required parameters were drawn from the discharge series and saved before it too was deleted; multiple rainfall or flow series were never stored permanently.

As discussed in Section 7.2.2.3, the characteristics drawn from any 1000-year discharge series were as follows. For each year of record, the peak instantaneous discharge was stored. The surrounding period of discharge was also retrieved from the record, and the time before and (separately) after the peak at which the discharge exceeded 3.5 m^3s^{-1} was recorded. The 1000 storms so recorded are then ranked by peak value and stored for later analysis.

7.2.4 Discharge Prediction Results

7.2.4.1 Flood Frequency Estimation

On completion of the processing of each simulation rainfall sequence using the rainfall-runoff model with corresponding parameter set, 1000 discharge series each of 1000 years were available in order to estimate the discharge associated with a range of return periods in the catchment. For each rank position in the 1000-year series, the 1000 possible realisations of discharge value were ordered and associated with the R^2 value as explained in Section 7.1.3.1. A weighted cumulative distribution of discharge for each of these return periods could therefore be created, and upper and lower limits at the required confidence level together with any other quantiles produced by interpolation. The return period-discharge relationship may be visualised by plotting all sets of limits together (Figures 7.3 and 7.4).

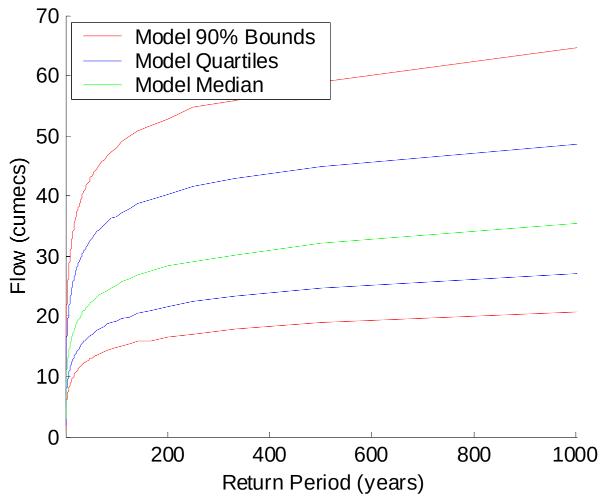

Figure 7.3: Modelled Discharge: Return Period Relation

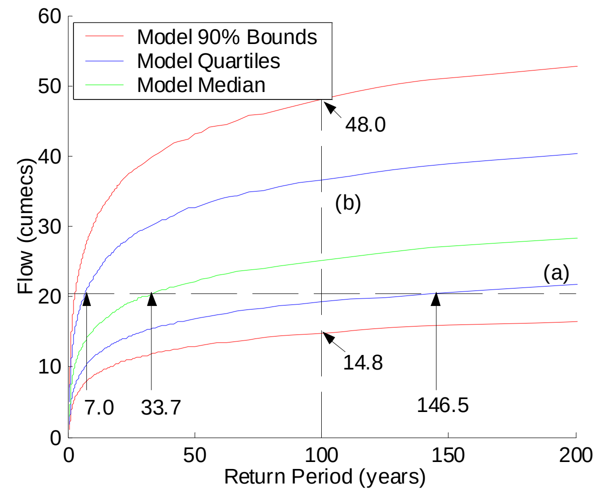

Figure 7.4: Detail of Modelled Discharge: Return Period Relation. Dashed lines show (a) Discharge associated with 2001 flood, with return period estimated from median and quartiles and (b)Discharge associated with 100-year flood.

The results demonstrate the high level of uncertainty associated with predictions made using the simulated rainfall series and rainfall-runoff model. As an example of this, consider a typical measure of susceptibility to flooding, the 100-year flood. A flood at this return period should be well-estimated by a 1000-year discharge record (Section 7.1.2.1). The confidence interval at a 90% level gives the possible range of discharge as 14.8 - 48.0 m^3s^{-1} (illustrated in Figure 7.4). The number of properties flooded by an event at the lower end of this range would probably fall in single figures; at the upper end of the interval widespread damage would be expected. In a similar vein, uncertainty in estimation of return period associated within a given discharge may also be considered. The estimated discharge of the October 2001 flood, 20.5 m^3s^{-1}, is also marked on Figure 7.4. In this case the return period associated with the event varies from 7 years to 146 years between the upper and lower quartiles (the return period estimated from the upper 90% bound was not captured within the 1000 series duration). The effects of the wide confidence intervals in turn impact on the cost-benefit ratio associated with any flood protection works, as is explored more fully in the following section using the floodplain hydraulic model to simulate inundation patterns.

7.2.4.2 Forming the Hydrograph: Flow-Discharge Relationship

As detailed in Section 7.2.2.3, a figure for the peak flow during a flood event is insufficient to create an input hydrograph for the floodplain inundation model, and therefore such hydrographs cannot be produced directly from the flood frequency analysis carried out in the previous section. In order to solve this problem, each annual flow maximum in the database was saved along with the time at which the discharge exceeded 3.5 m^3s^{-1} both before and after each flood peak. This allows the approximate recreation of hydrograph shape and volume for each event.

For each return period, a cumulative distribution of peak flow was produced. A flood hydrograph would typically be required for a given percentage point of this distribution. The simplest approach would be to run the floodplain model using a steady-state simulation based on this peak discharge. However, this was not felt to be a suitable approximation in this application (see Section 7.2.2.3). Another possible approach would be to find the recorded storm with peak discharge closest to this percentage point, and use the hydrograph reconstructed from the data on this storm. However, this might not produce a representative result if that particular storm had an unusual flow:volume relationship. Instead, an investigation was made into the reliability of using a generalised flow:volume relationship. To do this, the volume of each storm was calculated and this was graphed against the peak flow value. The assumption is made that the relationship follows a power law (this would be the case if hydrographs scale across the range of peak discharges such that they can be approximated as similar triangles). The results are shown below in Figure 7.5, plotted on a log-log scale, together with the best-fit regression relationship.

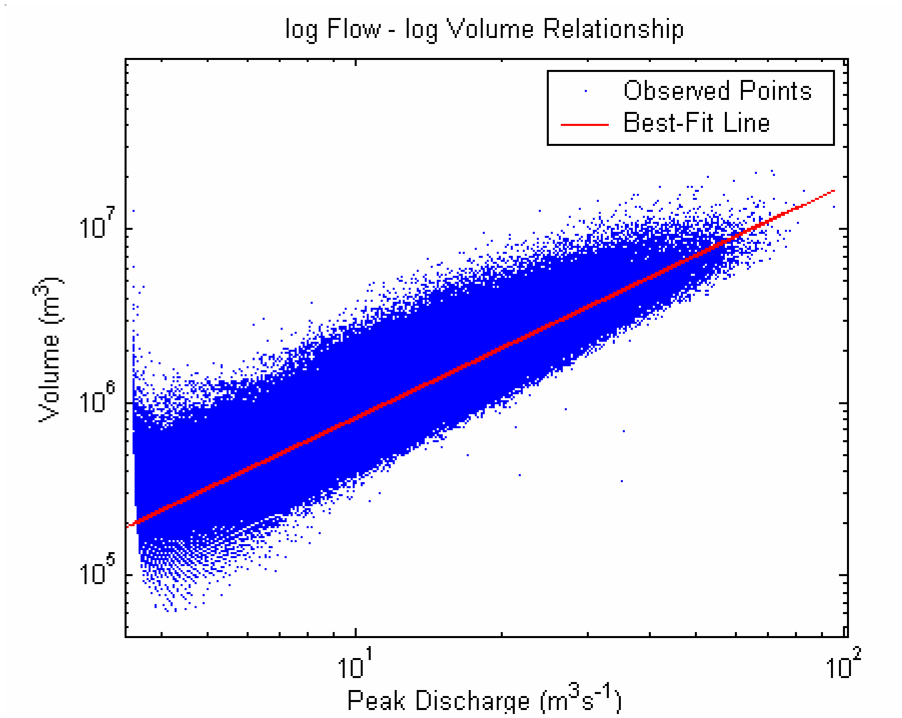

Figure 7.5: Peak Flow - Volume Relationship

Figure 7.5 shows a well-defined relationship between flow and volume, with a regression line defined by the following equation:

$$\text{Volume} = 36720 * \text{Flow}^{1.35}$$

Equation 7.1: Regression Relationship between Peak Flow (m^3s^{-1}) and Volume (m^3)

The strong correlation between flow and volume (correlation coefficient 0.90) justifies the use of a standardised hydrograph based on peak value. For each simulation, the peak value was identified, and Equation 7.1 used to predict the volume. The percentage of the hydrograph volume lying before and after the peak value was felt to be of less importance in controlling inundation extent than the total overbank volume. The median percentages of 23% before peak and 77% after peak were therefore used as a simple approximation. From this information the simplified input hydrograph relating to the peak value can be created ready for input into the inundation model.

7.2.4.3 Creation of Design Hydrographs

Following the approach described above, design hydrographs were derived for the range of return periods shown in Table 7.1. For each return period, hydrographs were produced with peak discharge at the median prediction and at the 5% and 95% points of the cumulative distribution.

Return Period (Years)	Cumulative Distribution Point (%)	Peak Discharge (m^3s^{-1})	Volume (m^3)	Time to Peak (Hours)	Time after Peak (Hours)
10	5	8.6	672000	1.0	33.4
	50	15.2	1450000	12.2	40.8
	95	30.0	3631000	15.5	51.8
50	5	13.0	1174000	11.5	38.6
	50	22.2	2418000	13.9	46.6
	95	43.1	5923000	17.6	58.8
100	5	14.8	1399000	12.1	40.4
	50	25.1	2854000	14.5	48.6
	95	48.0	6949000	18.2	61.0
500	5	19.0	1960000	13.2	44.1
	50	32.1	3979000	15.8	53.0
	95	58.8	9008000	20.0	65.5
1000	5	20.8	2215000	13.6	45.6
	50	35.5	4558000	16.4	54.9
	95	64.7	10249000	20.2	67.8

Table 7.1: Specifications for Design Hydrographs

The parameters may then be used to produce graphical representations of the hydrographs (Figure 7.6).

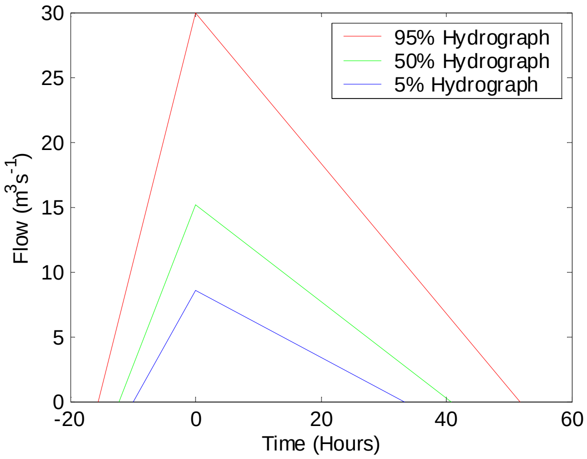

(a) 10 Year Return Period

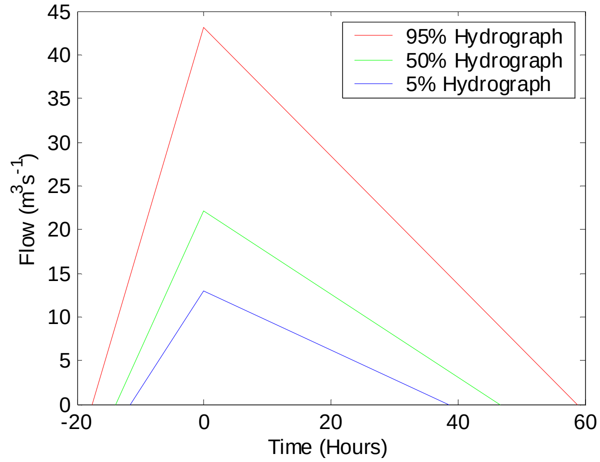

(a) 50 Year Return Period

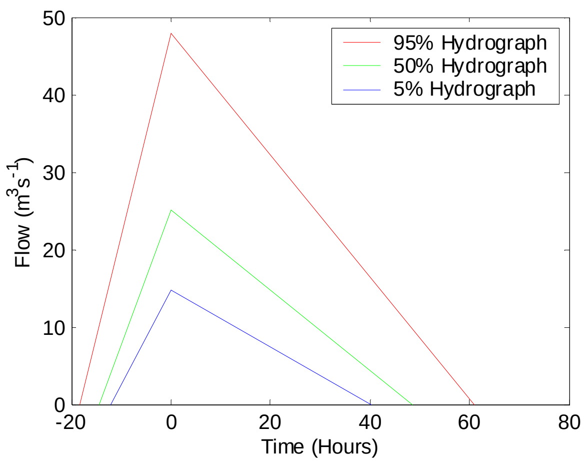

(a) 100 Year Return Period

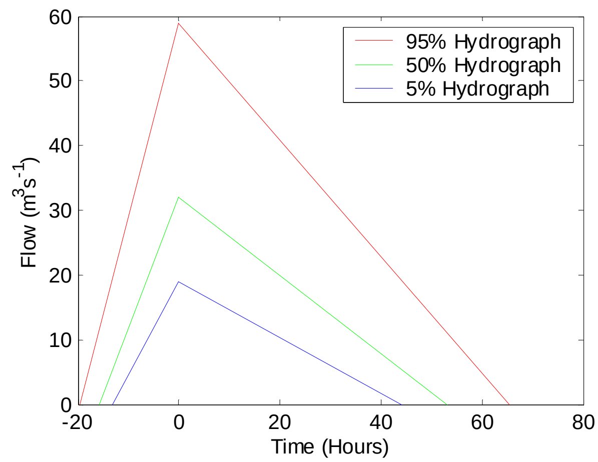

(a) 500 Year Return Period

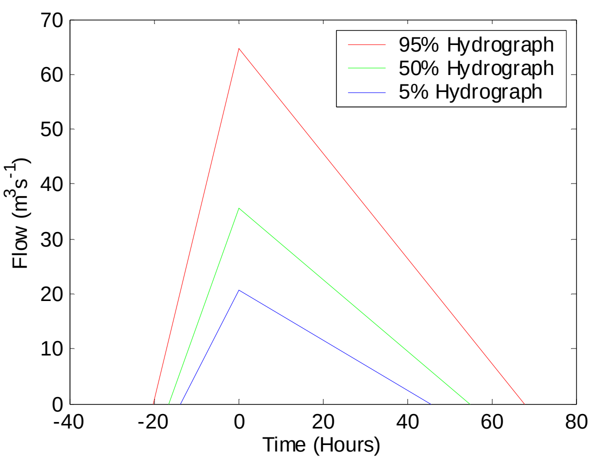

(a) 1000 Year Return Period

Figure 7.6: Design Hydrographs for each return period, at the 5%, 50% and 95% points of the cumulative distributions.

7.2.5 Inundation Extent and Depth Estimation Results

7.2.5.1 Inundation Extent of Design Events

The design hydrographs shown in the previous section (7.2.4.3) give discharge series for the gauging station at Linton, upstream of the town centre. The hydrographs were used to form the upstream boundary condition for the hydraulic model. Following the model evaluation presented in Chapter 6, the floodplain code was implemented at 10 m resolution using the sub-grid porosity treatment for maximum computational efficiency. The channel friction coefficient (Manning's n) was set at 0.05 $m^{-1/3}s$, which gave optimal performance in the multi-criteria validation for the 2001 flood event. For the reasons given in Section 7.2.2.3, uncertainty in value of channel friction is not considered at this stage. For a simple sensitivity analysis relating to this parameter, refer to Section 7.3.3.

For each of the 5 return periods (10 year, 50 year, 100 year, 500 year, 1000 year) the hydraulic model was used to produce an inundation simulation relating to the design hydrographs for the 5%, 50% and 95% points of the distribution of peak discharge magnitudes. The results are shown in Figure 7.7.

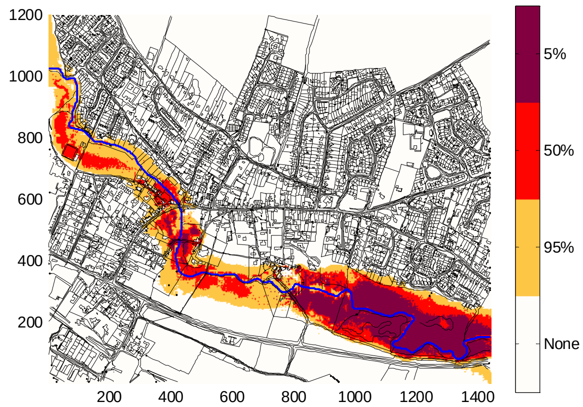

(a) *10-Year Return Period*

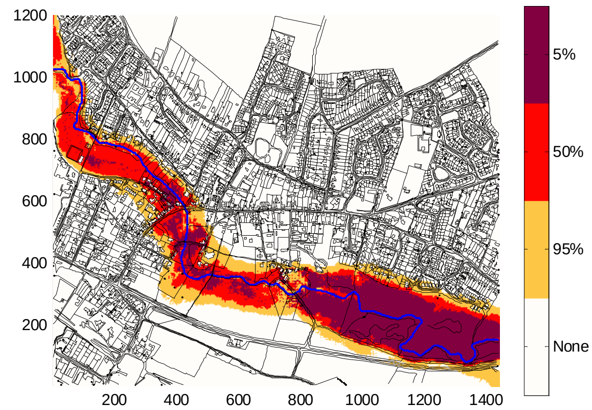

b) 50-Year Return Period

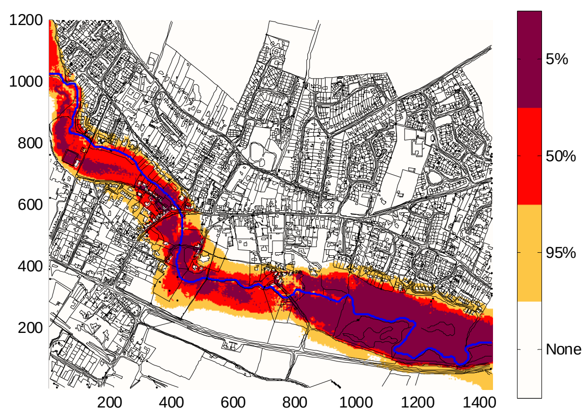

c) 100-Year Return Period

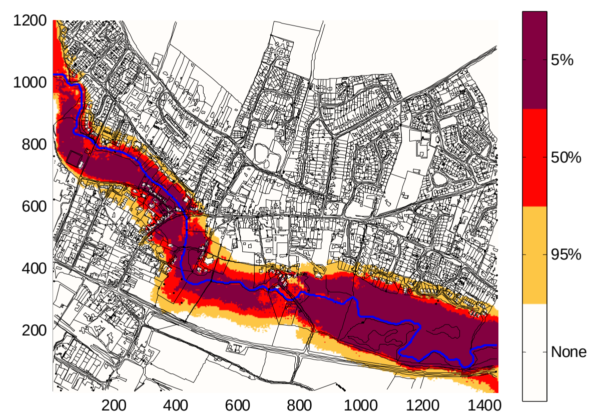

d) 500-Year Return Period

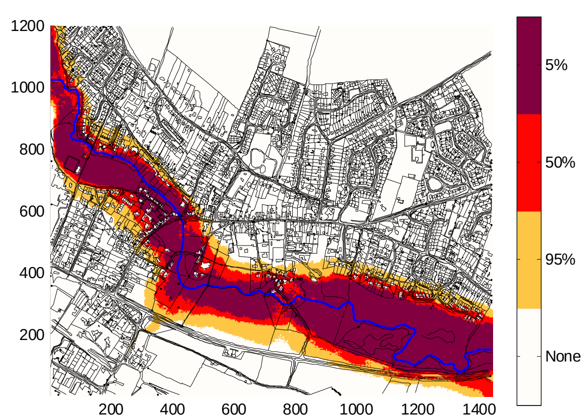

e) 1000-Year Return Period

Figure 7.7: Areas of Predicted Inundation at the 5%, 50% and 95% points of the cumulative distribution of peak discharge magnitudes

7.2.5.2 Communication of Results

The spatial pattern of inundation extent evident in Figure 7.7 is ultimately constrained by the valley morphology, so that despite large differences in the peak discharges of the extreme return periods, the maximal inundation envelope remains comparatively consistent. This is due to relatively steep topography at the natural boundaries of the floodplain which serves to constrain flood waters. However, it is also at this boundary that accuracy in prediction becomes more critical, as beyond the edge of the floodplain, density of housing increases dramatically. On the floodplain itself, there are few buildings, as waterlogged land and frequent flooding have constrained construction (Section 3.2.1.2).

The preceding paragraph usefully illustrates the importance of presenting results in a method sensitive to the intended use. The mapped inundation extents of Figure 7.7 would be useful for strategic and emergency planning at the local scale, for example to inform decisions on flood defence works or to prepare emergency evacuation and traffic routing plans. Information in a similar style from a deterministic forecast at return periods of 100 and 1000 years is presented online by the Environment Agency (Environment Agency, 2006) for public use and aimed particularly at homeowners (although the EA map is static and therefore does not allow the simulation of wetting up patterns which may be useful for emergency planning). However, for more specific applications such as a benefit-cost analysis for a structural flood defence scheme, statistics drawn from the inundation mapping would present the important trends more clearly. Figure 7.8 gives an example, plotting the number of houses flooded at each return period. The analysis for the figure counted a house as ‘flooded’ if flood water reached its perimeter at any point, and at any depth. It would be possible to tailor the analysis further, for example, counting only houses flooded to a depth at which it was no longer considered reasonable that they be protected by the use of sandbags or removable flood gates. The same analysis could also be used to recommend raised floor levels.

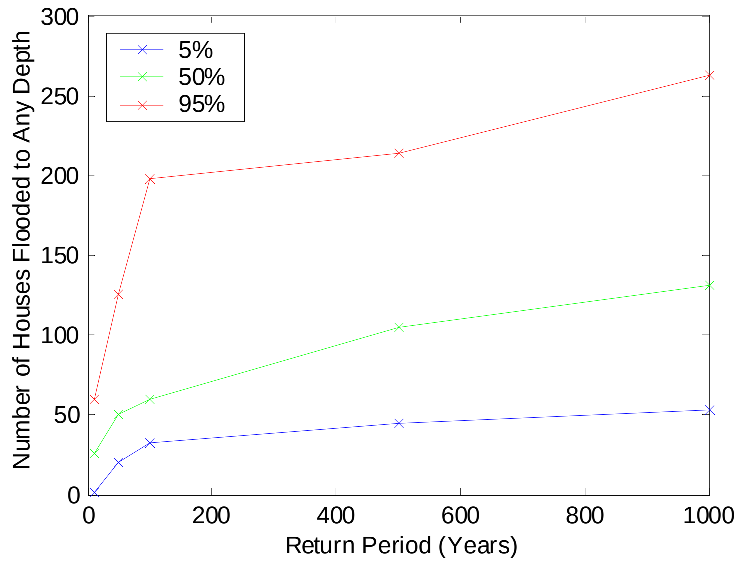

Figure 7.8: Number of houses flooded (to any depth) as a function of return period and point of peak discharge distribution

Figure 7.8 demonstrates a sharp rise in the number of properties flooded between the 10-year, 50-year and 100-year events; there is then a smaller increase up to the 500-year and 1000-year events. This type of analysis could be used to suggest a threshold return period beyond which the expenditure involved in containing the Granta would not be realised in terms of damage saving. In order to do this more fully, a worthwhile extension of the current work would be to link the properties in the area to a valuation, perhaps through zoning by postcode, in order to estimate the financial cost of each flood event. However, care should be taken not to discriminate against residents living in lower-cost accommodation when using this method, as noted in Section 1.2.3.2.

Another possible example of the use of inundation maps is to calculate the area flooded by each simulated event. This variable, as with the previous example of number of houses inundated, would be used directly within the DEFRA scoring system for capital works planning (DEFRA, 2002; see also Sections 1.3.2.2, 1.3.3). The results of such an analysis are shown in Figure 7.9. The analysis would be valuable in estimating the damage done to agricultural land (Section 1.2.4.3), and could be extended to examine the duration of inundation if appropriate. As previously, increase in flooded area is rapid up to the 100-year return period, less so for higher return periods.

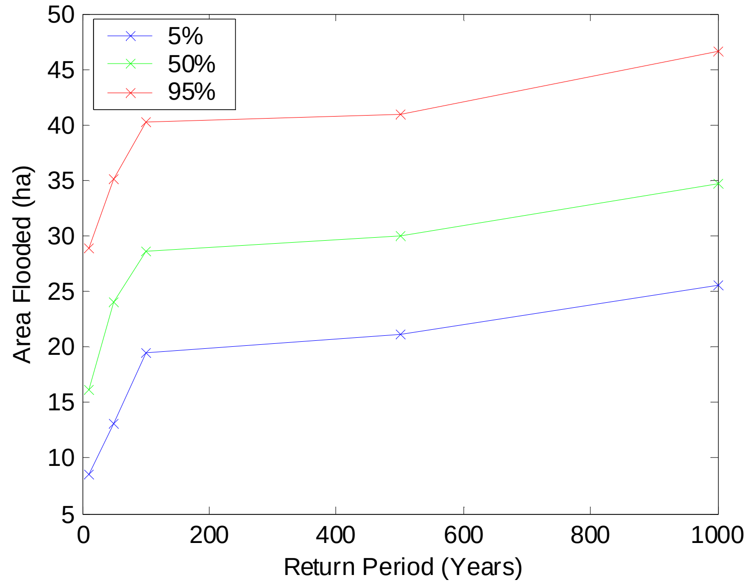

Figure 7.9: Area of land flooded (to any depth) as a function of return period and point of peak discharge distribution

7.2.5.3 Inundation Depth Results

In addition to maps of inundation extent, the simulations provide information on inundation depths and dynamic pattern of flood routing. Figure 7.10 gives an example of such output, showing the results from the 100-year event in more detail. The evolution of the flood is shown for the 5%, 50% and 95% points of the confidence interval, at 4-hour time intervals.

As highlighted in Section 1.2.4.3, depth mapping can be extremely useful in order to aid identification of areas of high risk to life and greater damage to property. Median expected depth of flooding, together with confidence bounds, may also be produced on a property-by-property basis for any given return period, allowing owners to choose the most appropriate flood protection measures.

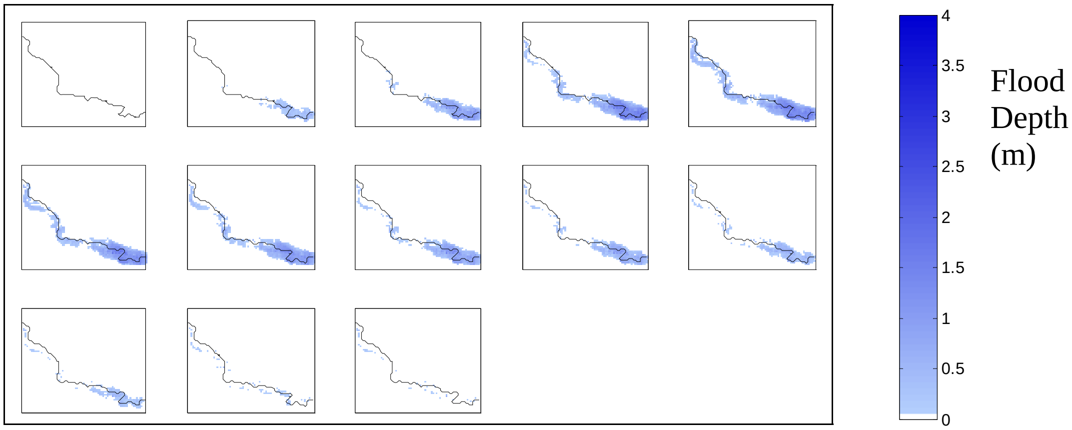

(a) Discharge Magnitude from 5% Lower Bound

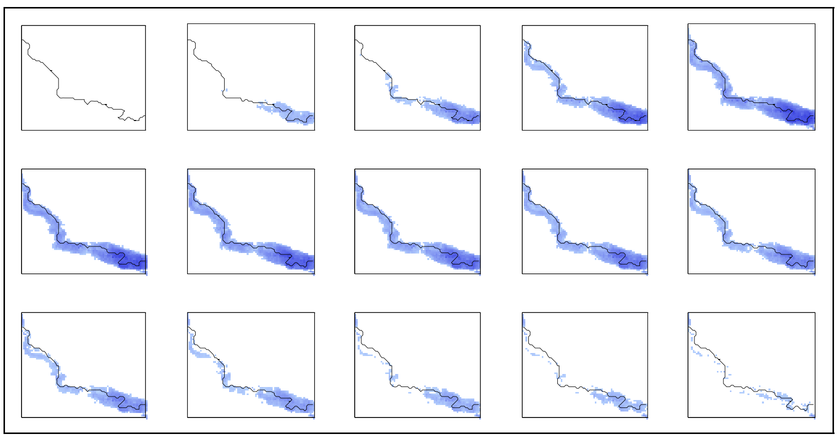

(b) Discharge Magnitude from 50% Median Point

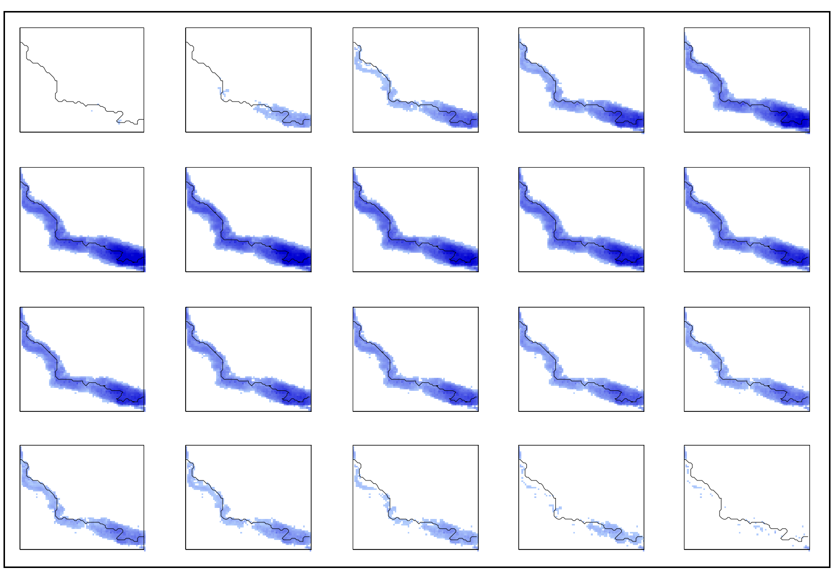

(c) Discharge Magnitude from 95% Upper Bound

Figure 7.10: Inundation Simulations at 4-hour intervals, using hydrographs based on the 5%, 50% and 95% points of the discharge magnitude distribution

7.3 Constraining Uncertainty in End-to-End Modelling

7.3.1 Constraining Uncertainty in Discharge

Given the wide confidence interval associated with discharge prediction, meaning that any estimate of flood peak magnitudes is associated with a high degree of uncertainty, it is important to improve understanding of the reasons that this uncertainty exists. Quantifying the uncertainty and analysing its provenance offers the scope to determine the main sources of uncertainty, and identify means of uncertainty reduction through refinement of model structure, parameterisation or boundary condition specification.

7.3.1.1 Effects of Uncertainty in Rainfall Series

Part of the uncertainty associated with high return period discharge estimation comes from the stochasticity of precipitation patterns that ultimately force the model chain. The combined rainfall and rainfall-runoff simulation accounted for this uncertainty by using an ensemble of 1000 individual climate scenarios. However, to consider the possible reduction in uncertainty that would be possible if improved knowledge of future rainfall behaviour was available, consider the extreme case where the full 1000-year series is known exactly. This can be simulated by selecting a single random series that is assumed to be 'correct' and re-running the Monte Carlo simulations using each of the possible rainfall-runoff model parameter sets as before, but all with the single rainfall series. The results are shown below in Figures 7.11 and 7.12, in the same format as the previous results.

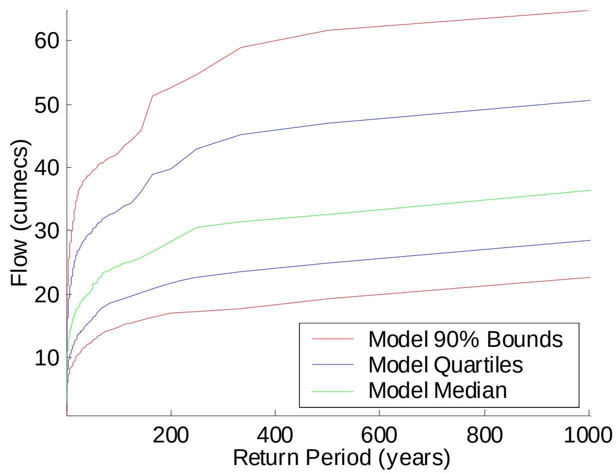

Figure 7.11: Modelled Discharge: Return Period Relation using single rainfall series

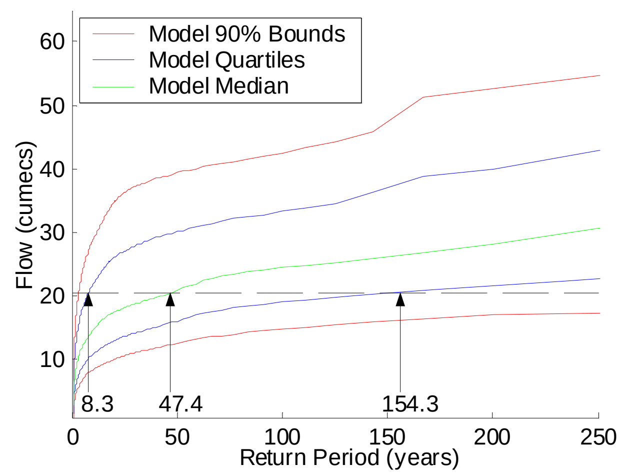

Figure 7.12: Detail of Modelled Discharge: Return Period Relation. Dashed line shows discharge associated with 2001 flood, with return period estimated from median and quartiles.

The return period-flow curves are, on first inspection, very similar to those using different rainfall series for each simulation. The curves are not as smooth, representing the increased dependence of the results on model response to particular rainfall events. Figure 7.12 shows a detail of the relationship for return periods of up to 250 years, and the return periods associated with the 2001 flood are marked as previously. The discharge of the 100-year event is slightly more constrained, the range between the 90% confidence bounds being reduced from [14.8, 48.0] to [14.8, 42.4]. The range of return periods between the first and third quartiles is very similar to that of the previous application; however there is a shift towards higher values signifying typically lower flood peak predictions in each simulation.

These results indicate that reducing the uncertainty in the rainfall series has only a small impact on the long term discharge prediction; similar variability is found within the response of models with different parameter sets but a single rainfall series as with multiple rainfall series. However, the estimate of particular quantities such as the return period associated with a particular discharge may be altered by a significant margin, e.g. the 2001 flood is estimated as having a return period of 47.4 years instead of 33.7. Hence improved information on rainfall patterns is predicted to improve accuracy but have only a minor affect on precision in discharge estimates. The limited effect of uncertainty in precipitation patterns however ultimately reflects the derivation of the rainfall model from a single 15-year gauged record. A longer rainfall series might contain implicit non-stationarity that exerts a significant control on discharge response: this question is discussed further in Section 8.3.2.

7.3.1.2 Effects of Uncertainty in Rainfall-Runoff Model

The above results suggested that the most significant source of uncertainty in the discharge prediction is in the parameterisation of the rainfall-runoff model. In order to test this, the suite of model simulations were rerun, using the same set of rainfall series as in the original experiment, but instead of using each of the behavioural rainfall-runoff parameter sets only that set with the optimal value of the performance measure was used. This mimics the situation where there is no uncertainty in the rainfall-runoff model parameterisation. The results are shown below in Figures 7.13 and 7.14.

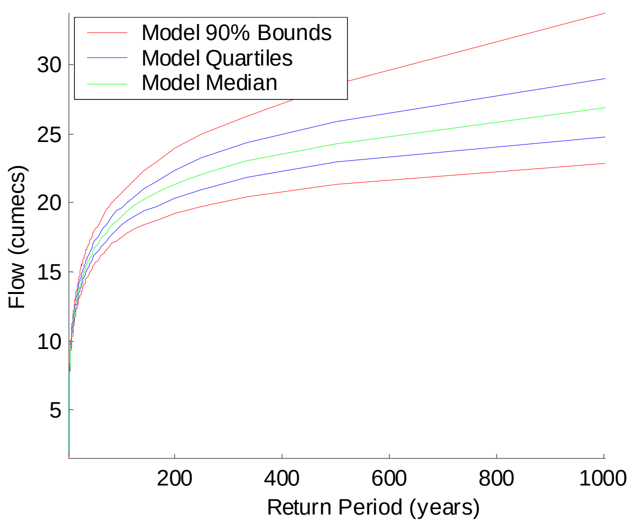

Figure 7.13: Modelled Discharge: Return Period Relation using optimum model parameter set

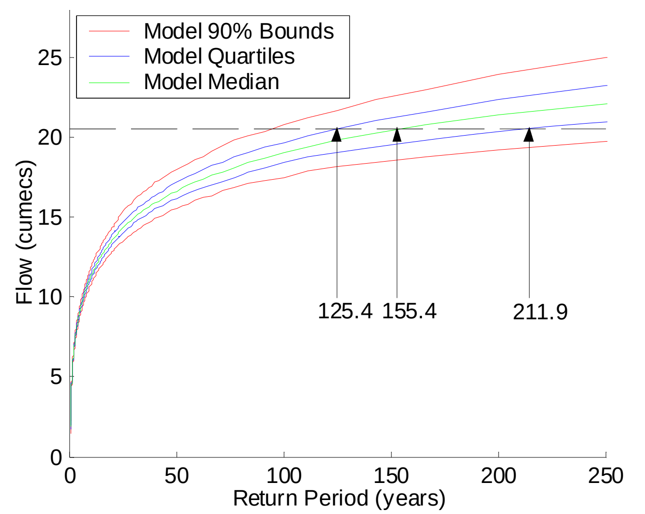

Figure 7.14: Detail of Modelled Discharge: Return Period Relation. Dashed line shows discharge associated with 2001 flood, with return period estimated from median and quartiles.

The graphs show that, as predicted, improved knowledge of the rainfall-runoff model parameters has the potential to greatly reduce the uncertainty associated with discharge estimates. The 90% confidence interval for the peak discharge of the 100-year flood has been constrained from [14.8, 48.0] to [17.5, 20.8] m^3s^{-1}. These narrower prediction bounds would be a significant advantage for any planning of flood defence works.

However, while this analysis shows the great benefits that would be associated with exact knowledge of rainfall-runoff model parameters, it must not be confused with the results of using a single set of parameters without the observed data and model structural knowledge required to justify this decision. Figures 7.13 and 7.14 show results using only the optimal parameter set as specified by comparison with the observed data. However, many of the alternative parameter sets used in the complete analysis showed an R^2 value within 0.01 of this optimum, and all were within 0.08, giving little reason to suppose that one set should be accepted against the rejection of all others. By using the single optimum set, the possibility of flow values within the wider confidence bounds has therefore been discounted without good supporting evidence. This may have particularly damaging consequences for flood risk assessments as the confidence limits fall at the lower end of the range of the wider bounds; the optimum set does not necessarily give values bracketing the median of the complete uncertainty analysis. These results show the potential problems of using an analysis without uncertainty estimation such as the model constructed for the Environment Agency (Section 3.5) which bases its conclusions on a single realisation of the flow associated with a given return period.

7.3.1.3 Uncertainty in Behavioural Threshold

Another source of uncertainty in the distributions of peak discharge prediction, also associated with the parameterisation of the rainfall-runoff model, is the threshold performance value above which models are deemed to be behavioural. Only parameter sets meeting this criterion are included in the analysis, however there is little physical basis for the choice of threshold which is made instead through operational reasoning and has therefore been seen as a weakness in the calibration methodology (Section 5.4.2.4). The threshold used in the preceding analysis was to require a mean R^2 value greater than 0.6 when the model simulations were compared with the observed levels for each winter season (Section 7.1.4.1). To test the effect of threshold choice on discharge prediction, this value was reduced to 0.5 and the procedure re-run. The updated discharge prediction results are shown in Figures 7.15 and 7.16.

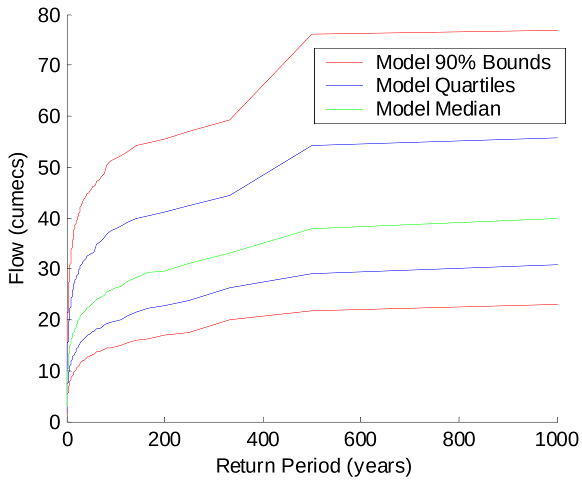

Figure 7.15: Modelled Discharge: Return Period Relation using behavioural threshold of 0.5

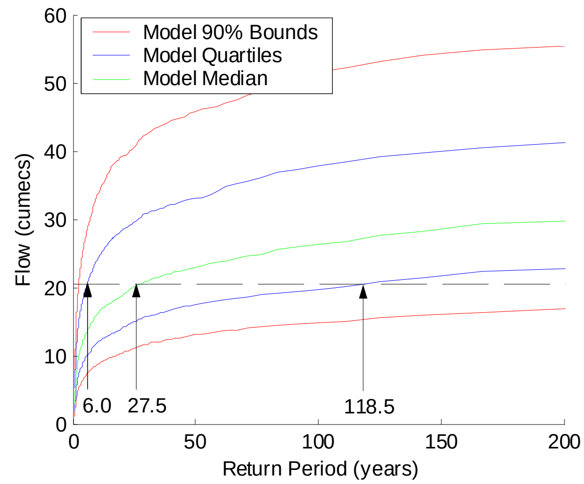

Figure 7.16: Detail of Modelled Discharge: Return Period Relation. Dashed line shows discharge associated with 2001 flood, with return period estimated from median and quartiles.

The results show a relatively small change in the discharge predictions at low return periods: the 90% confidence interval for the peak discharge of the 100-year flood has been widened from [14.8, 48.0] to [14.7, 51.6] m^3s^{-1}. At higher return periods the difference is more pronounced: the 90% confidence interval for the peak discharge of the 1000-year flood has been widened from [20.8, 64.7] to [23.1, 76.9] m^3s^{-1}. As expected, the less rigorous performance criterion has caused models with more disparate behaviour to be classed as behavioural and the range of simulation results has increased accordingly.

7.3.2 Propagating Uncertainty through Inundation Simulations

The preceding section analysed the relative effects of uncertainty in the rainfall input and rainfall-runoff model parameters, and also considered the influence of the behavioural threshold used to parse the ensemble simulations. In order to understand how such changes in discharge prediction distributions would affect inundation predictions in the coupled model structure, the uncertainty was propagated through the hydraulic model. As before, the peak discharge values were used to create triangular input hydrographs to form the upstream boundary condition for the floodplain inundation model. In this case, the 100-year event only was considered, as a standard for comparison between the different distributions. The hydrograph parameters are shown in Table 7.2.

Distribution Information	Cumulative Distribution Point (%)	Peak Discharge (m^3s^{-1})	Volume (m^3)	Time to Peak (Hours)	Time after Peak (Hours)
Single Rainfall Series	5	14.8	1395600	12.0	40.3
	50	24.5	2756000	14.4	48.1
	95	42.4	5778900	17.4	58.3
Single set of Rainfall-Runoff model Parameters	5	17.5	1749900	12.8	42.8
	50	19.0	1955300	13.1	44.0
	95	20.8	2209500	13.6	45.4
Behavioural Threshold at $r^2 = 0.5$	5	14.7	1382900	12.0	40.2
	50	26.3	3032800	14.7	49.3
	95	51.6	7533200	18.7	62.5

Table 7.2: Parameters for 100-Year Hydrographs Using Altered Discharge Distributions

The inundation pattern associated with each of these hydrographs was simulated using the hydraulic model. The patterns of inundation forecasts are shown in Figure 7.17. The plots of inundated area translate the effect of changing the uncertainty bounds into the consequences for flood extent:

- Plot (a) shows the original analysis of the 100-year flood, repeated for comparison with the other methods.

- Plot (b) shows the significant reduction in uncertainty of flood boundary position possible if the rainfall-runoff model parameters could be defined exactly. Although this is unlikely due to equifinality in parameter sets, caused by model structural deficiencies and limited calibration data, it reinforces the suggestion that significant benefits could be achieved by further work to reduce the number of models considered behavioural.

- Plot (c) shows the small reduction in uncertainty achievable if the future rainfall patterns were known exactly, however the relatively minor impact compared with that of Plot (b) suggests that improvements in rainfall-runoff modelling should take precedence over improvements in rainfall characterisation.

- Plot (d) shows the impact of changing the threshold value for model acceptance; this change has a relatively small effect on inundation extent at the 5% and 50% points of the discharge distribution, however at the upper 95% point the additional encroachment of the flood into the urbanised area suggests that many more households could be affected by flood waters if this additional uncertainty in the rainfall-runoff model parameterisation is considered valid.

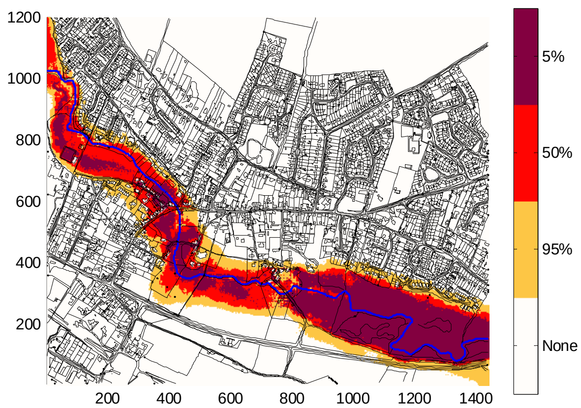

a) Original Analysis Repeated for Comparison

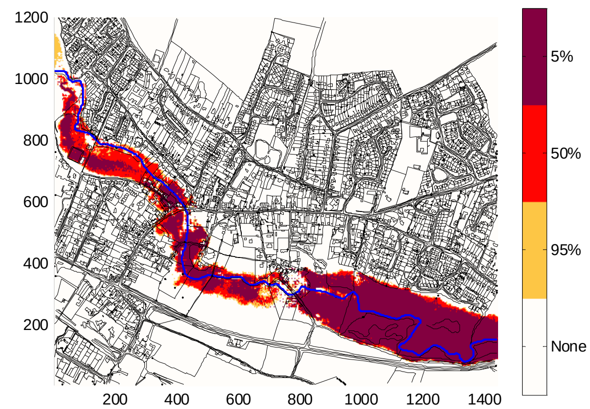

b) Single Set of Rainfall-Runoff Model Parameters

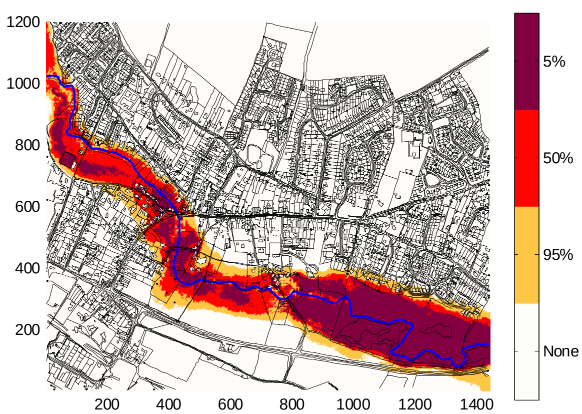

c) Single Rainfall Series

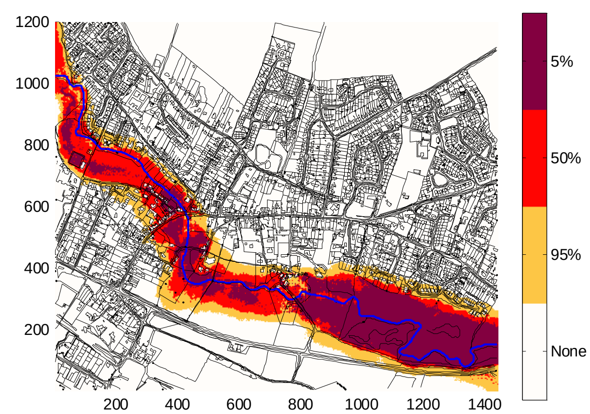

d) Behavioural Threshold at $r^2 = 0.5$

Figure 7.17: Areas of Predicted Inundation at the 5%, 50% and 95% points of the cumulative distribution of peak discharge magnitudes for the 100-year flood, using four alternative methods to calculate uncertainty bounds

7.3.3 Sensitivity to Inundation Model Parameterisation

As discussed in Section 7.2.2.3, the uncertainty analysis carried out in the preceding sections did not include consideration of uncertainty in the channel friction parameter used to calibrate the floodplain inundation model. Although computational restraints prevented such analysis under the framework of GLUE, it was felt to be important to gauge the comparative sensitivity of this parameter. Therefore a decoupled 'sensitivity analysis' procedure was undertaken to compare the scale of uncertainty associated with the channel friction parameter compared to those of the rainfall and rainfall-runoff model parameters.

For each return period, the 50% (median) hydrograph was routed through the floodplain using channel friction coefficients of 0.04 and 0.06 $m^{-1/3}s$, chosen to surround the previously selected optimum of 0.05 $m^{-1/3}s$ which represented a single, global maximum in the validation statistic response space. More extreme values were thought less likely to produce behavioural simulations; for example, validation scores were depressed for values below 0.04 $m^{-1/3}s$. Using the 100-year flood as a standard for comparison as before, the relative effects of the uncertainty sources on the flood envelope may be compared (Figure 7.18). It is observed that varying the friction parameter value within the specified range has a relatively small effect relative to the uncertainty sources previously considered. It is particularly noticeable that predictions using $n = 0.05$ $m^{-1/3}s$ and $n = 0.06$ $m^{-1/3}s$ give very similar flood outlines: this is consistent with the correspondingly close values of the combined validation statistic (Table 7.3).

Channel Friction ($m^{-1/3}s$)	Validation Statistic Value
0.04	0.705
0.05	0.766
0.06	0.732

Table 7.3: Combined validation statistic: variation with channel friction parameter value

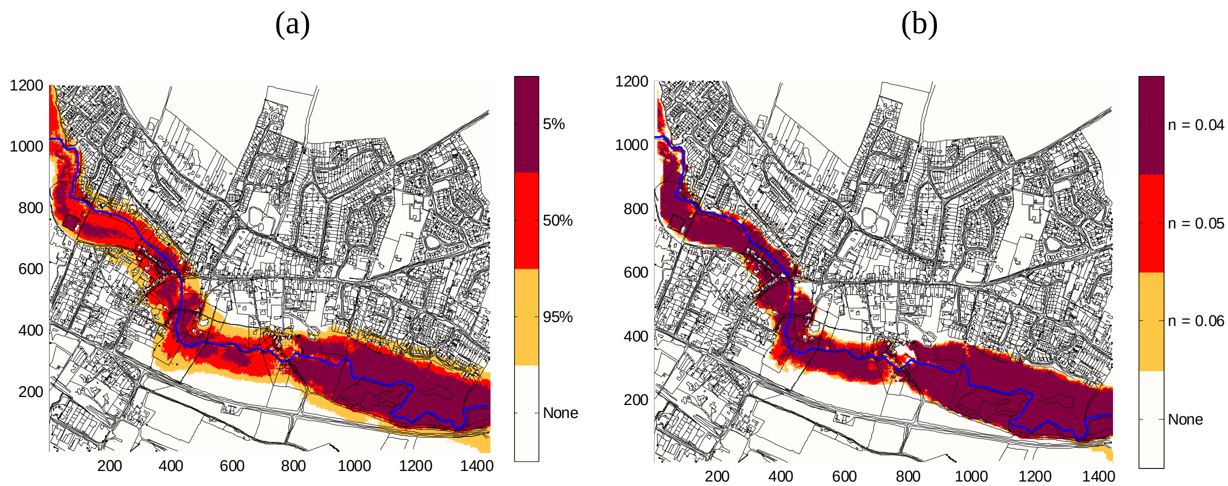

Figure 7.18: Variation in inundation envelope: Comparison of (a) Uncertainty in rainfall and rainfall-runoff model parameters and (b) Uncertainty associated with floodplain model channel friction parameter

In addition to mapping the flood envelope, the uncertainty may also be quantified in terms of number of houses flooded, as in Section 7.2.5.2. To visualise the relative uncertainties, the variation associated with a channel friction parameter in the range 0.04 – 0.06 $m^{-1/3}s$ was plotted as an error bar, superimposed on the graph showing previous uncertainty error bounds (Figure 7.19).

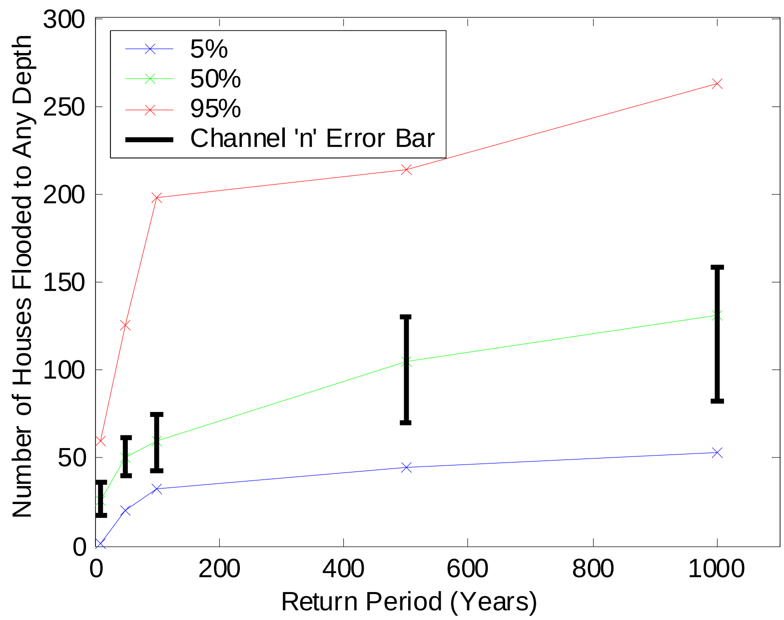

Figure 7.19: Uncertainty associated with variation in channel friction parameter in the range 0.04 – 0.06 $m^{-1/3}s$, compared with previous uncertainty bounds.

This graph again suggests that the effects of uncertainty in the channel friction parameter are of a smaller magnitude than those of uncertainty in the rainfall and rainfall-runoff model parameters. As with other uncertainty sources, the sensitivity increases with return period as marginal changes in the flood envelope become more significant in dense areas of housing. It should however be understood that a simplistic analysis of this kind cannot represent the nonlinear effects of uncertainty propagation through the model chain, and hence provides only a guide as to the likely effect of uncertainty on model results in a full application of the GLUE procedure to the coupled model system.

7.4 Discussion

The above analysis shows the results of propagating uncertainty through coupled rainfall, rainfall-runoff and floodplain inundation models. A number of key findings are made. First, extending the flood frequency analysis to include inundation simulations based on discharge magnitude estimates offers the opportunity to explore the relationships between discharge, inundation extent and depth, and likely damage to infrastructure and buildings. This emphasises the importance of including a hydraulic model in the chain of coupled models. This is especially relevant in the light of the recent trend away from structural flood defences and towards a greater reliance on integrated catchment management approaches (Section 1.3.2.2). While peak discharge measurements were sufficient for schemes which aimed to increase conveyance capacity to ensure that river flows remained in-bank, modern solutions instead aim to manage a 'functional floodplain'; using natural defences to attenuate flood peaks. The need for model results which simulate flow paths over the floodplain has therefore become a practical imperative.

An important aspect of the modelling procedure is the rejection of the principle of using single deterministic forecasts, replacing these with results in the form of distribution quantiles. To aid visualisation, these were presented using a confidence interval for predictions of inundation extent, with the median forecast also shown. The aim is to allow an intuitive interpretation of the effects of uncertainty on flood forecasts. Maps showing the confidence intervals allow an assessment of which areas of the floodplain are most sensitive to uncertainty in discharge predictions due to channel shape and local topography. The effects of uncertainty on inundation boundaries at different return periods can also be examined; at low return periods (10 – 50 years) boundaries are highly uncertain as small changes in water depths may create large differences in inundation extent as water spreads across shallow gradients of the floodplain. At return periods of 100 – 500 years the boundaries become more constrained by steepening topography at the natural edge of the floodplain, however at very high return periods (1000 years or greater) the uncertainty may increase again as water spreads across the shallower topography of the urban area.

The inclusion of uncertainty estimates in a flood frequency analysis is still a relatively rare occurrence outside academic research. This is demonstrated by the recent Standards of Protection Assessment commissioned by the Environment Agency for the River Granta, and summarised in Section 3.5, which uses a deterministic forecast. Section 7.3, however, demonstrates the narrowing of prediction bounds caused by the use of a single set of rainfall-runoff model parameters, even where uncertainty in rainfall patterns is still included in the analysis. Where insufficiency of validation data gives rise to equifinality in model calibration, this represents an unjustified suggestion of certainty in model results and may not correspond to the median prediction from a full uncertainty analysis thus giving biased estimates of flood risk. The results therefore suggest that it would be highly beneficial to catchment management agencies and to the general public that flood risk assessments should include analysis of uncertainty in predictions, and that such uncertainty should be communicated to the user. Although traditionally such an analysis might have been considered too complex to be conveyed effectively, it is becoming increasingly common to see probabilistic forecasts in the realm of weather prediction (e.g. Metcheck, 2006; Meteo France, 2006) and there is an expectation of greater customer demand in the future (Met Office, 2004). It is therefore reasonable to suggest that provision of uncertainty information should be extended to flood risk assessments.

A wider reporting of the effects of uncertainty on model predictions may also provide an impetus for further data collection in order to constrain uncertainty. By emphasising that observed floods may fall within wide prediction bounds rather than the more simplistic interpretation that the deterministic model is ‘wrong’, it becomes more obvious how additional data could aid future predictions. This is demonstrated in Section 7.3, which considers the effect of uncertainty from different sources on the confidence bounds. The results show that the major cause of uncertainty is equifinality in rainfall-runoff model parameterisation, and therefore suggests that future effort might best be directed at reducing the range of behaviour associated with the set of behavioural models. This could be achieved by constraining the parameters of the current model, for example by investing in a telemetered rain gauge closer to the subject site or a flow gauge that did not wash out at high discharge levels. Alternatively, a different model structure could be chosen which would enable the incorporation of internal state data such as water table levels at different points in the catchment, if funding were available to collect this data. The interrelations between model component complexity, sensitivity and magnitude of uncertainty are explored further in Section 8.3.2.

It is hoped that in the future this methodology could be extended to include uncertainty in hydraulic model parameterisation as part of the full GLUE application. The decoupled sensitivity analysis suggested that uncertainty in the Manning channel roughness coefficient was of smaller magnitude than that associated with the rainfall-runoff model. This conflicts with the findings of Hall et al. (2005), who found uncertainty in channel friction to be the factor with the greatest effect on predictions. Their study did however assume a relatively small uncertainty in upstream flow condition (assumed to have a normal distribution with mean 73 m^3s^{-1} and standard deviation 4 m^3s^{-1}) which is appropriate for flows measured at a gauging station, but would not be the case in a coupled modelled application where input is derived from a statistical analysis of continuously simulated discharge. While it would not be practical to propagate predictions from each discharge series through the hydraulic model, a concept such as that of functional similarity (Pappenberger et al., 2005) might be used to reduce computational effort. It is however unlikely that uncertainty in hydraulic model parameters could be significantly reduced before a further flood event in the town allowed a more complete archive of inundation data to be collected.

7.5 Conclusion

This chapter presents a method for using continuous simulation within the context of a chain of coupled models, to produce a flood frequency analysis including flood risk mapping. This technique would be valuable in data poor catchments where flood risk predictions are required for strategic planning purposes, a situation which has become more common in recent years due to perceived increases in flood events in small lowland catchments. Such catchments do not typically have a history of flow gauging, but the continuous simulation method allows predictions of high return period floods to be made.

The method draws together the models described in the previous three chapters: a stochastic rainfall model (Chapter 4), a rainfall-runoff model incorporating parallel fast and slow pathways (Chapter 5) and a 2d raster floodplain inundation model (Chapter 6). The stochastic nature of the rainfall model and equifinality in rainfall-runoff model parameter sets led the concept of an optimum model to be rejected in favour of the use of a set of behavioural models weighted by performance score. Methods of propagating the uncertainty in model inputs and predictions through the model chain were therefore considered. The GLUE methodology was used to cascade full pdfs of parameter values through the rainfall and rainfall-runoff models; a reduced set of hydraulic model simulations were then carried out to maintain efficiency, an important consideration if it is to become more widely used in commercial flood risk assessment applications.

The results of the flood frequency analysis showed that, given the modelling choices above, the uncertainty present in the estimates of flood extent for events at return periods of 10, 50, 100, 500 and 1000 years was significant and led to relatively wide confidence intervals for the number of houses which could be affected. The current use of deterministic flood risk analyses by the Environment Agency was therefore suggested to be unduly restrictive. This view was backed up by a further investigation of the relative effects of uncertainty from different causes, which identified uncertainty in rainfall-runoff model parameterisation as the major contributing factor. Using only the single optimum rainfall-runoff model parameter set was found to give conservative estimates of flood extent which did not reflect the possible risks identified in the full analysis.

Chapter 8

CONCLUSIONS

8.1 Thesis Summary

8.1.1 A Modern View on Flood Risk Modelling and Assessment

Hydrology is a fast-moving science and flood modelling in particular is in a period of rapid change with the recent introduction of many new concepts. Revolutions in data availability and computational resources have opened new avenues of research and facilitated the creation and application of hitherto unsupportable model structures. The principle aim of this thesis was to integrate the best of these emerging techniques with new thinking on reduced complexity modelling methods and opportunities for model coupling in order to establish an efficient, rigorous and modern structure for flood risk assessment.

Flood risk assessment currently has a high public and political profile due to recent floods in the UK and Europe which have highlighted the wide-ranging consequences of flooding and played onto public fears of the possible effects of climate change. Support and funding opportunities for data collection and modelling to aid understanding of flood risk and provide new catchment management solutions are at a high; however there is often a struggle to bridge the gap between specialist techniques developed for a single part of the flood modelling process and those that are perceived as providing a complete solution suitable for practical application. It is crucial that individual techniques are seen in their wider context as it is then that their ability to improve scientific understanding of catchment behaviour and response to management strategies can be fully appreciated. Importantly, the effects of uncertainty on model response in terms of impacts on dependant model components can also be evaluated.

Wheater (2002) considered a similar problem, at a time in which present techniques were still in their early developmental stages. In the light of the progress then achieved, he identified the following as among the priority research challenges in fluvial flood modelling:

1. Development of a national capability for continuous hydrological simulation of ungauged catchments.
2. Improved representation of urban flooding.
3. Appropriate parameterisations for hydraulic simulation of in-channel and floodplain flows, assimilating available ground observations and remotely sensed data.
4. A flexible decision-support modelling framework, incorporating developments in computing, data availability, data assimilation and uncertainty analysis.

This thesis has presented a preliminary structure to achieve the last of these aims, by means of coupled model components developed using ideas suggested by the first three and seeking to include the expertise expressed in the latest hydrological model developments. The chapters of this thesis consider in turn linked sub-models representing rainfall regime, runoff production and routing, and floodplain hydraulics. These are then drawn together as part of a coherent structure in Chapter 7.

8.1.2 Case Study

In order to provide context for each component, the models are applied to a catchment of the River Granta in Cambridgeshire. The catchment typifies the conditions in which flood models are increasingly expected to perform but which do not necessarily correspond to the characteristics of well-studied, highly instrumented research catchments. After the Granta suffered a flood in October 2001, which caused significant damage to listed buildings in the centre of the town of Linton, strong public pressure was exerted on management authorities to provide an increased level of flood protection. In order to achieve this, a standard flood risk assessment was carried out by the Environment Agency, relying on well-established techniques of design event creation and 1d hydraulic modelling.

Using Linton as a case study, the benefits of using the latest remote sensing data together with modern techniques of coupled modelling are demonstrated, providing a more comprehensive and rigorous flood risk assessment than that previously possible. In particular, continuous simulation methodology provides reliable estimates of flood magnitudes at each required return period while high-resolution 2d floodplain inundation simulation allows detailed representation of flood progression through an urban area. This is done without compromising the requirement to produce a framework which can be parameterised using only that data widely available within the UK for catchments which had not previously been considered at high flood risk. The technique is therefore verified as suitable for widespread implementation.

8.2 Focus on Technique Improvements

8.2.1 Continuous Simulation

Although the concept of continuous simulation is not new, it has not previously been considered as a suitable method for integration into a system of coupled models to provide a flood risk assessment framework. Previous examples of its use have included proof that it can be used to reproduce annual maximum floods and forecast those of greater return period (Cameron *et al.,* 1999) but not assimilation into an 'End-to-End' modelling system. Recent studies which have succeeded in linking numerical weather prediction models, rainfall-runoff models and hydraulic models have been focused around reproduction of single events in order to prove the concept of cascading model chains (Pappenberger *et al.,* 2005). Such studies are often constrained by model run times and have therefore been restricted to a relatively small number of simulations. This thesis has demonstrated that by using rainfall and rainfall-runoff models which have a low computational overhead, continuous simulation can be used as a practical and valuable tool to provide estimation of extreme discharge events. The short run time of the rainfall-runoff model deployed also allowed investigation of the effects of uncertainty within a Monte Carlo framework (Section 7.2.3).

The advantages of using continuous simulation within a flood risk assessment framework are numerous. By considering the flow regime of the catchment as a continuous process, antecedent conditions are automatically accounted for in the rainfall-runoff model. A strong annual cycle in the storage parameter of the rainfall-runoff model which controls runoff production showed this to be of great importance in the Linton catchment, demonstrating the strong dependency of the catchment response on groundwater levels. This behaviour, typical of catchments throughout the chalklands of South-East England, could not be modelled effectively using an event-based approach. Continuous simulation also reduces the dependency of the model on traditional statistical methods of extreme event prediction. It allows the whole rainfall - runoff record to be used to parameterise the model rather than purely the extreme event magnitudes, thus ameliorating the problems associated with short and unreliable flow records. For example, using continuous simulation in the Linton catchment enabled predictions of flood events even after gauge malfunction occurred. This proved a significant advantage over statistical methods for flood frequency analysis employed by the Environment Agency which were biased by the faulty gauge readings.

Furthermore, continuous simulation is a flexible methodology which may be manipulated to make predictions relating to climate or land-use change, through the adjustment of rainfall or rainfall-runoff model parameters. For example, Ivanov *et al*. (2004) discuss the use of continuous simulation with a distributed model sensitive to soil type distribution, which could therefore be used to study changes in catchment land-use. This ability is important in an age where flooding is seen as an evolving threat caused by human behaviour, and floodplain management strategies therefore require simulations of possible future scenarios to enable proper precautionary measures to be taken.

8.2.2 Urban Flood Modelling

One of the greatest challenges in the creation of a modern flood risk assessment framework is to produce a system capable of providing simulations and decision-making capabilities in complex urban environments. The ability to provide predictions in such environments is becoming a common requirement as awareness of flood risk is increased and limitations in the deployment of structural flood defences become apparent (Sharif *et al.,* 2006). Recent changes in attitude towards floodplains mean that they are no longer seen purely as areas which should be protected from overbank flow, and instead there is an increased understanding of their role as a functional part of the fluvial environment. As well as leading to improvements in catchment-wide management strategies, this new conceptualisation has also encouraged an expectation of self-sufficiency with regard to flood protection measures, as flooding is seen as a natural occurrence for homes located within the floodplain area. It is therefore important to provide accurate information on expected flood inundation extent and depth at different return periods, to allow homeowners to prepare for future flood events, and flood response strategies to be developed for urban areas.

Past attempts to incorporate flood risk mapping into flood risk analyses have typically used simple 1d models which provide predictions of water surface elevation for cross-sections perpendicular to the channel orientation. This type of model is unable to properly represent the complex flow patterns created through densely-populated areas where housing layout may cause combinations of directional blockages and preferential flow pathways. Instead, a 2d model structure is required, allowing a more complete representation of channel-floodplain coupling and floodplain flow behaviour which recognises the floodplain as an area providing dynamic flow pathways rather than simply as a static storage zone.

8.2.2.1 Incorporation of New Data Resources

The expectations of urban flood simulation capability have been driven by recent advances in remote sensing techniques such as LIDAR which provide high resolution mapping of vulnerable areas. Prior to such data availability, there was little to suggest that detailed urban flood modelling might be a realistic proposition. However, emphasising the inter-dependence between data collection advances and model structural improvements that was discussed in Section 2.1, expanding coverage of high resolution topographic data sets has pushed forward advances in models capable of providing spatially-distributed flood predictions.

Improvements in provision of topographic data have not always been matched by collection of validation data in terms of inundation datasets, especially in the case of small catchments displaying relatively flashy responses which do not lend themselves to aerial image capture. These catchments cannot benefit from advances in remote-sensing technology, and hence ‘post-flood’ reconstruction is inevitably required. This thesis has proved that it is still possible to reap the benefits of 2d floodplain inundation models in such catchments, using the simple strategy of a survey of residents to collect data on inundation extent and depth. Where this technique was used in a study relating to a more recent event, such information could be supplemented by trash line data. Although model calibration must then be conducted using point data rather than a complete flood outline, such disadvantages may be ameliorated by including additional data on flood depths which would not normally be collected from satellite SAR data, a deficiency which has been highlighted as an impediment to identification of correct model behaviour (Bates *et al.*, 1997; Werner *et al.*, 2005).

The influx of high resolution topographic data has brought new challenges to hydrological modelling for flood risk assessment. Model implementations in typical UK catchments are no longer restricted by low-resolution data produced by techniques such as contour digitalisation. Instead, the requirement to produce an efficient modelling structure means that models must often be applied at a resolution lower than that achieved by the topographic data set. Through the introduction of the concept of grid cell porosity, this thesis established a method which enabled the use of information on sub-grid scale variation in elevation to control the direction and rate of flow between cells.

The advantages of this concept in the field of urban flood modelling were demonstrated in a preliminary investigation by Yu and Lane (2006b) using topographic information at a scale half that of the model scale. This thesis extended the method to use a greater number of sub-grid cells, and hence enabled 2 m topographic information to be used within a 10 m model framework. This showed that elevation data at a scale at which the effect of building layout on flow pathway direction and conveyance capacity was accurately represented, could be included within a model running at an efficient and practical resolution. No previous raster model structures for floodplain inundation have enabled the use of such high-resolution information within a model suitable to run at the scale of a town or city. The ability to include this information was found to have a profound effect on flood inundation predictions and enabled replication of the results found when using a full high resolution (2 m) version of the model. This was achieved while reducing the running time to 1/38 of that of the high resolution implementation, with important consequences for both uncertainty analysis techniques and successful operational flood warning.

8.2.2.2 Communication and Visualisation

An important challenge in urban flood modelling is to provide predictions in a format that is useful and accessible to the wide range of end users towards whom the estimates are aimed. These users include residents, insurers and emergency and strategic planning authorities. Without consideration of the presentation format, simulation results may be considerably less valuable to these users; in contrast, where result format is made a priority, it may prove a powerful tool to encourage uptake of the new modelling framework proposed in this thesis. A demonstration of this was seen in the enthusiasm of local residents to understand and contribute to simulation of flood extent for the October 2001 event, when results were presented at a scale which clearly showed the relation of inundation depths and boundaries to individual buildings.

As an example, the benefits of coupling predictions of channel discharge (from rainfall and rainfall-runoff models) to a floodplain inundation model illustrate several of the relevant issues in visualisation of flood risk. First, that the variable through which the results are presented is very important. By integrating the inundation model within the coupled model framework, it is possible to present flood risk in terms of its spatial extent rather than as a river discharge level or depth. The results are then made accessible to many more users. For example, risk understanding for individual homeowners, and planning of likely road closures, are just two tasks that become easier and more accurate, no longer relying on basin-fill approximations from river level data. An example of the use of distributed flood data within an emergency planning model is given by Simovic and Ahmad (2005), and several other studies demonstrate the possibilities arising from further coupling to GIS data (e.g. Dutta *et al.*, 2006; Zerger, 2002; Zerger and Wealands, 2004).

The coupled inundation model may also be used to improve visualisation of flood evolution. By understanding the dominant breach points and flow paths within the floodplain, flood defences may be more efficiently sited. In effect, a spatially targeted response to the flood becomes possible. This point is becoming increasingly important as hard engineering solutions to flood protection fall out of favour due to improved understanding of the limitations and disadvantages associated with such interventions, and instead focus shifts to the role of the floodplain and riparian areas in flood peak attenuation (Section 1.3.2.3). Modern solutions more often rely on ‘soft engineering’ designed to restore the natural functions of the floodplain, together with greater emphasis on individual responsibility for building protection. These responses rely heavily on a spatial understanding of inundation patterns to identify respectively effective restoration measures and vulnerable areas of the floodplain.

8.2.3 Uncertainty Estimation

As identified by Wheater (2002), the modern decision support framework for flood risk assessment must include uncertainty estimation techniques in order to produce meaningful estimates. Although integration of uncertainty estimates into flood inundation modelling has been relatively slow compared to other branches of hydrology (Section 2.3), it is now being recognised as a vital part of flood risk assessment. A high level of uncertainty exists in boundary conditions and validation data for the typical lowland catchment; for example, the majority of gauges are not designed to function across the full spectrum of flow conditions and therefore do not record data relating to the complete range of dominant flow pathways which may be activated in different catchment wetness conditions. This is subsequently mirrored in high uncertainties and occurrence of equifinality in model parameterisation. It is therefore likely that the impression of certainty given by a deterministic forecast would be misleading.

The method used in this thesis to assess uncertainty in flood extent was the GLUE technique. Using Monte Carlo sampling of parameter values, many realisations of the model are created, and each one is tested for behaviourability with respect to some threshold criterion. Those that meet the criterion are weighted according to their success in replicating some validation data set. The set of weighted predictions is then used to give a cumulative distribution for any required output parameter. The method was explained fully in Chapter 5. The technique is extremely flexible and applicable to a wide range of natural phenomena which display nonlinear behaviour and may therefore preclude an analytical study of error propagation. In particular, GLUE is suitable for use within a system of coupled models such as that presented here, although it should be noted that as the number of models and associated parameters increase, the computational load also expands rapidly. This has been found in other studies of cascading models as the limiting factor in a full uncertainty analysis (Pappenberger *et al.*, 2005). In this thesis, reduced complexity model structures helped to decrease the simulation time required, together with imposed limitations on the sources of uncertainty considered and therefore the number of model realisations that had to be propagated through the complete model chain.

Although the assumptions required to reduce the simulation running time leave scope for the uncertainty analysis to be extended in the future, the method showed that GLUE is no longer a technique so specialised and resource-intensive that it is impractical to use in standard management decisions. Instead, with suitable simplifications, this extremely useful method may be rendered widely applicable. In addition to addressing efficiency issues, the inclusion of uncertainty information must be considered in relation to the ability of the end user to make use of the information. In Section 7.4, the increasing public acceptance and even expectation of uncertainty information presented with forecasts was discussed; however care must still be taken to present the magnitude and effects of uncertainty in an accessible way. Again, coupling of rainfall-runoff and floodplain inundation models proved a powerful way to achieve this, enabling uncertainty to be presented in terms of nested predictions of flood outline (Section 7.2.5).

Given an effective method of uncertainty estimation and presentation, continuous simulation within a GLUE framework compares very favourably with more traditional flood risk assessment approaches in giving a much more complete picture of flood risk possibility. This was demonstrated in the Linton catchment, by a comparison both with results using more limited uncertainty analyses, and also with the Flood Risk Assessment carried out on behalf of the Environment Agency with design event estimation using Flood Estimation Handbook methodology and inundation extent estimated using the 1d ISIS model. In Section 7.3, the effects on model output of methods ignoring uncertainty in rainfall estimates or rainfall-runoff model parameterisation were considered. The most significant disadvantage in the use of such reduced structures was found to be in the use of a single set of rainfall-runoff model parameters. Not only does such a structure fail to express the range of output which might be expected based on the results of the full model, but the median discharge predictions were greatly reduced. This is due to the characteristics of equifinality in model parameterisation, which give a wide range of parameter sets with approximately equal predictive value. The optimum parameter set produces only marginally better predictions than other behavioural sets and does not necessarily represent the median behaviour of these other sets.

The results of the uncertainty analysis showed that if the 90% confidence bounds on predictions were used, these demonstrated a very wide range when considered in term of discharge. For example, the median estimate for peak discharge of the 100-year flood at Linton was 25.1 m^3s^{-1} but the 90% confidence interval was [14.8 m^3s^{-1}, 48.0 m^3s^{-1}]. The perception of the effects of this uncertainty may vary depending on the variable through which uncertainty is presented. If the inundated area is used, the perceived uncertainty is reduced as the steeper gradient of the natural boundary of the floodplain serves to constrain the flood (Section 7.2.5). However this is also the distance from the channel at which the housing density rises, and therefore uncertainty expressed in terms of number of residential properties affected may appear to be of greater significance. Whichever variable is used, it is clear that the data currently available for the catchment does not justify a deterministic prediction of the inundation associated with a given return period. This may go some way to explaining the discrepancy between the results returned in this thesis and those from the Environment Agency report, as the latter gives no indication of uncertainty bounds. However, it is also affected by known gauging errors in the catchment, a problem which is ameliorated by the use of continuous simulation, as previously discussed (Section 8.2.1).

8.3 Reflections on the Results

The improvements in technique integrated into the end-to-end flood risk assessment framework, and summarised in the previous section, led to inundation predictions that are different in character to those from more conventional methods. In order to consider the advantages that the end-to-end technique could offer, these differences are explored in more detail. First, the results are compared with those of the Environment Agency risk assessment study previously discussed. The role of uncertainty as an integral part of the forecasts is a defining feature of the new framework, and therefore the extent to which uncertainty analysis results can be used to learn about the catchment is discussed. In particular, the use of inundation forecasts with uncertainty bounds in improving flood risk management strategies is considered.

8.3.1 Comparisons with Conventional Results

To illustrate the characteristic differences of the end-to-end flood risk assessment framework from conventional methodologies, the inundation predictions of Chapters 6 and 7 are compared with those of the Environment Agency study using the ISIS model and described in Section 3.5. Both methods use a hydrograph estimation technique, based on rainfall-runoff modelling, to provide an upstream boundary condition for an inundation model. However, the EA model uses a Flood Estimation Handbook estimate of design rainfall, routed through the rainfall-runoff model as a single event, which removes the influence of antecedent catchment wetness conditions on rainfall generation. The model therefore loses the ability to replicate the effects of either seasonal fluctuation in rainfall totals, or clustering of rainfall events. Further, the rainfall-runoff model results are calibrated against the statistical distribution of flows measured at the Linton gauge, introducing errors due to gauge malfunction. The end-to-end framework attempts to address these concerns by using continuous simulation methodology which provides implicit soil moisture accounting and allows representation of long-term groundwater level fluctuations. The contrasting nature of the techniques is reflected in the predictions of the 100-year flow peak magnitude: 10.22 m^3s^{-1} in the EA ISIS model versus 25.1 m^3s^{-1} median prediction in the end-to-end model.

Both techniques route the flood hydrograph along the channel to produce inundation envelope forecasts, and a comparison is made between the two forecasts in Figure 8.1. Comparing initially the deterministic ISIS forecast with the median forecast from the end-to-end system, the differences may be considered as a combination of magnitude and pattern. The constrained design event methodology of the ISIS implementation, leading to a flow peak prediction less than half that of the end-to-end technique, naturally gives rise to a much reduced flood envelope. However, the predicted pattern of inundation is also different, and the more complex routing mechanisms possible in a 2d model are evident. Particularly striking in the end-to-end inundation envelope are flow paths within the floodplain, and high resolution definition of the flood boundary.

The large difference in predictions of flood envelope, and hence the number of houses at risk from flooding, obviously has the potential to lead to vastly different approaches to flood risk mitigation within the catchment. However, it is hoped that the representation of uncertainty within the end-to-end forecast might also lead to a more comprehensive consideration of possible flood scenarios. This outcome is discussed more fully in Section 8.3.3.

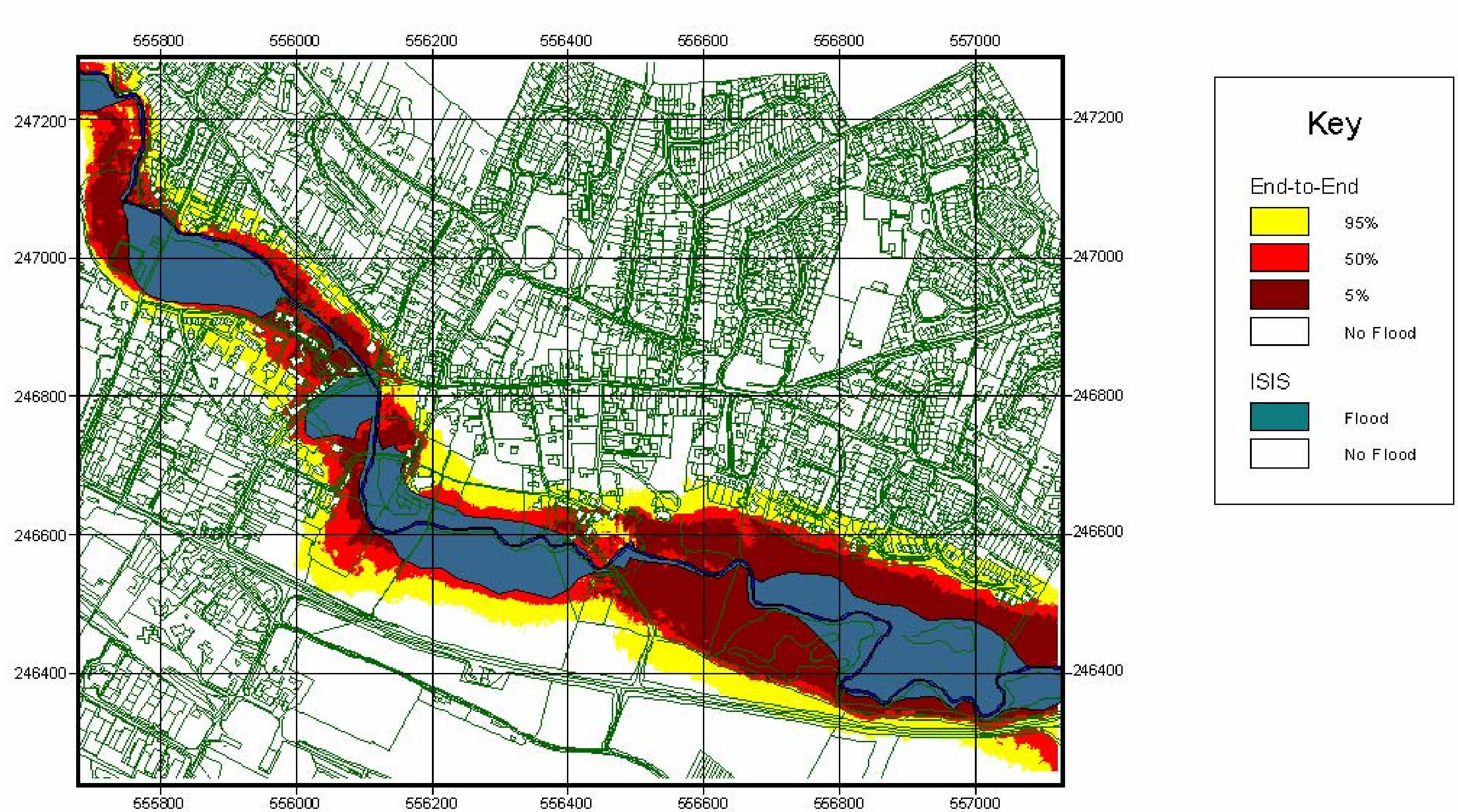

Figure 8.1: Comparison of 100-year flood envelopes predicted using End-to-End versus ISIS models

8.3.2 *Catchment Sensitivity*

The end-to-end flood risk assessment (FRA) framework goes beyond conventional FRA techniques in that it provides not only inundation forecasts, but also a chance to learn more about catchment sensitivity. One of the driving principles behind the FRA framework constructed in this study was the need for a process-based approach to flood modelling which could show the same sensitivities to climate and land-use change as a real-world catchment and therefore remain relevant in an era of accelerated flood risk and non-stationarity in the forcing factors of flood risk. It was hoped that such a model framework might enable recommendations to be made as to the model components which are most affected by uncertainty, and so hold the most opportunity to mitigate the uncertainty. The analysis required for such an appraisal relies on an assessment of the model component sensitivity to the data available for model conditioning, and hence also provides an indication of those components which may be most sensitive to non-stationarity of climate or land-use input conditions.

The application of the coupled model chain within a GLUE framework enabled an assessment of the contribution of individual uncertainty sources within the long term discharge and inundation predictions. It is not, however, justifiable to draw a direct link between this model component uncertainty and catchment process sensitivity. The component uncertainty is instead determined by the combined effects of catchment process sensitivity, data available for model conditioning, choice and complexity of model and validation methodology.

In Section 7.3, it was found that uncertainty in the rainfall-runoff model parameterisation was dominant over that in rainfall series realisation or in floodplain inundation model calibration. However, this result must be considered in terms of the relative complexity of parameterisation in each of these components. The uncertainty in the rainfall series results not from model parameterisation, as the rainfall generator relies on direct sampling from empirical distributions of storm characteristics, but instead only from the stochastic nature of the sampling procedure and the corresponding clustering of simulated storm events. The relatively short data series from which the distributions are created therefore limits the uncertainty in the simulated rainfall series. The uncertainty in the inundation model is also constrained by the use of a single calibration parameter; calibration using a distributed floodplain friction parameter having been rejected due to model insensitivity caused by the flow limiter. In contrast, the rainfall-runoff model has seven parameters to be calibrated, despite having one of the simplest structures in common use.

In trying to distinguish the most sensitive part of the hydrological system - the climate forcing, the nonlinear runoff generator or the flood routing process - we have therefore perhaps learnt more about the relative complexity of each component and our ability to characterise the dominant processes. In the case of the rainfall and floodplain components, the attempt to use the data available in the context of physical understanding of catchment process has been relatively successful. Returning to the discussion of Section 2.1, these aspects of catchment behaviour have been well conditioned by data that can be measured remotely: precipitation series for the rainfall model and the topographic boundary condition for the inundation model. This success has allowed the use of physically-based models which capture the dominant processes and require relatively little calibration. In contrast, the nonlinear mechanisms of runoff generation and catchment-scale routing remain elusive. Subsurface processes are known to control the catchment response and yet the techniques to monitor them are unavailable. This is exacerbated by the sensitivity of such processes to small-scale heterogeneity and structural features in the soil and bedrock, leading to model representations and parameterisations which are highly scale dependant. The model structure used in the lumped rainfall-runoff model is therefore necessarily a crude simplification requiring the calibration of ‘effective’ parameters which cannot be directly measured in the catchment.

8.3.3 Useful Uncertainty

The previous section suggested that the investigation of the relative contribution of uncertainty sources could lead to conclusions about the conditioning of each model in response to the available data. It is important that this result is seen not only in its academic context but also that the consequences in term of flood risk assessment procedure are explored. Without this context, uncertainty estimation is in danger of gaining a reputation as a theoretical game without useful or meaningful results (Morss *et al.,* 2005).

8.3.3.1 Improving forecast precision

High levels of uncertainty in a flood forecast make strategic and emergency planning more difficult. Therefore it is hoped that a more detailed understanding of uncertainty sources will aid hydrologists in their efforts to constrain the total uncertainty. There are three factors relating to each model component which could be considered in deciding where future work could best be directed in this aim. First, how great are the current uncertainty levels? Second, to what extent would it be possible to reduce these? Third, does the uncertainty analysis carried out to date represent a fair assessment of the model sensitivity or could there be additional uncertainty sources not currently quantified?

The rainfall model currently shows relatively low uncertainty magnitude. However, this does not necessarily mean it should be ignored in terms of future improvements. This relates to the third factor described above: the current model provides only a representation of rainfall characteristics over the past 15 years, a sufficiently short period that climate change is unlikely to be well represented and will therefore show essentially stationary conditions. The possible model sensitivity to non-stationarity in the climate driver is therefore a source of uncertainty that has not been included in the analysis, and is an area in which future investigation would be valuable.

The rainfall-runoff model is currently the dominant source of uncertainty. However, this only recommends it as a subject for further work if there exist the methods to reduce this uncertainty. Although a very simple structure was chosen for the model, it clearly still exhibits ill-conditioning, evidenced by equifinality in parameter set choice. In the long term, the best solution to this problem is to collect a longer series of rainfall-runoff data to capture a fuller description of catchment behaviour including response to extreme conditions, and hence allowing parameter identification for a model of similar or more complex structure. To achieve this, structural improvements should also be made to the Linton gauge to allow accurate measurement of flood flows where additional flow pathways or processes may become active. This solution, however, does not provide an answer for the immediate problem. In the past, a traditional response would have been to use a physically-based model whose parameters could be measured directly in the catchment and which therefore reduces the need for calibration. However, improved understanding of parameter scale dependence has led to a rejection of this philosophy (Beven, 1996). One possible alternative is to attempt the alter the rainfall-runoff model structure to enable increased use of catchment data that is available or could be collected, without increasing the number of parameters. This type of modification might provide a more immediate approach to reducing model uncertainty. For example, the topographic index of TOPMODEL allows explicit use of a DEM to represent the control of catchment form on runoff response, although this may not be appropriate in a groundwater-dominated catchment where surface gradient does not follow bedrock slope. Another possibility would be to make use of regional data, using results from similar catchments to constrain the range of the effective parameters.

The floodplain model was not included in the full GLUE application; however a sensitivity analysis was carried out to gauge the relative scale of uncertainty in this component. As with the rainfall model, it was found to make a relatively minor contribution to overall uncertainty. However, during the modelling process it was noted that use of a flow limiter caused insensitivity to floodplain friction. Therefore an additional cause of uncertainty related to choice of limiter and roughness caused by floodplain vegetation may exist, which is not currently included in the uncertainty estimation procedure.

8.3.3.2 Integrating uncertainty into risk assessment

Given the arguments in the previous section, it is likely that uncertainty will continue to play an important role in flood risk forecasts. In order to utilise knowledge of uncertainty, procedures should be implemented which embed uncertainty analysis into flood risk assessment procedures. Section 2.3.2 discussed conventional methods of dealing with uncertainty such as using the ‘worst case scenario’ or using an arbitrary safety factor. However, more complete specifications of inundation risk distributions would allow management decisions to be based on data rather than guesswork.

Using concepts from mathematical decision theory, candidate strategies may be assessed on the basis of a risk function which quantifies the danger associated with the decision (e.g. Lund, 2002). This is calculated using the distribution of possible flood outcomes from the coupled model chain, together with a function which attempts to evaluate the ‘loss’ expected as a result of a particular flood magnitude occurring in a community adopting the given flood mitigation strategy. The loss function could be interpreted in a narrow, financial, ‘cost’ sense; or in a broader sense to incorporate the vulnerability of the community as discussed in Section 1.3.2.2.

This type of assessment would be very valuable as it provides an evidence-based methodology for assessing flood risk guidance which considers the spectrum of possible flood outcomes rather than a single deterministic prediction. Therefore the cost savings associated with minimum intervention strategies in the case of unusually low-volume floods are included as well as the benefits of planning for low-probability, high–risk events. The end-to-end framework proposed here provides the best information available on the probability distribution of flood magnitudes required for such an assessment.

8.4 End-to-End Modelling: Future Directions

The challenges found in the creation and application of the flood risk assessment framework in many ways reflect the wider questions being asked of catchment hydrology today. The cascade of coupled models – stochastic rainfall model, rainfall-runoff model and floodplain inundation model – has emphasised the interdependence of each part of the modelling process and the importance of an assessment of model structure, uncertainty and finally flood risk, made in the context of the complete system. The understanding of the need to take a holistic view of catchment process mirrors the increasing rejection of hydrologic modelling techniques based on laboratory-scale process descriptions. Sivapalan (2005) voices this philosophy in his call for a unified theory of hydrology at the catchment scale, based on new multi-scale process theories.

Although superficially this concept might seem to conflict with modern perceptions of small-scale heterogeneity and "uniqueness of place" (Beven, 2000), it is in fact a response to many of the same drivers. Current technologies for hydrological data collection are not sufficient to allow the perceived complexity and spatial heterogeneity of catchment rainfall-runoff response to be incorporated in a model structure without causing ill-conditioning. This was demonstrated in Chapter 5 where 15 years of rainfall-runoff data was found insufficient to parameterise a model with 9 parameters. Recent attempts integrate detailed observations from specific areas of a catchment within current simplified model structures have concluded that this could instead lead to model bias (e.g. Freer *et al.*, 2004). The unified theory would try to circumvent these problems by relating signatures of hydrological variability to predictor variables rather than relying on measured data. For example, spatial densities of preferential flow pathways would be considered in terms of the climate or geological driving forces.

This type of approach suggests a solution to the typical lack of data available in small urban catchments increasingly at risk from flooding. By considering the geomorphic or land-forming processes which control catchment response, connections may be made between observations in different catchments by study of pattern and process. This would allow transfer of information between catchments, and hence facilitate the type of region-based identification of catchment process proposed as a solution to data scarcity in Section 8.3.3.1. By relating catchment response to predictor variables, progress may also be made towards the goal of understanding catchment sensitivity to human impacts on climate and land-use. Discussed in Section 1.2.2, this aim is at the root of many of today's efforts to understand, model, predict and mitigate future flood risk. The type of integrated, process-based methodology that is proposed in this thesis will be an integral part of the drive to achieve this aim.

REFERENCES

Acreman, M.C. and Sinclair, C.D., 1986. Classification of drainage basins according to their physical characteristics; an application for flood frequency analysis in Scotland. *Journal of Hydrology*, 84: 365-380.

Allen, J.C., 1976. Modified Sine Wave Method for Calculating Degree Days. *Environmental Entomology*, 5(3): 388-396.

Anderson, M.G. and Bates, P.D., 2001. Hydrological Science: Model Credibility and Scientific Integrity. In: M.G. Anderson and P.D. Bates (Editors), *Model Validation: Perspectives in Hydrological Science*. Wiley, Chichester, pp. 1-10.

Anderson, M.G., Bates, P.D. and Walling, D.E., 1996. General Context for Floodplain Process Research. In: M.G. Anderson, D.E. Walling and P.D. Bates (Editors), *Floodplain Processes*. Wiley, Chichester.

Andreadis, K.M. and Lettenmaier, D.P., In Press. Assimilating remotely sensed snow observations into a macroscale hydrology model. *Advances in Water Resources*.

Antoniadis, A., 1995. Matlab Smoothing Toolbox. http://www.unizh.ch/biostat/Software/, Zurich.

Apel, H., Thieken, A.H., Merz, B. and Bloschl, G., 2004. Flood risk assessment and associated uncertainty. *Natural Hazards and Earth System Sciences*, 4(2): 295-308.

Archer, D., 1991. Practical application of historical flood information to flood estimation. In: L. Gottschalk, J.C. Olivry, D. Reed and D. Rosbjerg (Editors), *Hydrological Extremes: Understanding, Predicting, Mitigating*. IAHS, Birmingham, pp. 191-199.

Arnaud, P. and Lavabre, J., 1999. Using a stochastic model for generating hourly hyetographs to study extreme rainfalls. *Hydrological Sciences Journal*, 44(3): 433-446.

Arnell, N.W. and Reynard, N.S., 1996. The effects of climate change due to global warming on river flows in Great Britain. *Journal of Hydrology*, 183(3-4): 397-424.

Arnell, N.W., Liu, C., Compagnucci, R., da Cunha, L., Hanaki, k., Howe, C., Mailu, G. & Shiklomanov, I., 2001. *Climate Change 2001: Impacts, Adaptation and Vulnerability*. IPCC.

Aronica, G., Hankin, B. and Beven, K., 1998. Uncertainty and equifinality in calibrating distributed roughness coefficients in a flood propagation model with limited data. *Advances in Water Resources*, 22(4): 349-365.

Aronica, G., Bates, P.D. and Horritt, M.S., 2002. Assessing the uncertainty in distributed model predictions using observed binary pattern information within GLUE. *Hydrological Processes*, 16: 2001-2016.

AT&T_Laboratories, 2005. Cambridge Raw Daily Weather Data. http://www.cl.cam.ac.uk/Research/DTG/attarchive/cgi-bin/dailyWeatherHistory-cgi

Axelsson, 1998. Improved Fourier Modelling of Soil Temperature Using FFT Algorithms. *IEEE Transactions on Geoscience and Remote Sensing*, 36(5): 1519-1523.

BADC, 2005. Met Office - UK Land Surface Stations data (1900-present). http://badc.nerc.ac.uk/cgi-bin/data_browser/data_browser/badc/ukmo-surface/data/united_kingdom/cambridgeshire/cambridge_botanic_garden.

Bardossy, A., 2005. Fuzzy sets in rainfall/runoff modelling. In: M.G. Anderson and J.J. McDonnell (Editors), *Encyclopedia of Hydrological Sciences*. Wiley, Chichester, pp. 2007-2014.

Barrington Local History and Conservation Society, 1979. *Cam or Rhee*.

Bartholmes, J. and Todini, E., 2005. Coupling meteorological and hydrological models for flood forecasting. *Hydrology and Earth System Sciences*, 9(4): 333-346.

Bates, P.D., 2004. Remote sensing and flood inundation modelling. *Hydrological Processes*, 18: 2593-2597.

Bates, P.D. and De Roo, A.P.J., 2000. A simple raster-based model for flood inundation simulation. *Journal of Hydrology*, 236: 54-77.

Bates, P.D., Horritt, M.S., Smith, C.N. and Mason, D.C., 1997. Integrating remote sensing observations of flood hydrology and hydraulic modelling. *Hydrological Processes*, 11: 1777-1795.

Bates, P.D., Stewart, M.D., Siggers, G.B., Smith, C.N., Hervouet, J.M. & Sellin, R.J.H., 1998. Internal and External validation of a two-dimensional finite element code for river flood simulations. *Proceedings of the Institute of Civil Engineers*, 130: 127-141.

Bates, P.D. and Hervouet, J.M., 1999. A new method for moving boundary hydrodynamic problems in shallow water. *Proceedings of the Royal Society of London, Series A: Mathematical and Physical Sciences*, 455: 3107-3128.

Bates, P.D., Marks, K.J. and Horritt, M.S., 2003. Optimal use of high-resolution topographic data in flood inundation models. *Hydrological Processes*, 17(3): 537-557.

Bayliss, A.C., 1999. Validation and update of flood peak data, *Flood Estimation Handbook*. Institute of Hydrology, Wallingford, pp. 261-272.

Bayliss, A.C. and Jones, R.C., 1992. *The Peaks-Over-Threshold flood database at the Institute of Hydrology: Report to MAFF*.

Bayliss, A.C. and Reed, D., 2001. *The use of historical data in flood frequency estimation. Report to MAFF.*, Centre for Ecology and Hydrology.

Beck, M.B., 1987. Water quality modelling: a review of the analysis of uncertainty. *Water Resources Research*, 23: 1393-1442.

Beck, U., 1992. *Risk society: Towards a New Modernity*. Sage, London.

Beffa, C. and Connell, R.J., 2001. Two-dimensional flood plain flow. I: Model Description. *Journal of Hydrologic Engineering*, 6(5): 382-396.

Bencala, K.E., Huff, J.H., Harvey, A.W., Jackman, A.P. and Tiska, F.J., 1993. Modelling within the stream-catchment continuum. In: A.J. Jakeman, M.B. Beck and M.J. McAleer (Editors), *Modelling Change in Environmental Systems*. Wiley, Chichester.

Bender, M.J., 1996. Fuzzy compromise approach to water resources systems planning under uncertainty. In: J.J. Bogardi and Z.W. Kundzewicz (Editors), *Risk, Reliability, Uncertainty, and Robustness of Water Resources Systems*. Cambridge University Press, Cambridge, pp. 122-130.

Beven, 1987. Towards the use of catchment geomorphology in flood frequency predictions. *Earth Surface Processes and Landforms*, 12: 69-82.

Beven, K., 1993. Prophecy, reality and uncertainty in distributed hydrological modelling. *Advances in Water Resources*, 16(1): 41-51.

Beven, K., 1995. Linking parameters across scales: subgrid parameterisations and scale dependant hydrological models. In: J.D. Kalma and M. Sivapalan (Editors), *Scale issues in Hydrological Modelling*. Wiley, New York, pp. 263-282.

Beven, K., 1996. The limits of splitting. *The Science of the Total Environment*, 183: 89-97.

Beven, K., 2000. Uniqueness of place and process representations in hydrological modelling. *Hydrology and Earth System Sciences*, 4(2): 203-213.

Beven, K., 2001a. Calibration, Validation and Equifinality in Hydrological Modelling - a Continuing Discussion... In: M.G. Anderson and P.D. Bates (Editors), *Model Validation: Perspectives in Hydrological Science*. Wiley, Chichester.

Beven, K., 2001b. *Rainfall-Runoff Modelling: The Primer*. Wiley, Chichester.

Beven, K. and Binley, A., 1992. The future of distributed models - model calibration and uncertainty prediction. *Hydrological Processes*, 6(3): 279-298.

Beven, K. and Freer, J., 2001. Equifinality, data assimilation, and uncertainty estimation in mechanistic modelling of complex environmental systems using the GLUE methodology. *Journal of Hydrology*, 249(1-4): 11-29.

Beven, K. and Kirkby, M.J., 1979. A physically-based, variable contributing area model of basin hydrology. *Hydrological Sciences Bulletin*, 24: 43-69.

Birikundaugi, S. and Rouselle, J., 1992. Some problems involved in using partial duration series for regional flood frequency analysis. In: G. Rossi, N. Harmancioglu and V. Yevjevich (Editors), *Coping with Floods*. Kluwer, Dordrecht.

Birks, C.J., Pickles, M.L., Bray, C.W. and Taylor, K., 1992. *Standards of Service for flood defence - A framework for planning and monitoring*, BHR Group Conference on Floods and Flood Management, Florence, pp. 13.

Black, A.R. and Law, F.M., 2004. Development and utilization of a national web-base chronology of hydrological events. *Hydrological Sciences Journal*, 49: 237-246.

Blazkova, S. and Beven, K., 2000. Flood frequency estimation by continuous simulation for a catchment treated as ungauged. *Water Resources Research*., 38(8): 14.

Blazkova, S. and Beven, K., 2002. Flood frequency estimation by continuous simulation for a catchment treated as ungauged (with uncertainty). *Water Resources Research*, 38(8).

Blazkova, S. and Beven, K., 2004. Flood frequency estimation by continuous simulation of subcatchment rainfalls and discharges with the aim of improving dam safety assessment in a large basin in the Czech Republic. *Journal of Hydrology*, 292(1-4): 153-172.

Bloschl, G., 2005. Statistical Upscaling and Downscaling in Hydrology. In: M.G. Anderson and J.J. McDonnel (Editors), *Encyclopaedia of Hydrological Sciences*. Wiley, Chichester, pp. 135-154.

Boardman, J., 2003. Soil erosion and flooding on the eastern South Downs, southern England, 1976-2001. *Transactions of the Institute of British Geographers*, 28(2): 176-196.

Boardman, J., Ligneau, L., Deroo, A. and Vandaele, K., 1994. Flooding of Property by Runoff from Agricultural Land in Northwestern Europe. *Geomorphology*, 10(1-4): 183-196.

Bogardi, J.J. and Kundzewicz, Z.W., 1996. Introduction. In: J.J. Bogardi and Z.W. Kundzewicz (Editors), *Risk, Reliability, Uncertainty, and Robustness of Water Resources Systems*. Cambridge University Press, Cambridge, pp. 1-3.

Bormann, H. et al., 2005. From local hydrological process analysis to regional hydrological model application in Benin: Concept, results and perspectives. *Physics and Chemistry of the Earth, Parts A/B/C*, 30(6-7): 347-356.

Botterweg, P., 1995. The user's influence on model calibration results: an example of the model SOIL, independently calibrated by two users. *Ecological Modelling*, 81(1-3): 71-81.

Boughton, W. and Droop, O., 2003. Continuous simulation for design flood estimation - a review. *Environmental Modelling & Software*, 18(4): 309-318.

Bradbrook, K.F., Lane, S.N., Waller, S.G. and Bates, P.D., 2004. Two dimensional diffusion wave modelling of flood inundation using a simplified channel representation. *International Journal of River Basin Management*, 2(3): 211-223.

Bradford, S.F. and Sanders, B.F., 2002. Finite-volume model for shallow-water flooding of arbitrary topography. *Journal of Hydraulic Engineering*, 128(3): 289-298.

Brasington, J. and Richards, K., 1998. Interactions between model predictions, parameters and DTM scales for topmodel. *Computers & Geosciences*, 24(4): 299-314.

Brodtkorb, P.A. et al., 2000. WAFO - *A Matlab Toolbox for Analysis of Random Waves and Loads*, 10th International Offshore and Polar Engineering Conference, Seattle, USA, pp. 343-350.

Brookes, A., Baker, J. and Redmond, C., 1996. Floodplain restoration and riparian zone management. In: A. Brookes, F. Douglas and J. Shields (Editors), *River Channel Restoration*. Wiley, Chichester.

Brouwer, R. and van Ek, R., 2004. Integrated ecological, economic and social impact assessment of alternative flood control policies in the Netherlands. *Ecological Economics*, 50(1-2): 1-21.

Bullen Consultants, 2002. *Standard of Protection Studies, River Cam and Granta (Draft Report)*, Environment Agency.

Burlando, P. and Rosso, R., 1991. Comment on parameter estimation and sensitivity analysis for the modified Bartlett–Lewis rectangular pulses mode of rainfall by S. Islam et al. *Journal of Geophysical Research*, 96(D5): 9391-9395.

Cadavid, L., Obeysekera, J.T.B. and Shen, H.W., 1991. Flood-frequency derivation from kinematic wave. *Journal of Hydraulic Engineering*, 117(4): 489–510.

Calenda, G. and Napolitano, F., 1999. Parameter estimation of Neyman–Scott processes for temporal point rainfall simulation. *Journal of Hydrology*, 225(1-2): 45-66.

Calver, A., 1993. Flood generation Modelling. *Institution of Wat. Environ. Management Journal*, 7: 614:620.

Cambridgeshire County Council, C., 1998. *Cambridgeshire and Peterborough's State of the Environment Report*. http://www.cambridgeshire.gov.uk/environment/policy/Env_Report_1998.htm

Cambridgeshire County Council, C., 2005. *Cambridgeshire Environment Report*. http://www.cambridgeshire.gov.uk/environment/policy/cer/

Cameron, D.S., Beven, K.J. and Tawn, J., 1999. Flood frequency estimation by continuous simulation for a gauged upland catchment (with uncertainty). *Journal of Hydrology*., 219(3-4): 169-187.

Cameron, D.S., Beven, K. and Tawn, J., 2000. An evaluation of three stochastic rainfall models. *Journal of Hydrology*, 228(1-2): 130-149.

Cameron, D.S., Beven, K., Tawn, J. and Naden, P., 2000. Flood frequency estimation by continuous simulation (with likelihood based uncertainty estimation). *Hydrology and Earth System Sciences*, 4(1): 23-34.

Camorani, G., Castellarin, A. and Brath, A., 2005. Effects of land-use changes on the hydrologic response of reclamation systems. *Physics and Chemistry of the Earth*, 30(8-10): 561-574.

Cernesson, F., Lavabre, J. and Masson, J.M., 1996. Stochastic model for generating hourly hyetographs. *Atmospheric Research*, 42(1-4): 149-161.

Chapman, T.G., 1996. Common unitgraphs for sets of runoff events. Part 2: comparisons and inferences for rainfall loss models. *Hydrological Processes*, 10: 783-792.

Charlton, R.A., 1999. Initial stages in the development of a coupled hillslope hydrology-floodplain inundation model. *Physics and Chemistry of the Earth* Part B - Hydrology, Oceans and Atmosphere, 24(1-2): 37-41.

Chen, J.M., Chen, X., Weimin, J. and Geng, X., 2005. Distributed hydrological model for mapping evapotranspiration using remote sensing inputs. *Journal of Hydrology*, 305(1-4): 15-39.

Chen, L., Rabitz, H., Considine, D.B., Jackman, C.H. and Shorter, J.A., 1997. Chemical reaction rate sensitivity and uncertainty in a two-dimensional middle atmosphere ozone model. *Journal of Geophysical Research* - Atmospheres, 102: 16201-16214.

Chetty, K. and Smithers, J., 2005. Continuous simulation modelling for design flood estimation in South Africa: Preliminary investigations in the Thukela catchment. *Physics and Chemistry of the Earth*, 30(11-16): 634-638.

Chow, V.T., 1959. *Open-Channel Hydraulics*. McGraw-Hill, New York.

Chow, V.T., Maidment, D.R. and Mays, L.W., 1988. *Applied Hydrology*. McGraw-Hill, Singapore.

Cocke, S. and LaRow, T.E., 2000. Seasonal predictions using a regional spectral model embedded within a coupled ocean-atmosphere model. *Monthly Weather Review*, 128: 689-708.

Coles, S., 2001. The use and misuse of extreme value models in practice., *SEMSTAT: Extreme value theory and applications*.

Coles, S. and Dixon, M.J., 1999. Likelihood-based inference for extreme value models. *Extremes*, 2: 5-23.

Coles, S., Pericchi, L.R. and Sisson, S., 2003. A fully probabilistic approach to extreme rainfall modelling. *Journal of Hydrology*, 273: 35-50.

Collier, C.G., 1999. Precipitation Measuring Weather Radar. In: R.W. Herschy (Editor), *Hydrometry: Principles and Practices*. Wiley, Chichester.

Collier, C.G. and Hardaker, P.J., 1996. Estimating probable maximum precipitation using a storm model approach. *Journal of Hydrology*, 183(3-4): 277-306.

Connell, R.J., Beffa, C. and Painter, D.J., 1998. Comparison of observations by flood plain residents with results from a two-dimensional flood plain model: Waihao River, New Zealand. *Journal of Hydrology* (NZ), 37: 55-79.

Connell, R.J., Painter, D.J. and Beffa, C., 2001. Two-dimensional flood plain flow. II: Model Validation. *Journal of Hydrologic Engineering*, 6(5): 406-415.

Correia, F.N. et al., 1994. The planning of flood alleviation measure: interface with the public. In: E. Penning-Rowsell and M. Fordham (Editors), *Floods across Europe: hazard assessment, modelling and management*. Middlesex University Press, London, pp. 167-193.

Cowpertwait, P.S.P., 1994. A Generalised Point Process Model for Rainfall. *Proc. R. Soc. Lond. A*, 447: 23-37.

Cowpertwait, P.S.P., 1995. A generalised spatial-temporal model based on a clustered point process. *Proc. R. Soc. Lond. A*, 450: 162-175.

Cowpertwait, P.S.P. and O'Connell, P.E., 1997. A regionalised Neyman-Scott model of rainfall with convective and stratiform cells. *Hydrology and Earth System Sciences*, 1: 71-80.

Cox, D.R., Isham, V.S. and Northrop, P.J., 2002. Floods: some probabilistic and statistical approaches. *Philos T Roy Soc A*, 360(1796): 1389-1408.

Croke, B.F.W. and Jakeman, A.J., 2004. A catchment moisture deficit module for the IHACRES rainfall-runoff model. *Environmental Modelling and Software*, 19: 1-5.

Crooks, S. and Davies, H., 2001. Assessment of land use change in the Thames catchment and its effect on the flood regime of the river. *Physics and Chemistry of the Earth* Part B-Hydrology Oceans and Atmosphere, 26(7-8): 583-591.

Cunge, J.A., Holly Jr, F.A. and Verwey, A., 1976. *Practical aspects of computational river hydraulics*. Pitman, London.

Dai, A., Fung, I.Y. and DelGenio, A.D., 1997. Surface observed global land precipitation variations during 1900-88. *Journal of Climate*, 10(11): 2943-2962.

Davies, G.L., 1992. Catchment management planning in the NRA of England and Wales. In: A. Saul (Editor), *Floods and Flood Management*. Kluwer, Dordrecht.

Davison, A.C. and Smith, R.L., 1990. Models for Exceedances over High Thresholds. *J. Roy. Statist. Soc. B.*(52): 393-442.

De Roo, A.P.J., Wesseling, C.G. and Van Deursen, W.P.A., 2000. Physically based river basin modelling within a GIS: the LISFLOOD model. *Hydrological Processes*, 14(11-12): 1981-1992.

De Roo, A.P.J., Odijk, M., Schmuck, G., Koster, E. and Lucieer, A., 2001. Assessing the effects of land use changes on floods in the Meuse and Oder catchment. *Phys. Chem. Earth (B)*, 26(7-8): 593-599.

De Roo, A.P.J., Schmuck, G., Perdigao, V. and Thielen, J., 2003. The influence of historic land use changes and future planned land use scenarios on floods in the Oder catchment. *Phys. Chem. Earth (B)*, 28(33-36): 1291-1300.

De Roo, P.J., Gouweleeuw, B., Thielen, J., Bartholmes, J., Bongioannini-Cerlini, P., Todini, E., Bates, P.D., Horritt, M., Hunter, N., Beven, K.J., Pappenberger, F., Heise, E., Rivin, G., Hils, M., Hollingsworth, A., Holst, B., Kwadijk, J., Reggiani, P., Van Dijk, M., Sattler, K. & Sprokkereef, E., 2003. Development of a European Flood Forecasting System. *International Journal of River Basin Management*., 1(1): 49-59.

Defina, A., 2000. Two-dimensional shallow flow equations for partially dry areas. *Water Resources Research*, 36(11): 3251-3264.

Defina, A., D'Alpaos, L. and Matticchio, B., 1994. A new set of equations for very shallow water and partially dry areas suitable to 2D numerical models. In: P. Molinaro and L. Natale (Editors), *Modelling Flood Propagation Over Initially Dry Areas*. American Society of Civil Engineers, New York, pp. 72-81.

DEFRA, 2000. *Project Appraisal Guidance 3 - Economic Appraisal*. http://www.defra.gov.uk/environ/fcd/pubs/pagn/fcdpag3/default.htm

DEFRA, 2002. *Flood Management - Capital Grant Allocations for Flood and Coastal Defence*. http://www.defra.gov.uk/environ/fcd/policy/grantaid.htm#scorecalc

DEFRA, 2003. *Wetlands, Land Use Change and Flood Management - A Jointly Agreed Paper*. Joint statement with English Nature, EA, DEFRA and Forestry Commission

Diaz-Granados, M.A., Valdes, J.B. and Bras, R.L., 1984. A physically based flood frequency distribution. *Water Resources Research*, 20(7): 995–1002.

Dibike, Y.B. and Coulibaly, P., 2005. Hydrologic impact of climate change in the Saguenay watershed: comparison of downscaling methods and hydrologic models. *Journal of Hydrology*, 307(1-4): 145-163.

Dietrich, W.E. and Montgomery, D.R., 1998. Hillslopes, Channels, and Landscape Scale. In: G. Sposito (Editor), *Scale Dependence and Scale Invariance*. Cambridge University Press, Cambridge, pp. 30-60.

Duan, Q., Sorooshian, S. and Gupta, V.K., 1992. Effective and Efficient Global Optimization for Conceptual Rainfall-Runoff Models. *Water Resources Research*, 28(4): 1015-1031.

Dunbar, M., 2004. *Heavily Modified Waters in Europe: Case Study on the Great Ouse Catchment*, CEH Wallingford.

Dunne, T., 1982. Relation of field studies and modeling in the prediction of storm runoff. *Journal of Hydrology*, 65(1-3): 25-48.

Dutta, D., Herath, S. and Musiake, K., 2006. An application of a flood risk analysis system for impact analysis of a flood control plan in a river basin. *Hydrological Processes*, 20(6): 1365-1384.

Eagleson, P.S., 1972. Dynamics of Flood Frequency. *Water Resources Research*, 8(4): 878-898.

Easterling, D.R. et al., 2000. Observed variability and trends in extreme climate events: A brief review. *Bulletin of the American Meteorological Society*, 81(3): 417-425.

Egozcue, J.J. and Ramis, C., 2001. Bayesian Hazard Analysis of Heavy Precipitation in Eastern Spain. *International Journal of Climatology*, 21: 1263-1279.

Entekhabi, D., Rodrigues-Iturbe, I. and Eagleson, P.S., 1989. Probabilistic representation of the temporal rainfall process by a modified Neymann-Scott rectangular pulses model - parameter estimation and validation. *Water Resources Research*, 25(2): 295-302.

Environment Agency, 1998. *Groundwater Vulnerability of England and Wales, Policy and Practice for the Protection of Groundwater*.

Environment Agency, 2001. *Lessons Learned: Autumn 2000 Floods*.

Environment Agency, 2006. *Am I at risk of Flooding?* http://www.environment-agency.gov.uk/subjects/flood/826674/829803/

Ericksen, N.J., 1986. *Creating Flood Disasters?*, National Water and Soil Conservation Agency, Wellington.

Estrela, T. and Quintas, L., 1994. Use of a GIS in the modelling of flows on floodplains. In: W.R. White and J. Watts (Editors), *Proceedings of the 2nd International Conference on River Flood Dynamics*. Wiley, Chichester.

Evans, J.P. and Jakeman, A.J., 1998. Development of a simple, catchment-scale, rainfall-evapotranspiration-runoff model. *Environmental Modelling and Software*, 13(3-4): 385-393.

Fahmy, T., Parent, E. and Gatel, D., 1996. Controlling three levels of uncertainties in ecological risk models. In: J.J. Bogardi and Z.W. Kundzewicz (Editors), *Risk, Reliability, Uncertainty, and Robustness of Water Resources Systems*. Cambridge University Press, Cambridge, pp. 76-83.

Famiglietti, J.S. and Wood, E.F., 1994a. Application of multiscale water and energy balance models on a tallgrass prairie. *Water Resources Research*, 30(11): 3079-3094.

Famiglietti, J.S. and Wood, E.F., 1994b. Multiscale modelling of spatially variable water and energy balance processes. *Water Resources Research*, 30(11): 3061-3078.

Famiglietti, J.S. and Wood, E.F., 1995. Effects of spatial variability and scale on areally averaged evapotranspiration. *Water Resources Research*, 31: 699-712.

Fanok, S.F. and Wohl, E.E., 1997. Assessing the accuracy of paleohydrologic indicators, Harpers Ferry, West Virginia. *Journal of the American Water Resources Association*, 33(5): 1091-1102.

Faulkner, D. and Wass, R., 2005. Flood estimation by continuous simulation in the Don catchment, South Yorkshire, UK. *Water and Environment Journal*, 19(2): 78-84.

Feidas, H., Cartalis, C. and Lagouvardos, C., 2002. Temporal simulation of diurnal temperature and relative humidity at a forested mountainous site in Attica, Greece. *International Journal of Wildland Fire*, 11(2): 95-106.

Flury, M., Fluhler, H., Jury, W.A. and Levenberger, J., 1994. Susceptibility of soils to preferential flow of water: A field study. *Water Resources Research*, 30: 1945-54.

Folland, C.K. et al., 2001. Observed climate variability and change. In: J.T. Houghton et al. (Editors), *Climate change 2001: the scientific basis, contribution of Working Group I to the third assessment report of the Intergovernmental Panel on Climate Change*. Cambridge University Press, Cambridge, pp. 99-181.

Forsyth, T., 2005. Land Use Impacts on Water Resources. In: M.G. Anderson and J.J. McDonnell (Editors), *Encyclopedia of Hydrological Sciences*. Wiley, Chichester, pp. 2911-2924.

Franchini, M., Hashemi, A.M. and O'Connell, P.E., 2000. Climatic and basin factors affecting the flood frequency curve: PART II - A full sensitivity analysis based on the continuous simulation approach combined with a factorial experimental design. *Hydrology and Earth System Sciences*, 4(3): 483-498.

Franks, S.W., Gineste, P., Beven, K. and Merot, P., 1998. On constraining the predictions of a distributed model: The incorporation of fuzzy estimates of saturated areas into the calibration process. *Water Resources Research*, 34(4): 787-797.

Frappart, F., Seyler, F., Martinez, J.-M., Leon, J.G. and Cazenave, A., In Press. Floodplain water storage in the Negro River basin estimated from microwave remote sensing of inundation area and water levels. *Remote Sensing of Environment*.

Freer, J., Beven, K. and Ambroise, B., 1996. Bayesian estimation of uncertainty in runoff prediction and the value of data: An application of the GLUE approach. *Water Resources Research*, 32(7): 2161-2173.

Freer, J., McDonnell, J.J., Beven, K., Peters, N.E., Burns, D.A., Hooper, R.P., Aulenbach, B. & Kendall, C., 2002. The role of bedrock topography on subsurface storm flow. *Water Resources Research*, 38(12): 1269.

Freer, J.E., McMillan, H.K., McDonnell, J.J. and Beven, K.J., 2004. Constraining dynamic TOPMODEL responses for imprecise water table information using fuzzy rule based performance measures. *Journal of Hydrology*, 291: 254-277.

Freeze, R.A., 1980. A stochastic conceptual analysis of rainfall-runoff processes on a hillslope. *Water Resources Research*, 16: 391-408.

Freeze, R.A. and Harlan, R.L., 1969. Blueprint for a physically-based digitally simulated hydrological response model. *Journal of Hydrology,* 9: 237-258.

French, J.R., 2003. Airborne LIDAR in support of geomorphological and hydraulic modelling. *Earth Surface Processes and Landforms*, 28(3): 321-335.

Gelegenis, 1999. Estimation of hourly temperature data from their monthly average values: case study of Greece. *Renewable Energy*, 18: 49-60.

Giddens, A., 1998. *The Third Way*. Polity Press, Cambridge.

Gilard, o., 1996. Flood risk management: Risk cartography for objective negotiation. In: J.J. Bogardi and Z.W. Kundzewicz (Editors), *Risk, Reliability, Uncertainty, and Robustness of Water Resources Systems*. Cambridge University Press, Cambridge, pp. 47-52.

Goel, N.K., Kurothe, R.S., Mathur, B.S. and Vogel, R.M., 2000. A derived flood frequency distribution for correlated rainfall intensity and duration. *Journal of Hydrology*, 228: 56-67.

Gouweleeuw, B.T., Thielen, J., Franchello, G., De Roo, A.P.J. and Buizza, R., 2005. Flood forecasting using medium-range probabilistic weather prediction. *Hydrology and Earth System Sciences*, 9(4): 365-380.

Grayson, R. and Bloschl, G., 2000a. Spatial Modelling of Catchment Dynamics. In: R. Grayson and G. Bloschl (Editors), *Spatial Patterns in Catchment Hydrology: Observations and Modelling*. Cambridge University Press, Cambridge, pp. 51-81.

Grayson, R. and Bloschl, G., 2000b. Spatial Observations and Interpolation. In: R. Grayson and G. Bloschl (Editors), *Spatial Patterns in Catchment Hydrology: Observations and Modelling*. Cambridge University Press, Cambridge, pp. 17-50.

Grayson, R. and Bloschl, G., 2000c. Spatial Processes, Organisation and Patterns. In: R. Grayson and G. Bloschl (Editors), *Spatial Patterns in Catchment Hydrology: Observations and Modelling*. Cambridge University Press, Cambridge, pp. 1-16.

Grayson, R.B. and Western, A.W., 1998. Towards areal estimation of soil water content from point measurements: time and space stability of mean response. *Journal of Hydrology*, 207(1-2): 68-82.

Green, C., Van der Veen, A., Wiersta, E. and Penning-Rowsell, E., 1994. Vulnerability Refined: Analysing Full Flood Impacts. In: E. Penning-Rowsell and M. Fordham (Editors), *Floods across Europe: hazard assessment, modelling and management*. Middlesex University Press, London.

Grimshaw, S.D., 1993. Computing Maximum Likelihood Estimates for the Generalized Pareto Distribution. *Technometrics*, 35(2): 185-191.

Groisman, P.Y. et al., 2004. Contemporary changes of the hydrological cycle over the contiguous United States: Trends derived from in situ observations. *Journal of Hydrometeorology*, 5(1): 64-85.

Guenni, L., Hutchinson, M.F., Hogarth, W., Rose, C.W. and Braddock, R., 1996. A model for seasonal variation of rainfall at Adelaide and Turen. *Ecological Modelling*, 85(2-3): 203-217.

Guo, S.L. and Cunnane, C., 1991. Evaluation of the usefulness of historical and paleological floods in quantile estimation. *Journal of Hydrology*, 129: 245-262.

Gupta, V.K. and Sorooshian, S., 1998. Toward improved calibration of hydrologic models: Multiple and noncommensurable measures of information. *Water Resources Research*, 34(4): 751-763.

Gupta, V.K. and Waymire, E.C., 1998. Spatial Variability and Scale Invariance in Hydrologic Representation. In: G. Sposito (Editor), *Scale Dependence and Scale Invariance*. Cambridge University Press, Cambridge, pp. 61-87.

Gupta, H.V., Sorooshian, S. and Yapo, P.O., 1998. Toward improved calibration of hydrologic models: multiple and noncommensurable measures of information. *Water Resources Research*, 34(4): 751-763.

Gupta, V.K., Beven, K. and Wagener, T., 2005. Model Calibration and Uncertainty Estimation. In: M.G. Anderson and J.J. McDonnell (Editors), *Encyclopedia of Hydrological Sciences*. Wiley, Chichester, pp. 2015-2032.

Halcrow, 2003. Audit of the Cam and Granta Hydraulic Model, Environment Agency.

Halcrow, 2004. *Rivers Cam and Granta Model Improvements: Model Construction and SOP Assessment. Final Report.*, Environment Agency.

Hall, J.W., Tarantola, S., Bates, P.D. and Horritt, M.S., 2005. Distributed Sensitivity Analysis of Flood Inundation Model Calibration. *Journal of Hydraulic Engineering*, 131(2): 117-126.

Handmer, J.W., 1990. Flood insurance and relief in the U.S. and Britain. *Natural Hazard Research*; working paper 68., Boulder.

Hansen, D.P., Jakeman, A.J., Kendall, C. and Weizu, G., 1997. Identification of internal flow dynamics in two experimental catchments. *Mathematics and Computers in Simulation*, 43(3-6): 367-375.

Hardle, W., 1991. *Smoothing Techniques, with Implementations in S*. Springer, New York.

Hardy, R.J., Bates, P.D. and Anderson, M.G., 2000. Modelling suspended sediment deposition on a fluvial floodplain using a two-dimensional dynamic finite element model. *Journal of Hydrology*, 229(3-4): 202-218.

Hart, D. and Hart, I., 2005. *The River Thames - The effect of weather and tides*.

Hashemi, A.M., Franchini, M. and O'Connell, P.E., 2000. Climatic and basin factors affecting the flood frequency curve: PART I-A simple sensitivity analysis based on the continuous simulation approach. *Hydrology and Earth System Sciences*, 4(3): 463-482.

Hebson, C. and Wood, E.F., 1982. A derived flood frequency distribution using Horton order ratios. *Water Resources Research*, 18(5): 1509–1518.

Hervouet, J.M. and Janin, J.M., 1994. Finite element algorithms for modelling flood propagation. In: P. Molinaro and L. Natale (Editors), *Modelling Flood Propagation Over Initially Dry Areas*. American Society of Civil Engineers, New York, pp. 102-113.

Hey, R.W. and Perrin, R.M.S., 1980. *Geology and Soils of Cambridgeshire*. Cambridge Natural History Society.

Holt, C.P. and Jones, J.A.A., 1996. Equilibrium and transient global, warming scenario implications for water resources in Wales. *Water Resources Bulletin*, 32(4): 711-721.

Hopmans, J.W. and Shoups, G., 2005. Soil Water Flow at Different Spatial Scales. In: M.G. Anderson and J.J. McDonnell (Editors), *Encyclopedia of Hydrological Sciences*. Wiley, Chichester, pp. 999-1010.

Hornberger, G.M. and Boyer, E.W., 1995. Recent advances in watershed modelling. *Reviews of Geophysics*, 33(949-958).

Hornberger, G.M. and Beven, K., Cosby, B.J. and Sappington, D.E., 1985. Shenandoah watershed study: calibration of a topography-based, variable contributing area hydrological model to a small forested catchment. *Water Resources Research*, 21(12): 1841-1850.

Horritt, M.S., 2000. Calibration and validation of a 2-dimensional finite element flood flow model using satellite radar imagery. *Water Resources Research*, 36(11): 3279-3291.

Horritt, M.S. and Bates, P.D., 2001a. Effects of spatial resolution on a raster based model of flood flow. *Journal of Hydrology*, 253(1-4): 239-249.

Horritt, M.S. and Bates, P.D., 2001b. Predicting floodplain inundation: raster-based modelling versus the finite-element approach. *Hydrological Processes*, 15(5): 825-842.

Horritt, M.S. and Bates, P.D., 2002. Evaluation of 1D and 2D numerical models for predicting river flood inundation. *Journal of Hydrology*, 268(1-4): 87-99.

Horritt, M.S., Mason, D.C. and Luckman, A.J., 2001. Flood boundary delineation from Synthetic Aperture Radar imagery using a statistical active contour model. *International Journal of Remote Sensing*, 22(13): 2489-2507.

Horritt, M.S., Mason, D.C., Cobby, D.M., Davenport, I.J. and Bates, P.D., 2003. Waterline mapping in flooded vegetation from airborne SAR imagery. *Remote Sensing of the Environment*, 85: 271-281.

Horton, R.E., 1945. Erosional development of streams and their drainage basin; hydrophysical approach to quantitative morphology. *Geological Society of America Bulletin*, 56: 275-370.

Hosking, J.R.M., 1990. L-Moment - Analysis and Estimation of Distributions Using Linear-Combinations of Order-Statistics. *Journal of the Royal Statistical Society Series B-Methodological*, 52(1): 105-124.

Hosking, J.R.M., Wallis, J.R. and Wood, E.F., 1985. Estimation of the generalised extreme-value distribution by the method of probability-weighted moments. *Technometrics*, 27: 251-261.

Hossain, F., Anagnostou, E.N. and Lee, K.H., 2004. A non-linear and stochastic response surface method for Bayesian estimation of uncertainty in soil moisture simulation from a land surface model. *Nonlinear Processes in Geophysics*, 11(4): 427-440.

Houghton-Carr, H., 1999. *Flood Estimation Handbook Volume 4: Restatement and application of the Flood Studies Report rainfall-runoff method*. Institute of Hydrology, Wallingford.

Hsieh, L.S., Hsu, M.H. and Li, M.H., 2006. An assessment of structural measures for flood-prone lowlands with high population density along the Keelung River in Taiwan. *Natural Hazards*, 37(1-2): 133-152.

Hulme, M. and Osborn, T.J., 1998. Precipitation sensitivity to global warming: Comparison of observations with HadCM2 simulations. *Geophysical Research Letters*, 25(17): 3379-3382.

Hunter, N.M., Horritt, M.S., Bates, P.D. and Werner, M.G.F., 2004. Theoretical and practical limits to the use of storage cell codes for flood inundation modelling. In: D. Reeve (Editor), *Flood risk assessment*. Institute of Mathematics and its Applications, Southend-on-Sea.

Huntington, T.G., 2006. Evidence for intensification of the global water cycle: Review and synthesis. *Journal of Hydrology*, 319(1-4): 83-95.

Huxtable, D., 2005. *The Lynmouth Floods of 1952, Exmoor*. Exmoor National Park Portal.

Islam, S., Entekhabi, D., Bras, R.L. and Rodriguez-Iturbe, I., 1990. Parameter estimation and sensitivity analysis for the modified Bartlett-Lewis rectangular pulses model of rainfall. *Journal of Geophysical Research*, 95(2093-2100).

Islam, N., Wallender, W.W., Mitchell, J.P., Wicks, S. and Howitt, R.E., In Press. Performance evaluation of methods for the estimation of soil hydraulic parameters and their suitability in a hydrologic model. *Geoderma*.

Ivanov, V.Y., Vivoni, E.R., Bras, R.L. and Entekhabi, D., 2004. Preserving high-resolution surface and rainfall data in operational-scale basin hydrology: a fully-distributed physically-based approach. *Journal of Hydrology*, 298(1-4): 80-111.

Jakeman, A.J. and Hornberger, G.M., 1993. How much complexity is warranted in a rainfall-runoff model? *Water Resources Research*, 29(8): 2637-2649.

Jakeman, A.J., Littlewood, I.G. and Whitehead, P.G., 1990. Computation of the instantaneous unit hydrograph and identifiable component flows with application to two small upland catchments. *Journal of Hydrology*, 117: 275-300.

Jamieson, D., 1990. Managing the Future. In: D. Scherer (Editor), *Upstream / Downstream. Issues in Environmental Ethics*. Temple, Philadelphia.

Jasper, K., Gurtz, J. and Lang, h., 2002. Advanced flood forecasting in Alpine watersheds by coupling meteorological observations and forecasts with a distributed hydrological model. *Journal of Hydrology*, 267(1-2): 40-52.

Jin, M. and Stedinger, J.R., 1989. Flood Frequency Analysis with Regional and Historical Information. *Water Resources Research*, 25: 925-936.

Karbowski, A., 1995. Statistically safe sets methodology for optimal management of resevoirs in risk situations. In: Z.W. Kundzewicz (Editor), *New Uncertainty Concepts in Hydrology and Water Resources*. Cambridge University Press, Cambridge, pp. 284-292.

Kasischke, E.S., Melack, J.M. and Dobson, M.C., 1997. The use of imaging radars for ecological applications - A review. *Remote Sensing of Environment*, 59(2): 141-156.

Katz, R.W., 2002. Statistics of Extremes in Hydrology. *Advances in Water Resources*, 25: 1287-1304.

Keys, C., 1997. The Total Flood Warning System. In: J. Handmer (Editor), *Flood Warning: Issues and Practice in Total System Design*, Middlesex University Flood Hazard Research Centre, pp. 13-22.

Kidson, R., 2004. *Extreme hydrology in the monsoon tropics: the Mae Chaem catchment, Northern Thailand*, Cambridge University.

Kidson, R. and Richards, K.S., 2005. Flood frequency analysis: assumptions and alternatives. *Progress in Physical Geography*, 29(3): 392-410.

Kidson, R., Richards, K.S. and Carling, P.A., 2005. Reconstructing the ca. 100-year flood in Northern Thailand. *Geomorphology*, 70(3-4): 279-295.

Kidson, R.L., Richards, K.S. and Carling, P.A., 2006. Hydraulic model calibration for extreme floods in bedrock-confined channels: case study from northern Thailand. *Hydrological Processes*, 20(2): 329-344.

Kindler, J. and Tyszewski, S., 1995. On the value of fuzzy concepts in hydrology and water resources management. In: Z.W. Kundzewicz (Editor), *New Uncertainty Concepts in Hydrology and Water Resources*. Cambridge University Press, Cambridge, pp. 126-132.

Kirkby, M.J., 2005. Organisation and Process. In: M.G. Anderson and J.J. McDonnell (Editors), *Encyclopedia of Hydrological Sciences*. Wiley, Chichester, pp. 41-58.

Kleinn, J. et al., 2005. Hydrologic simulations in the Rhine basin driven by a regional climate model. *Journal of Geophysical Research*-Atmospheres, 110(D4): D04102.

Klemes, V., 1986. Dilettantism in Hydrology - Transition or Destiny. *Water Resources Research*, 22(9): S177-S188.

Klemes, V., 1996. Risk analysis: The unbearable cleverness of bluffing. In: J.J. Bogardi and Z.W. Kundzewicz (Editors), *Risk, Reliability, Uncertainty, and Robustness of Water Resources Systems*. Cambridge University Press, Cambridge, pp. 22-29.

Knight, R., 2001. Ground penetrating radar for environmental applications. *Annual Review of Earth and Planetary Sciences*, 29: 229-255.

Konikow, L.F. and Bredehoeft, J.D., 1992. Ground-water models cannot be validated. *Advances in Water Resources*, 15(1): 75-83.

Koster, R.D. and Suarez, M.J., 1992. Modelling the land surface boundary in climate models as a composite of independent vegetation stands. *Journal of Geophysical Research* - Atmospheres, 97(D3): 2697-2715.

Kotwicki, V. and Kundzewicz, Z.W., 1995. Hydrological Uncertainty - floods of Lake Eyre. In: Z.W. Kundzewicz (Editor), *New Uncertainty Concepts in Hydrology and Water Resources*. Cambridge University Press, Cambridge, pp. 32-37.

Koutsoyiannis, D. and Mamassis, N., 2001. On the representation of hyetograph characteristics by stochastic rainfall models. *Journal of Hydrology*, 251: 65-87.

Kozlowski, A. and Lodzinski, A., 1995. Risk assessment in control of reservoir systems. In: Z.W. Kundzewicz (Editor), *New Uncertainty Concepts in Hydrology and Water Resources*. Cambridge University Press, Cambridge, pp. 293-298.

Krzysztofowicz, R., 1996. Probabilistic hydrometeorological forecasting. In: J.J. Bogardi and Z.W. Kundzewicz (Editors), *Risk, Reliability, Uncertainty, and Robustness of Water Resources Systems*. Cambridge University Press, Cambridge, pp. 41-45.

Kuchment, L.S. and Gelfan, A.N., 2002. Estimation of extreme flood characteristics using physically based models of runoff generation and stochastic meteorological inputs. *Water International*, 27(1): 77-86.

Kuczera, G. and Mroczkowski, M., 1998. Assessment of hydrologic parameter uncertainty and the worth of multiresponse data. *Water Resources Research*, 34(6): 1481-1489.

Kundzewicz, Z.W., 1995. Hydrological Uncertainty in Perspective. In: Z.W. Kundzewicz (Editor), *New Uncertainty Concepts in Hydrology and Water Resources*. Cambridge University Press, Cambridge, pp. 3-12.

Kurothe, R.S., Goel, N.K. and Mathur, B.S., 1997. Derived Flood Frequency Distribution for correlated rainfall intensity and duration. *Water Resources Research*, 33(9): 2103-2107.

Lamb, R., 1999. Calibration of a conceptual rainfall-runoff model for flood frequency estimation by continuous simulation. *Water Resources Research*, 35(10): 3103-3114.

Lamb, R. and Kay, A.L., 2004. Confidence intervals for a spatially generalized, continuous simulation flood frequency model for Great Britain. *Water Resources Research*, 40(7).

Lamb, R., Beven, K. and Myrabo, S., 1998. Use of spatially distributed water table observation to constrain uncertainty in a rainfall-runoff model. *Advances in Water Resources*, 22(4): 305-317.

Lane, S.N., 2005. Roughness - time for a re-evaluation. *Earth Surface Processes and Landforms*, 30: 251-253.

Lane, S.N. and Bates, P.D., 2000. Introduction. In: P.D. Bates and S.N. Lane (Editors), High Resolution Flow Modelling in Hydrology and *Geomorphology*. Wiley, Chichester.

Lane, L.J., Hernandez, M. and Nichols, M., 1997. Processes controlling sediment yield from watersheds as functions of spatial scale. *Environmental Modelling and Software*, 12(4): 355-369.

Lane, S.N., James, T.D. and Pritchard, H., 2003. Photogrammetric and laser altimetric reconstruction of water levels for extreme flood event analysis. *Photogrammetric Record*, 18(104): 293-307.

Lane, S.N., Brookes, C.J., Kirkby, A.J. and Holden, J., 2004. A network-index based version of TOPMODEL for use with high-resolution digital topographic data. *Hydrological Processes*, 18(1): 191-201.

Leung, L.R. and Ghan, S.J., 1999. Pacific Northwest climate sensitivity simulated by a regional climate model driven by a GCM. Part 1: Control Simulations. *Journal of Climate*, 12: 2010-2030.

Liang, X., Lettenmaier, D.P., Wood, E.F. and Burges, S.J., 1994. A simple hydrologically based model of land surface water and energy fluxes for general circulation models. *Journal of Geophysical Research*, 99(D7): 14415-14428.

Linton Parish Council, 1982. *Linton: The Story of a Market Town*.

Liu, Y.B., De Smedt, F., Hoffmann, L. and Pfister, L., 2004. Assessing land use impacts on flood processes in complex terrain by using GIS and modelling approach. *Environmental Modelling & Assessment*, 9(4): 227-235.

Loukas, A., 2002. Flood frequency estimation by a derived distribution procedure. *Journal of Hydrology*, 255((1-4)): 69-89.

Lund, J.R., 2002. Floodplain planning with risk-based optimization. *Journal of Water Resources Planning and Management-Asce*, 128(3): 202-207.

Madsen, H., Pearson, C.P. and Rosbjerg, D., 1997. Comparison of Annual Maximum Series and Partial Duration Series methods for modelling extreme hydrological events. 2:Regional Modelling. *Water Resources Research*, 33(4): 75-769.

MAFF, 2001. *Flood and Coastal Defence Project Appraisal Guidance - Overview*, MAFF, London.

MAFF & the Welsh Office, 1993. *Strategy for Flood and Coastal Defence for England and Wales*: PB 1471.

Marchette, D.J., Priebe, C.E., Rogers, G.W. and Solka, J.L., 1996. Filtered kernel density estimation. *Computational Statistics*, 11(2): 95-112.

Marco, J.B., 1992. Flood Risk Mapping. In: G. Rossi, N. Harmancioglu and V. Yevjevich (Editors), *Coping with Floods*. Kluwer, Dordrecht, pp. 353-373.

Marks, K.J. and Bates, P.D., 2000. Integration of high-resolution topographic data with floodplain flow models. *Hydrological Processes*, 14: 2109-2122.

Marr, J.E. and Shipley, A.E.E., 1904. *Natural History of Cambridgeshire*. Cambridge University Press, Cambridge.

Marron, J.S. and Nolan, D., 1988. Canonical kernels for density estimation. *Statistics & Probability Letters*, 7(3): 195-199.

Marshall, L., Nott, D. and Sharma, A., 2004. A comparative study of Markov chain Monte Carlo methods for conceptual rainfall-runoff modelling. *Water Resources Research*, 40(2): W02501.

Martins, E.S. and Stedinger, J.R., 2000. Generalized maximum-likelihood generalized extreme-value quantile estimators for hydrologic data. *Water Resources Research*, 36: 737-744.

Martins, E.S. and Stedinger, J.R., 2001. Historical information in a generalized maximum likelihood framework with partial duration and annual maximum series. *Water Resources Research*, 37(10): 2559-2567.

Maskey, S., Guinot, V. and Price, R.K., 2004. Treatment of precipitation uncertainty in rainfall-runoff modelling: a fuzzy set approach. *Advances in Water Resources*, 27(9): 889-898.

Mason, D.C., Cobby, D.M., Horritt, M.S. and Bates, P.D., 2003. Floodplain friction parameterization in two-dimensional river flood models using vegetation heights derived from airborne scanning laser altimetry. *Hydrological Processes*, 17(9): 1711-1732.

McGlynn, B.L., McDonnel, J.J. and Brammer, D.D., 2002. A review of the evolving perceptual model of hillslope flowpaths at the Maimai catchment, New Zealand. *Journal of Hydrology*, 257(1-4): 1-26.

McMillan, H.K., 2002. *The estimation of discharges in ungauged sub-catchments of the River Eden in Cumbria*. Unpublished Masters Thesis, Lancaster University.

Melching, C.S., 1995. Reliability Estimation. In: V.P. Singh (Editor), *Computer Models of Watershed Hydrology*. Water Resources Publications, Highlands Ranch, pp. 69-118.

Merz, B., Kreibich, H., Thieken, A. and Schmidtke, R., 2004. Estimation uncertainty of direct monetary flood damage to buildings. *Natural Hazards and Earth System Sciences*, 4(1): 153-163.

Met Office, 2004. *Three year National Meteorological Programme 2004/5-2006/7*. http://www.meto.gov.uk/corporate/nmp/3_year_Met_prog.pdf

Met Office, 2006. *Heavy rainfall - east UK*. http://www.met-office.gov.uk/climate/uk/interesting/oct2001rain2.html

Metcheck, 2006. *Metcheck GFS Ensembles*. http://metcheck.com/V40/UK/FREE/ensembles.asp

Meteo France, 2006. *Indice de confiance*. http://www.meteofrance.com/FR/glossaire/designation/1036_curieux_view.jsp

Moffiet, T., Mengersen, K., Witte, C., King, R. and Denham, R., 2005. Airborne laser scanning: Exploratory analysis indicates potential variables for classification of individual trees or forest stands according to species. *ISPRS Journal of Photogrammetry and Remote Sensing*, 59(5): 289-309.

Moglen, G.E., Eltahir, E.A.B. and Bras, R.L., 1998. On the sensitivity of drainage density to climate change. *Water Resources Research,* 34: 855-862.

Montgomery, D.R. and Dietrich, W.E., 1992. Channel initiation and the problem of landscape scale. *Science,* 255: 826-830.

Moore, R.J., 1996. Aspects of uncertainty, reliability, and risk in flood forecasting systems incorporating weather radar. In: J.J. Bogardi and Z.W. Kundzewicz (Editors), *Risk, Reliability, Uncertainty, and Robustness of Water Resources Systems*. Cambridge University Press, Cambridge, pp. 30-40.

Moore, R.J. and Clarke, R.T., 1981. A distribution function approach to rainfall-runoff modelling. *Water Resourses Research*, 17: 1367-1382.

Morris, D.G. and Flavin, R.W., 1996. *Flood Risk Map for England and Wales: IH Report 130*, Institute of Hydrology, Wallingford.

Morss, R.E., Wilhelmi, O.V., Downton, M.W. and Gruntfest, E., 2005. Flood risk, uncertainty, and scientific information for decision making - Lessons from an interdisciplinary project. *Bulletin of the American Meteorological Society*, 86(11): 1593-+.

Moughamian, M.S., McLaughlin, D.B. and Bras, R.L., 1987. Estimation of flood frequency: an evaluation of two derived distribution procedures. *Water Resources Research*, 23(7): 1309–1319.

Muhlherr, I.H. and Hiscock, K.M., 1997. A preliminary assessment of nitrous oxide in Chalk groundwater in Cambridgeshire, U.K. *Applied Geochemistry*, 12: 797-802.

Naden, P.S., 1992. Analysis and use of peaks-over-threshold data in flood estimation, BHR Group Conference on *Floods and Flood Management*, Florence, pp. 13.

Naef, F., Scherrer, S. and Weiler, M., 2002. A process based assessment of the potential to reduce flood runoff by land use change. *Journal of Hydrology*, 267(1-2): 74-79.

Nash, J.E. and Sutcliffe, J.V., 1970. River flow forecasting through conceptual models. 1. A discussion of principles. *Journal of Hydrology*, 10: 282-290.

Nash, J.E., 1959. Systematic determination of unit hydrograph parameters. *Journal of Geophysical Research*, 64: 111-115.

National River Flow Archive, N., 2002. *Concise Register of Gauging Stations*.

Newson, M., 1975. *Flooding and Flood Hazard in the U.K.* Oxford University Press, Oxford.

Newson, M. and Chalk, L., 2005. Public Participation in River Basin Planning and Management: Quality-of-Life Capital as an Information Aid to Sustainable Decisions. In: M.G. Anderson and J.J. McDonnell (Editors), *Encyclopedia of Hydrological Sciences*. Wiley, Chichester, pp. 2973-2985.

Nicholas, A.P. and Mitchell, C.A., 2003. Numerical simulation of overbank processes in topographically complex floodplain environments. *Hydrological Processes*, 17: 727-746.

Nikuradse, J., 1933. Laws of Flow in Rough Pipes. Verein deutscher Ingenieure, Forschungsheft. Quoted in Chow, V.T. (1959)(361).

Oberstadler, R., Honsch, H. and Huth, D., 1997. Assessment of the mapping capabilities of ERS-1 SAR data for flood mapping: A case study in Germany. *Hydrological Processes*, 11(10): 1415-1425.

Ocampo, C.J., Sivapalan, M. and Oldham, C.E., In Press. Field exploration of coupled hydrological and biogeochemical catchment responses and a unifying perceptual model. *Advances in Water Resources*.

O'Connell, D.R.H., 2005. Nonparametric Bayesian flood frequency estimation. *Journal of Hydrology*, 313(1-2): 79-96.

O'Connell, D.R.H., Ostenaa, D.A., Levish, D.R. and Klinger, R.E., 2002. Bayesian flood frequency analysis with paleohydrologic bound data. *Water Resources Research*, 38(5).

ODPM, 2000. *Planning Policy Guidance 3: Housing*. http://www.odpm.gov.uk/index.asp?id=1143943#P19_1240

ODPM, 2004. *Planning Policy Guidance 25: Development and Flood Risk*.

ODPM, 2005. *News Release: Strengthened planning policy for flood risk areas will ensure sustainable development*. http://www.odpm.gov.uk/index.asp?id=1002882&PressNoticeID=1852

Office of Science and Technology, 2004. *Foresight: Future Flooding*.

Olsson, J. and Burlando, P., 2002. Reproduction of temporal scaling by a rectangular pulses rainfall model. *Hydrological Processes*, 16(3): 611-630.

Onof, C. and Wheater, H.S., 1993. Modelling of British Rainfall using a random parameter Bartlett-Lewis rectangular pulse model. *Journal of Hydrology*, 149: 67-95.

Onof, C. and Wheater, H.S., 1994. Improvements to the modelling of British rainfall using a modified random parameter Barlett-Lewis rectangular pulse model. *Journal of Hydrology*, 157: 177-195.

Onof, C., Faulkner, D. and Wheater, H.S., 1996. Design rainfall modelling in the Thames catchment. *Hydrological Sciences Journal-Journal Des Sciences Hydrologiques*, 41(5): 715-733.

Oreskes, N. and Belitz, K., 2001. Philosophical Issues in Model Assessment. In: M.G. Anderson and P.D. Bates (Editors), *Model Validation: Perspectives in Hydrological Science*. Wiley, Chichester, pp. 23-42.

Orr, H.G. and Carling, P.A., 2006. Hydro-climatic and land use changes in the river Lune catchment, North West England, implications for catchment management. *River Research and Applications*, 22(2): 239-255.

Osborn, T.J. and Hulme, M., 2002. Evidence for trends in heavy rainfall events over the UK. *Phil. Trans. R. Soc. Lond. A*, 360(1796): 1313-1325.

Pandit, A. and Gopalakrishnan, G., 1996. Estimation of annual storm runoff coefficients by continuous simulation. *Journal of Irrigation and Drainage Engineering-Asce*, 122(4): 211-220.

Pappenberger, F., Beven, K., Hunter, N., Bates, P., Gouweleeuw, B., Thielen, J. & de Roo, A., 1999. *A European Flood Forecasting System: The Implementation of a Methodology for Estimating the Predictive Uncertainty of Flood Forecasts.*

Pappenberger, F., Beven, K.J., Hunter, N.M., Bates, P.D., Gouweleeuw, B.T., Thielen, J. & de Roo, A.P.J., 2005a. Cascading model uncertainty from medium range weather forecasts (10 days) through a rainfall-runoff model to flood inundation predictions within the European Flood Forecasting System (EFFS). *Hydrology and Earth System Sciences*, 9(4): 381-393.

Pappenberger, F., Beven, K., Horritt, M.S. and Blazkova, S., 2005b. Uncertainty in the calibration of effective roughness parameters in HEC-RAS using inundation and downstream level observations. *Journal of Hydrology*, 302(1-4): 46-69.

Park, B.U. and Turlach, B.A., 1992. Practical performance of several data driven bandwidth selectors. *Computational Statistics*, 7: 251-270.

Parker, D.J. and Handmer, J.W., 1998. The Role of Unofficial Flood Warning Systems. *Journal of Contingencies and Crisis Management*, 6(1): 45-58.

Pask, N., 1992. Washland management in the Ouse Washes Conservation Area. In: A. Saul (Editor), *Floods and Flood Management*. Kluwer, Dordrecht.

Pauwels, V.R.N., Hoeben, R., Verhoest, N.E.C. and De Troch, F.P., 2001. The importance of the spatial patterns of remotely sensed soil moisture in the improvement of discharge predictions for small-scale basins through data assimilation. *Journal of Hydrology*, 251(1-2): 88-102.

Penning-Rowsell, E. and Parker, D.J., 1973. *Control of floodplain development - A preliminary analysis*. Flood Hazard Research Project, Report 4., Middlesex Polytechnic.

Perrin, C., Michel, C. and Andreassian, V., 2001. Does a large number of parameters enhance model performance? Comparative assessment of common catchment model structures on 429 catchments. *Journal of Hydrology*, 242(3-4): 275-301.

Peters, R.T. and Evett, S.R., 2004. Modelling Diurnal Canopy Temperature Dynamics Using One-Time-Of-Day Measurements And A Reference Temperature Curve. *Agronomy Journal*, 96: 1553-1561.

Pilling, C. and Jones, J.A.A., 1999. High resolution climate change scenarios: implications for British runoff. *Hydrological Processes*, 13: 2877-2895.

Pilon, P.J. and Adamowski, K., 1993. Asymptotic Variance of Flood Quantile in Log Pearson Type-Iii Distribution with Historical Information. *Journal of Hydrology*, 143(3-4): 481-503.

Plate, E.J., 1995. Stochastic approach to non-point pollution of surface waters. In: Z.W. Kundzewicz (Editor), *New Uncertainty Concepts in Hydrology and Water Resources*. Cambridge University Press, Cambridge, pp. 273-283.

Plate, E.J., 1996. Risk management for hydraulic systems under hydrological loads. In: J.J. Bogardi and Z.W. Kundzewicz (Editors), *Risk, Reliability, Uncertainty, and Robustness of Water Resources Systems*. Cambridge University Press, Cambridge, pp. 209-219.

Post, D.A. and Jakeman, A.J., 1996. Relationships between physical attributes and hydrological response characteristics in small Australian mountain ash catchments. *Hydrological Processes*, 10: 877-892.

PUB Science Steering Group, 2003. *PUB Science and Implementation Plan,* IAHS.

Ragab, R., Finch, J. and Harding, J., 1997. Estimation of groundwater recharge to chalk and sandstone aquifers using simple soil models. *Journal of Hydrology*, 190(1-2): 19-41.

Rasid, H. and Haider, W., 2002. Floodplain residents' preferences for non-structural flood alleviation measures in the Red River basin, Manitoba, Canada. *Water International*, 27(1): 132-151.

Raupach, M.R. and Finnigan, J.J., 1995. Scale issues in boundary-layer meteorology: surface energy balances in heterogeneous terrain. In: J.D. Kalma and M. Sivapalan (Editors), *Scale issues in Hydrological Modelling*. Wiley, New York, pp. 354-368.

Reed, D., 1992. Some notes on generalised methods of flood estimation in the United Kingdom. In: G. Rossi, N. Harmancioglu and V. Yevjevich (Editors), *Coping with Floods*. Kluwer, Dordrecht.

Reed, D., 1999. *Flood Estimation Handbook Volume 1: Overview*. Institute of Hydrology, Wallingford.

Reed, D.W., 2002. Reinforcing Flood Risk Estimation. *Phil. Trans. R. Soc. Lond. A*, 360: 1373-1387.

Reeves, M. and Miller, E.E., 1975. Estimating infiltration for erratic rainfall. *Water Resources Research*, 11: 102-110.

Refsgaard, J.C., 1997. Parameterisation, calibration and validation of distributed hydrological models. *Journal of Hydrology*, 198: 69-97.

Reis, D.S. and Stedinger, J.R., 2005. Bayesian MCMC flood frequency analysis with historical information. *Journal of Hydrology*, 313(1-2): 97-116.

Reitano, B., 1992. Floodin vulnerability analysis at basin-wide scale. In: G. Rossi, N. Harmancioglu and V. Yevjevich (Editors), *Coping with Floods*. Kluwer, Dordrecht.

Reynard, N.S., Prudhomme, C. and Crooks, S.M., 1998. *The potential impacts of climate change on the flood characteristics of a large catchment in the UK*, Second International Conference on Climate and Water. Finland, Espoo.

Reynard, N.S., Prudhomme, C. and Crooks, S.M., 2001. The flood characteristics of large UK Rivers: Potential effects of changing climate and land use. *Climatic Change*, 48(2-3): 343-359.

Richards, K., Brasington, J. and Hughes, F., 2002. Geomorphic dynamics of floodplains: ecological implications and a potential modelling strategy. *Freshwater Biology*, 47(4): 559-579.

Rinaldo, A. and Rodriguez-Iturbe, I., 1998. Scaling in River Networks. In: G. Sposito (Editor), *Scale Dependence and Scale Invariance*. Cambridge University Press, Cambridge, pp. 61-87.

Roberts, G., 1998. The effects of possible future climate change on evaporation losses from four contrasting UK water catchment areas. *Hydrological Processes*, 12: 727-739.

Robinson, M. et al., 1997. Land Use Change. In: M. Acreman (Editor), *The Hydrology of the UK*. Routledge, London, pp. 30-54.

Robson, A.J., 2002. Evidence for trends in UK flooding. *Phil. Trans. R. Soc. Lond. A*, 360(1796): 1327-1343.

Robson, A. and Reed, D., 1999. *Flood Estimation Handbook Volume 3: Statistical procedures for flood frequency estimation*. Institute of Hydrology, Wallingford.

Robson, A.J., Jones, T.K., Reed, D.W. and Bayliss, A.C., 1998. A study of national trend and variation in UK floods. *International Journal of Climatology,* 18(2): 165-182.

Rodriguez-Iturbe, I., Gupta, V.K. and Waymire, E., 1984. Scale Considerations in the Modelling of Temporal Rainfall. *Water Resources Research,* 20(11): 1611-1619.

Rodriguez-Iturbe, I., Cox, D.R., Isham, F.R.S. and Isham, V., 1987. Some models for rainfall based on stochastic point processes. *Proc. R. Soc. Lond. A.*, 410: 269-288.

Rodriguez-Iturbe, I., Cox, D.R. and Isham, V., 1988. A Point Process Model for Rainfall - Further Developments. *Proc. R. Soc. Lond. A.*, 417(1853): 283-298.

Romanowicz, R. and Beven, K., 2003. Estimation of flood inundation probabilities as conditioned on event inundation maps. *Water Resources Research*, 39(3): 1061-1073.

Romanowicz, R.J., Dooge, J.C.I. and O'Kane, J.P., 1995. Spatial variability of evaporation from the land surface - random initial conditions. In: Z.W. Kundzewicz (Editor), *New Uncertainty Concepts in Hydrology and Water Resources*. Cambridge University Press, Cambridge, pp. 197-205.

Romanowicz, R., Beven, K. and Tawn, J., 1996. Bayesian calibration of flood inundation models. In: M.G. Anderson, D.E. Walling and P.D. Bates (Editors), *Floodplain Processes*. Wiley, Chichester.

Rosso, R. and Rulli, M.C., 2002. An integrated simulation method for flash-flood risk assessment: 2. Effects of changes in land-use under a historical perspective. *Hydrology and Earth System Sciences*, 6(2): 285-294.

Rumsby, B.T. and Macklin, M.G., 1994. Channel and Floodplain response to recent abrupt climate-change - the Tyne basin, northern England. *Earth Surface Processes and Landforms*, 19(6): 499-515.

Salas, J.B., Wohl, E.E. and Jarrett, R.D., 1992. Determination of flood characteristics using systematic, historical and paleoflood data. In: G. Rossi, N. Harmancioglu and V. Yevjevich (Editors), *Coping with Floods*. Kluwer, Dordrecht.

Saraiva, M.d.G., Pinto, P., Rabaca, J., Ramos, A. and Revez, M., 1992. *Protection, Reclamation and Improvement of small watercourses in the suburbs of Evora, Portugal, The Ecological Basis for River Mangement*, Leicester, U.K.

Sattler, K. and Feddersen, H., 1999. *A European Flood Forecasting System: Study on the treatment of uncertainties in limited-area NWP rainfall using different ensemble approaches.* http://effs.wldelft.nl/

Schmugge, T.J., Kustas, W.P., Ritchie, J.C., Jackson, T.J. and Rango, A., 2002. Remote sensing in hydrology. *Advances in Water Resources*, 25(8-12): 1367-1385.

Schultz, G.A., 1988. Remote sensing in hydrology. *Journal of Hydrology*, 100(1-3): 239-265.

Scott, D.W., 1992. *Multivariate Density Estimation: Theory, Practice and Visualization*. Wiley, Chichester.

Seaman-Turner, G.W., 1984. *A walk around Linton*.

Seaman-Turner, G.W., 1987. *Linton: An Early Market Town*.

Sear, D., Wilcock, D., Robinson, M. and Fisher, K., 1997. River Channel Modification in the UK. In: M. Acreman (Editor), *The Hydrology of the UK*. Routledge, London, pp. 55-81.

Sear, D.A., Armitage, P.D. and Dawson, F.H., 1999. Groundwater Dominated Rivers. *Hydrological Processes*, 13(3): 255-276.

Sefton, C.E.M. and Boorman, D.B., 1997. A regional investigation of climate change impacts on UK streamflows. *Journal of Hydrology*, 195: 26-44.

Sefton, C.E.M. and Howarth, S.M., 1998. Relationships between dynamic response characteristics and physical descriptors of catchments in England and Wales. *Journal of Hydrology*, 211: 1-16.

Seibert, J. and McDonnell, J.J., 2002. On the dialog between experimentalist and modeler in catchment hydrology: Use of soft data for multicriteria model calibration. *Water Resources Research*, 38(11): 1241.

Shakya, N.M. and Chander, S., 1998. Modelling of hillslope runoff processes. *Environmental Geology*, 35(2-3): 115-123.

Sharif, H.O., Yates, D., Roberts, R. and Mueller, C., 2006. The use of an automated nowcasting system to forecast flash floods in an urban watershed. *Journal of Hydrometeorology*, 7(1): 190-202.

Sheffer, N.A. et al., 2003. Paleofloods and historical floods of the Ardeche River, France. *Water Resources Research*, 39(12).

Shige-Eda, M. and Akiyama, J., 2003. Numerical and experimental study on two-dimensional flood flows with and without structures. *Journal of Hydraulic Engineering*, 129(10): 817-821.

Shorter, J.A. and Rabitz, H., 1997. Risk analysis by the guided Monte Carlo technique. Journal of Statistical Computation and Simulation, 57(1-4): 321-336.

Shuttleworth, W.J., 1988. Macrohydrology - the new challenge for process hydrology. *Journal of Hydrology*, 100: 31-56.

Silberstein, R.P., In Press. Hydrological models are so good, do we still need data? *Environmental Modelling and Software*.

Silverman, B.W., 1982. Kernel Density Estimation using the Fast Fourier Transform. *Journal of the Royal Statistical Society Series C*, 31(1): 93-99.

Silverman, B.W., 1986. *Density estimation for statistics and data analysis. Monographs on statistics and applied probability*. Chapman and Hall, London.

Simonovic, S.P. and Ahmad, S., 2005. Computer-based model for flood evacuation emergency planning. *Natural Hazards*, 34(1): 25-51.

Singh, V.P.E. (Editor), 1995. *Computer Models of Watershed Hydrology*. Water Resources Publications, Highlands Ranch.

Sivapalan, M., 2005. Pattern, Process and Function: Elements of a Unified Theory of Hydrology at the Catchment Scale. In: M.G. Anderson and J.J. McDonnell (Editors), *Encyclopedia of Hydrological Sciences*. Wiley, Chichester, pp. 193-219.

Sivapalan, M. and Wood, E.F., 1987. A multidimensional model of nonstationary space-time rainfall at the catchment scale. *Water Resources Research*, 22: 1289-1299.

Sklash, M.G. and Farvolden, R.N., 1979. The role of groundwater in storm runoff. *Journal of Hydrology*, 43: 43-65.

Smith, R.L., 1999. *Trends in Rainfall Extremes*. www.stat.unc.edu/faculty/rs/papers/RLS_Papers.html

Smith, R.L., 2001. Extreme value statistics in meteorology and the environment., *Environmental Statistics*.

Smithers, J.C., Pegram, G.G.S. and Schulze, R.E., 2002. Design rainfall estimation in South Africa using Bartlett–Lewis rectangular pulse rainfall models. *Journal of Hydrology*, 258(1-4): 83-99.

Sorooshian, S. and Dracup, J.A., 1980. Stochastic parameter estimation procedures for hydrologic rainfall-runoff models: correlated and heteroscedastic error cases. *Water Resources Research*, 16(2): 430-442.

Sorooshian, S. and Gupta, V.K., 1995. Model Calibration. In: V.P. Singh (Editor), *Computer Models of Watershed Hydrology*. Water Resource Publications, Highlands Ranch.

South Cambridgeshire District Council, S., 2001. *Contaminated Land strategy*.

Spear, R.C., Grieb, M. and Shang, N., 1994. Parameter uncertainty and interaction in complex environmental models. *Water Resources Research*, 30(11): 3159-3169.

Spencer, P., 2005. *HiFlows-UK*. The Environment Agency.

Staeger, T., Grieser, J. and Schonwiese, C.D., 2003. Statistical separation of observed global and European climate data into natural and anthropogenic signals. *Climate Research*, 24(1): 3-13.

Staff, E., 1946. *Basin of the River Cam: A Geographical Survey of Cambridgeshire and the Adjoining Counties around the Rivers Cam, Granta and Bourn Brook*.

Stedinger, J.R. and Cohn, T.A., 1986. Flood frequency analysis with historical and paleoflood information. *Water Resources Research*, 22(5): 785-793.

Steel, M.E., Black, A.R., Werrity, A. and Littlewood, I.G., 1999. Reassessment of flood risk for Scottish rivers using synthetic runoff data. *Hydrological Extremes: Understanding, Predicting, Mitigating*. IAHS publication No. 255., Wallingford.

Steers, J.A.E., 1965. *The Cambridge Region*. The British Association for the Advancement of Science, Cambridge.

Strupczewski, W.G. and Mitosek, H.T., 1995. Some aspects of hydrological design under non-stationarity. In: Z.W. Kundzewicz (Editor), *New Uncertainty Concepts in Hydrology and Water Resources*. Cambridge University Press, Cambridge, pp. 39-44.

Sullivan, A., Ternan, J.L. and Williams, A.G., 2004. Land use change and hydrological response in the Camel catchment, Cornwall. *Applied Geography*, 24(2): 119-137.

Tarrant, O., Todd, M., Ramsbottom, D. and Wicks, J., 2005. 2D floodplain modelling in the tidal Thames - Addressing the residual risk. *Water and Environment Journal*, 19(2): 125-134.

Taylor, C., 1973. *Cambridgeshire Landscape: Cambridgeshire and the Southern Fens*. Hodder and Stoughton, London.

Thorndycraft, V.R. et al., 2005. A long-term flood discharge record derived from slackwater flood deposits of the Llobregat River, NE Spain. *Journal of Hydrology*, 313(1-2): 16-31.

Tollan, A., 2002. Land-use change and floods: what do we need most, research or management? *Water Science and Technology*, 45(8): 183-190.

Troch, P.A., Smith, J.A., Wood, E.F. and de Troch, F.P., 1994. Hydrologic controls of large floods in a small basin: central Appalachian case study. *Journal of Hydrology*, 156: 285:309.

Troutman, B.M., 1983. Runoff prediction errors and bias in parameter estimation induced by spatial variability of precipitation. *Water Resources Research*, 19(3): 791-810.

Troutman, B.M., 1985. Errors and Parameter-Estimation in Precipitation-Runoff Modelling .1. Theory. *Water Resources Research*, 21(8): 1195-1213.

Tucciarelli, T. and Termini, D., 2000. Finite-element modelling of floodplain flow. *Journal of Hydraulic Engineering*, 126(6): 416-424.

US Army Corps of Engineers, 2005. *HEC History*. http://www.hec.usace.army.mil/whoweare/history.html

USNWS, 2006. *Advanced Hydrological Prediction Service*. http://www.weather.gov/ahps/about/about.php

van Stokkom, H.T.C., Smits, A.J.M. and Leuven, R., 2005. Flood defense in the Netherlands - A new era, a new approach. *Water International*, 30(1): 76-87.

Velghe, T., Troch, P.A., De Troch, F.P. and Van de Velde, J., 1994. Evaluation of cluster-based rectangular pulses point process models for rainfall. *Water Resources Research*, 30(10): 2847-2857.

Verhoest, N., Troch, P.A. and De Troch, F.P., 1997. On the applicability of Bartlett-Lewis rectangular pulse models in the modelling of design storms at a point. *Journal of Hydrology*, 202(108-120).

Vinnikov, K.Y., Robock, A., Grody, N.C. and Basist, A., 2004. Analysis of diurnal and seasonal cycles and trends in climatic records with arbitrary observation times. *Geophysical Research Letters*, 31(6).

Vionnet, C.A., Tassi, P.A. and J.P., M.-V., 2004. Estimates of flow resistance and eddy viscosity coefficients for 2D modelling on vegetated floodplains. *Hydrological Processes*, 18(15): 2907-2926.

Vogel, R.M., Thomas, W.O. and McMahon, T.A., 1993. Flood-flow frequency model selection in southwestern United States. *Journal of Water Resources Planning and Management*, 119: 353-366.

Vrugt, J.A., Gupta, V.K., Bouten, W. and Sorooshian, S., 2003. A Shuffled Complex Evolution Metropolis algorithm for optimisation and uncertainty assessment of hydrologic model parameters. *Water Resources Research*, 39(8): 1201.

Wallingford Software Ltd, 2006. *ISIS Flow / Hydrology*. http://www.wallingfordsoftware.com/products/isis/

Walshaw, D., 1994. Getting the most from your extreme wind data: A step-by-step guide. *Journal of Research of the National Institute of Standards and Technology.*, 99(4): 399-411.

Waterstone, M., 1977. Hazard Mitigation Behaviour of Urban Floodplain Residents. *Natural Hazard Research*; working paper 35., Boulder.

Watts, G., 1996. Can Science Reassure? In: S. Dunant and R. Porter (Editors), *The Age of Anxiety*, pp. 167-187.

Wealands, S.R., Grayson, R.B. and Walker, J.P., 2005. Quantitative comparison of spatial fields for hydrological model assessment - some promising approaches. *Advances in Water Resources*, 28(1): 15-32.

Weightman, C., 2004. *Cambridge and Peterborough Biodiversity Action Plan: Pack for Farmers.*

Werner, M., Blazkova, S. and Petr, J., 2005. Spatially distributed observations in constraining inundation modelling uncertainties. *Hydrological Processes*, 19(16): 3081-3096.

Wheater, H.S., 2002. Progress in and Prospects for Fluvial Flood Modelling. *Phil. Trans. R. Soc. Lond. A*,, 360: 1409-1431.

Wheater, H.S., 2006. Flood Risk and Flood Management. *Phil. Trans. R. Soc. Lond. A*, In Press.

Wheater, H.S., Jakeman, A.J. and Beven, K., 1993. Progress and direction in rainfall-runoff modelling. In: A.J. Jakeman, M.B. Beck and M.J. McAleer (Editors), *Modelling Change in Environmental Systems*. Wiley, Chichester, pp. 101-132.

Whiting, P.J. and Stamm, J., 1995. The hydrology and form of spring-dominated channels. *Geomorphology*, 12(3): 233-240.

Wigmosta, M. and Prasad, R., 2005. Upscaling and Downscaling - Dynamic Models. In: M.G. Anderson and J.J. McDonnell (Editors), *Encyclopedia of Hydrological Sciences*. Wiley, Chichester, pp. 165-176.

Wiltshire, S.E. and Beran, M., 1986. Multivariate techniques for the identification of homogeneous flood frequency regions. In: V.P. Singh (Editor), *Flood Frequency and Risk Analysis*. Reidal, Dordrecht, pp. 133-146.

Wohl, E.E., 1998. Uncertainty in flood estimates associated with roughness coefficient. *Journal of Hydraulic Engineering*-ASCE, 124(2): 219-223.

Wood, E.F., 1995. Scaling behaviour of hydrological fluxes and variables: empirical studies using a hydrological model and remote sensing data. In: J.D. Kalma and M. Sivapalan (Editors), *Scale issues in Hydrological Modelling*. Wiley, New York, pp. 89-104.

Wood, E.F., 1997. Effects of soil moisture aggregation on surface evaporative fluxes. *Journal of Hydrology*, 190: 397-412.

Wood, E.F., 1998. Scale Analyses for Land-Surface Hydrology. In: G. Sposito (Editor), *Scale Dependence and Scale Invariance*. Cambridge University Press, Cambridge, pp. 1-29.

Wood, E.F., Beven, K., Sivapalan, M. and Band, L., 1988. Effects of spatial variability and scale with implication to hydrology modelling. *Journal of Hydrology*, 102: 29-47.

Wood, A.W., Leung, L.R., Sridhar, V. and Lettenmaier, D.P., 2004. Hydrologic implications of dynamical and statistical approaches to downscaling climate model outputs. *Climate Change*, 62: 189-216.

Wood-Gee, V., 2001. *River Restoration and Chalk Streams*, The River Restoration Centre, University of Hertfordshire.

Woods, R., 2005. Hydrologic Concepts of Variability and Scale. In: M.G. Anderson and J.J. McDonnell (Editors), *Encyclopedia of Hydrological Sciences*. Wiley, Chichester, pp. 23-40.

Xiong, L. and O'Connor, 2000. Analysis of the response surface of the objective function by the optimum parameter curve: how good can the optimum parameter values be? *Journal of Hydrology*, 234: 187-207.

Ye, W., Bates, B.C., Viney, N.R., Silvaplan, M. and Jakeman, A.J., 1997a. Performance of conceptual rainfall-runoff models in low-yielding catchments. *Water Resources Research*, 33: 153-166.

Ye, W., Hansen, D.P., Jakeman, A.J., Sharma, P. and Cooke, R., 1997b. Assessing the natural variability of runoff: Clarence Basin catchments, NSW, Australia. *Mathematics and Computers in Simulation*, 43(3-6): 251-260.

Ye, W., Jakeman, A.J. and Young, P.C., 1998. Identification of improved rainfall-runoff models for an ephemeral low-yielding Australian catchment. *Environmental Modelling and Software*, 13: 59-74.

Yen, B.C., 1996. System and component uncertainties in water resources. In: J.J. Bogardi and Z.W. Kundzewicz (Editors), *Risk, Reliability, Uncertainty, and Robustness of Water Resources Systems*. Cambridge University Press, Cambridge, pp. 133-139.

Young, P.C., 1984. *Recursive Estimation and Time Series Analysis*. Springer-Verlag, Berlin.

Young, P.C., 1993. Data-Based Mechanistic Models. In: P.C. Young (Editor), *Concise Encylopedia of Environmental Systems*. Pergamon, Oxford.

Young, P.C., 2003. Top-down and data-based mechanistic modelling of rainfall-flow dynamics at the catchment scale. *Hydrological Processes*, 17: 2195-2217.

Young, P.C. and Beven, K., 1991. Computation of the instantaneous unit hydrograph and identifiable component flows with application to two small upland catchments - comment. *Journal of Hydrology*, 129(1-4): 389-396.

Young, P.C. and Beven, K., 1994. Data-based mechanistic modelling and the rainfall-flow nonlinearity. *Environmetrics*, 5(3): 335-363.

Young, P.C. and Jakeman, A.J., 1980. Refined instrumental variable methods of recursive time series analysis: Part I, single input single output systems. *International Journal of Control*, 29: 1-30.

Young, P.C., Taylor, C.J., Tych, W., Pedregal, D.J. and McKenna, P.G., 2004. *The Captain Toolbox*. Centre for Research on Environmental Systems and Statistics, Lancaster University.

Yu, D. and Lane, S.N., 2006a. Urban fluvial flood modelling using a two-dimensional diffusion-wave treatment, part 1: mesh resolution effects. *Hydrological Processes*, 20(7): 1541-1565.

Yu, D. and Lane, S.N., 2006b. Urban fluvial flood modelling using a two-dimensional diffusion-wave treatment, part 2: development of a sub-grid-scale treatment. *Hydrological Processes*, 20(7): 1567-1583.

Zerger, A., 2002. Examining GIS decision utility for natural hazard risk modelling. *Environmental Modelling & Software*, 17(3): 287-294.

Zerger, A. and Wealands, S., 2004. Beyond modelling: Linking models with GIS for flood risk management. *Natural Hazards*, 33(2): 191-208.

Appendix A

COMPUTER CODE FOR FLOODPLAIN INUNDATION MODELS

Matlab Function Code: FloodWave

```
%This function routes a flood wave down the river channel
%Calls function which routes water over floodplain

%Hilary McMillan
%Department of Geography
%Cambridge University

function [Flows, Flows2, Flows3, FloodplainDepth, Times, MassBalance] =
FloodWave(ChInfoArray,InitDepths,InitFlow,hydrotime,hydroflow,EndTime,DEMresolution,
DEMarray,RoughArray,InitFloodplainDepths)

%------Inputs

%ChInfoArray has columns: Channel x-position, channel y-pos, width, slope, friction coeff, bankfull depth
%InitDepths: initial upstream depth (m)
%InitFlow: Initial channel flow (m^3/s)
%[hydrotime, hydroflow]: upstream hydrograph
%EndTime: Time to end simulation (s)
%DEMresolution: Distance between sample points (m)

%--These are passed straight to floodplain depth calculator FloodplainRoute
%DEMarray: Ground height of floodplain
%RoughArray: Roughness of each grid square on floodplain
%InitFloodplainDepths: Initial depth of water in each floodplain cell

%------Outputs
%Flows, Flows2, Flows3: Channel hydrograph at specified locations
%Floodplain Depth: maximum depth occurring at each grid cell
%Times: Time (s) at which hydrograph data is recorded
%MassBalance: Record of any water volume change during model run (accuracy check)

tic  %record time taken

%--------- Declare global variables ----------------------------------------------------------------------------

%Array of volume of water in each grid cell
global VolumeArray

%---------Set up constants -------------------------------------------------------------------------------------

%Find delta-x array of length of channel in each grid cell
%    depending on whether consective channel cells are adjacent or diagonal

%Create intermediate variables
Channelx = ChInfoArray(1:end-1,1);
Channelx2 = ChInfoArray(2:end,1);
Channely = ChInfoArray(1:end-1,2);
Channely2 = ChInfoArray(2:end,2);
%Calculate distance between centres of each two channel cells (= 1 or sqrt(2))
deltax = (((Channelx2-Channelx)+(Channely2-Channely)-1)*(sqrt(2)-1))+1;
%Clear intermediate variables
clear Channelx2,Channely2;
```

```
%Split up channel info array for readability
ChannelXpos = ChInfoArray(:,1);
ChannelYpos = ChInfoArray(:,2);
ChannelWidth = ChInfoArray(:,3);
%And cut width if greater than cell size
ChannelWidth=min(ChannelWidth,DEMresolution);
ChannelSlope = ChInfoArray(:,4);
ChannelFriction = ChInfoArray(:,5);
ChannelBankfull = ChInfoArray(:,6);

%Clear ChInfo array
clear ChInfoArray;

%Set positions at which to output hydrograph
OutHydPosition = 891;
OutHydPosition2 = 366;
OutHydPosition3 = 253;

%Set folder in which to store output video
VideoFolder = 'H:\VideoFolder';

%Set folder in which to store output files
OutputFolder = 'H:\OutputFolder';

%--------- Create Arrays to stop dynamic allocation -----------------------------------------------------------

%Store time values in seconds corresponding to timesteps j
StoredTime = zeros(30000,1);

%Store Q (flow) values
Q = zeros(length(ChannelWidth),2);
%And put in intial flows
Q(:,1) = InitFlow*ones(length(ChannelWidth),1);
Q(:,2) = Q(:,1);

%Store Output hydrograph values
OutputFlow = zeros(1,30000);
OutputFlow2 = zeros(1,30000);
OutputFlow3 = zeros(1,30000);

%Store water depths y
y = zeros(length(ChannelWidth),2);
%And put in initial depths
y(:,1) = (ChannelFriction.*Q(:,1)./((ChannelSlope.^0.5).*ChannelWidth)).^(0.6);
y(:,2) = y(:,1);

%Store Channel Inflow q
qq1 = zeros(length(ChannelWidth),1);
qq2=qq1;
qq2_old = qq1;

%Create variable alpha used in calculations of Q
alpha = [(ChannelFriction.*ChannelWidth.^(2/3))./ChannelSlope.^(1/2)].^0.6;

%Depth of water on floodplain
```

```
sz2 = size(DEMarray);
FloodplainDepth1 = zeros(sz2(1),sz2(2));
FloodplainDepth2=FloodplainDepth1;
FloodplainDepth1 = InitFloodplainDepths;
FloodplainMaxDepth = zeros(sz2(1),sz2(2));

%Initialise floodplain flows
Flow_S = 0;
Flow_E = 0;
Flow_SE = 0;
Flow_NE = 0;

%Array of floodplain volumes
VolumeArray = zeros(sz2(1),sz2(2));

%Find fraction of channel in channel cells for volume finding-----------------------------------------------------
---------

%Calculate length of channel occurring within each cell
%Set up temporary arrays
%Add beginning and end coordinates as if adjacent channel cells existed
Channelxoffset1 = [ChannelXpos(1);ChannelXpos(1:end-1)];
Channelyoffset1 = [ChannelYpos(1)-1;ChannelYpos(1:end-1)];
Channelxoffset2 = ChannelXpos(1:end);
Channelyoffset2 = ChannelYpos(1:end);
Channelxoffset3 = [ChannelXpos(2:end);ChannelXpos(end)];
Channelyoffset3 = [ChannelYpos(2:end);ChannelYpos(end)+1];
%Calculate lengths
ChannelLength = sqrt(abs(Channelxoffset2-Channelxoffset1)+abs(Channelyoffset2-Channelyoffset1))/2 +
...
        sqrt(abs(Channelxoffset3-Channelxoffset2)+abs(Channelyoffset3-Channelyoffset2))/2;

ChannelFraction=zeros(length(ChannelLength),1);
%Cell type 1: straight channel
CL1=find(ChannelLength==1);
%Cell type 2: straight/diagonal
CL12=find(ChannelLength==((1/2)+(sqrt(2)/2)));
%Cell type 3: all diagonal
CL2=find(ChannelLength==sqrt(2));
%Calculate volume for each cell type
ChannelFraction(CL1)=(ChannelWidth(CL1).*ChannelLength(CL1))/DEMresolution;
ChannelFraction(CL12)=((ChannelWidth(CL12).*ChannelLength(CL12))/DEMresolution)/2+...
   ((((2^0.5).*ChannelWidth(CL12))./DEMresolution)-
((ChannelWidth(CL12).*ChannelWidth(CL12))./(2*(DEMresolution^2))))/2;
ChannelFraction(CL2) = (((2^0.5).*ChannelWidth(CL2))./DEMresolution)-
((ChannelWidth(CL2).*ChannelWidth(CL2))./(2*(DEMresolution^2)));
%Put in due to errors when Channel takes up whole square
ChannelFraction=min(ChannelFraction,0.8);
%Save as sparse matrix
sparse_channel_vol = sparse(ChannelYpos,ChannelXpos,ChannelFraction,sz2(1),sz2(2));

%clear up
clear Channelxoffset1 Channelyoffset1 Channelxoffset2 Channelyoffset2 Channelxoffset3 Channelyoffset3
%Initialise total water for mass balance calculations
WaterIn = sum(y(:,1).*ChannelLength.*ChannelWidth*DEMresolution);
WaterOut = 0;
```

```
OldTotalWater = sum(y(:,1).*ChannelLength.*ChannelWidth*DEMresolution);

%---------Initialise loop variables------------------------------------------------------------------------------

%Initialise timestep
delta_t = 0;

%time in seconds
t=0;

%timestep number
j = 1;

%--------- Calculate variable values from initial conditions ---------------------------------------------------

%Q(:,1) = InitFlow;
FloodplainDiff = [0];

%Find timesteps at which to record picture of flood
Step = floor(EndTime/60);
Step = Step:Step:Step*60;
StepCounter=1;

%Find point at which drying begins
[MaxChannelFlow, MaxChannelFlowIndex] = max(hydroflow);
DryingTime = hydrotime(MaxChannelFlowIndex);

%-------- Loop for timesteps-------------------------------------------------------------------------------------

while t < (EndTime-delta_t)

%-------- Find delta-t by using Courant condition ----------------------------------------------------------------

%Find kinematic wave celerity c_k = dQ/dA = 1/B.dQ/dY       B = channel width, y = water depth
%Mannings equation Q = [By.Sf^(1/2).R^(2/3)]/n    (A=By)  s0 = sf  R~=y
%Differentiate to get c_k = [s0^(1/2).(5/3).y^(2/3)]/n
%We assume surface slope s0 = bed slope

%c_k is found for each cell
c_k = [ChannelSlope.^(1/2)*(5/3).*y(:,2).^(2/3)]./ChannelFriction;

%delta-t is found for each cell, and min value gives timestep
delta_t = min(DEMresolution./c_k)*1;

%--------- Advance to next time step -----------------------------------------------------------------------------

t = t + delta_t;

%Store timestep value
StoredTime(j+1) = t;

t %print time

%---------- Now route water overbank and into floodplain where appropriate -------------------------------------
---
```

```
%Find overbank height by subtracting bankfull height from total water depth
ChannelHeight = y(:,2) - ChannelBankfull;

%update variables
chheight = ChannelHeight;
FloodplainDepth1 = FloodplainDepth2;
qq1_old = qq2_old;
qq1=qq2;

%Find out whether this step needs to be stored to be part of flood video
if (StoredTime(j+1)>Step(StepCounter))&&(StoredTime(j)<Step(StepCounter))
   VideoFile = [VideoFolder,'\VideoFrame',num2str(StepCounter,'%02i'),'.asc'];
   save(VideoFile, 'FloodplainDepth1', '-ASCII')
   if StepCounter < length(Step)
      StepCounter=StepCounter+1;
      if StepCounter==11
         stop=1;
      end;

   end
end

%Variable should not include within-reach inflow
if ((t > 82000)&&(t < 143000))
   qqtemp=qq1_old-0.0116;
else
   qqtemp=qq1_old;
end;

%Find out whether we are in drying phase
if t > DryingTime;Drying=1;else;Drying=0;end;

%Calculate new floodplain depths and channel inflow for next timestep using FloodplainRoute function
[FloodplainDepth2, qq2,Flow_S,Flow_E,vol_edge] = FloodplainRoute(DEMarray,RoughArray, ...

FloodplainDepth1,DEMresolution,ChannelXpos,ChannelYpos,ChannelHeight,ChannelWidth,delta_t,Flow
_S,Flow_E,qqtemp,
ChannelFraction,Drying);

%Add within-reach lateral inflow
if ((t > 82000)&&(t < 143000))
   qq2=qq2+0.0116;
end;
qq2_old=qq2;

%Record maximum depths
FloodplainMaxDepth = max(FloodplainMaxDepth,FloodplainDepth2);

%--------- Calculate correct upstream flow value for this data point ------------------------------------------------

%Update flow variable
Q(:,1) = Q(:,2);

%If hydrograph does not start at time zero then add a zero
if min(hydrotime > 0)
   hydrotime = [0;hydrotime];
```

```
    hydroflow = [hydroflow(1);hydroflow];
end;

%Find position of time t within hydrograph times series
tlessthan = (hydrotime <= t);
tposition = sum(tlessthan);
%Hence find interpolated flow at time t
Q(1,2) = hydroflow(tposition) + ((t-hydrotime(tposition))/(hydrotime(tposition+1)-hydrotime(tposition)))
...
    *(hydroflow(tposition+1)-hydroflow(tposition));


%--------- Loop to calculate downstream discharges ---------------------------------------------------------------

%Length of channel array = number of channel cells
for i = 1:length(ChannelWidth)-1

%--------- Solve for discharge at point x + delta-x ---------------------------------------------------------------

if ((Q(i+1,1)+Q(i,2)) > (10^(-15)))
    Q(i+1,2) =
((delta_t/(DEMresolution*ChannelLength(i+1)))*Q(i,2)+alpha(i+1)*0.6*Q(i+1,1)*((Q(i+1,1)+Q(i,2))/2).^-
0.4+ ...
        (delta_t/(DEMresolution*ChannelLength(i+1)))*(qq2(i+1)+qq1(i+1))/2)/ ...
        ((delta_t/(DEMresolution*ChannelLength(i+1))) + alpha(i+1)*0.6*((Q(i+1,1)+Q(i,2))/2).^-0.4);

else
    Q(i+1,2) = 0;
end;


%-----------------------------------------------------------------------------------------------------------------

end; %End downstream loop

%Save Output flow for Output hydrograph
OutputFlow(j+1)=Q(OutHydPosition,2);
OutputFlow2(j+1)=Q(OutHydPosition2,2);
OutputFlow3(j+1)=Q(OutHydPosition3,2);

%-------- Transform flows into depths ---------------------------------------------------------------------------

%Water depth is found for each cell
%from Mannings equation y = (nQ/(s0^(1/2).B))^(3/5)
y(:,1) = y(:,2);
y(:,2) = (ChannelFriction.*Q(:,2)./((ChannelSlope.^0.5).*ChannelWidth)).^(0.6);

%------- Find total volume of water to check conservation -------------------------------------------------------

%Water on floodplain
TotalWater = VolumeArray;
TotalWater = sum(TotalWater(:));
%Add water depth in channel
TotalWater = TotalWater + sum(y(:,1).*ChannelLength.*ChannelWidth*DEMresolution);

%Find volume of water added to model
```

```
WaterIn = WaterIn + Q(1,2)*delta_t;
WaterOut = WaterOut + Q(length(ChannelXpos),2)*delta_t;

%Account for water flowing off edge of model
WaterOut = WaterOut - vol_edge;

%wo = Q(length(ChannelXpos),2)*delta_t;
WaterBalance = (WaterIn-WaterOut-TotalWater)/WaterIn;

%Save for next timestep
OldTotalWater = TotalWater;

%Increment timestep
j = j+1;

end; %End timestep loop

%--------- Write outputs variable ---------------------------------------------------------------------------------

Flows = OutputFlow(1:j);
Flows2 = OutputFlow2(1:j);
Flows3 = OutputFlow3(1:j);
FloodplainDepth = FloodplainMaxDepth;
Times = StoredTime(1:j);
MassBalance = WaterBalance*100;

%--------- Save all outputs -------------------------------------------------
flowfile = [OutputFolder,'\OutputFlows.dat'];
flowfile2 = [OutputFolder,'\OutputFlows2.dat'];
flowfile3 = [OutputFolder,'\OutputFlows3.dat'];
depthsfile = [OutputFolder,'\OutputDepths.dat'];
timesfile = [OutputFolder,'\OutputTimes.dat'];
waterbalfile = [OutputFolder,'\WaterBalance.dat'];

save(flowfile,'Flows','-ascii');
save(flowfile2,'Flows2','-ascii');
save(flowfile3,'Flows3','-ascii');
save(depthsfile,'FloodplainDepth','-ascii');
save(timesfile,'Times','-ascii');
save(waterbalfile,'MassBalance','-ascii');

ttoc=toc
tocfile = [OutputFolder,'\tocfile.dat'];
save(tocfile,'ttoc','-ascii');


%--------------------------------------End of Kinematic Wave ----------------------------------------------------------
```

```
%-----------------------------------FloodplainRoute subfunction for 2D floodplain flow ---------------------

function [Floodplain_depths, Inchannel_Flow,Flow_S,Flow_E,vol_edge] =
FloodplainRoute(DEMarray,RoughArray,DepthsArray,
...DEMresolution,Channelx,Channely,ChannelHeight,ChannelWidths,delta_t,ChannelFrac,Drying)

%DEMarray = Land Height for each gridsquare (m)
%RoughArray = Mannings n for each gridsquare
%DepthsArray = previous depths of water on floodplain (m)
%DEM resolution: Distance between sample points (m)
%Channelx = channel square x-position
%Channely = channel square y-position
%Channel Height = overbank height of water
%ChannelWidths = width of channel in each cell
%delta_t = timestep over which flow can take place
%ChannelFrac: Fraction of each channel cell containing channel not floodplain
%Drying: boolean to specify if we are in drying phase

%Returns
%Floodplain_depths = new heights of water on floodplain
%Inchannel_Flow = Flow rate of water returning to channel
%Floodplain_depths = new heights of water on floodplain
%Flow_S/Flow_E: Floodplain flows
%vol_edge: volume of water leaving edge of floodplain


%--------- Declare global variables ----------------------------------------------------------------------------

global VolumeArray

%------- Set up constants ------------------------------------------------------------------------------------------------
-

%Get size of DEM array
sz = size(DEMarray);
%Size of DEM
DEMsizeNS = sz(1);
DEMsizeWE = sz(2);

%------- Create mask of active points within floodplain ----------------------------------------------------------------
------

activepoints = (DepthsArray > 0);
ap_pack = bwpack2(activepoints);                    %bwpack is used for efficiency
se_dilate = strel2([0, 1, 0;1, 1, 1;0, 1, 0]);       %Each point with positive depth has its four surrounding
points made active
ap_dilate = imdilate2(ap_pack,se_dilate,'ispacked');
ap_unpack = bwunpack2(ap_dilate,size(activepoints,1));

%------- First Calculate 'down/south' flows in relation to DEM ------------------------------------------------------
---------

%Initialise arrays
DepthsTotal = DepthsArray+DEMarray;
```

```
%Create offset maps
DEMoffset1 = DEMarray(1:end-1,:);
DEMoffset2 = DEMarray(2:end,:);

Depthoffset1 = DepthsTotal(1:end-1,:);
Depthoffset2 = DepthsTotal(2:end,:);

RoughOffset1 = RoughArray(1:end-1,:);
RoughOffset2 = RoughArray(2:end,:);

%Initialise Flow matrix
Flow_S = zeros(sz(1)-1,sz(2));

%Find active flows
aps1 = ap_unpack(2:end,:);
aps = find(aps1);

%Calculate flows
Flow_S(aps) = sign(Depthoffset1(aps)-Depthoffset2(aps)).*[((max(Depthoffset1(aps),Depthoffset2(aps))-
max(DEMoffset1(aps),DEMoffset2(aps))).^(5/3)) ...
        .*(abs(Depthoffset1(aps)-Depthoffset2(aps)).^0.5).*(DEMresolution.^(7/6))]./ ...

[((RoughOffset1(aps)+RoughOffset2(aps))./2).*((DEMresolution+2*(max(Depthoffset1(aps),Depthoffset2(
aps))-max(DEMoffset1(aps),DEMoffset2(aps)))).^(2/3))];


%Check that water is not allowed to flow such that depth in receiving cell > depth in source cell
%Calculate max flow lost from cell 1 = (av. depth - prev depth).*area./timestep
aps_add1 = aps + ceil(aps/(DEMsizeNS-1));
MaxFlowS = abs((VolumeArray(aps_add1)-VolumeArray(aps_add1-1))./2)./delta_t;
Flow_S(aps) = sign(Flow_S(aps)).*min(abs(Flow_S(aps)),MaxFlowS);

%------- Calculate 'right/east' flows in relation to DEM ------------------------------------------------------------

%Initialise arrays

%Create offset maps
DEMoffset1 = DEMarray(:,1:end-1);
DEMoffset2 = DEMarray(:,2:end);

Depthoffset1 = DepthsTotal(:,1:end-1);
Depthoffset2 = DepthsTotal(:,2:end);

RoughOffset1 = RoughArray(:,1:end-1);
RoughOffset2 = RoughArray(:,2:end);

%Initialise Flow matrix
Flow_E = zeros(sz(1),sz(2)-1);

%Find active flows
ape1 = ap_unpack(:,2:end);
ape = find(ape1);

%Calculate flows
Flow_E(ape) = sign(Depthoffset1(ape)-Depthoffset2(ape)).*[((max(Depthoffset1(ape),Depthoffset2(ape))-
max(DEMoffset1(ape),DEMoffset2(ape))).^(5/3))...
```

```
    .*(abs(Depthoffset1(ape)-Depthoffset2(ape)).^0.5).*(DEMresolution.^(7/6))]./ ...

[((RoughOffset1(ape)+RoughOffset2(ape))./2).*((DEMresolution+2*(max(Depthoffset1(ape),Depthoffset2
(ape))-max(DEMoffset1(ape),DEMoffset2(ape)))).^(2/3))];

%Check that water is not allowed to flow such that depth in receiving cell > depth in source cell
%Calculate max flow lost from cell 1 = (av. depth - prev depth).*area./timestep
ape_add1 = ape + ceil(ape/(DEMsizeWE-1));
MaxFlowE = abs((VolumeArray(ape)-VolumeArray(ape+DEMsizeNS))./2)./delta_t;
Flow_E(ape) = sign(Flow_E(ape)).*min(abs(Flow_E(ape)),MaxFlowE);

%------Clear up
clear DEMoffset1 DEMoffset2 RoughOffset1 RoughOffset2 DepthOffset1 DepthOffset2 aps1 ape1
clear aps_add1 ape_add1 depthindices flows_xsec flows_wp max depths

%------- Now Calculate flows to and from Channel -----------------------------------------------------------------
-

%Create array of floodplain cells corresponding to channel cells
%Get size of DEM array
sz = size(DEMarray);
%Uses linear index to retrieve scattered elements of DEM array
DEMChannelCell = DEMarray(sz(1)*(Channelx-1)+Channely);
%And similarly for roughness
RoughChannelCell = RoughArray(sz(1)*(Channelx-1)+Channely);
%And water heights
DepthsChannelCell = DepthsArray(sz(1)*(Channelx-1)+Channely);

%Calculate length of channel occurring within each cell
%Set up temporary arrays
%Add beginning and end coordinates as if adjacent channel cells existed
Channelxoffset1 = [Channelx(1);Channelx(1:end-1)];
Channelyoffset1 = [Channely(1)-1;Channely(1:end-1)];
Channelxoffset2 = Channelx(1:end);
Channelyoffset2 = Channely(1:end);
Channelxoffset3 = [Channelx(2:end);Channelx(end)];
Channelyoffset3 = [Channely(2:end);Channely(end)+1];
%Calculate lengths
ChannelLength = sqrt(abs(Channelxoffset2-Channelxoffset1)+abs(Channelyoffset2-Channelyoffset1))/2 +
...
            sqrt(abs(Channelxoffset3-Channelxoffset2)+abs(Channelyoffset3-Channelyoffset2))/2;

ChannelTransform = sparse(Channely,Channelx,ChannelFrac,DEMsizeNS,DEMsizeWE);

%For each channel cell, work out flow from cell into channel
Inchannel_Flow = sign(DepthsChannelCell-
ChannelHeight).*[(max(ChannelHeight,DepthsChannelCell).^(5/3)).*(abs(DepthsChannelCell-
ChannelHeight).^0.5).* ...

((2*ChannelLength*DEMresolution).^(7/6))]./[RoughChannelCell.*((2*ChannelLength*DEMresolution)+
2*(max(ChannelHeight,DepthsChannelCell)).^(2/3))];

%Check that water is not allowed to flow such that depth in receiving cell > depth in source cell
%Calculate Channel area
ChannelArea = (DEMresolution^2)*ChannelFrac;
%Calculate total volume of water available
```

```
TotalVolume = ChannelHeight.*ChannelArea + DepthsChannelCell.*(DEMresolution^2-ChannelArea);
%Calculate equilibrium depths
EquilDepths = TotalVolume./((DEMresolution^2));
%Calculate depth lost from channel
LostDepths = ChannelHeight - EquilDepths;
%Calculate vol lost from channel
LostVolume = LostDepths.*ChannelArea;
%Calculate flow from channel to cell
ChtoCellFlowMax = LostVolume./delta_t;

%-------------- Cut off flows if greater than allowed then cut off (as flow would actually decrease as level
difference decreased
Inchannel_Flow = sign(Inchannel_Flow).*min(abs(Inchannel_Flow),abs(ChtoCellFlowMax));

%Find new area of interest
dpS = find(Flow_S);
dpE = find(Flow_E);

%------- Transform flows to volumes --------------------------------------------------------------------------

%Initialise
Vol_S = Flow_S;
Vol_E = Flow_E;

%Find flowing volume by transforming flow
Vol_S(dpS) = Vol_S(dpS)*delta_t;
Vol_E(dpE) = Vol_E(dpE)*delta_t;
Vol_Ch = -Inchannel_Flow.*delta_t;

%------ Clear up
clear Flow Depthoffset1 Depthoffset1E Depthoffset2 Depthoffset2E MaxFlowE MaxFlowS
Channelxoffset1 Channelyoffset1 Channelxoffset2 Channelyoffset2 Channelxoffset3 Channelyoffset3

%-------- Add flowing volumes to each cell --------------------------------------------------------------------

%Find water that flows out of each cell
%Initially zero
VolOut = zeros(DEMsizeNS,DEMsizeWE);
%At same time find min height difference between central and neighbouring outflow cells
HeightDiff1 = zeros(DEMsizeNS, DEMsizeWE);
HeightDiff2 = zeros(DEMsizeNS, DEMsizeWE);
HeightDiff3 = zeros(DEMsizeNS, DEMsizeWE);
HeightDiff4 = zeros(DEMsizeNS, DEMsizeWE);
HeightDiffch = zeros(DEMsizeNS, DEMsizeWE);

HeightDiff = zeros(DEMsizeNS, DEMsizeWE);

%And count flows out of each cell
NumFlows = zeros(DEMsizeNS, DEMsizeWE);

%Find direction of flow at each point
dpS_south = find(Vol_S(dpS)>0);
dpS_south = dpS(dpS_south);
dpS_north = find(Vol_S(dpS)<0);
dpS_north = dpS(dpS_north);
dpE_east = find(Vol_E(dpE)>0);
```

```
dpE_east = dpE(dpE_east);
dpE_west = find(Vol_E(dpE)<0);
dpE_west = dpE(dpE_west);

%Now at each point add all the negative flows
%Find flow to vol matrix index conversion
dpS_add1 = dpS + ceil(dpS/(DEMsizeNS-1));
dpS_south_add1 = dpS_south + ceil(dpS_south/(DEMsizeNS-1));
dpS_north_add1 = dpS_north + ceil(dpS_north/(DEMsizeNS-1));
%South flowing
VolOut(dpS_south_add1-1) = VolOut(dpS_south_add1-1) + Vol_S(dpS_south);
HeightDiff1(dpS_south_add1-1)=DepthsTotal(dpS_south_add1-1)-DepthsTotal(dpS_south_add1);
%North flowing
VolOut(dpS_north_add1) = VolOut(dpS_north_add1) - Vol_S(dpS_north);
HeightDiff2(dpS_north_add1)=DepthsTotal(dpS_north_add1)-DepthsTotal(dpS_north_add1-1);
%East flowing
VolOut(dpE_east) = VolOut(dpE_east) + Vol_E(dpE_east);
HeightDiff3(dpE_east)=DepthsTotal(dpE_east)-DepthsTotal(dpE_east+DEMsizeNS);
%West Flowing
VolOut(dpE_west+DEMsizeNS) = VolOut(dpE_west+DEMsizeNS) - Vol_E(dpE_west);
HeightDiff4(dpE_west+DEMsizeNS)=DepthsTotal(dpE_west+DEMsizeNS)-DepthsTotal(dpE_west);


%Now include channel cells
%Find indices of channel cells
ChCells = sz(1)*(Channelx-1)+Channely;
%Find flows into channel
Into_channel = find((Vol_Ch)<0);
%Add flows
VolOut(ChCells(Into_channel)) = VolOut(ChCells(Into_channel)) - Vol_Ch(Into_channel);
HeightDiffch(ChCells(Into_channel))=min(DepthsChannelCell(Into_channel),DepthsChannelCell(Into_cha
nnel)-(ChannelHeight(Into_channel).*(1-ChannelFrac(Into_channel))));

%Find out max flow from each cell
ActiveHeights=find(HeightDiff1+HeightDiff2+HeightDiff3+HeightDiff4+HeightDiffch);
ah1=HeightDiff1(ActiveHeights);
ah2=HeightDiff2(ActiveHeights);
ah3=HeightDiff3(ActiveHeights);
ah4=HeightDiff4(ActiveHeights);
ahch=HeightDiffch(ActiveHeights);

MaxHeights=max([ah1,ah2,ah3,ah4,ahch],[],2);

%Any flows less than 1/20 of max are deleted
MinHeights=MaxHeights./20;
%Find indices of bad heights
delheights1=find(ah1<MinHeights);
delheights2=find(ah2<MinHeights);
delheights3=find(ah3<MinHeights);
delheights4=find(ah4<MinHeights);
delheightsch=find(ahch<MinHeights);

%And remove
ah1(delheights1)=0;
ah2(delheights2)=0;
ah3(delheights3)=0;
```

```
ah4(delheights4)=0;
ahch(delheightsch)=0;

%Find number of flows at each point
NumFlowsVector=(ah1>0)+(ah2>0)+(ah3>0)+(ah4>0)+(ahch>0);
%Find height diff minima
%First set 0 values high
ah1(find(ah1==0))=1000;
ah2(find(ah2==0))=1000;
ah3(find(ah3==0))=1000;
ah4(find(ah4==0))=1000;
ahch(find(ahch==0))=1000;
HeightDiffVector = min([ah1,ah2,ah3,ah4,ahch],[],2);

%Put back into matrix
HeightDiff(ActiveHeights)=HeightDiffVector;
NumFlows(ActiveHeights)=NumFlowsVector;


%Include estimated flows for cells on edge of floodplain to allow water to flow along floodplain
%Find flows out
Edge_out = find(Vol_E(1:DEMsizeNS)<0);
VolOut(Edge_out) = VolOut(Edge_out) - Vol_E(Edge_out);      %Western edge
NumFlows(Edge_out) = NumFlows(Edge_out) + 1;

%Find points where volume flowing out is too great
FlowRatio=(1+1./NumFlows).*VolOut;
FlowRatio(ChCells)=FlowRatio(ChCells)./(1-ChannelFrac);

[ii jj] = find((FlowRatio > HeightDiff*DEMresolution^2)+(VolOut > VolumeArray));

if length(ii) > 0

%---------------------------------------------------Normalise flows
%Find normalisation coefficient
%Find indices of bad points
norm_position = DEMsizeNS*(jj-1) + ii;

[channel_norm_position,inp,ics] = intersect(norm_position,ChCells);

find_norm_coeff =
(HeightDiff(norm_position)*DEMresolution^2)./((1+1./NumFlows(norm_position)).*VolOut(norm_positi
on));
find_norm_coeff(inp)=find_norm_coeff(inp).*(1-ChannelFrac(ics));
find_norm_coeff = min(find_norm_coeff,(VolumeArray(norm_position))./(VolOut(norm_position)));

%--------Extra code for drying case -----------------------
%This allows cells to drain to zero volume when they are already very low

if (Drying==1)
   %Find points where outflowing vol is too great and low depth
   drying_cells = find(VolumeArray(norm_position) < (0.01*DEMresolution^2));
   %Check that these cells do have some water in
   drying_cells = drying_cells(find(VolumeArray(drying_cells) > 0));

   if(length(drying_cells)>0)
```

```
    %Save index of drying cells
    drying_cells_index = drying_cells;
    %Get index into vol array for these point
    drying_cells = norm_position(drying_cells);
    %Check that these cells do not have an inflow
    %Find Volumes of surrounding cells
    %Check surrounding cells are not off the edge of array
    drying_cells_plus =
(((drying_cells+DEMsizeNS)<=(DEMsizeNS*DEMsizeWE)).*(drying_cells+DEMsizeNS))+ ...
        (((drying_cells+DEMsizeNS)>(DEMsizeNS*DEMsizeWE)).*drying_cells);
    drying_cells_minus = (((drying_cells-DEMsizeNS)>=1).*(drying_cells-DEMsizeNS))+(((drying_cells-
DEMsizeNS)<1).*drying_cells);
    %Then collect values of surrounding cells
    CheckInflowArray =
[DepthsTotal(drying_cells),DepthsTotal(min(drying_cells+1,DEMsizeNS*DEMsizeWE)),DepthsTotal(ma
x(drying_cells-1,1)),...
            DepthsTotal(drying_cells_plus),DepthsTotal(drying_cells_minus)];
    %Check that centre cell has highest depth
    CheckInflowArray =
((max(max(max(max(CheckInflowArray(:,1),CheckInflowArray(:,2)),CheckInflowArray(:,3)),CheckInflo
wArray(:,4))...
        ,CheckInflowArray(:,5)))==CheckInflowArray(:,1));
    %Find cells with no inflow
    drying_cells = drying_cells(CheckInflowArray);
    drying_cells_index = drying_cells_index(CheckInflowArray);
    %Set normalisation coefficient to reduce volume to zero in these cells
    find_norm_coeff(drying_cells_index) =
VolumeArray(norm_position(drying_cells_index))./VolOut(norm_position(drying_cells_index));
end;

end;

%----------------------------------------------------------

%Convert back to indices in flow/vol matrices
norm_north = norm_position - ceil(norm_position/(DEMsizeNS));
norm_south = norm_north+1;
norm_east = norm_position;
norm_west = norm_position - DEMsizeNS;

%Take subset of flow indices which apply only to those flows in the correct direction
%i.e. do not apply to inflows in problem cells
%Return point,index into active points vector, index into norm coeff vector
[norm_south,ips,ins] = intersect(dpS_south,norm_south);
[norm_north,ipn,inn] = intersect(dpS_north,norm_north);
[norm_east,ipe,ine] = intersect(dpE_east,norm_east);
[norm_west,ipw,inw] = intersect(dpE_west,norm_west);
[norm_channel,ipc,inc] = intersect(ChCells(Into_channel),norm_position);

%Now normlalise flow volumes
Vol_S(norm_south) = Vol_S(norm_south).*find_norm_coeff(ins);
Vol_S(norm_north) = Vol_S(norm_north).*find_norm_coeff(inn);
Vol_E(norm_east) = Vol_E(norm_east).*find_norm_coeff(ine);
Vol_E(norm_west) = Vol_E(norm_west).*find_norm_coeff(inw);
```

```
if length(ipc)>0
   %Apply to flow into channel from problem cells
   Vol_Ch(Into_channel(ipc)) = Vol_Ch(Into_channel(ipc)).*find_norm_coeff(inc);
   Inchannel_Flow(Into_channel(ipc)) = Inchannel_Flow(Into_channel(ipc)).*find_norm_coeff(inc);
end;

end;

%-----------------------------------------------------Recalculate new depths


%Record previous volume
OldVol = VolumeArray;

%Recoded for better efficiency
VolumeArray(dpS_add1) = VolumeArray(dpS_add1) + Vol_S(dpS);         %NS Flows
VolumeArray(dpS_add1-1) = VolumeArray(dpS_add1-1) - Vol_S(dpS);

VolumeArray(dpE+DEMsizeNS) = VolumeArray(dpE+DEMsizeNS) + Vol_E(dpE); %WE Flows
VolumeArray(dpE) = VolumeArray(dpE)-Vol_E(dpE);

%Include estimated flows for cells on edge of floodplain to allow water to flow along floodplain
VolumeArray(1:DEMsizeNS) = VolumeArray(1:DEMsizeNS) + Vol_E(1:DEMsizeNS);      %Western
edge

%Add water flowing into floodplain on channel cells
VolumeArray(ChCells) = VolumeArray(ChCells) + Vol_Ch;

%Record water lost for mass balance
vol_edge = sum(Vol_E(1:DEMsizeNS));

%Allow for small numerical errors
VolumeArray = max(VolumeArray,0);

%---------- Transform volumes in cells to new depths-------------------

DepthsArray = VolumeArray./(DEMresolution^2);
DepthsArray(ChCells)=DepthsArray(ChCells)./(1-ChannelFrac);

%Clear up
clear indices1 indices2 indices3 indices DepthLower DepthUpper VolumeLower VolumeUpper

%clear up
clear ExtraDepth AddedVol sparse_norm_s sparse_norm_E norm_coeff_channel dpS dpS_add1 dpE
DepthsArray2

%-------- Function returns new floodplain depths and new channel overbank height -----------------------------
--------

%Floodplain depths have already been calculated
Floodplain_depths = DepthsArray;

clear DepthsArray
```

Matlab Function Code: FloodWave_Porosity

```
%This function routes a flood wave down the river channel
%Calls function which routes water over floodplain: uses porosity values

%Hilary McMillan
%Department of Geography
%Cambridge University
```

function [Flows, FloodplainDepth, Times, MassBalance] = FloodWave_Porosity(ChInfoArray,hydrotime,hydroflow,DEMresolution,DEMarray,RoughArray,InitFloodplainDepths,DilatedChannel,PorosityAtDepths,WettedPMatrix_NS,WettedPMatrix_WE,XSecAreaMatrix_NS,XSecAreaMatrix_WE)

```
%------Inputs

%ChInfoArray has columns: Channel x-position, channel y-pos, width, slope, friction coeff, bankfull depth
%[hydrotime, hydroflow]: upstream hydrograph
%DEMresolution: Distance between sample points (m)
%DilatedChannel: Channel area if channel covers more than single line of grid cells
%PorosityAtDepths: Look-up table of porosity values
%WettedPMatrix_WE/NS: Look-up tables of wetted perimeters
%XSecAreaMatrix_WE/NS: Look-up tables of cross-sectional areas

%--These are passed straight to floodplain depth calculator FloodplainRoute
%DEMarray: Ground height of floodplain
%RoughArray: Roughness of each grid square on floodplain
%InitFloodplainDepths: Initial depth of water in each floodplain cell

%------Outputs

%Flows: Channel hydrograph at specified locations
%FloodplainDepth: maximum depth occurring at each grid cell
%Times: Time (s) at which hydrograph data is recorded
%MassBalance: Record of any water volume change during model run (accuracy check)

%--------- Declare global variables ---------------------------------------------------------------------------

global Porosities
global VolumeArray
global VolumeArray2
global PorosityVolumes
global WettedP_NS
global WettedP_WE
global XSecArea_NS
global XSecArea_WE

%Assign input parametes to global variables
WettedP_NS = WettedPMatrix_NS;
WettedP_WE = WettedPMatrix_WE;
XSecArea_NS = XSecAreaMatrix_NS;
XSecArea_WE = XSecAreaMatrix_WE;
%and clear original variables
clear WettedPMatrix_NS WettedPMatrix_WE XSecAreaMatrix_NS XSecAreaMatrix_WE
```

```
%---------Set up constants ----------------------------------------------------------------------------------------

%Time for simulation to end
EndTime=hydrotime(end);
%Inital channel flow
InitFlow=hydroflow(1);

%Find delta-x array of length of channel in each grid cell
%    depending on whether consective channel cells are adjacent or diagonal
%Create intermediate variables
Channelx = ChInfoArray(1:end-1,1);
Channelx2 = ChInfoArray(2:end,1);
Channely = ChInfoArray(1:end-1,2);
Channely2 = ChInfoArray(2:end,2);
%Calculate distance between centres of each two channel cells (= 1 or sqrt(2))
deltax = (((Channelx2-Channelx)+(Channely2-Channely)-1)*(sqrt(2)-1))+1;
%Clear intermediate variables
clear Channelx2,Channely2;

%Split up channel info array for readability
ChannelXpos = ChInfoArray(:,1);
ChannelYpos = ChInfoArray(:,2);
ChannelWidth = ChInfoArray(:,3);
ChannelSlope = ChInfoArray(:,4);
ChannelFriction = ChInfoArray(:,5);
ChannelBankfull = ChInfoArray(:,6);

%Clear ChInfo array
clear ChInfoArray;

%Set folder in which to store output video
VideoFolder = 'H:\VideoFolder';

%Set folder in which to store output files
OutputFolder = 'H:\OutputFolder';

%----------Calculate volumes corresponding to known depths --------------------------------

%Depths where porosity is recorded
p_depths = [0;0.25;0.5;0.75;1;1.5;2;2.5;3;4;5;6;7;8;9;10;11;12];

%Also find volumes corresponding to known depths and porosities
Porosities = PorosityAtDepths;
PorosityVolumes = Porosities;

for i = 1:length(p_depths)
   PorosityVolumes(:,:,i) = (DEMresolution^2).*p_depths(i).*Porosities(:,:,i);
end;


%---------Set up matrix to change between dilated channel and central channel-----------------------------------
-

%------ Find x,y position of elements in dilated channel matrix
[dchi dchj dchv] = find(DilatedChannel);
```

```
%------ Find single index position of channel elements
dchindex = find(DilatedChannel);
dchindexnot = find(DilatedChannel==0);

%Create sparse matrix for transform
ChannelTransform = sparse(dchv,[1:length(dchv)]',ones(length(dchv),1));

%------ Find cells which represent inflow into channel
DilatedChannel2=(DilatedChannel>0);
Channel_S = DilatedChannel2(1:(end-1),:) + 2.*DilatedChannel2(2:end,:);
InflowCellsS = (Channel_S==2) + (Channel_S==1);
InflowS = find(InflowCellsS);
InChannelS = find(Channel_S==3);

Channel_E = DilatedChannel2(:,(1:end-1)) + 2.*DilatedChannel2(:,2:end);
InflowCellsE = (Channel_E==2) + (Channel_E==1);
InflowE = find(InflowCellsE);
InChannelE = find(Channel_E==3);

%Clear up
clear Channel_S Channel_E InflowCellsS InflowCellsE DilatedChannel2

%--------- Create Arrays to stop dynamic allocation ------------------------------------------------------------

%Store time values in seconds corresponding to timesteps j
StoredTime = zeros(30000,1);
%StoredTime = zeros(2,1);

%Store Q (flow) values
%Q = zeros(length(ChannelWidth),30000);
Q = zeros(length(ChannelWidth),2);
%And put in intial flows
Q(:,1) = InitFlow*ones(length(ChannelWidth),1);
Q(:,2) = Q(:,1);

%Store Output hydrograph values
OutputFlow = zeros(1,30000);

%Store water depths y
y = zeros(length(ChannelWidth),2);
%And put in initial depths
y(:,1) = (ChannelFriction.*Q(:,1)./((ChannelSlope.^0.5).*ChannelWidth)).^(0.6);
y(:,2) = y(:,1);

%Store Channel Inflow q
qq1 = zeros(length(ChannelWidth),1);
qq2=qq1;
inflow = zeros(1000,1);

%Create variable alpha used in calculations of Q
alpha = [(ChannelFriction.*ChannelWidth.^(2/3))./ChannelSlope.^(1/2)].^0.6;

%Depth of water on floodplain
sz2 = size(DEMarray);
FloodplainDepth1 = zeros(sz2(1),sz2(2));
```

```
FloodplainDepth2=FloodplainDepth1;
FloodplainDepth1 = InitFloodplainDepths;
FloodplainMaxDepth = zeros(sz2(1),sz2(2));

%Initialise floodplain flows
Flow_S = 0;
Flow_E = 0;
Flow_SE = 0;
Flow_NE = 0;

%Array of floodplain volumes
VolumeArray = zeros(sz2(1),sz2(2));
VolumeArray2 = zeros(sz2(1),sz2(2));
VolumeArray2(dchindex)=y(dchv,1).*(DEMresolution^2);
VolumeArray2(dchindex)=(y(dchv,1)-ChannelBankfull(dchv)).*(DEMresolution^2);


%Find fraction of channel in channel cells for volume finding-----------------

%Calculate length of channel occurring within each cell
%Set up temporary arrays
%Add beginning and end coordinates as if adjacent channel cells existed
Channelxoffset1 = [ChannelXpos(1);ChannelXpos(1:end-1)];
Channelyoffset1 = [ChannelYpos(1)-1;ChannelYpos(1:end-1)];
Channelxoffset2 = ChannelXpos(1:end);
Channelyoffset2 = ChannelYpos(1:end);
Channelxoffset3 = [ChannelXpos(2:end);ChannelXpos(end)];
Channelyoffset3 = [ChannelYpos(2:end);ChannelYpos(end)+1];
%Calculate lengths
ChannelLength = sqrt(abs(Channelxoffset2-Channelxoffset1)+abs(Channelyoffset2-Channelyoffset1))/2 +
...
            sqrt(abs(Channelxoffset3-Channelxoffset2)+abs(Channelyoffset3-Channelyoffset2))/2;

ChannelFraction = (ChannelWidth.*ChannelLength)/DEMresolution;
sparse_channel_vol = sparse(ChannelYpos,ChannelXpos,ChannelFraction,sz2(1),sz2(2));

%Now use calculated channel fraction as part of Porosity Array
for i = 1:length(p_depths)
   temp=PorosityVolumes(:,:,i);
   temp(find(DilatedChannel))=p_depths(i).*(DEMresolution^2);
   PorosityVolumes(:,:,i)=temp;
end;

%And put into Porosities matrix as well
for i = 1:length(p_depths)
   temp=Porosities(:,:,i);
   temp(find(DilatedChannel))=1;
   Porosities(:,:,i)=temp;
end;

%clear up
clear Channelxoffset1 Channelyoffset1 Channelxoffset2 Channelyoffset2 Channelxoffset3 Channelyoffset3
%Initialise total water for mass balance check
WaterIn = sum(y(:,1).*ChannelLength.*ChannelWidth*DEMresolution);
WaterOut = 0;
OldTotalWater = sum(y(:,1).*ChannelLength.*ChannelWidth*DEMresolution);
```

```
%---------Initialise loop variables--------------------------------------------------------------------------------

%Initialise timestep
delta_t = 0;

%time in seconds
t=0;

%timestep number
j = 1;

%--------- Calculate variable values from initial conditions ---------------------------------------------------

FloodplainDiff = [0];

%Find timesteps at which to record picture of flood
%hours of simulation
NumHours = floor(EndTime/(60*60));
%every hour
Step = [3600:3600:3600*NumHours];

StepCounter=1;

%Find point at which drying begins
[MaxChannelFlow, MaxChannelFlowIndex] = max(hydroflow);
DryingTime = hydrotime(MaxChannelFlowIndex);

%-------- Loop for timesteps-------------------------------------------------------------------------------------

while t < (EndTime-delta_t)

%-------- Find delta-t by using Courant condition --------------------------------------------------------------------

%Find kinematic wave celerity c_k = dQ/dA = 1/B.dQ/dY       B = channel width, y = water depth
%Mannings equation Q = [By.Sf^(1/2).R^(2/3)]/n    (A=By)  s0 = sf  R~=y
%Differentiate to get c_k = [s0^(1/2).(5/3).y^(2/3)]/n
%We assume surface slope s0 = bed slope

%c_k is found for each cell
c_k = [ChannelSlope.^(1/2)*(5/3).*y(:,1).^(2/3)]./ChannelFriction;

%delta-t is found for each cell, and min value gives timestep
delta_t = min(DEMresolution./c_k);

%--------- Advance to next time step ---------------------------------------------------------------------------------

t = t + delta_t;

%Store timestep value
StoredTime(j+1) = t;

%Print time
t
```

```
%---------- Now route water overbank and into floodplain where appropriate -------------------------------------
---

%Find overbank height by subtracting bankfull height from total water depth
ChannelHeight = y(:,2) - ChannelBankfull;

FloodplainDepth1 = FloodplainDepth2;
qq1 = qq2;

%Add overbank heights to all cells in Dilated Channel
FloodplainDepth1(dchindex)=ChannelHeight(dchv);
VolumeArray2(dchindex)=(ChannelBankfull(dchv)+ChannelHeight(dchv)).*DEMresolution^2;
VolumeArray(dchindex)=(ChannelHeight(dchv)).*DEMresolution^2;

%Find out whether this step needs to be stored to be part of flood video
if (StoredTime(j+1)>Step(StepCounter))&&(StoredTime(j)<Step(StepCounter))
   VideoFile = [VideoFolder,'\VideoFrame',num2str(StepCounter,'%02i'),'.asc'];
   save(VideoFile, 'FloodplainDepth1', '-ASCII')
   if StepCounter < length(Step)
      StepCounter=StepCounter+1;
   end
end

%Remove within-reach lateral inflow
if ((t > 7300)&&(t < 68300))
   qqtemp=qq1-0.0116;
else
   qqtemp=qq1;
end

%Find out whether we are in drying phase
if t > DryingTime;Drying=1;else;Drying=0;end;

%Calculate new floodplain depths and channel inflow for next timestep using FloodplainRoute function
[FloodplainDepth2,Flow_S,Flow_E,vol_edge] = FloodplainRoute(DEMarray,RoughArray, ...

FloodplainDepth1,DEMresolution,ChannelXpos,ChannelYpos,ChannelHeight,ChannelWidth,delta_t,Flow
_S,Flow_E,...
   qqtemp,InflowS,InflowE,InChannelS,InChannelE,dchindex,dchindexnot, Drying);

%Depths in channel are recorded as overbank height
FloodplainDepth2(dchindex)=FloodplainDepth2(dchindex)-ChannelBankfull(dchv);

%Record maximum depths
FloodplainMaxDepth = max(FloodplainMaxDepth,FloodplainDepth2);

%Add together all flow for each dilated channel cell corresponding to central channel cells
qq2 = (ChannelTransform*(FloodplainDepth2(dchindex)-
FloodplainDepth1(dchindex)))*((DEMresolution)^2)/delta_t;

%Add within-reach lateral inflow
if ((t > 7300)&&(t < 68300))
   qq2=qq2+0.0116;
end

%--------- Calculate correct upstream flow value for this data point -----------------------------------------------
```

```
%Update Flow variable
Q(:,1) = Q(:,2);

%If hydrograph does not start at time zero then add a zero
if min(hydrotime > 0)
   hydrotime = [0;hydrotime];
   hydroflow = [hydroflow(1);hydroflow];
end;

%Find position of time t within hydrograph times series
tlessthan = (hydrotime <= t);
tposition = sum(tlessthan);
%Hence find interpolated flow at time t
Q(1,2) = hydroflow(tposition) + ((t-hydrotime(tposition))/(hydrotime(tposition+1)-hydrotime(tposition)))
...
   *(hydroflow(tposition+1)-hydroflow(tposition));
%Add any in/outflow from the floodplain
Q(1,2)=Q(1,2)+qq2(1);


%--------- Loop to calculate downstream discharges ---------------------------------------------------------------

%Length of channel array = number of channel cells
for i = 1:length(ChannelWidth)-1

%--------- Solve for discharge at point x + delta-x ----------------------------------------------------------------

if ((Q(i+1,1)+Q(i,2)) > (10^(-15)))
   Q(i+1,2) =
((delta_t/(DEMresolution*ChannelLength(i+1)))*Q(i,2)+alpha(i+1)*0.6*Q(i+1,1)*((Q(i+1,1)+Q(i,2))/2).^-
0.4+ ...
      (delta_t/(DEMresolution*ChannelLength(i+1)))*(qq2(i+1)+qq1(i+1))/2)/ ...
      ((delta_t/(DEMresolution*ChannelLength(i+1))) + alpha(i+1)*0.6*((Q(i+1,1)+Q(i,2))/2).^-0.4);
else
   Q(i+1,2) = 0;
end

%----------------------------------------------------------------------------------------------------------------

end; %End downstream loop

%Save Output flow for Output hydrograph
OutputFlow(j+1)=Q(length(ChannelWidth),2);

%-------- Transform flows into depths ----------------------------------------------------------------------------

%Water depth is found for each cell
%from Mannings equation y = (nQ/(s0^(1/2).B))^(3/5)
y(:,1) = y(:,2);
y(:,2) = (ChannelFriction.*Q(:,2)./((ChannelSlope.^0.5).*ChannelWidth)).^(0.6);

%------- Find total volume of water to check conservation --------------------------------------------------------

%Water on floodplain (reduced in cells where channel takes up part of the area)
TotalWater = VolumeArray;
```

```
TotalWater(dchindex)=0;
TotalWater = sum(TotalWater(:));
%Add water depth in channel
TotalWater = TotalWater + sum(y(:,1).*ChannelLength.*ChannelWidth*DEMresolution);

%Find volume of water added to model
WaterIn = WaterIn + Q(1,2)*delta_t;

%And leaving model
WaterOut = WaterOut + Q(length(ChannelXpos),2)*delta_t;

%Account for water flowing off edge of model
WaterOut = WaterOut - vol_edge*(DEMresolution^2);

WaterBalance = (WaterIn-WaterOut-TotalWater)/WaterIn;

%Save for next timestep
OldTotalWater = TotalWater;

%Increment timestep
j = j+1;

end; %End timestep loop

%--------- Write outputs variable --------------------------------------------------------------------------------

Flows = OutputFlow(1:j);
FloodplainDepth = FloodplainMaxDepth;
Times = StoredTime(1:j);
MassBalance = WaterBalance*100;

%--------- Save all outputs ------------------------------------------------
flowfile = [OutputFolder,'\OutputFlows.dat'];
depthsfile = [OutputFolder,'\OutputDepths.dat'];
timesfile = [OutputFolder,'\OutputTimes.dat'];
waterbalfile = [OutputFolder,'\WaterBalance.dat'];

save(flowfile,'Flows','-ascii');
save(depthsfile,'FloodplainDepth','-ascii');
save(timesfile,'Times','-ascii');
save(waterbalfile,'MassBalance','-ascii');


%---------------------------------------End of Kinematic Wave -----------------------------------------------------------
```

```
%------------------------------------- Start FloodplainRoute subfunction -----------------------------------------

%Function to route water over floodplain

%Hilary McMillan
%Department of Geography
%Cambridge University

function [Floodplain_depths,Flow_S,Flow_E,vol_edge] =
FloodplainRoute(DEMarray,RoughArray,DepthsArray,DEMresolution,Channelx,Channely,
ChannelHeight,ChannelWidths,delta_t,InS,InE,ChS,ChE,dchindex,dchindexnot,Drying)

%DEMarray = Land Height for each gridsquare (m)
%RoughArray = Mannings n for each gridsquare
%DepthsArray = previous depths of water on floodplain (m)
%DEM resolution: Distance between sample points (m)
%Channelx = channel square x-position
%Channely = channel square y-position
%Channel Height = overbank height of water
%ChannelWidths = width of channel in each cell
%delta_t = timestep over which flow can take place
%InS/InE: flow paths into channel
%ChS/ChE: flow paths intra-channel
%dchindex: location of channel
%dchindexnot: cells not in channel
%Drying: boolean to specify if we are in drying phase

%Returns
%Floodplain_depths = new heights of water on floodplain
%Flow_S/Flow_E: Floodplain flows
%vol_edge: volume of water leaving edge of floodplain

%--------- Declare global variables -----------------------------------------------------------------------------

global Porosities
global VolumeArray
global VolumeArray2
global PorosityVolumes
global WettedP_NS
global WettedP_WE
global XSecArea_NS
global XSecArea_WE

%------- Set up constants ---------------------------------------------------------------------------------------------
-

%Set lateral inflow damping
DampingLateral = 0.0;

%Set intra-floodplain damping
DampingFloodplain = 0.0;

%Get size of DEM array
sz = size(DEMarray);
%Size of DEM
```

```
DEMsizeNS = sz(1);
DEMsizeWE = sz(2);

%Depths where porosity is recorded
p_depths = [0;0.25;0.5;0.75;1;1.5;2;2.5;3;4;5;6;7;8;9;10;11;12];
num_pdepths = length(p_depths);

%------- Create mask of active points within floodplain ------------------------------------------------------------------

activepoints = (DepthsArray > 0);
ap_pack = bwpack2(activepoints);                    %bwpack is used for efficiency
se_dilate = strel2([0, 1, 0;1, 1, 1;0, 1, 0]);       %Each point with positive depth has its four surrounding points made active
ap_dilate = imdilate2(ap_pack,se_dilate,'ispacked');
ap_unpack = bwunpack2(ap_dilate,size(activepoints,1));

%------- First Calculate 'down/south' flows in relation to DEM ------------------------------------------------------------

%Initialise arrays
DepthsTotal = DepthsArray+DEMarray;

%Create offset maps
DEMoffset1 = DEMarray(1:end-1,:);
DEMoffset2 = DEMarray(2:end,:);

Depthoffset1 = DepthsTotal(1:end-1,:);
Depthoffset2 = DepthsTotal(2:end,:);

Depthonlyoffset1 = DepthsArray(1:end-1,:);
Depthonlyoffset2 = DepthsArray(2:end,:);

RoughOffset1 = RoughArray(1:end-1,:);
RoughOffset2 = RoughArray(2:end,:);

%Initialise Flow matrix
Flow_S = zeros(sz(1)-1,sz(2));

%Find active flows
aps1 = ap_unpack(2:end,:);
aps = find(aps1);
%Get rid of points in/to channel
aps=setdiff(aps,InS);
aps=setdiff(aps,ChS);

%Flow depends on cross-section areas and wetted perimeters - these in turn depend on depth
%Get depth indices closest to actual depth - first get max depth over each two squares
maxdepths = max(Depthoffset1(aps),Depthoffset2(aps)) - max(DEMoffset1(aps),DEMoffset2(aps));
depthindices = interp1(p_depths,[1:length(p_depths)],maxdepths);
%Round to nearest integer
depthindices1 = floor(depthindices);
depthindices2 = depthindices1+1;
%Index used to reference cross-section area - find upper and lower points
flows_xsec1 = XSecArea_NS((depthindices1-1).*((sz(1)-1)*sz(2))+aps);
flows_xsec2 = XSecArea_NS((depthindices2-1).*((sz(1)-1)*sz(2))+aps);
```

```
%Find actual xsec as combination
flows_xsec = flows_xsec1 + ((depthindices-depthindices1)./(depthindices2-depthindices1)).*(flows_xsec2 -
flows_xsec1);

%Index used to reference cross-section area - find upper and lower points
flows_wp1 = WettedP_NS((depthindices1-1).*((sz(1)-1)*sz(2))+aps);
flows_wp2 = WettedP_NS((depthindices2-1).*((sz(1)-1)*sz(2))+aps);
%Find actual xsec as combination
flows_wp = flows_wp1 + ((depthindices-depthindices1)./(depthindices2-depthindices1)).*(flows_wp2 -
flows_wp1);

%Set flows to zero where no wetted perimeter
zero_indices = find(flows_wp == 0);
flows_wp(zero_indices) = 1;
flows_xsec(zero_indices) = 0;

%Calculate flows
Flow_S(aps) = sign(Depthoffset1(aps)-Depthoffset2(aps)).*[(flows_xsec.^(5/3)).*(abs(Depthoffset1(aps)-
Depthoffset2(aps)).^0.5)] ./ ...
   [(flows_wp.^(2/3)).*((RoughOffset1(aps)+RoughOffset2(aps))./2)];

Flow_S(InS) = sign(Depthonlyoffset1(InS)-
Depthonlyoffset2(InS)).*[(max(Depthonlyoffset1(InS),Depthonlyoffset2(InS)).^(5/3)) ...
        .*(abs(Depthonlyoffset1(InS)-Depthonlyoffset2(InS)).^0.5).* (DEMresolution.^(7/6))]./ ...

[((RoughOffset1(InS)+RoughOffset2(InS))./2).*((DEMresolution+2*(max(Depthonlyoffset1(InS),Depthon
lyoffset2(InS)))).^(2/3))];

%Check that water is not allowed to flow such that depth in receiving cell > depth in source cell
%Calculate max flow lost from cell 1 = (av. depth - prev depth).*area./timestep
aps_add1 = aps + ceil(aps/(DEMsizeNS-1));
MaxFlow1 = abs((VolumeArray(aps_add1)-VolumeArray(aps_add1-1))./2)./delta_t;
MaxFlow2 = abs(((Depthonlyoffset2(InS)-Depthonlyoffset1(InS))./2).*(DEMresolution^2)./delta_t);

%Extra step to ensure inflow channel cells are not overwritten by floodplain max flows
Flow1 = sign(Flow_S(aps)).*min(abs(Flow_S(aps)),MaxFlow1);
Flow2 = sign(Flow_S(InS)).*min(abs(Flow_S(InS)),MaxFlow2);

%Cut off flow if greater
Flow_S(aps) = Flow1;
Flow_S(InS) = Flow2;

%Clear flows between channel cells (as we discount these)
Flow_S(ChS) = 0;

%------- Calculate 'right/east' flows in relation to DEM ---------------------------------------------------------------

%Initialise arrays

%Create offset maps
DEMoffset1 = DEMarray(:,1:end-1);
DEMoffset2 = DEMarray(:,2:end);

Depthoffset1 = DepthsTotal(:,1:end-1);
Depthoffset2 = DepthsTotal(:,2:end);
```

```
Depthonlyoffset1 = DepthsArray(:,1:end-1);
Depthonlyoffset2 = DepthsArray(:,2:end);

RoughOffset1 = RoughArray(:,1:end-1);
RoughOffset2 = RoughArray(:,2:end);

%Initialise Flow matrix
Flow_E = zeros(sz(1),sz(2)-1);

%Find active flows
ape1 = ap_unpack(:,2:end);
ape = find(ape1);
%Get rid of points in/to channel
ape=setdiff(ape,InE);
ape=setdiff(ape,ChE);

%Flow depends on cross-section areas and wetted perimeters - these in turn depend on depth
%Get depth indices closest to actual depth - first get max depth over each two squares
maxdepths = max(Depthoffset1(ape),Depthoffset2(ape)) - max(DEMoffset1(ape),DEMoffset2(ape));
depthindices = interp1(p_depths,[1:length(p_depths)],maxdepths);
%Round to nearest integer
depthindices1 = floor(depthindices);
depthindices2 = depthindices1+1;
%Index used to reference cross-section area - find upper and lower points
flows_xsec1 = XSecArea_WE((depthindices1-1).*((sz(1)-1)*sz(2))+ape);
flows_xsec2 = XSecArea_WE((depthindices2-1).*((sz(1)-1)*sz(2))+ape);
%Find actual xsec as combination
flows_xsec = flows_xsec1 + ((depthindices-depthindices1)./(depthindices2-depthindices1)).*(flows_xsec2 -
flows_xsec1);

%Index used to reference cross-section area - find upper and lower points
flows_wp1 = WettedP_WE((depthindices1-1).*((sz(1)-1)*sz(2))+ape);
flows_wp2 = WettedP_WE((depthindices2-1).*((sz(1)-1)*sz(2))+ape);
%Find actual xsec as combination
flows_wp = flows_wp1 + ((depthindices-depthindices1)./(depthindices2-depthindices1)).*(flows_wp2 -
flows_wp1);

%Set flows to zero where no wetted perimeter
zero_indices = find(flows_wp == 0);
flows_wp(zero_indices) = 1;
flows_xsec(zero_indices) = 0;

%Calculate flows
Flow_E(ape) = sign(Depthoffset1(ape)-Depthoffset2(ape)).*[(flows_xsec.^(5/3)).*(abs(Depthoffset1(ape)-
Depthoffset2(ape)).^0.5)] ./ ...
    [(flows_wp.^(2/3)).*((RoughOffset1(ape)+RoughOffset2(ape))./2)];

Flow_E(InE) = sign(Depthonlyoffset1(InE)-
Depthonlyoffset2(InE)).*[(max(Depthonlyoffset1(InE),Depthonlyoffset2(InE)).^(5/3)) ...
        .*(abs(Depthonlyoffset1(InE)-Depthonlyoffset2(InE)).^0.5).* (DEMresolution.^(7/6))]./ ...

[((RoughOffset1(InE)+RoughOffset2(InE))./2).*((DEMresolution+2*(max(Depthonlyoffset1(InE),Deptho
nlyoffset2(InE)))).^(2/3))];


%Check that water is not allowed to flow such that depth in receiving cell > depth in source cell
```

```
%Calculate max flow lost from cell 1 = (av. depth - prev depth).*area./timestep
ape_add1 = ape + ceil(ape/(DEMsizeWE-1));
MaxFlow1 = abs((VolumeArray(ape)-VolumeArray(ape+DEMsizeNS))./2)./delta_t;
MaxFlow2 = abs(((Depthonlyoffset2(InE)-Depthonlyoffset1(InE))./2).*(DEMresolution^2)./delta_t);

%Extra step to ensure inflow channel cells are not overwritten by floodplain max flows
Flow1 = sign(Flow_E(ape)).*min(abs(Flow_E(ape)),MaxFlow1);
Flow2 = sign(Flow_E(InE)).*min(abs(Flow_E(InE)),MaxFlow2);

%Cut off flow if greater
Flow_E(ape) = Flow1;
Flow_E(InE) = Flow2;

%Clear flows between channel cells (as we discount these)
Flow_E(ChE) = 0;

%------Clear up
clear DEMoffset1 DEMoffset2 Depthoffset1 Depthoffset2 Depthonlyoffset1 Depthonlyoffset2
RoughOffset1 RoughOffset2 aps1 ape1 MaxFlow1 MaxFlow2 Flow1 Flow2

%Find new area of interest
dpS = find(Flow_S);
dpE = find(Flow_E);

%Get rid of points in/to channel
dpS=setdiff(dpS,InS);
dpS=setdiff(dpS,ChS);

dpE=setdiff(dpE,InE);
dpE=setdiff(dpE,ChE);


%------- Transform flows to volumes --------------------------------------------------------------------------

%Initialise
Vol_S = Flow_S;
Vol_E = Flow_E;

%Find flowing volume by transforming flow
Vol_S(dpS) = Vol_S(dpS)*delta_t;
Vol_E(dpE) = Vol_E(dpE)*delta_t;

%------ Clear up
clear Flow Depthoffset1 Depthoffset1E Depthoffset2 Depthoffset2E MaxFlowE MaxFlowS
Channelxoffset1 Channelyoffset1 Channelxoffset2 Channelyoffset2 Channelxoffset3 Channelyoffset3


%-------- Begin normalisation procedure --------------------------------------------------------------------

%Find water that flows out of each cell
%Initially zero
VolOut = zeros(DEMsizeNS,DEMsizeWE);
%At same time find min height difference between central and neighbouring outflow cells
HeightDiff1 = zeros(DEMsizeNS, DEMsizeWE);
HeightDiff2 = zeros(DEMsizeNS, DEMsizeWE);
HeightDiff3 = zeros(DEMsizeNS, DEMsizeWE);
```

```
HeightDiff4 = zeros(DEMsizeNS, DEMsizeWE);
HeightDiff = zeros(DEMsizeNS, DEMsizeWE);
%And count flows out of each cell
NumFlows = zeros(DEMsizeNS, DEMsizeWE);


%Find direction of flow at each point
dpS_south = find(Vol_S(dpS)>0);
dpS_south = dpS(dpS_south);
dpS_north = find(Vol_S(dpS)<0);
dpS_north = dpS(dpS_north);
dpE_east = find(Vol_E(dpE)>0);
dpE_east = dpE(dpE_east);
dpE_west = find(Vol_E(dpE)<0);
dpE_west = dpE(dpE_west);

%Now at each point add all the negative flows
%Find flow to depth matrix index conversion
dpS_add1 = dpS + ceil(dpS/(DEMsizeNS-1));
dpS_south_add1 = dpS_south + ceil(dpS_south/(DEMsizeNS-1));
dpS_north_add1 = dpS_north + ceil(dpS_north/(DEMsizeNS-1));

%South flowing
VolOut(dpS_south_add1-1) = VolOut(dpS_south_add1-1) + Vol_S(dpS_south);
HeightDiff1(dpS_south_add1-1)=DepthsTotal(dpS_south_add1-1)-DepthsTotal(dpS_south_add1);

%North flowing
VolOut(dpS_north_add1) = VolOut(dpS_north_add1) - Vol_S(dpS_north);
HeightDiff2(dpS_north_add1)=DepthsTotal(dpS_north_add1)-DepthsTotal(dpS_north_add1-1);

%East flowing
VolOut(dpE_east) = VolOut(dpE_east) + Vol_E(dpE_east);
HeightDiff3(dpE_east)=DepthsTotal(dpE_east)-DepthsTotal(dpE_east+DEMsizeNS);

%West Flowing
VolOut(dpE_west+DEMsizeNS) = VolOut(dpE_west+DEMsizeNS) - Vol_E(dpE_west);
HeightDiff4(dpE_west+DEMsizeNS)=DepthsTotal(dpE_west+DEMsizeNS)-DepthsTotal(dpE_west);


%Find direction of flow at each point
InS_south = find(Vol_S(InS)>0);
InS_south = InS(InS_south);
InS_north = find(Vol_S(InS)<0);
InS_north = InS(InS_north);
InE_east = find(Vol_E(InE)>0);
InE_east = InE(InE_east);
InE_west = find(Vol_E(InE)<0);
InE_west = InE(InE_west);

%Add negative flows into channel
InS_add1 = InS + ceil(InS/(DEMsizeNS-1));
InS_south_add1 = InS_south + ceil(InS_south/(DEMsizeNS-1));
InS_north_add1 = InS_north + ceil(InS_north/(DEMsizeNS-1));
%South flowing
VolOut(InS_south_add1-1) = VolOut(InS_south_add1-1) + Vol_S(InS_south);
HeightDiff1(InS_south_add1-1)=DepthsTotal(InS_south_add1-1)-DepthsTotal(InS_south_add1);
```

```
%NumFlows(InS_south_add1-1)=NumFlows(InS_south_add1-1)+1;

%North flowing
VolOut(InS_north_add1) = VolOut(InS_north_add1) - Vol_S(InS_north);
HeightDiff2(InS_north_add1)=DepthsTotal(InS_north_add1)-DepthsTotal(InS_north_add1-1);
%NumFlows(InS_north_add1)=NumFlows(InS_north_add1)+1;

%East flowing
VolOut(InE_east) = VolOut(InE_east) + Vol_E(InE_east);
HeightDiff3(InE_east)=DepthsTotal(InE_east)-DepthsTotal(InE_east+DEMsizeNS);
%NumFlows(InE_east)=NumFlows(InE_east)+1;

%West Flowing
VolOut(InE_west+DEMsizeNS) = VolOut(InE_west+DEMsizeNS) - Vol_E(InE_west);
HeightDiff4(InE_west+DEMsizeNS)=DepthsTotal(InE_west+DEMsizeNS)-DepthsTotal(InE_west);
%NumFlows(InE_west+DEMsizeNS)=NumFlows(InE_west+DEMsizeNS)+1;

%Find out max flow from each cell
ActiveHeights=find(HeightDiff1+HeightDiff2+HeightDiff3+HeightDiff4);
ah1=HeightDiff1(ActiveHeights);
ah2=HeightDiff2(ActiveHeights);
ah3=HeightDiff3(ActiveHeights);
ah4=HeightDiff4(ActiveHeights);


%Count number of flows coming out of each cell
NumFlowsVector=(ah1>0)+(ah2>0)+(ah3>0)+(ah4>0);

%Temporary array of first porosity value
tempPorosities = Porosities(:,:,2);

%For each direction work out the value of the parameter which is minimised
%South flowing
if min(DepthsArray(dpS_south_add1-1))<=0
   stop=1
end
if length(dpS_south)>0
CentralPorosity = VolumeArray(dpS_south_add1-1) ./ (DepthsArray(dpS_south_add1-
1).*DEMresolution^2);
OutflowPorosity = VolumeArray(dpS_south_add1) ./ (DepthsArray(dpS_south_add1).*DEMresolution^2);
OutflowPorosity(find(isnan(OutflowPorosity)+(OutflowPorosity==0))) =
tempPorosities(dpS_south_add1(find(isnan(OutflowPorosity)+(OutflowPorosity==0))));
[FlowPoints, ifl, iah] = intersect(dpS_south_add1-1,ActiveHeights);
HeightDiff1(dpS_south_add1-1)=HeightDiff1(dpS_south_add1-
1)./((1./CentralPorosity)+(1./(NumFlowsVector(iah).*(OutflowPorosity))));
end

%North flowing
if min(DepthsArray(dpS_north_add1))<=0
   stop=1
end

if length(dpS_north)>0
CentralPorosity = VolumeArray(dpS_north_add1) ./ (DepthsArray(dpS_north_add1).*DEMresolution^2);
OutflowPorosity = VolumeArray(dpS_north_add1-1) ./ (DepthsArray(dpS_north_add1-
1).*DEMresolution^2);
```

```
OutflowPorosity(find(isnan(OutflowPorosity)+(OutflowPorosity==0))) =
tempPorosities(dpS_north_add1(find(isnan(OutflowPorosity)+(OutflowPorosity==0)))-1);
[FlowPoints, ifl, iah] = intersect(dpS_north_add1,ActiveHeights);
HeightDiff2(dpS_north_add1)=HeightDiff2(dpS_north_add1)./((1./CentralPorosity)+(1./(NumFlowsVector
(iah).*(OutflowPorosity))));
end

%East flowing
if min(DepthsArray(dpE_east))<=0
   stop=1
end

if length(dpE_east)>0
CentralPorosity = VolumeArray(dpE_east) ./ (DepthsArray(dpE_east).*DEMresolution^2);
OutflowPorosity = VolumeArray(dpE_east+DEMsizeNS) ./
(DepthsArray(dpE_east+DEMsizeNS).*DEMresolution^2);
OutflowPorosity(find(isnan(OutflowPorosity)+(OutflowPorosity==0))) =
tempPorosities(dpE_east(find(isnan(OutflowPorosity)+(OutflowPorosity==0)))+DEMsizeNS);
[FlowPoints, ifl, iah] = intersect(dpE_east,ActiveHeights);
HeightDiff3(dpE_east)=HeightDiff3(dpE_east)./((1./CentralPorosity)+(1./(NumFlowsVector(iah).*(Outflo
wPorosity))));
end

%West flowing
if min(DepthsArray(dpE_west+DEMsizeNS))<=0
   stop=1
end

if length(dpE_west)>0
CentralPorosity = VolumeArray(dpE_west+DEMsizeNS) ./
(DepthsArray(dpE_west+DEMsizeNS).*DEMresolution^2);
OutflowPorosity = VolumeArray(dpE_west) ./ (DepthsArray(dpE_west).*DEMresolution^2);
OutflowPorosity(find(isnan(OutflowPorosity)+(OutflowPorosity==0))) =
tempPorosities(dpE_west(find(isnan(OutflowPorosity)+(OutflowPorosity==0))));
[FlowPoints, ifl, iah] = intersect(dpE_west+DEMsizeNS,ActiveHeights);
HeightDiff4(dpE_west+DEMsizeNS)=HeightDiff4(dpE_west+DEMsizeNS)./((1./CentralPorosity)+(1./(Nu
mFlowsVector(iah).*(OutflowPorosity))));
end

if length(InS_south)>0
CentralPorosity = VolumeArray(InS_south_add1-1) ./ (DepthsArray(InS_south_add1-
1).*DEMresolution^2);
OutflowPorosity = VolumeArray(InS_south_add1) ./ (DepthsArray(InS_south_add1).*DEMresolution^2);
OutflowPorosity(find(isnan(OutflowPorosity)+(OutflowPorosity==0))) =
tempPorosities(InS_south_add1(find(isnan(OutflowPorosity)+(OutflowPorosity==0))));

[FlowPoints, ifl, iah] = intersect(InS_south_add1-1,ActiveHeights);
HeightDiff1(InS_south_add1-1)=HeightDiff1(InS_south_add1-
1)./((1./CentralPorosity)+(1./(NumFlowsVector(iah).*(OutflowPorosity))));

end
if length(InS_north)>0
CentralPorosity = VolumeArray(InS_north_add1) ./ (DepthsArray(InS_north_add1).*DEMresolution^2);
OutflowPorosity = VolumeArray(InS_north_add1-1) ./ (DepthsArray(InS_north_add1-
1).*DEMresolution^2);
```

```
OutflowPorosity(find(isnan(OutflowPorosity)+(OutflowPorosity==0))) =
tempPorosities(InS_north_add1(find(isnan(OutflowPorosity)+(OutflowPorosity==0)))-1);

[FlowPoints, ifl, iah] = intersect(InS_north_add1,ActiveHeights);
HeightDiff2(InS_north_add1)=HeightDiff2(InS_north_add1)./((1./CentralPorosity)+(1./(NumFlowsVector(
iah).*(OutflowPorosity))));

end
if length(InE_east)>0
CentralPorosity = VolumeArray(InE_east) ./ (DepthsArray(InE_east).*DEMresolution^2);
OutflowPorosity = VolumeArray(InE_east+DEMsizeNS) ./
(DepthsArray(InE_east+DEMsizeNS).*DEMresolution^2);
OutflowPorosity(find(isnan(OutflowPorosity)+(OutflowPorosity==0))) =
tempPorosities(InE_east(find(isnan(OutflowPorosity)+(OutflowPorosity==0)))+DEMsizeNS);

[FlowPoints, ifl, iah] = intersect(InE_east,ActiveHeights);
HeightDiff3(InE_east)=HeightDiff3(InE_east)./((1./CentralPorosity)+(1./(NumFlowsVector(iah).*(Outflo
wPorosity))));

end
if length(InE_west)>0
CentralPorosity = VolumeArray(InE_west+DEMsizeNS) ./
(DepthsArray(InE_west+DEMsizeNS).*DEMresolution^2);
OutflowPorosity = VolumeArray(InE_west) ./ (DepthsArray(InE_west).*DEMresolution^2);
OutflowPorosity(find(isnan(OutflowPorosity)+(OutflowPorosity==0))) =
tempPorosities(InE_west(find(isnan(OutflowPorosity)+(OutflowPorosity==0))));

[FlowPoints, ifl, iah] = intersect(InE_west+DEMsizeNS,ActiveHeights);
HeightDiff4(InE_west+DEMsizeNS)=HeightDiff4(InE_west+DEMsizeNS)./((1./CentralPorosity)+(1./(Nu
mFlowsVector(iah).*(OutflowPorosity))));

end

ah1=HeightDiff1(ActiveHeights);
ah2=HeightDiff2(ActiveHeights);
ah3=HeightDiff3(ActiveHeights);
ah4=HeightDiff4(ActiveHeights);

MaxHeights=max([ah1,ah2,ah3,ah4],[],2);

%Any flows less than 1/20 of max are deleted
MinHeights=MaxHeights./20;
%Find indices of bad heights
delheights1=find(ah1<MinHeights);
delheights2=find(ah2<MinHeights);
delheights3=find(ah3<MinHeights);
delheights4=find(ah4<MinHeights);
%And remove
ah1(delheights1)=0;
ah2(delheights2)=0;
ah3(delheights3)=0;
ah4(delheights4)=0;

%Find number of flows at each point
NumFlowsVector=(ah1>0)+(ah2>0)+(ah3>0)+(ah4>0);
%Find height diff minima
```

```
%First set 0 values high
ah1(find(ah1==0))=1000;
ah2(find(ah2==0))=1000;
ah3(find(ah3==0))=1000;
ah4(find(ah4==0))=1000;
HeightDiffVector = min([ah1,ah2,ah3,ah4],[],2);

%Put back into matrix
HeightDiff(ActiveHeights)=HeightDiffVector;
NumFlows(ActiveHeights)=NumFlowsVector;

%Include estimated flows for cells on edge of floodplain to allow water to flow along floodplain
%Find flows out
Edge_out = find(Vol_E(1:DEMsizeNS)<0);
VolOut(Edge_out) = VolOut(Edge_out) - Vol_E(Edge_out);       %Western edge

%Find points where volume flowing out is too great
CheckDepth = ((VolOut > HeightDiff*DEMresolution^2)+(VolOut > VolumeArray));
CheckDepth(dchindex)=0;
[ii jj] = find(CheckDepth > 0);


if length(ii) > 0

%--------------------------------------------------Normalise flows
%Find normalisation coefficient
%Find indices of bad points
norm_position = DEMsizeNS*(jj-1) + ii;

find_norm_coeff = (HeightDiff(norm_position)*DEMresolution^2)./(VolOut(norm_position));
find_norm_coeff = min(find_norm_coeff,(VolumeArray(norm_position))./(VolOut(norm_position)));

%--------Extra code for drying case -----------------------
%This allows cells to drain to zero volume when they are already very low

if (Drying==1)
   %Find points where outflowing vol is too great and low depth
   drying_cells = find(VolumeArray(norm_position) < (0.01*DEMresolution^2));
   %Check that these cells do have some water in
   drying_cells = drying_cells(find(VolumeArray(drying_cells) > 0));
   %Save index of drying cells
   drying_cells_index = drying_cells;

   if length(drying_cells_index)>0

   %Get index into vol array for these point
   drying_cells = norm_position(drying_cells);
   %Check that these cells do not have an inflow
   %Find Volumes of surrounding cells
   %Check surrounding cells are not off the edge of array
   drying_cells_plus =
(((drying_cells+DEMsizeNS)<=(DEMsizeNS*DEMsizeWE)).*(drying_cells+DEMsizeNS))+ ...
      (((drying_cells+DEMsizeNS)>(DEMsizeNS*DEMsizeWE)).*drying_cells);
   drying_cells_minus = (((drying_cells-DEMsizeNS)>=1).*(drying_cells-DEMsizeNS))+(((drying_cells-
DEMsizeNS)<1).*drying_cells);
   %Then collect values of surrounding cells
```

```
   CheckInflowArray =
[DepthsTotal(drying_cells),DepthsTotal(min(drying_cells+1,DEMsizeNS*DEMsizeWE)),DepthsTotal(ma
x(drying_cells-1,1)),...
         DepthsTotal(drying_cells_plus),DepthsTotal(drying_cells_minus)];
   %Check that centre cell has highest depth
   CheckInflowArray =
((max(max(max(max(CheckInflowArray(:,1),CheckInflowArray(:,2)),CheckInflowArray(:,3)),CheckInflo
wArray(:,4))...
      ,CheckInflowArray(:,5)))==CheckInflowArray(:,1));
   %Find cells with no inflow
   drying_cells = drying_cells(CheckInflowArray);
   drying_cells_index = drying_cells_index(CheckInflowArray);
   %Set normalisation coefficient to reduce volume to zero in these cells
   find_norm_coeff(drying_cells_index) =
VolumeArray(norm_position(drying_cells_index))./VolOut(norm_position(drying_cells_index));
end;
end;
%---------------------------------------------------------

%Convert back to indices in flow/vol matrices
norm_north = norm_position - ceil(norm_position/(DEMsizeNS));
norm_south = norm_north+1;
norm_east = norm_position;
norm_west = norm_position - DEMsizeNS;

norm_north_2 = norm_north;
norm_south_2 = norm_south;
norm_east_2 = norm_east;
norm_west_2 = norm_west;

%Take subset of flow indices which apply only to those flows in the correct direction
%i.e. do not apply to inflows in problem cells
%Return point,index into active points vector, index into norm coeff vector
[norm_south,ips,ins] = intersect(dpS_south,norm_south);
[norm_north,ipn,inn] = intersect(dpS_north,norm_north);
[norm_east,ipe,ine] = intersect(dpE_east,norm_east);
[norm_west,ipw,inw] = intersect(dpE_west,norm_west);

[norm_c_south,ipsc,insc] = intersect(InS_south,norm_south_2);
[norm_c_north,ipnc,innc] = intersect(InS_north,norm_north_2);
[norm_c_east,ipec,inec] = intersect(InE_east,norm_east_2);
[norm_c_west,ipwc,inwc] = intersect(InE_west,norm_west_2);

%Now normlalise flow volumes
Vol_S(norm_south) = Vol_S(norm_south).*find_norm_coeff(ins);
Vol_S(norm_north) = Vol_S(norm_north).*find_norm_coeff(inn);
Vol_E(norm_east) = Vol_E(norm_east).*find_norm_coeff(ine);
Vol_E(norm_west) = Vol_E(norm_west).*find_norm_coeff(inw);

%Now normlalise flow volumes
Vol_S(norm_c_south) = Vol_S(norm_c_south).*find_norm_coeff(insc);
Vol_S(norm_c_north) = Vol_S(norm_c_north).*find_norm_coeff(innc);
Vol_E(norm_c_east) = Vol_E(norm_c_east).*find_norm_coeff(inec);
Vol_E(norm_c_west) = Vol_E(norm_c_west).*find_norm_coeff(inwc);

end;
```

```
%Record previous volume
OldVol = VolumeArray;

%Recoded for better efficiency
VolumeArray(dpS_add1) = VolumeArray(dpS_add1) + Vol_S(dpS);          %NS Flows
VolumeArray(dpS_add1-1) = VolumeArray(dpS_add1-1) - Vol_S(dpS);

VolumeArray(dpE+DEMsizeNS) = VolumeArray(dpE+DEMsizeNS) + Vol_E(dpE); %WE Flows
VolumeArray(dpE) = VolumeArray(dpE)-Vol_E(dpE);

%Include estimated flows for cells on edge of floodplain to allow water to flow along floodplain
VolumeArray(1:DEMsizeNS) = VolumeArray(1:DEMsizeNS) + Vol_E(1:DEMsizeNS);       %Western
edge

VolumeArray(InS_add1) = VolumeArray(InS_add1) + Vol_S(InS);          %NS Flows
VolumeArray(InS_add1-1) = VolumeArray(InS_add1-1) - Vol_S(InS);

VolumeArray(InE+DEMsizeNS) = VolumeArray(InE+DEMsizeNS) + Vol_E(InE); %WE Flows
VolumeArray(InE) = VolumeArray(InE)-Vol_E(InE);



%Recoded for better efficiency
VolumeArray2(dpS_add1) = VolumeArray2(dpS_add1) + Vol_S(dpS);          %NS Flows
VolumeArray2(dpS_add1-1) = VolumeArray2(dpS_add1-1) - Vol_S(dpS);

VolumeArray2(dpE+DEMsizeNS) = VolumeArray2(dpE+DEMsizeNS) + Vol_E(dpE); %WE Flows
VolumeArray2(dpE) = VolumeArray2(dpE)-Vol_E(dpE);

%Include estimated flows for cells on edge of floodplain to allow water to flow along floodplain
VolumeArray2(1:DEMsizeNS) = VolumeArray2(1:DEMsizeNS) + Vol_E(1:DEMsizeNS);       %Western
edge

VolumeArray2(InS_add1) = VolumeArray2(InS_add1) + Vol_S(InS);          %NS Flows
VolumeArray2(InS_add1-1) = VolumeArray2(InS_add1-1) - Vol_S(InS);

VolumeArray2(InE+DEMsizeNS) = VolumeArray2(InE+DEMsizeNS) + Vol_E(InE); %WE Flows
VolumeArray2(InE) = VolumeArray2(InE)-Vol_E(InE);

%Record water lost for mass balance
vol_edge = sum(Vol_E(1:DEMsizeNS));

%Allow for small computational errors
VolumeArray(dchindexnot(find(VolumeArray(dchindexnot)<0)))=0;
VolumeArray2(dchindexnot(find(VolumeArray2(dchindexnot)<0)))=0;

%---------- Transform volumes in cells to new depths-------------------

%Find known volume/porosity points that volume lies between
VolumeArrayCheck = PorosityVolumes;
for i = 1:num_pdepths
   VolumeArrayCheck(:,:,i) = max(sign(VolumeArray2 - VolumeArrayCheck(:,:,i)+0.000001),0);
end;
%Sum known volume points less than Volume Array to find point number
```

```
VolumePointNumbers = sum(VolumeArrayCheck,3);
%Now extract indices to find lower volume points
indices1=repmat([1:DEMsizeNS].',DEMsizeWE,1);
indices2=reshape(repmat([1:DEMsizeWE],DEMsizeNS,1),[],1);
indices3=VolumePointNumbers(:);

indices = sub2ind(size(PorosityVolumes),indices1,indices2,indices3);
%Use index to find volume
VolumeLower = PorosityVolumes(indices);
%And finally reshape array
VolumeLower=reshape(VolumeLower,DEMsizeNS,DEMsizeWE);
%Use index to find depths
DepthLower = p_depths(indices3);
%And reshape
DepthLower=reshape(DepthLower,DEMsizeNS,DEMsizeWE);

%And upper volume points
indices3=indices3+1;
indices = sub2ind([DEMsizeNS,DEMsizeWE,length(p_depths)],indices1,indices2,indices3);
%Use index to find volume
VolumeUpper = PorosityVolumes(indices);
%And finally reshape array
VolumeUpper=reshape(VolumeUpper,DEMsizeNS,DEMsizeWE);
%Use index to find depths
DepthUpper = p_depths(indices3);
%And reshape
DepthUpper=reshape(DepthUpper,DEMsizeNS,DEMsizeWE);

%Now calculate intermediate volume point
DepthsArray = DepthLower + ((VolumeArray2-VolumeLower)./(VolumeUpper-
VolumeLower)).*(DepthUpper-DepthLower);

%Clear up
clear indices1 indices2 indices3 indices DepthLower DepthUpper VolumeLower VolumeUpper
clear ExtraDepth AddedDepth sparse_norm_s sparse_norm_E norm_coeff_channel dpS dpS_add1 dpE
DepthsArray2

%-------- Function returns new floodplain depths -------------------------------------

%Floodplain depths have already been calculated
Floodplain_depths = DepthsArray;

clear DepthsArray
```

Appendix B

FLOODPLAIN INUNDATION SURVEY RESPONSES

Survey Responses by House Number

House number (see map)	Maximum flood depth	Flood water came from river?	Flood water came as surge from fields?	Time house was first flooded	Time for water to reach 1ft deep	Comments
1	2 ft	Y	N	2.30 pm	45 min	
2	3 ft 6 in	Y	?	Pre- 2.30 pm		
3	2 ft 10 in	Y	Y	2.30-3 pm	15 min	
4	4-5 ft	Y	Y	5 pm		
5	18 in – 2 ft	Y	Y	1 pm?		
6	3 ft	?	?	?		
7	2 ft (cellar)	N	N	?		
8	2 ft	Y	?	?		
9	4 ft (cellar)	Y	N	Mid-afternoon	1 hr	
10	1 ft	?	Y	7 pm	1 hr	
11	2 ft	Y	Y	2-2.30 pm	30 min	
12	3 ft 6 in	Y	N	3 pm	45 min	
13	2 ft	Y	Y	12.30 pm		Vacated 1pm
14	5 ft 6 in	Y	Y	?	20 min	
15	4 ft	Y	Y	12.30 pm	15 min	
16	3 ft 6 in	Y	Y	1 pm	1 hr	
17	3 ft 6 in	Y	Y	1 pm	15 min	
18	3 ft	Y	Y	1 pm	Minutes	
19	3 ft 10 in (cellar)	Y	N	4 pm	30 min	Flooded through cellar walls
20	2 ft	Y	N	4 pm		2 in inside (sandbags)
21	1 ft 2 in	?	?	?		Owners absent
22	1 in	Y	?	?		3 ft in cellar
23	3 ft (cellar)	?	N	4 pm	1 hr	Flooded through floor
24	3 ft	Y	Y	1.30 pm	30-60 min	
25	3 in	Y	Y	3 pm	30 min	House raised by 3 ft above surrounding land
26	1 ft	Y	Y	2.30 pm	10-15 min	
27	3 ft 6 in	?	Y	?		Owners absent
28	3 ft	?	Y	4 pm	Immediately	
29	1 ft 2 in	Y	N	3 pm	1 hr	
30	1 ft 6 in	Y	?	2 pm	< 1 hr	
31	13 in	Y	N	4 pm	1 hr	House raised by 20 in above surrounding land
32	18 in	?	Y	1.30 pm		
33	1 ft	Y	?	?		Owners absent
34	3 ft	?	Y	?		Owners absent
35	3 ft	Y	N	4 pm		
36	2-3 ft	Y	N	1 pm	30 min	
37	10-15 in	Y	?	2 pm		
38	5 ft (cellar)	?	N	2 pm	1 hr 30 min	

Map of House Locations

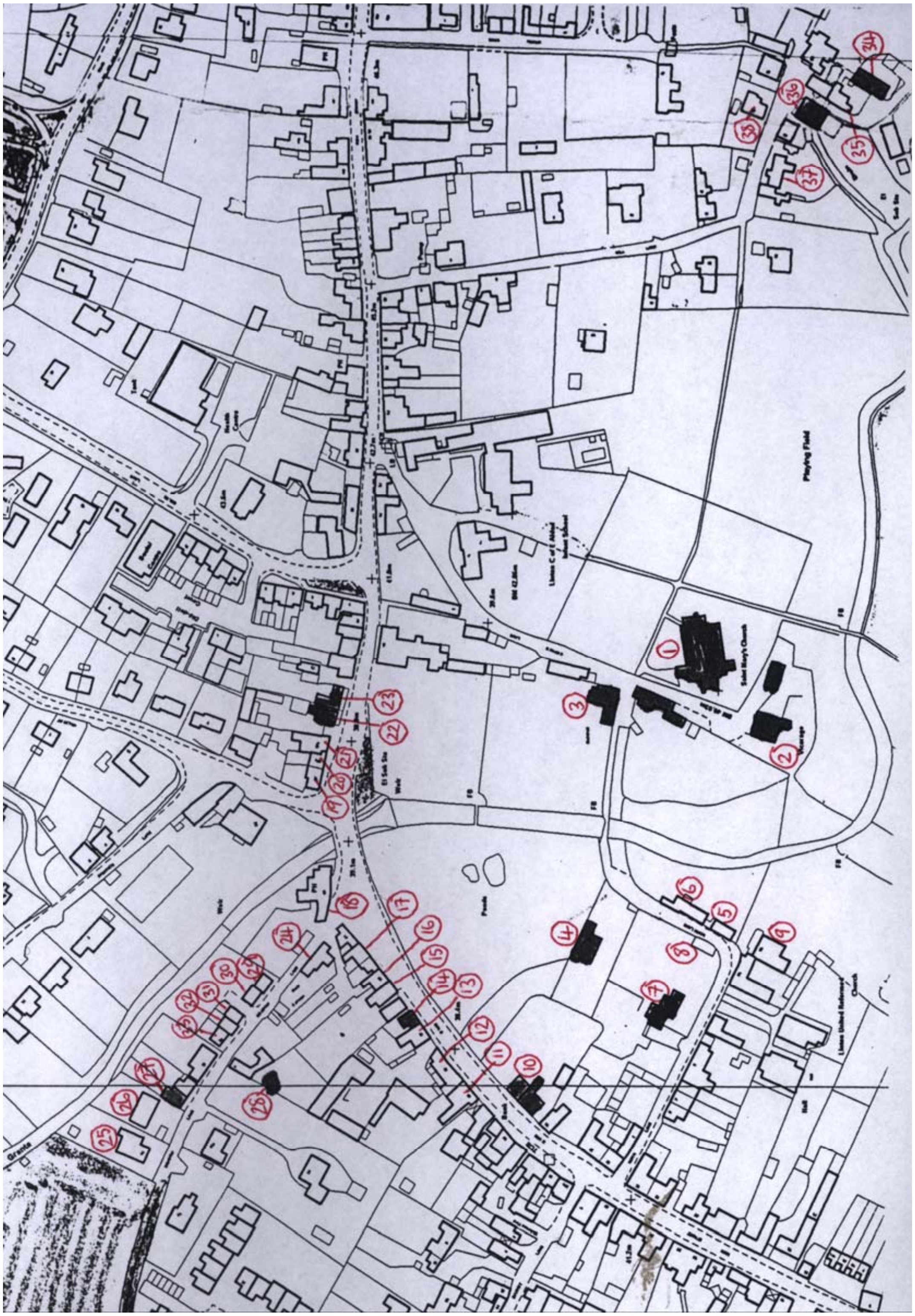

Figure B1: House locations in Linton as referenced by Survey Response table